Comparative study of amino acids utilisation in *Leishmania mexicana*

Archana Nayak BSc, MSc, MRes

Submitted in fulfilment of the requirements for the degree of a Doctor of Philosophy

May 2018

Institute of Infection, Immunity and Inflammation
College of Medical, Veterinary and Life Sciences
University of Glasgow

Abstract

Critical metabolic steps of the central carbon metabolism pathways have been of primary focus for the discovery of novel drug targets against Leishmaniasis, a neglected tropical disease caused by *Leishmania*. It is known that this particular protozoan parasite also relies on exogenous amino acids; however, comparative studies between exogenous amino acids utilisation and their essentiality for parasite growth and metabolism were often less emphasised.

In this thesis, a novel approach was used to apply metabolomics techniques in a newly developed amino acids rich chemically defined medium for *in vitro* culture of *Leishmania* promastigotes. The chemically defined medium allowed for controlled customisable environment for deeper understanding of amino acids metabolism and parasite growth. A previously reported semi-defined growth medium (REIX (Steiger and Black, 1980)) was selected as a starting point. Undefined components of REIX were omitted and the composition of the resulting defined medium was varied through the addition, individually or in groups of amino acids and trace components (including magnesium, calcium, zinc, iron salts, biopterin, folate, riboflavin and lipoic acid). Growth assays were performed to identify a medium composition, referred to as Nayak medium, that supported robust growth over serial passages, at a similar rate to a conventional, serum supplemented rich growth medium (HOMEM (Berens et al., 1976)).

Subsequently, the importance of individual amino acids was studied by systematic analysis in media containing equimolar quantities of each proteogenic amino acid, bar one (termed “amino acid knock out media”). Growth rate, concentration dependent growth, cell body length, total cell protein and acetate secretion were all recorded. Based on these results, it was found that exogenous supply of L-Tryptophan, L-Phenylalanine, L-Arginine, L-Lysine, L-Leucine and L-Valine as most critical for viability of promastigotes. Hence, it was of interest to further investigate the intracellular composition of the other 14 amino acids and their anabolic and catabolic pathways within *L. mexicana* promastigotes.

Comparative investigation of intracellular amino acid metabolism was conducted using a metabolomic finger-printing technique in log phase *L. mexicana* promastigotes cultured in defined medium. Previous studies on amino acid pathways were mostly based on genome annotation or reductionist experimental approaches, however, network mapping of metabolomics data as shown in Chapter 5 allowed to understand new insights about compensatory amino acid metabolic pathways, not predicted before. The 45 known components of the defined medium allowed for easier distinction from ~400 metabolites of the intracellular samples. The free amino acids pool showed increased abundance of L-Alanine, L-Glycine, L-Proline, L-Histidine, L-Asparagine, L-Threonine and L-Tyrosine in the intracellular metabolome which partly explains the dispensability of these amino acids in culture media as observed in single amino acid knock out experiments. Approximately 64 metabolites, putatively identified as related to amino acid metabolism were analysed by pathway mapping. This showed a unique utilisation pattern amongst all amino acids following a two-step transamination and a decarboxylation with significant NADH production. The downstream intermediates were secreted into the environment, rather than elaborate degradation pathways as followed within the mammalian systems.

Validation of the observed secretion pattern of amino acid degradation was conducted using metabolic foot-printing technique at six different time points, which provided data on relative quantification of metabolite uptake and secretion from the culture media at different growth stages. About ~200 metabolites were putatively identified from across the replicates in the dataset collected over a growth period of 9 days in both the positive and negative ionisation mode and only ~70 metabolites could be identified with authentic standards for individual mass/charge ratio and retention time comparison. Depletion profiling of the culture media showed that L-Tryptophan, L-Aspartate, L-Glutamate, L-Arginine, L-Methionine and L-serine were continuously utilised with more than 50% consumed over the 9-day growth period. Amino acids such as L-Leucine, L-Threonine, L-Valine, L-Phenylalanine, L-Tyrosine and L-Lysine were partially utilised, while L-Glycine, L-Glutamine, L-Asparagine, L-Proline and L-Alanine were continuously secreted during the growth period under conditions tested. Overall, ~25 % of the total metabolites were found depleted from the medium, ~15% not changed significantly, 20% un-identified metabolites and interestingly, about ~40% of metabolites were significantly enriched in the medium.

Systematic analysis of the 40% secreted small molecules secreted in the culture media constituted the exometabolome. The proportion of keto acids exceeded the other constituents of the exometabolome, confirming the partial degradation and overflow metabolism. Hence, the possibility that keto acids could also contribute to virulence was speculated. Early results from various biochemical analysis allowed new insights about amino acid derived enol lactones, especially the aromatic pyruvates to support the establishment of parasitism, with macrophage cells as *in vitro* experimental model. However, targeted molecular biology studies are required to further understand the role of exometabolome in parasitism; especially by inhibition of the *Leishmania* enzymes L-Tryptophan transaminase or phenyl pyruvate dehydrogenase as they are non-homologous to mammalian systems.

In summary, this study has shown simple, customisable platform for *in vitro* culture of *Leishmania* promastigotes in defined medium, intracellular and exometabolome of *Leishmania* adaptable for various studies. L-Tryptophan and L-Phenylalanine were found as the most critical exogenous amino acids for parasite viability and their analogues inhibited parasite growth. Hence, warrants further studies for their effectiveness as drugs in the field. Also, *Leishmania* exometabolome could serve as diagnostic signature for species identification, taxonomical comparisons, virulence patterns, physiological comparisons within varied nutrient systems.

Table of Contents

List of tables

List of Figures

Acknowledgements

Firstly, my sincere thanks to supervisor Dr. Richard Burchmore for his guidance, support and help during the course of my Ph.D. studies. Many thanks to Prof Mike Barrett, Dr. Karl Burgess and Dr. Daniel Walker for the time and kind consideration during the supervisory and review process for their guidance and support.

Special thanks to all present and past group members of Burchmore, Barrett, Glasgow Polyomics members including and not limited to Najad Zaki, Hazel Hamilton, Dr. Snezhana Akpunarlieva, Dr. Julie Kovarova, Dr. Katharina Johnston, Dr. Fiona Achcar, Dr. Isabel Vincent, Dr. Christina Naula, Dr. Gavin Blackburn, Dr. Yoann Gloaguen; Dr. Naomi Rankin, Carina Conceicao; Dr. Leandro Lemgruber Soares, Helena De Torre, Mottram and McCulloch group members and all members of Institute of Infection, Immunity & Inflammation, University of Glasgow, Glasgow, Scotland, UK.

Many thanks to Mrs. Angela Woolton and present administrator, supervisors and colleagues associated with the DTC in Cell & Proteomic Technologies program.

Most of all, to God Almighty in presence and grace with my husband Mr. Krishnananda Nayak, and son Master Ishaan Nayak, parents and parents-in-laws, extended family and friends both in UK and India, thank you one and all for your constant encouragements and support at all times.

Author's Declaration

I declare that, except where explicit reference is made to the contribution of others, this dissertation is the result of my own work and has not been submitted for any other degree at The University of Glasgow or any other institution.

Archana Nayak

List of abbreviations

µM
micromolar, 127

acetyl-CoA
acetyl - coenzyme A, 29

ADP
adenosine diphosphate, 172

AMP
adenosine monophosphate, 157

ATP
adenosine triphosphate, 178

blast
Basic local alignment search tool, 170

BSA
Bovine serum albumin, 45

CMW
Chloroform methanol water, 47

Da
Daltons, 27

HCA
hierarchical clustering analysis, 188

HILIC
hydrophilic interaction chromatography, 187

IDEOM
Identification of metabolites, 188

KEGG
Kyoto Encyclopedia of Genes and Genomes, 225

LC-MS
liquid chromatography mass spectrometry, 216

mL
milliliter, 94

NADH
Nicotinamide adenine dinucleotide, 164
Nicotinamide adenine dinucleotide (reduced form), 170

nM
nano molar, 94

NMR
Nuclear magnetic resonance, 221

ºC
degree Celsius, 51

PCA
principal component analysis, 188

PLS-DA
Partial Least-Squares Regression and Discriminant Analysis, 188

ppm
parts per million, 143

Chapter 1 Introduction

1.1 Leishmaniasis

Leishmaniasis is an infectious disease affecting some of the poorest parts of the world. Leishmaniasis is caused by parasitic protozoa of the genus *Leishmania*. It has been recorded that there are more than 20 species of *Leishmania* pathogenic to human causing a wide range of clinical diseases (Ross et al;1903, Lainson et al; 1987, Shaw et al; 1994). According to the World Health Report, leishmaniasis is classified under the neglected tropical diseases since 1.3 million people develop the symptomatic disease each year resulting in 20,000 to 30,000 deaths annually affecting poorest people in Asia, Africa and Latin America.

Leishmaniasis is transmitted to the mammalian host by the bite of insect vectors from particular sandfly species. Killickkendrick et al. emphasise that these particular species of sand-flies, belonging to the subfamily-Phlebotominae are found in places with high temperature and lead to rapid disease transmission (Killickkendrick et al; 1990). However, there have been evidences of cases reported in non-endemic areas favouring the spread of disease carrying insect vectors mainly owing to the factors such as disorganised waste management, heavily populated areas of people with signs of malnutrition, weaker immunity and migration (Vecsei et al., 2001).

The endemicity of leishmaniasis as shown in Figure 1.1. Parasitic diseases in different hosts exhibit several debilitating clinical symptoms with different forms of leishmaniasis (Shaw et al, 1994) in human hosts described as follows:

- In cutaneous leishmaniasis, skin ulcers usually form on exposed areas, such as the face, arms and legs. Most cases heal within a few months although certain scars could remain on the skin.

- Diffuse cutaneous leishmaniasis produces disseminated and chronic skin lesions resembling those of lepromatous leprosy and poses more difficulty for complete treatment.

- In mucocutaneous forms, the lesions can partially or totally destroy the mucous membranes of the nose, mouth and throat cavities and surrounding tissues.

- Visceral leishmaniasis, also known as kala azar, is characterised by high fever, substantial weight loss, swelling of the spleen and liver, and anaemia. The disease has been reported to have high fatality rate (Croft and Coombs, 2003).

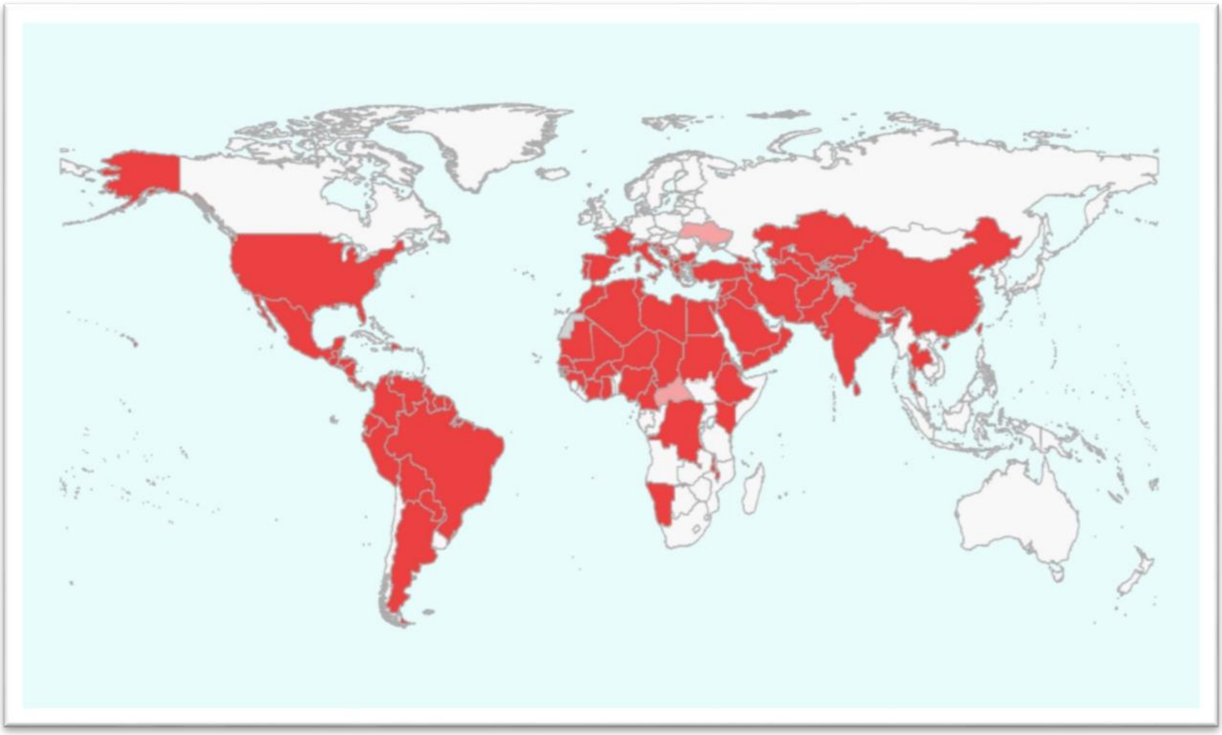

Figure 1.1 Endemicity of leishmaniasis

Data according to WHO report 2015. Those highlighted in red shows areas reported with positive cases of leishmaniasis adopted from http: //apps.who.int/neglected_diseases/ntddata/leishmaniasis/leishmaniasis.html

1.2 Life cycle of *Leishmania*

Leishmania, a protozoan parasite, require female sand-fly as insect vector during the promastigotes stage and mammalian hosts during the amastigotes stage in one complete life cycle as shown in Figure 1.2.

Broadly, parasitism has been defined to exhibit three basic properties such as infectiousness, establishment and transmission (Zelmer, 1998) between host systems. The first step involves the short term process of tolerance during an instantaneous exposure to a new environment described as infectiousness. The new environment could be other living organisms of multiple species as known for the *Leishmania* parasite. The second crucial step in parasitism is establishment within the host system. Zelmer et al explain that successful establishment of the parasite is its ability to tolerate or to evade the host immune system. The third step of transmission mainly involves virulent factors to malfunction host cells or host manipulation to facilitate rapid transference to other new host systems as a result of other various virulence mechanisms.

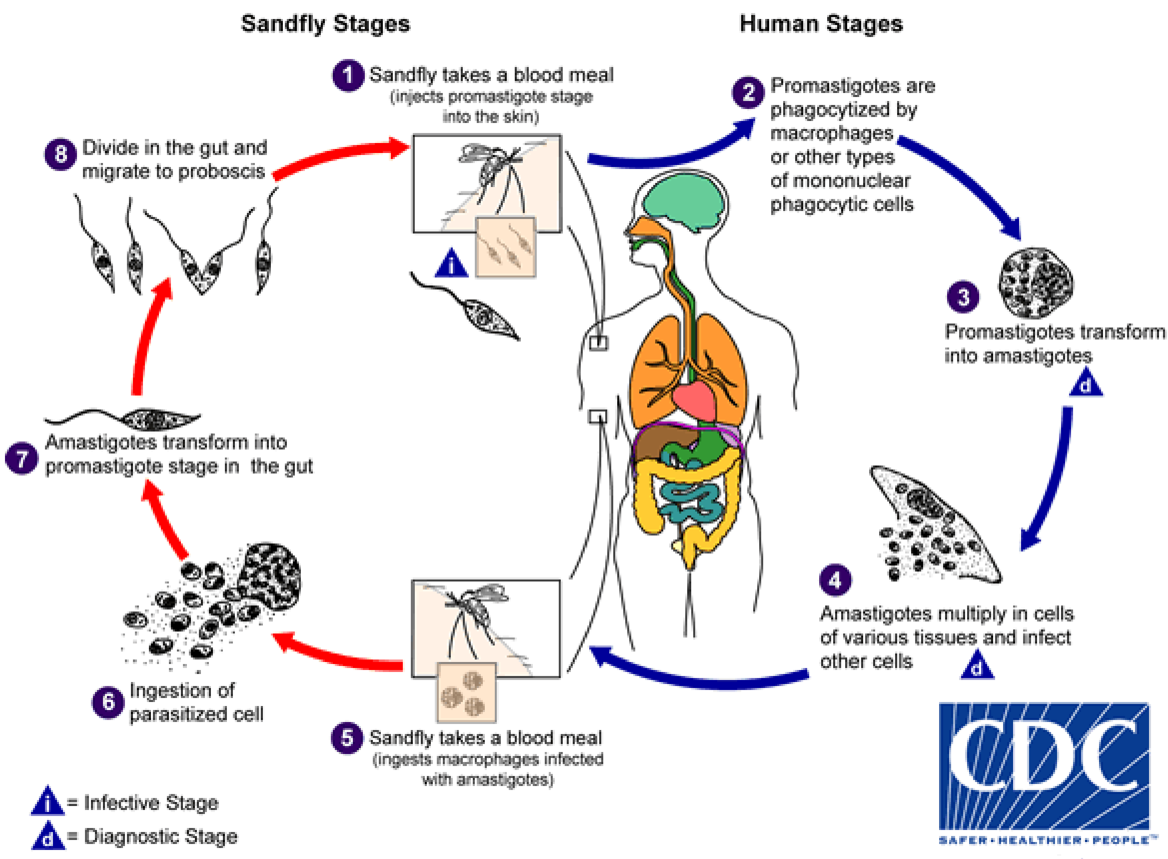

Figure 1.2 Life cycle of Leishmania parasites between the host systems.

Adapted from https://www.cdc.gov/parasites/leishmaniasis/biology.html available freely under public domain. Numbered stages with description as follows: **1.** Promastigotes injected within the host during insect bite

2. Promastigotes engulfed by macrophages or mononuclear cells.

3. Stage of promastigotes transformed to amastigotes within the macrophages.

4. Amastigotes multiply within cells and infect other neighbouring cells.

5. Subsequent sand-fly bites result in ingestion of infected cells with amastigotes.

6, 7, and 8. Within the sand-fly, the amastigotes transform into promastigotes and continue as stage 1 of the life cycle.

Promastigotes undergo a dynamic transformation from procyclics reported to undertake in 24-48 hours then the nectomonands in 48-72 hours, leptomonads in 4-7 days and metacyclics in 5-7 days which infect the host cells and haptomonads in 7-9 days forms the lining of the salivary duct (Dostalova and

Volf, 2012). The dynamic transformation from procyclics to haptomonad forms the lining of the salivary duct of the sand-fly adapted and modified from (Dostalova and Volf, 2012) is as shown in
Figure 1.3 are associated with morphological changes from shorter and stout cell body to metacyclics with longer flagella and longer, slender cell body. These extracellular flagellated promastigotes at metacylic stages are transmitted into the mammalian hosts during infection.

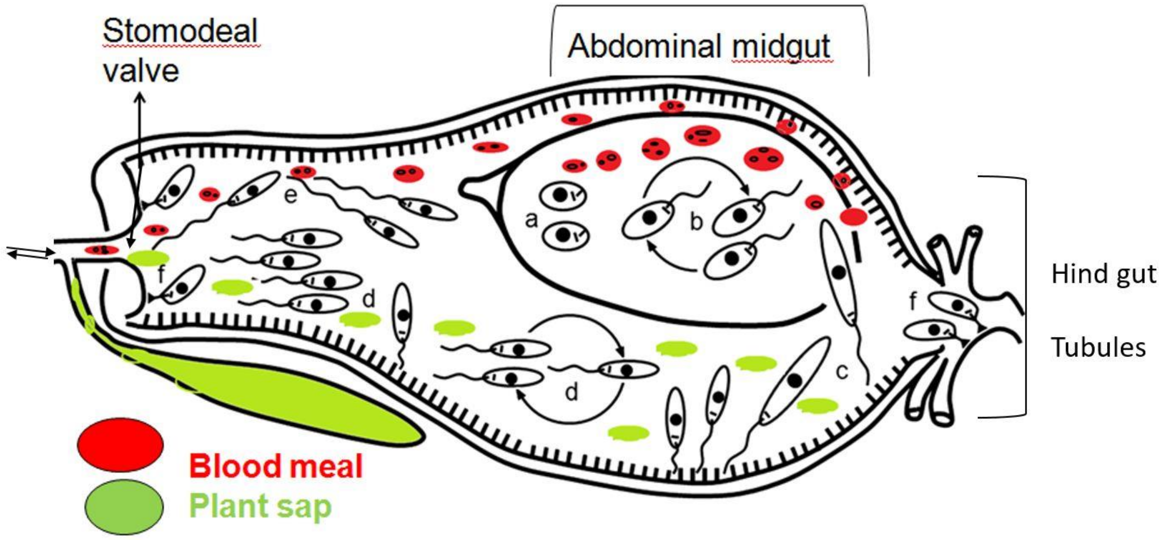

a. amastigotes **b.** procyclics **c.** nectomonands,
d. leptomonads **e.** metacyclics **f.** haptomonads

Figure 1.3 Promastigotes development within the sand-fly

Picture modified from (Dostalova and Volf, 2012) to describe the transformation of promastigotes in the sand-fly digestive tract. Special emphasis has been laid on nutrient utilisation required during promastigotes development dependent on the blood meal (red) or sugar meal (green) of the sandfly insect feed.

The development of promastigotes within the sand-fly highly depends upon the nutrients from the blood meal and plant sap meals fed by the insect alternatively. It has been reported that the sugar gradient in the alimentary tract of the sand-fly facilitates the differentiation of procyclics leading up to metacyclics that accumulate at the pharynx of the sand-fly. The sand-fly regurgitates the parasites to the mammalian host during its blood meal (Murray et al., 2005). The neutrophils are the first immune cells to engulf the parasites and then undergo cell lysis. The lysed neutrophils along with the parasites are phagocytosed by the macrophages. The macrophages become the major host cells for *Leishmania*. The parasites within self-sustaining membrane-bounded parasitophorous vacuoles at high temperature (~37ºC) and acidic pH promotes the development of non-dividing, metacyclic promastigotes to amastigotes (Biegel et al., 1983, Bates and Tetley, 1993). Electron micrographs of macrophages have shown a fusion of secondary lysosomes with vacuoles containing *L. mexicana* amasitogotes after internalisation within the macrophages to form the phagolysosome (Alexander and Vickerman, 1975).

The phagolysosome is a highly acidic, hydrolytic compartment with many characteristics of a late endosomal compartment, which is responsible for the final stage of the phagocytosis process in an uninfected macrophage. Within the phagolysosome, the promastigotes differentiate into amastigotes before proliferation. The differentiation process is associated with pre-adaptive metabolic changes that enable the *Leishmania* amastigotes to thrive in an acidic condition suitable to the new host environment (Mcconville and Naderer, 2011).

Wenynon et al in 1926 described the intracellular form of amastigotes of *L. donovani* as round-ovoid with a rod like kinetoplast and a nucleus within a homogenous mass of cytoplasm unlike the promastigotes with an elongated anterior flagellum. Chang et al describe the ultrastructure of *Leishmania* by thin sectioning of the two different life forms for the comparison of promastigotes and amastigotes (Chang et al 1955).The structural comparison described for amastigotes in the parasitophorous vacuole within macrophages were reported as 2-4 microns however, the promastigotes in the insect midgut reach up to 14-20 microns in length and 1.5-3.5 microns in breadth. Thus, the amastigotes undergo series of developmental changes for transformation into infective promastigotes in the midgut of the sand-fly.

These morphological and metabolic transformations of the parasite within the host system largely depends upon nutrient utilisation capabilities of *Leishmania*. The factors for nutrient sequestration remains critical on the metabolic ability of the parasite to divert host cell resources for their own needs (Glaser and Mukkada, 1992). Though the *Leishmania* genome encodes for a diverse enzymatic profile, the dynamics of nutrients salvage remains largely unknown. The competition for substrate molecules between the host and parasitic transporters, the metabolic capability of the parasite to adapt to diverse host environments at different temperature, pH and enzymatic repertoire (Darling et al., 1989) of the parasite are the key factors that determines the viability of the parasites within the host system (Mcconville and Naderer, 2011). Thus, in this study efforts have been made in this direction for deeper understanding about the nutrients required for the viability, growth and development of *Leishmania*.

1.3 Taxonomy

The taxonomy of *Leishmania* as described in Table 1-1belong to domain Eukaryota, kingdom Protista and phylum euglenzoa. Importantly, *Leishmania* belongs to the order Kinetoplastida and to the sub order Trypanosomatina. Vickerman et al, 1994 described the evolutionary expansion of Trypanosomatina as exclusively parasitic with species containing one flagellum, which notably includes *Trypanosoma* and *Leishmania* species (Vickerman, 1994). The evolutionary hierarchy of *Leishmania* is as shown in Table 1-1. The other sub order of Kinetoplastida is Bodonina which includes ecto-commensal and free living species which are biflagellate. Lainson et al, 1987 classified the 53 species recognised in this genus based on their location within the insect gut (Lainson et al., 1987). However, the classification of the genus to sub genus has been of considerable debate, some studies define three subgenera such as *Leishmania*, *Sauroleishmania*, and *Viannia and* the position of the two other genera called the *Euleishmania* and *Paraleishmania* has been placed under the division of *Leishmania*, yet a need for a sub genera to be differentiated by their unique metabolic traits (Franco and Grimaldi, 1999, Momen and Cupolillo, 2000, Akhoundi et al., 2016).

Table 1-1 Taxonomical classification of *Leishmania*

Domain	Eukaryota
Kingdom	Protista
Phylum	Euglenozoa
Subphylum	Sarcomastigophora
Superclass	Mastigophora
Class	Zoomastigophora
Order	Kinetoplastida
Family	Trypanosomatina
Genus	*Leishmania*

1.4 Diagnosis

Current methods for the diagnosis of Leishmaniasis are based on antigen detection and serological techniques from patient samples. The advantages and disadvantages of few of the techniques have been briefly described here. Microscopy serves as a primary technique for identification of *Leishmania* in many clinical laboratories. Giemsa stained smears of lesions, biopsies or scrapings allows direct identification of amastigotes and in combination of culture methods improves to 85% sensitivity (Ramirez et al, 2000, Blum et al, 2004). However, microscopy and culture are time consuming, requires skilled personnel and clinical laboratory instruments; not easily applicable in endemic field areas.

Immunochromatograhic techniques based on target interaction between parasite antigens and monoclonal antibodies have been designed in various kit formats as dipsticks or cassette based. Rapid diagnostic tests (RDTs) detect different antigens such as L-Histidine rich protein 2 (HRP2), parasite lactate dehydrogenase (pLDH) and aldolase (Piper et al., 1999). Immunofluorescent antibody test (IFA), another antigen-based test has been reported with sensitivity between 87-100% and specificity in range of 77-100% for positive cases in early infection stages.

However, IFA test can only be conducted within clinical laboratory standards and not directly applied on field (Iqbal et al, 2002).

Different diagnostic procedures are required depending upon the level of infection. For example, asymptomatic *Leishmania* carriers who carry low levels of circulating parasites within their system with not enough accumulation of antigen for reliable detection; PCR based methods are adopted (Salotra et al., 2001). In the case of leishmaniasis in the dog, anti-*leishmania* antibodies were reported as present in urine with urinary protein/creatinine (U P/C) ratios higher than one. ELISA test to detect protein A and IgG2 were found to be positive in the urine of *Leishmania* infected dogs (Solano-Gallego et al., 2001).

KAtex, a latex agglutination test is used to detect *Leishmania* antigens in urine (Attar et al., 2001). The efficacy of KAtex has been monitored in different disease prone areas such as Spain (Sarkari et al., 2002), India (Sundar et al., 2005) and the middle-east. Latex agglutination tests hold great promise because of good specificity (80-100%) and also useful for detection even in immunocompromised patients (Vilaplana et al, 2004). However, the moderate sensitivity range of 47% to 95% poses questionable results to separate the weak positive cases from negative results (Diro et al, 2007; Malaei et al, 2006) and requires longer sample preparation procedure such as boiling urine to eliminate false positive results (Attar et al, 2001).

Thus, the different species of *Leishmania* and its geographical distribution brings an enormity of variations amongst the level of parasitic infections in host systems (Badaró et al, 1983; Boelaert et al, 2004). These different levels of parasite infections pose a challenging bottleneck for faster and reliable detection of different types of parasite antigens or serological markers. Thus, there is an increasing demand for better diagnostic techniques for early intervention.

Discovery of novel antigens is imperative to accelerate diagnosis especially for different species of *Leishmania*. Isolation of antigens depends upon a stable platform of *in vitro* culture of *Leishmania*; addressed in this thesis by development of a defined medium as described in Chapter 3.

1.5 Current treatment

Leishmaniasis affected endemic countries have traditionally used pentavalent antimonials, pentostam or glucantime, chemically sodium stibogluconate and N-methylglucamine antimonate respectively. These drugs are known to be required for continuous consumption over a long period of time leading to adverse consequences administered parenterally for 10-30 days. The exact mode of action of these drugs are yet to be elucidated; there have been reports of toxic side effects in variable degrees depending upon the immune comprised state of the patient (Basselin et al., 2002).

Another widely used drug in the treatment of leishmaniasis in dogs is allopurinol, riboside analogue which prevents protein production. Allopurinol serves as a substrate of hypoxathine guanine phosphoribosyl transferase enzyme located in parasite specific organelle, glycosomes (Pfaller and Marr, 1974). Clinical trails with human patients have not shown consistent success. Recent formulations such as amphotericin B and miltefosine with a novel mode of delivery using liposomal formulation (AmBisome) for oral consumption have been reported to have better efficacy for the treatment of visceral and cutaneous leishmaniasis (Rakotomanga et al., 2007).

Current treatment also involves vaccination against leishmaniasis, however, the combination of antigens and right delivery system for the long lasting central memory of the immune system has been a challenging milestone. A short summary of different types of vaccines, advantages and disadvantages have been listed in Table 1-2 below (Gillespie et al., 2016, Handman, 2001):

Table 1-2 Vaccines used in treatment of Leishmaniasis

Type of vaccines	Organisms used	Advantages	Disadvantages
First generation vaccines	whole killed/ live attenuated	Prophylaxis Asymptomatic immune memory	Relapse of virulence and infection.
Second generation vaccines	Laboratory produced recombinant protein products of *Leishmania* specific antigens	Safer alternatives to the first generation Ease of customisation	Need for soluble stable emulsions and extensive clinical development.
Third generation vaccines	Naked DNA	Less immunogenic Different mixture of conserved antigens	The cost of development and clinical trials.

Similar to other protozoan parasite with a dynamic life cycle involving multiple hosts, *Leishmania* with female sand-fly as vector affects multiple host systems such as humans, cattle and dogs (Kaye and Scott, 2011). Leishmaniasis being a vector borne has been difficult to control the spread of the disease(Kaye and Scott, 2011). The rise in global warming have caused widespread of sand-flies and measures of surveillance and controls are less emphasised than required (Dujardin et al., 2008). The increasing problem of vector control, emerging drug resistance and hospitalisation expenses amongst other factors demand the need for novel therapies for the treatment of diseases caused by the parasitic protozoa. Also, increased cost, poor accessibility to disease affected areas and emergence of drug resistance have necessitated the need for new and better drugs.

Therefore, greater understanding of the metabolic cues required for the survival of the parasite within the host system could accelerate the discovery of novel targets for desperately needed anti-parasitic drugs (Tiuman et al., 2011, Monge-Maillo and Lopez-Velez, 2013, Croft and Coombs, 2003, Ameen, 2010). Propagation of the *Leishmania* within the host depends upon the various environmental niche encountered and critically on the nutrient availability within the host system. Mapping the metabolic requirements during the life cycle of the parasite would highlight parasitic specific metabolic pathways that could serve as potential drug targets. Hence, metabolomics of promastigotes cultured in in-house developed defined medium at various time points was used in this study to deciphering the same.

1.6 Metabolomics

High throughput "omics" technologies help in analysing complicated biological systems by a holistic approach. These methods examine the interacting elements of the different biological entities in a global manner. Using omics technologies, a particular hypothesis of the experiment could be examined to derive a vast amount of data revealing new scientific insights that would have been previously inconspicuous. The most challenging aspect of high-throughput techniques is that each analytical platform is best chosen depending upon the research question; and subsequent integration of data from multiple platforms caters to more holistic view than a single technique alone (De Souza et al, 2006, Karimpour et al., 2016).

Metabolomics has been defined as study of diverse nature of small molecules constituting the metabolic composition of a cell or biofluid; within a range of molecular weight of less than 1500Da (Oliver et al, 1998, Lindon et al; 2003). Metabolomics evaluates molecules that arise due to enzymatic processing within single cells and forms a subset of metabonomics (Raamsdonk et al; 2001). A broad range of information can be captured; for example, about the level of metabolites consumed by the system but also provides relative quantitative information about the metabolites produced by the organism (Cuperlovic-Culf et al., 2010). Both diagnosis and treatment of leishmaniasis can be vastly developed by applying high-throughput techniques such as metabolomics (Vincent et al, 2012; Saunders et al; 2011, Creek et al; 2014).

Some of the strategies of metabolomics have been listed below as follows:

- **Targeted metabolomics** involves a priori knowledge about particular metabolite(s) of interest with tailored extraction and optimisation protocols. This technique is mostly followed to obtain quantitative information about the metabolites of interest. For example, recent advances in the diagnosis of inborn errors of metabolism have been shown to have employed targeted metabolomics to derive specific information about acylcarnitines (Scolamiero et al, 2015). Stable isotope labelling is based on targeted metabolomics which allows for heavy stable molecule incorporation for tracing metabolic pathways of interest and flux monitoring.

- **Untargeted metabolomics** allows relative changes of metabolites between comparative samples to be gain new insights on the system of interest. A particular study with samples from patients with crohn's disease compared to healthy individuals revealed differentiating metabolites in the synthesis of bile acids, arachidonic acid attributing the contribution of gut microbiota to the disease status of the host (Hisamatsu et al, 2012).
- **Metabolite profiling** is based on untargeted metabolomics aimed to obtain maximum coverage of the metabolome of the system of interest. Often multiple analytical platforms with complementing extraction procedures are used to achieve the same. Human plasma metabolomics is a typical example which has been extensively studied combining different platforms due to the complexity of the mixture and importance of the wholesome information required for practical purposes (Noguchi et al, 2006, Capacci et al, 1984, Saiki et al, 2013, Cui et al, 2017).
- **Metabonomics** refers to study of endogenous and exogenous metabolites of dynamic or static biological fluids with particular emphasis to extract molecular information (Lindon et al; 2003). Analytical platforms such as NMR and mass spectrometers have been used for the study of metabolites in biological fluids. NMR as an analytical platform provides more quantitative data; whilst mass spectrometer provides more broad comprehensive coverage of metabolites with minimal sample preparation steps. Particularly, LC-MS offers more advantages for broad coverage of metabolites without the need for volatilisation, derivatisation, particular feature selection which may be required for gas chromatography-mass spectrometry sample preparations (Nicolson et al; 1989). Bio-fluids such as urine and plasma were analysed by H-1 based NMR metabonomics and metabolites such as L-Arginine, succinate, 3-hydroxybutyrate, alpha-ketobutyrate and L-Valine were indicated as biomarkers after validated

using pepsin activity and ROC analysis for chronic atrophic gastritis (Cui et al, 2017).

- **Metabolite finger-printing** has been used mostly for intracellular samples, for example, studies to measure the effect of salinity on tomato fruit cultivation allowed classification of salt treated from control fruits. Metabolite finger-printing technique allowed to precisely map the identification of functional groups such as nitrile containing compounds and amino radicals in the spectra as an important response to salinity compared to normal conditions (Johnson et al, 2003).
- **Metabolite foot-printing** involves the analysis of metabolites in the extracellular environment of the system of interest. Thus, metabolite foot-printing acts as a dynamic reflection of the intracellular activity since biological systems function under the principles of homeostasis and any change due to external stimuli such as temperature, pH or genetic/drug perturbations can be monitored non-invasively (Behrends et al., 2009, Allen et al., 2003, Palmer et al., 2007).

Metabolomics has been applied in the field of parasitic protozoa for drug discovery, biomarkers, novel metabolic pathways, etc. Earliest studies of metabolomics in *T. brucei* belonging to kinetoplastida dates back to Mackenzie et al, 1983, with the tracing of anaerobic glycolysis using [U-^{13}C] glucose by NMR studies (Mackenzie et al., 1983). Similar studies of [U-^{13}C] glucose incorporation in *Leishmania* promastigotes (Rainey et al., 1991, Saunders et al., 2011) has provided many insights on glucose metabolism. Metabolomics has been useful technique to unravel drug mode of action, for example, the mechanistic action of the anti-parasitic drugs eflornithine through the polyamine pathway against trypanosomiasis was elucidated using a metabolomics approach (Vincent et al., 2012), wherein the level of ornithine accumulated and downstream concentration of putrescine decreased in treated cells compared to untreated cells. The changes of the metabolites provides holistic phenotypic insights of the system as the metabolite levels reflect the dynamic changes of the underlying proteomic and genomic expression.

With improvements in high end analytical platforms and advances in mass spectrometry; targeted metabolomics with heavy stable isotope incorporation into the culture medium has been used for tracking metabolic pathways of interest and also for quantification of metabolites in *Leishmania* (Chokkathukalam et al., 2013, Saunders et al, 2014, Westrop et al, 2015). Using ^{13}C NMR, labelled carbon tracing in $H^{13}CO_3$- and succinate, acetate, and L-Alanine as partially oxidised end products confirmed the existence of succinate fermentation pathway. Also, the *Leishmania* specific metabolic pathway for the conversion of acetyl-CoA to acetate via the mitochondrial acetate: succinyl-CoA transferase unique to Kinetoplastida was uncovered using metabonomics (Rainey et al., 1991).

Data analysis plays a crucial role in the interpretation of results from metabolomics experiments (Tikunov et al., 2005). Apart from the univariate and multivariate analysis for clusters and patterns within the data, information from metabolomics experiments are visualised in the form of metabolic pathways. Discovery of novel metabolic routes or critical nodes within individual metabolic pathways unique to the system of interest is best suited as potential drug targets within pharmacological research (Vincent et al., 2012).

The main goal of this study was to capture information about the amino acid requirements of *Leishmania* parasite required for the growth and development during the promastigotes stages. This would allow highlight those essential amino acid pathways that could be useful as potential drug targets. Amongst the different methods of metabolomics; untargeted metabolomics proved to be promising strategy for this study. This would allow prediction of metabolic pathways directly based on dynamic unbiased metabolomics data unlike inference obtained from gene pathway correlations. The important techniques employed in this study were metabolomic finger printing and foot printing techniques according to protocols described in Chapter 2.

Metabolic finger printing was conducted with log phase cells grown in defined medium. This first step was carried out at this one particular time point to understand the dynamic intracellular composition in the most active growth phase at log stage. Thus, the captured snapshot of molecular information gave significant insights about the defined medium composition used for *in vitro* culture and also, allowed to differentiate metabolites derived from the parasite. This has been further analysed using unbiased network mapping to gain new insights about the amino acid metabolic pathways as described in Chapter 5.

The metabolic foot printing technique was conducted in time course manner to interpret the dynamic state of the medium at various stages of the parasite growth. Changes in metabolite levels allows detailed analysis of uptake of environmental constituents of defined medium in culture; which has been referred to as the depletion profile and also the secretion of metabolites by the cells referred to as the exometabolome described in chapter 5 and 6. This allowed the amino acids to be evaluated both for the relative rates of uptake/secretion and to integrate with the knowledge of amino acid essentiality as derived from the growth assays. Finally, this approach was used to classify amino acids based on utilisation of *Leishmania* and highlight those essential pathways that have greater potential as new drug targets over other less dispensable pathways as discussed in Chapter 5, 6 and 7.

1.7 Development of *in vitro* culture medium for metabolomics

Study of small molecules using metabolomics techniques generates a vast amount of data that could provide holistic information of the biological system of interest. Data analysis and interpretation within the biological context requires careful filtration of background noise and signals occurring at the base line of the experiment. Previously, *in vitro* culture of *Leishmania* has been based in elaborate medium compositions with additional supplementation of undefined serum up to various concentrations explained in Chapter 1. Results from the metabolomics experiments provide snapshot of metabolism under conditions tested. It has been rightly described by Kell et al (Kell et al., 2005) that results for metabolomics rely on the composition of the *in vitro* medium used for culture of the organism. In this study, *Leishmania* metabolism had been reported using unbiased mapping of metabolic finger-printing and foot-printing of *L. mexicana* promastigotes in defined media not been reported before. Untargeted metabolic finger printing for tracing parasitic specific metabolic pathways was carried out to highlight as potential parasite specific pathways as drug targets as shown in Chapter 5.

Minimizing the metabolites in the defined medium allowed for a significant decrease in the background signals in high throughput LC-MS experiment. In turn, leads to pronounced changes in relative levels of metabolites during the growth of the parasite in the defined medium. This allowed deriving snapshots of metabolic capabilities of the parasite and aid in unbiased metabolic mapping as described in Chapter 5 and 6. It opens new venues for hierarchal visualisation of the metabolic maps and could potentially be used to integrate dynamic information about underlying genes and protein expression in a qualitative and quantitative manner within genome scale and kinetic models in future research (Zech et al., 2013).

Metabolic foot-printing allowed to determine nutrient salvage pathways throughout the growth of *L. mexicana* promastigotes and elucidation of the changing exo-metabolome in time resolved manner reflecting the intracellular activities as shown in Chapter 6. Efforts have been made isolate and characterise small molecules enriched in the spent media of the defined media by biochemical and functional analysis as shown in Chapter 6.

1.8 Overview of *Leishmania* metabolism

Nutrients salvage by the parasite depends upon many factors such as competition for available nutrients with the host system, regulated expression of transport proteins, and enzymatic repertoire of the parasite to metabolise the nutrients to high energy intermediates (Mcconville and Naderer, 2011). Nutrients can be broadly classified as macronutrients containing the carbohydrates, lipids and amino acids/proteins and micro nutrients including metal salts and vitamins. Nutrients together contribute to energy, the fundamental driving force of living organisms for viability, growth and proliferation. Energy is obtained from the efficient use of all of the available nutrients in the immediate environment. As a parasitic protozoon, *Leishmania* during the life cycle encounters the insect and vertebrate hosts as their immediate environment with pronounced differences in nutrient levels determined by host conditions, pH and temperature. However, the ability of the parasite to salvage nutrients from the host system is critical for the transmission and infection to a new host, disease manifestation and central component of pathogenesis. In this study, efforts were made to study the nutrient salvage by *L. mexicana* promastigotes to highlight parasite specific metabolic routes as drug targets.

Perturbation of permeases responsible for critical nutrients has been reported as drug targets (Landfear, 2011, Dean et al., 2014). Few of permeases involved in import of certain nutrients such as purines (Ortiz et al., 2010), hexoses (Naula et al., 2010, Burchmore et al., 2003), iron (Wilson et al., 2002), polyamines (Colotti and Ilari, 2011) and amino acids transporters of L-Arginine (Shaked-Mishan et al., 2006), L-Lysine (Inbar et al., 2012), L-Proline/L-Alanine (Inbar et al., 2013) and L-Glutamate (Paes et al., 2008) in *Leishmania* have been well studied. Genome sequencing have accelerated the identification and functional characterisation of these permeases. However, genome sequences alone have not been able to predict the functional diversification and changing permease activity to a broad range of substrates adaptive to the dynamic environment encountered during their life cycle in *Leishmania* parasitic protozoa (Dean et al, 2014).

Here, using untargeted metabolomics in defined medium, unbiased insights about nutrient salvage of *L. mexicana* promastigotes throughout their growth have been reported. Both intracellular and extracellular metabolomics reported as changes from the naïve medium without cells as base line in Chapter 5 and 6. In this study, special emphasis has been placed on amino acids in relation to other nutrients metabolism in *L. mexicana* promastigotes.

1.8.1 Amino Acids

Amino acids make up the fundamental building blocks for proteins required for many different biological processes. *Leishmania* parasites have been reported to possess well adapted mechanisms to suit different nutrient environments conserved through evolution. The regulated expression of nutrient transporters and enzymes of metabolic pathways differs depending upon the growth stages of the parasites within the host system (Landfear, 2011). Disruption of the metabolic pathways will block the biosynthesis/catabolic process essential for parasite viability and transmission and lead to novel treatment therapies against diseases caused by parasitic protozoa (Dean et al, 2014).

Glucose is the primary source of energy for promastigote thriving within the sugar rich conditions of the midgut of the sandfly host; however, amino acids serve as their major carbon source in the scarcity of carbohydrates. This has been elucidated with previous results reported by our group (Burchmore et al., 2003, Akpunarlieva et al; 2017) in glucose transporter knock out promastigotes show an increased amino acids uptake compared to wildtype.

Amino acids are essential for the viability, growth and proliferation of *Leishmania* promastigotes (Hart and Coombs; 1982, Opperdoes and Coombs; 2007, Simon et al., 1983). Perturbation of specific amino acid pathway could lead to loss of viability and parasite development within the host system. However, identification of specific amino acid pathway as a drug target must fulfil certain considerations such as essential for viability, unique target metabolic steps not homologous to the host system and specificity of target metabolic steps of interest (Vincent et al, 2012; Creek et al, 2014). Previous classifications of amino acid essentiality was based on the studies in *L. tertentolae* which is lizard parasite (Krassner and Flory, 1971) and *L. donovani parasite which* causes visceral leishmaniasis (Steiger and Steiger, 1977). In this study, systematic investigation of amino acids important for the viability of the parasites has been conducted by growth analysis in *L. mexicana* known to cause cutaneous leishmaniasis by defined medium development as reported in Chapter 4. Furthermore, individual metabolites of amino acid pathways have been mapped (Chapter 5) and data on relative changes of metabolites during the different growth stages have been elucidated (Chapter 6).

In previous studies, L-Proline has been shown as the prime source of energy in glucose deprived condition supplementing the production of L-Methionine, L-Alanine, L-glutamic acid, L-isoleucine and L-aspartic acid in *Leishmania* promastigotes (Simon et al., 1983, Zilberstein and Gepstein, 1993, Bringaud et al., 2012, Burchmore et al., 2003). Also, L-Aspartate has been shown to contribute significantly to the carbon pool other than glucose by heavy stable isotope metabolomics (Saunders et al., 2011). Other amino acids such as L-Arginine has been of interest owing to its contribution to the *Leishmania* specific polyamine pathway (Darlyuk et al., 2009, Westrop et al., 2015, Shaked-Mishan et al., 2006, Colotti and Ilari, 2011), whilst L-Arginine in host cells functions to regulate iNOS production for clearing the parasitic burden and for the activation of the immune system (Wanasen and Soong, 2008, Goldman-Pinkovich et al., 2011). Also, L-Arginine is noted for phosphoinositide phosphates synthesis which are major players of lipid membrane dynamics of the phagolysosome and membrane lipid organisation (Wanasen and Soong, 2008). Thus, L-Arginine metabolism has been reported as one of the amino acids of interest for drug target (Wanasen and Soong, 2008, Shaked-Mishan et al., 2006, Kandpal et al., 1996). However, comparative investigation of all amino acids systematically in *L. mexicana* promastigotes under identical conditions has not been reported before, which has been the prime focus in this study.

Studies on amino acid requirements of other intracellular obligate pathogens, e.g.; *Mycobacterium leprae* have shown that the pathogens alters the degree of proteolysis and rates of acidification within the macrophages (Podinovskaia et al., 2013). A significant reduction in intra-phagosomal lipolysis allowing host lipids to be a potential source of nutrients for *Mycobacterium* within the macrophages was demonstrated. Metabolomics studies in *Leishmania* showed that amastigotes within macrophages exhibited more quiescent metabolism, with a shift of nutrient utilisation from glucose to lipids (Saunders et al., 2014). Geraldo et al characterised the *L. amazonensis* gene (La-PAT1) encoding a putative amino acid transporter by screening a probable list of sequences from the genomic library. The functional clone was validated by submitting the translated coding sequence to the GenBank protein database. They found that this particular gene is conserved within the Kinetoplastida family of parasites. Northern blot results of the genomic DNA revealed that La-PAT1 was upregulated in amastigotes. Interestingly, this gene belongs to the AAAP (Amino Acid/Auxin Permease; TC 2.A.18) family which is H^+/amino acid symporters required to maintain pH homeostasis (Geraldo et al., 2005), vital for parasite survival in the host system. Also, the exchange of amino acids is crucial in maintaining osmolality (Blum et al; 1996) both in promastigotes and amastigotes and pH homeostasis within the host system.

1.8.2 Amino acids metabolism linked to carbohydrate metabolism

Broadly, both amino acids and carbohydrates are metabolised via the TCA cycle leading to oxidative phosphorylation for energy generation. Different amino acids follow different metabolic pathways in mammalian systems culminating in various TCA cycle intermediates as follows: L-Arginine, L-Glutamine, L-Histidine, L-Proline undergoes transamination to L-Glutamate and alpha-ketoglutarate, while isoleucine, L-Methionine, L-Threonine, L-Valine broken down to succinyl CoA. Others including L-Alanine, cysteine, glycine, serine, L-Threonine, and L-Tryptophan to pyruvate. Aromatic amino acids such as L-Phenylalanine, L-Tyrosine to fumarate and L-Asparagine, L-Aspartate to oxaloacetate. Oxaloacetate is converted to phosphoenol pyruvate leading to glucose production via gluconeogenesis. Amino acids are classified as glycogenic and ketogenic, while the former can be converted to glucose; the latter amino acids are degraded directly to acetyl-CoA. Ketogenic amino acids such as isoleucine, L-Leucine, L-Threonine, L-Tryptophan leads to acetyl CoA and L-Leucine, L-Lysine, L-Phenylalanine, L-Tryptophan, L-Tyrosine leads to aceto-acetyl-CoA converted to citrate in the TCA cycle (Lehninger Principles of Biochemistry, Cox and Nelson).

Acetyl CoA to acetate and ATP is unique pathway occurring in *Leishmania*. The presence of unique enzyme acetyl: succinate CoA transferase (ASCT) involved in succinyl-CoA and succinate conversion to acetyl CoA to acetate and ATP adds further complexity in the link between carbohydrate and amino acid metabolism in *Leishmania*. Interestingly, ketogenesis is a process that is triggered in locations where there is a lack of glucose and increase amino acids/fatty acid oxidation for energy generation, leading to increase in accumulation of acetyl-CoA. The acetyl-CoA so formed leads to ketone bodies such as acetoacetate and beta-hydroxybutyrate, increase in the level of ketone bodies causes a drop in pH as they are highly acidic in nature. Unlike mammalian cells which have cholesterol in the cell membrane; *Leishmania* have ergosterol like sterols forming the membrane domains. Acetyl CoA plays an important part for steroid biosynthesis. The first step involves the enzyme acetoacetyl-CoA thiolase; which links two units of acetyl CoA as substrate to form acetoacetyl CoA. Subsequent steps in the pathway lead to generation of sterols such as mevalonate and ergosterol highlighting the importance of acetyl CoA in steroids biosynthesis in *Leishmania* (Reithinger et al; 2007, Lepesheva et al; 2011). Acetyl-CoA in post translational modifications has been used in histone acetylation which changes gene expression and hence promotes proliferation (Wellen and Thompson et al; 2012). Acetylation and glycosylation have been suggested to be the key modulators regulating both cell signalling and metabolism (Hellemond et al; 1997).

Carbohydrates are mainly metabolised through glycolysis and the pentose phosphate pathway for energy generation and/or production of reducing equivalents (NAD/NADH), and precursors for nucleotides biosynthesis. There have been certain distinct differences reported between promastigotes and amastigotes life stages of *Leishmania* with respect to glucose metabolism (Meade et al., 1984). Glucose utilisation has been observed to be greater in promastigotes with the rate of glucose catabolism to CO_2 per number of cells was up to 10-fold higher than that of amastigotes (Hart and Coombs; 1982). Promastigotes exhibited optimal rates of glucose uptake at pH 7 while amastigotes were optimal between pH 4-5; Pro-1 gene encoding glucose transport in *L. enriettii* was upregulated in the promastigotes, while downregulated in amastigotes (Cairns et al., 1989). It has been observed that promastigotes exhibit approximately 10% higher activity of the glycolytic enzymes compared to amastigotes. This is in line with the physiological adaptation of the promastigotes to survive within the changing dynamic environment of the sand-fly gut.

It has been shown D-glucose transporter have similar affinity to glucose molecules in both promastigotes and amastigotes (Burchmore and Hart, 1995). However, the parasite transporter has been shown to have higher affinity compared to host cell glucose transporter, hence might serve as a valid drug target (Burchmore et al., 2003). Glucose transporter knock out parasites maintains viability by relying on alternative carbon sources as demonstrated by increased amino acids uptake using radiolabelled and heavy stable isotope metabolomics studies (Akpunarlieva et al, 2017). Mukkada et al (Mukkada et al; 1985) have shown experiments with amastigote suspensions incorporated with radiolabelled glucose and L-Proline. A significant proportion of labelled CO_2 from both glucose and L-Proline was observed. Thus, *Leishmania* exhibits a preference for both glucose and amino acids as a carbon source.

Interestingly, Rainey et al compared models of the axenic continuous culture of *L. pifanoi* promastigotes with amasitogotes using uniformly ^{13}C-labeled [U-^{13}C] glucose under aerobic and anaerobic conditions and reported a significant proportion of un-metabolised glucose in both life stage forms of *Leishmania*. Excess glucose is stored as glycogen in mammals, similar storage carbohydrates had been reported in *Leishmania* by Rainey et al, but the identity was not very clear from the NMR peaks; although some could be attributed to glycogen and trehalose. They found that the NMR peaks did neither resemble PO_4-6Gal (β1, 4) which is the repeating unit of lipophosphoglycan of *L. donovani*; nor does it belong to the major surface glycoprotein, gp63 (Rainey et al., 1991). Almost a decade later, evidence has been found for that the storage carbohydrate was beta 1-2 mannanoligosaccharides, a homopolymer with 4-40 residues constituting 80-90% of the cellular carbohydrate (Ralton et al., 2003).

Low glucose conditions triggered mannan catabolism suggesting a reserve function to sustain the parasite growth under extreme conditions. Stress activators like mild heat shock or heat shock protein-90 inhibitors have been shown to increase mannan levels by 10-25 fold (Ralton et al., 2003, Sernee et al., 2006). However, it was uncertain whether mannan was required for parasite differentiation and survival within the macrophages. Comparison of *L. major* null mutant for the gene fructose-1, 6, bisphosphatase; an enzyme which catalyses the final committed step converting fructose 1, 6 bisphosphate to fructose 6 phosphate in the gluconeogenesis pathway to wild type promastigotes cultivated in synthetic medium with glucose or glycerol showed higher levels of intracellular beta 1, 2-mannan; however, the FBP mutant had decreased level of intracellular mannan indicating that the FBP mutant was hexose limited. The FBP mutants show a rapid depletion of oligosaccharides, which confirms that gluconeogensis is an essential pathway, required for supplying the hexose requirements of *L. major* promastigotes. Also, similar rates of infection between wild type and FBP mutant parasites of host cells was observed indicating storage carbohydrates like mannan does not modulate infection level in the host (Naderer et al., 2006).

Research for the identification of key molecules that modulate infection level in the host could bring new insights about potential drug targets; necessary to block transmission of the widespread diseases caused by these parasitic protozoa. It has been previously shown that the parasite abrogates host immune responses for its own replication (Dogra et al., 2007) and much has been centered around parasitic proteins that modulate host infection. However, the effect of small molecules to promote infection of *Leishmania* with host cells have not been reported much. Efforts in this study have been made to elaborate on the impact of amino acids and its metabolism on infection with host cells as reported in Chapter 6. Studies in other species, for example, anaerobic human microflora and aerobic pathogenic bacteria in septic patients have shown phenolic acids of microbial origin regulate oxidative stress contributing to the pathophysiology of the disease (Beleborodava et al; 2012). Patients suffering from malaria due to infections with *Plasmodium yoelii*, have shown that amino acids and amino acid derived intermediates could change the metabolic dynamics of host parasite interaction (Saiki et al., 2013).

1.8.3 Role of amino acids in nucleotides, NADPH and antioxidant biosynthesis

The genetic material of any organism is made of fundamental building blocks of nucleotides synthesised by the pentose phosphate pathway (PPP) to a large extent. Nucleotides, especially purines are imported from the host environment in *Leishmania* (Ortiz et al., 2010, Carter et al., 2001). The pentose phosphate pathway also contributes to other cellular processes such as the production of reducing equivalents in NADPH, the inter conversion of three and six carbon sugar phosphates to ribose-5-phosphate, in-turn used in pyrimidine biosynthesis demonstrated in *Leishmania*, and generation of erythrose-4-phosphate which acts as a precursor for aromatic amino acid biosynthesis (Wood, 1986).

Amastigotes have a greater turn-over of nucleotides probably facilitating the developmental switch from promastigotes. However, amastigotes have lower dividing rate, rather passive state, with lesser DNA compared to RNA. Mukkada et al have shown a rate of uridine incorporation to be greater than thymidine reflecting increased RNA synthesis (Mukkada, 1985). Amino acids not only contribute the nitrogen group for pyrimidines but also involved in regulation of cellular oxidative stress conditions to optimise nucleotide biosynthesis. For example, cysteine plays very important role in reducing oxidative stress within the cell. Cysteine is sulphur containing amino acid required for various biological processes within the system, but it could be of utmost importance to *Leishmania* because it contributes to thiols (glutathione, trypanothione) production required to survive against high oxidative stress within macrophages. The unique aspect about trypanosomatids is their dual ability for de-novo synthesis by the assimilatory route and also trans-sulphuration pathway for cysteine synthesis (Sanderson et al., 2000). Proteome profiling of axenically differentiated amastigote life stage of *L. panamensis* in comparison to promastigotes by two-dimensional electrophoresis (2DE) in neutral pH revealed upregulation of cysteine proteinase suggesting the importance of this enzyme for the amastigotes (Walker J et al., 2006).

There have been other studies emphasising the importance of the pentose phosphate pathway (Barrett, 1997, Cronin et al., 1989, Funayama et al., 1977) as an important NADPH source and also an instance of increased expression of pentose phosphate shunt enzyme, 6-phosphogluconate dehydrogenase in *L. infantum* mutant as an adaption to nitric oxide stress (Moreira et al,2014).

Maugeri et al characterised each enzyme of the pentose phosphate pathway for *L. mexicana* promastigotes. They subjected the cells to oxidative stress by methylene blue and found an increased proportion of radiolabelled glucose contributing to the PPP. They also showed that free ribose can be taken up more efficiently through a carrier mediated process and the presence of ribokinase activity was also found in the cells. These results suggest that a high build-up of reducing equivalents such as NADPH required for the survival of the parasites within the host system and regeneration of cellular antioxidants to combat oxidative stress encountered by parasites (Maugeri et al., 2003).

In this study, efforts have been made to understand the role of amino acid metabolic pathways and antioxidants that could facilitate parasitism within host cells as shown in Chapter 6.

1.8.4 Amino acids profile as diagnostic index

The amino index has been used as a diagnostic marker for detection and monitoring of disease progression and treatment. For example, studies on amino acid profiling between cirrhotic patients and control subjects have postulated amino acid index as ratio of concentrations of taurine, citrate, L-Methionine and L-Arginine over the pooled concentration of serine and L-Leucine as an additive component to ratio of pooled concentration of L-Phenylalanine and ornithine by the pool of L-Glutamate and L-Tryptophan in studies related to liver injury (Capacci et al., 1984). Liver cirrhosis has been associated with abnormal L-Methionine metabolism reported in the 1950s, however, it is only recently that amino acid concentrations have been used to investigate the underlying gene expression. The rate of clearance of L-Methionine pool in cirrhotic patients was found to be slow due to low activity of the enzyme L-Methionine adenosyltransferase (EC 2.5.1.6) responsible for the conversion of L-Methionine to S-adenosyl-L-Methionine (Ramani et al, 2011). Abnormalities of the urea cycle utilise citrate and ornithine concentrations as markers for diagnosis (Machado et al, 2014). Fischer's ratio between the branched chain amino acids and aromatic amino acids have been used to differentiate fibrosis (Ishikawa et al, 2012). A recent study showed the novel combinatorial algorithm to generate an amino acid index based on molar ratios to discriminate diabetic rat models from nondiabetic rats (Noguchi et al., 2006). This kind of diagnostic profile has been less studied in infection related cases. A recent study on amino acid profiling referred to as aminogram has been reported as new diagnostic markers for *Plasmodium falciparum* infected blood as a method for disease detection (Saiki et al., 2013). The use of amino acid profile in all potential combinations could be used to harness data to advance biomedical and nutritional investigations. The first step in this direction as being taken in this study by amino acid profiling in serum and protein free defined medium of *L. mexciana* promastigotes in a culture. The knowledge from this study also allowed deeper insights about the requirements of extracellular nutrients and metabolism in *L. mexicana* promastigotes in a controlled environment for the proposal of novel drug targets.

1.9 Aims and objectives of this study

Genome sequencing has accelerated the identification and characterisation of various nutrient transporters that could serve as drug targets (Dean et al., 2014, Landfear, 2011). However, diverse metabolic capabilities of the parasite demand novel approaches to understanding the assimilation and metabolism of the broad range of nutrients by these parasites. In this study, a novel approach has been made for a detailed understanding of unbiased mapping of *Leishmania* metabolism in a chemically defined medium to derive new insights about the physiological adaptations occurring during its life cycle. Hence, the aims were set as follows:

- To develop serum and protein free defined medium for *in vitro* culture of the insect stage of the parasites.
- To evaluate the importance of amino acids for parasite viability.
- To identify and highlight *Leishmania* specific amino acid pathways which could serve as a potential drug target.

The key objective was to elucidate utilisation of important nutrients in human infective species, *L. mexicana* promastigotes as a model organism. This was conducted by development and establishment of chemical defined media by testing individual components and their concentrations required to support viability and growth of *L. mexicana* promastigotes in culture. Furthermore, single amino acid knock out media customised to 20 different amino acid conditions were analysed for protein quantification, energy determination and morphometric studies. Nutrient utilisation was inspected using metabolic finger-printing and metabolic foot-printing at different growth stages of the life cycle to highlight unique metabolic routes as drug targets. For the first time, exometabolome of *Leishmania* in defined medium were isolated and characterised using biochemical assays. These results demonstrated the unique role of certain amino acid intermediates in the establishment of infection with host cells; and potentially modulates the parasite and host interaction dynamics during infection.

Chapter 2 Materials and Methods

2.1 Cell culture of *Leishmania* promastigotes

Promastigotes of *Leishmania mexicana* (MNYC/BZ/62/M379) were derived from amastigotes of mouse lesions and stabilates were created and maintained. Promastigotes only within few passages (5 passages maximum) from stabilates were used for growth analysis and metabolomics experiment. Mid log phase parasites were sub-passaged thrice in a week into 5 ml of HOMEM prepared according to (Berens et al., 1976) supplemented with 10% (v/v) heat-inactivated foetal calf serum (FCS), 1% penicillin-streptavidin and maintained at 27^{o}C, pH 7.4. Initial parasite concentration was 5 x10^{5} cells / ml. Parasites were grown until mid-log phase (5 X 10^{6} cells/ml) about 3-4 days from the day of culture initiation and passaged in 1:10 dilution subsequently into fresh medium. Promastigotes were cultured in commercial HOMEM (Invitrogen, Paisley, Scotland) supplemented with 10% (v/v) heat inactivated-foetal calf serum (FCS, example supplier Biosera, Ringmer, UK). HOMEM was also prepared in the laboratory following the protocol from Berens et al; 1976. The routine culture was carried out using vented culture flasks (25 cm_2 Corning).

For all the growth analysis experiments, cultures were initiated in triplicate and growth was monitored in appropriate media (REIX/BM/NM/DM as explained in 2.3). 5 X 10^{6} cells /mL of promastigotes from mid log phase (day 4) of the culture were collected in sterile test tubes and subjected to centrifugation to about 1000 g and the supernatant discarded. The cell pellet was briefly washed with appropriate media with 1000 g slow acceleration and slow deceleration prior to re-suspending in the media to an appropriate volume such that starting density of promastigotes at 5 X10^{5} cells/mL for growth analysis experiment. Viability and integrity of the cells were assessed using the trypan blue dye exclusion test. Samples from the culture flask were diluted at 1:1 ratio and assessed by manual examination under a microscope for the number of cells that appeared blue in colour (non-viable) amongst the total number of cells counted. Only culture flasks with more than 98% viability were considered for further experiments. Growth monitored after fixing cells in 2% formaldehyde in PBS by counting cell numbers with an improved Neubauer haemocytometer.

2.2 Creating and maintaining stabilates record

L. mexicana promastigotes from the clonal population were preserved routinely by the creation of stabilates of cells in mid-log phase 1:1 (v/v) of a mixture of 80% culture media and 20% glycerol to confluent cells at a density of 1 X 10^6 cells/mL. The cryovials were wrapped in cotton wool and stored overnight at -80°C, subsequently transferred to liquid nitrogen for long term storage and appropriate placement of the vials recorded.

2.3 Preparation of Defined medium

Stock solutions of individual components (example supplier-Sigma Aldrich) were prepared and the REIX composition (Steiger and Black, 1980) was modified accordingly as stated in the results section Table 3-2. Briefly, stocks of salts including sodium chloride, potassium chloride, sodium phosphate monobasic dehydrate and sodium pyruvate were prepared in 4X concentration. To the required salt concentration, sodium bicarbonate and HEPES were added directly before use. Individual amino acids, L-glucose, adenosine and hemin were added from pre-filtered stocks to the aliquots immediately before use. Vitamin mixture containing choline chloride, D-calcium, pantothenate, nicotinamide, pyridoxal hydrochloride, thiamine hydrochloride, myo-inositol, biotin at concentrations specified in Table 3-2 were added from pre-filtered individual stocks for growth tests and commercial source (example supplier-Sigma Aldrich- B 6891) for defined medium preparation. Individual cofactor stock solutions (1mM) of folic acid, riboflavin, biotin, lipoic acid, Biopterin and para-amino benzoic acid dissolved in 1N sodium hydroxide solution and added at required concentrations from pre-filtered stocks for growth tests. Individual metal stock solutions (1mM) of magnesium septa-hydrate, calcium chloride, iron (III) nitrate nona-hydrate, zinc chloride, manganese chloride and cobalt chloride was dissolved in water with drop with concentrated acid or alkali added from the side of the tubes for complete dissolution. Cofactors and metals with concentrations specified in the medium composition were added as cocktail during medium preparation. The pH of the medium was adjusted to 7.4, the medium was filter sterilised using 0.22 mm (Millipore filter unit) and stored in aliquots. All components from Sigma Aldrich unless otherwise mentioned. Concentrations of individual components of Base Medium (BM), Nayak Medium (NM), Single amino acid knock out media (NM-specified amino acid), Nayak minimal media (NMM) and Defined medium (DM) are as listed in Chapter 3, 4, and 5.

Promastigotes were grown in HOMEM for 4 days prior to inoculation. The cells were centrifuged at 1000 g for 10 min. The cell pellet washed with BM twice and starting cell density adjusted to 5 x 10^5 cells/mL. A metal mixture of magnesium, calcium, zinc, iron, copper, manganese and cobalt were tested at various orders of magnitude each at 0.5mM, 0.05mM and 0.005mM. REIX medium was prepared according to Steiger et al, 1980 (Steiger and Black, 1980) and the relative importance of individual amino acids, co-factors and metals were tested by omitting each one from the medium composition. Growth analysis monitored as stated above and doubling time of cells calculated with co-factors tested were biopterin, folate, PABA, lipoic acid, riboflavin and metal salts of magnesium, calcium, zinc, iron, manganese, copper and cobalt both individually and in combination.

2.4 Image analysis

For studying the impact of individual amino acid on the cell morphology, cell body length of promastigotes grown in single amino acid knock out media was assessed by Giemsa staining as described by Bates et al 1993. Briefly, aliquots from day 6 of the culture were smeared on glass slides and air dried. The cells were fixed using absolute methanol and slides submerged in 10% Giemsa in 10mM phosphate buffer at pH 7.2. The slides were examined under a Zeiss Axiovision upright light microscope using bright-field. Images captured on an AxioCam MRm camera and a scale bar of 10μm bar was used to measure the cell body length of promastigotes cultured in single amino acid knock out media. For statistical significance, cell body length measurements of the several pairs of populations in different amino acid starved and replete conditions were measured using Fiji-ImageJ software and plotted as their frequency distribution.

2.5 Evaluation of Defined Medium using infectivity test

The mononuclear cell line, THP1 was used for testing the infectivity of cells grown in DM according to the protocol to Jain et al, 2012 with slight modifications. Briefly, THP1 cells were cultured in RPMI 1640 (Gibco, Life technologies) plus 10% FCS with a starting density of $5x10^5$ cells/ml. These cells were sub-passaged in 1:5 dilutions every five days. The viability of the cells was tested using trypan blue (Sigma) exclusion test (Dutta et al., 2005). Briefly, 0.4% trypan blue solution (3:1 ratio vol/vol) were added to each well containing macrophages and assessed microscopically using haemocytometer. The stained cells were counted as dead cells and percent viability of more than 98% were considered for further experiments of infection with *L. mexicana* promastigotes.

THP1 cells were plated on chamber slides for 3 days at 37 ^oC at 5% CO_2 and differentiated using 100nM PMA (phorbol myristate acetate) 24 hours prior to infection. Promastigotes were prepared at 10^6 cells in NM/HOMEM after careful consideration of cell numbers in HOMEM serially diluted two fold to recover a similar percentage of metacyclics on day 6 from the start of culture initiation.
For infectivity test, the macrophage monolayers were overlaid with 1:10 ratio with 5×10^6 cells of *L. mexicana* grown until stationary phase (Day 6 from the start of the culture initiation) in either medium containing HOMEM or NM. The cells were incubated for 4, 24, 48, 96 and 144 hours at 37^oC in 5% CO_2. The wells were then washed thrice with PBS to remove unbound promastigotes at various time as specified in figure legends. The cells in the chamber slides were fixed by brief treatment using ice cold methanol and air dried. Alternative chambers were treated with DAPI for nuclear staining (Sigma Aldrich) or Giemsa stain for cell body length staining (Sigma Aldrich) for 20 minutes and sealed with a coverslip. The slides were visualised using a light microscope (Axiovision) and analysed using Fiji-Image J software. The number of infected macrophages was based on counting an average of 100 macrophages and the equation used to calculate is as follows:
Number of amastigotes/100 THP1 cells= (Number of amastigotes nuclei counted/Number of THP1 nuclei counted) * 100

Also, the percentage of a total number of infected macrophages were compared between NM or HOMEM media conditions.

2.6 Alamar blue assay

Alamar blue assays developed by Raz et al assess the toxicity of drugs on the viability of the cells (Raz et al., 1997). Required drugs for testing were prepared in appropriate medium (HOMEM/NM) at twice the maximum concentration tested. The first well of the 96 well micro-titre plate (Corning) were added with 200 µL of the drug. To the remaining wells, 100 µL appropriate media were added. The drug in the first well was serially diluted at 1:2 ratio across 10 wells, leaving the last wells drug free. Cells from log phase in serum containing rich medium were counted using haemocytometer and diluted to $5x10^5$ cells/ml with fresh medium and added to the plate to a final volume of 200µL per well. Cells incubated for 48 hours at 37 °C, 5% CO_2, followed by addition of (20µL of 10% of sample volume) 0.49mM resazurin (Sigma) in 1 X PBS, pH 7.4 and incubation for another 24 hours. Fluorescence was measured on a Pherastar spectrometer (BMG Labtech), with excitation wavelength of 544 nm and emission wavelength of 590 nm.

2.7 Growth in single amino acid knock out media

For studying the amino acid requirements of *Leishmania mexicana* promastigotes, single amino acid “knock out” media, containing 0.5 mM of all 20 proteogenic amino acids bar one, were prepared. *L. mexicana* promastigotes were cultured in complete HOMEM medium for 4 days prior to the start of amino acid starvation conditions. Cells were collected by centrifugation at 1000 g for 10 minutes. The pellet was washed by a quick spin by centrifugation to remove any traces of HOMEM medium with defined medium lacking all amino acids referred to as NM-AA and re-suspended in NM-AA. This was used as an inoculation media for 20 mL/flask in triplicates of single amino acid knock out medium such that the starting cell density set to 10^6 cells/ml. The integrity of the cells was assessed by trypan blue dye exclusion test and cultures were only considered for counting with more than 98% viability. Parasite growth was followed daily for 9 days by diluting a 0.01mL aliquot 50X with cold 2 % (w/v) formaldehyde-PBS and counting using improved Neubauer haemocytometer and growth curves plotted for the calculated of doubling time (hours). HOMEM, NM and NM-AA (no amino acids) were treated similar inoculation as single amino acid knock out media to assess the effect of the absence of each amino acid on the growth of the promastigotes. Further reductions in the number of amino acids were prepared by modification of NM as appropriate provisionally referred to as Nayak minimal medium as stated in Chapter 4. Data were derived from several independent assays (n=9) each carried out in triplicates. All statistical analysis was carried using Graph-pad Prism software with significance threshold set at $P<0.0001$ between comparisons, using one way ANOVA with Dunnett's multiple comparison tests.

2.8 Protein determination in single amino acid knock out media

L. mexicana promastigotes were cultured in complete HOMEM medium for 4 days prior to the start of amino acid starvation conditions. Cells were collected by centrifugation at 1000 g for 10 minutes. The pellet was washed by a quick spin by centrifugation to remove any traces of HOMEM medium with Nayak medium lacking all amino acids referred to as NM-AA and re-suspended in NM-AA. This was used as inoculation media for 20 mL/flask in triplicates of single amino acid knock out medium such that the starting cell density set to 10^6 cells/ml. The integrity of the cells was assessed by trypan blue dye exclusion test and cultures were only considered for counting with more than 98% viability. Subsequently, 10^7cells were collected on day 6 of single amino acid knock out media (NM-and suspended in ice cold lysis buffer in PBS containing triton (0.05%), Glycerol (5%), NaCl (150mM) and cocktail of protease inhibitors containing (1,10,Phenanthroline (2mM), Leupeptin (10µM), Pepstatin (7µM) and E64 (10µM) where are compatible with Bradford reagent (from the manufacturer's manual, example-Biorad) and cell lysed by brief pulses of sonication on ice. Bradford protein assay was used to determine the amount of protein extracted from an equal number of cells recovered from single amino acid knock out media. 96 well flat bottom plates were used to test protein concentrations of the sample in different dilutions. Briefly, serial dilution of BSA was used as standards (1.0, 0.5, 0.25, 0.125, 0.06, 0 mg ml^{-1}) prepared in the same lysis buffer, diluted 1:5 with Bradford reagent simultaneously added to the standards and samples. The plates placed on the rotating mixer for 15 min at room temperature and absorbance measured at 595 nm. Simple linear regression was used to determine protein concentration in the samples. Results were derived from three independent experiments (n=9) each performed in triplicate.

2.9 Acetate Assay

Sample preparation for secreted acetate determination was carried out as follows: Briefly, *L. mexicana* promastigotes were cultured in complete HOMEM medium for 4 days prior to the start of amino acid starvation conditions. Cells were collected by centrifugation at 1000 g for 10 minutes. The pellet was washed by a quick spin by centrifugation to remove any traces of HOMEM medium with either NM, NM-glucose or NM-AA and re-suspended in respective media. These were used as inoculation media for 20 mL/flask in triplicates for each of NM, NM-glucose and NM-specified amino acid in single amino acid knock out media respectively, such that the starting cell density set to 10^6 cells/ml. The integrity of the cells was assessed by trypan blue dye exclusion test and cultures were only considered for counting with more than 98% viability.

1 x 10^7 cells/mL were collected on day 6 from the start of culture initiation and centrifuged at 1000 g for 10 minutes and the supernatant transferred to pre-chilled test tubes on ice without disturbing the pellet. Acetate secreted in the extracellular medium by *Leishmania* promastigotes were quantified in the culture supernatant *of* NM, NM-glucose and single amino acid knock out media conditions according to the protocol from the manufacturer instructions (Sigma MAK086). Briefly, 50µL of the samples were taken into micro-titre plate (example supplier, Corning) were mixed with reaction mixture from the commercial kit prepared by mix of acetate assay Buffer (42 µL), Acetate enzyme mix (2 µL), ATP (2 µL), Acetate substrate mix (2 µL) and Probe (2 µL). ATP and NADH in the samples have been described to generate background signal; thus, sample blank without the addition of acetate enzyme mix was set up for individual conditions. The plate was placed on rotating shaker for 40 minutes of incubation time and absorbance measured at 450 nm using Pherastar spectrometer (BMG Labtech).

2.10 Sample preparation for metabolite finger-printing of intracellular extraction

L. mexicana promastigotes were inoculated at 5 X 10^5 cells/ml in 50 ml Corning flask in triplicates, in HOMEM medium (Berens et al., 1976), and cultured for 4 days. On day 4, the cells were collected by centrifugation 1000 g for 10 minutes in mid logarithmic growth phase. The cell pellets were washed with DM twice and re-suspended in the same medium used as inoculation for three individual flasks containing 200mL/flask of DM maintained at 27°C, pH 7.4 with starting cell density adjusted to 1 x 10^6 cells/mL.

Growth was monitored for 9-day period and integrity of the cells was assessed by trypan blue dye exclusion test and cultures were only considered for counting with more than 98% viability. Parasite growth was followed daily for 9 days by sample dilution at 1:5 ratio with ice cold 2 % (w/v) formaldehyde-PBS and counted using improved Neubauer haemocytometer. Defined medium without cells was maintained in similar conditions set as positive control. Sample preparation was carried out according to (Vincent et al., 2014) with modifications to the protocol by omitting the washing step meant for removing traces of serum adhering to cells.

Briefly, On Day 3 from the day of culture initiation, 4x10^7 cells were pipetted out from each flask individually to a 50 mL pre chilled falcon tubes and quenched by rapidly cooling cells to 10^0C using a thermometer, by submerging tube in dry ice/ethanol bath for approximately 10 seconds. During the procedure, it was ensured that the tubes were constantly shaken in a circular motion to avoid cell clumping or freezing or lysis and placed on ice bath whilst handling other samples. The tubes were centrifuged at 1000 g, 10 min at 4^0C. The supernatant was pipetted into another falcon tube without disturbing the cell pellet. The cell pellet (metabolite finger-print profiling), supernatant (metabolite foot-print profiling) and naïve medium without cells (blank control) were treated with 1:1 ratio with CMW extraction solvent (chloroform/methanol/water -CMW extraction solvent, 1:3:1, v/v/v, example supplier-Thermo Scientific, analytical standard reagent) in a pre-chilled Eppendorf tubes and placed on shaker set at maximum speed and temperature of 4^0C for an hour. Subsequently, the Eppendorf tubes were centrifuged at 16000 g, 10 min at 4^0C. Individual samples each at 90µL were suspended into an MS glass vial under argon. From each individual samples 5µL were taken and mixed together into one Eppendorf (pre-chilled) used as quality control (QC). Samples were placed on dry ice during the transfer to Glasgow Polyomics building and the samples were stored in -80^{0}C until sample injections into the mass spectrometer.

2.11 Sample processing on the mass spectrometer

Metabolomics samples were processed at Glasgow Polyomics, University of Glasgow, UK in standardised methods as specified in protocol from (Mwenechanya et al, 2017; Akpunarlieva et al, 2017, Van der Hooft JJJ et al; 2017). Briefly, the samples were run on zwitterions permanent hydrophilic interaction liquid chromatography (Zic-pHILIC column with 150 mm × 4.6 mm, 5 µm column, Merck Sequant on a Dionex UltiMate 3000 RSLC system. The mobile phase of the pHILIC column consisted of two solvents maintained at 30^{o}C with solvent A with 20mM ammonium carbonate in water and solvent B of 100% acetonitrile. The order of the solvents used were 80% B to 20% B at 30 min and 5% B at 32 min and held to 39 min for washing, then 80% B at 40 min. The samples eluted in linear gradient over 46 min flow rate at 0.3ml/min. The injection volume was 10µL and 4^{o}C prior to injection. The chromatography system was coupled to high-resolution exactive orbitrap mass spectrometer (Thermo Scientific). The settings of mass spectrometer for certain other parameters were as follows: Probe temperature 150^{o}C, Capillary temperature 275^{o}C, resolution 50,000; m/z range 70-1400 and the samples were run in both positive and negative ionisation modes.

2.12 Data analysis

The data-sets from mass spectrometer was analysed according to (Creek et al., 2012b, Scheltema et al., 2011) with manual verification at each step. Briefly, the raw data files from the LC-MS analysis were grouped manually in different folders according to their respective biological conditions under each master folder for positive and negative ionisation modes. Supporting software such as Proteowizard library (version 3) has the msconvert utility to convert raw files to mzXML open data format and XCMS (version 3.0.1) has the CentWave feature detection algorithm that extracts all the chromatographic peaks (Smith et al; 2006).

The core software mzMatch (version 1.0.2)was applied to filter the noise from the signal noise by manual setting of parameters for mass and retention time error as below 5% so that all peaks arising from artefacts during sample preparation and solvent memory (Scheltema et al., 2011) are removed. The PeakML files are further processed to discard peaks that are not reproducibly detected in all the replicates involved. Peaks from every sample are then aligned on the basis of their retention time (RT) and m/z values to be collated as combined PeakML file. Information about the RT and m/z from each peak are matched to online databases in alignment with metabolomics profiling initiative forum.

To obtain more robust metabolite identification, 250 authentic standards were run in parallel during sample processing. These standards files were processed using TOXID software (version 2.1) to derive experimental retention time of the standard metabolites. These files were used to update the predicted retention time as calculated by IDEOM software (version 19c). The peak shape and intensity of above $5X10^3$ was selected as appropriate peak for each of the metabolites. The relative standard deviation was evaluated to understand about the sample variation between replicates and instrument response consistency. Multiple macro chosen within IDEOM software filtered the metabolites into the identification and rejected list. Manual curation at each stage was carried out to pick false rejections and add them to the identification list or vice versa. All steps carried out individually for positive and negative mode separately and then used to combine all data sets for comparison across samples in the study with schematic as shown in appendix figure 4. Multi-variant data analysis was carried out by writing scripts using in R and Matlab programming with details as shown in appendix code 1 to appendix code 4.

2.13 Sample preparation for metabolite foot-printing of extracellular metabolome extraction

Sample preparation was carried out according to metabolite finger-printing elaborated in Section 4.4. Briefly, On Day 1, 2, 3, 6, and 9 from the day of culture initiation, $4x10^7$ cells were pipetted out from each flask individually from the three different flasks to a 50 ml pre chilled falcon tubes and quenched by rapidly cooling cells to 10^0C as measured by thermometer in dry ice/ethanol bath. At the same time, 10 mL of naïve medium without cells (sterile media placed in incubator) was also aliquoted at similar times and processed as control samples as above represented as Day 0 in the data. All sample tubes were centrifuged at 1000 g, 10 min at 4^0C. The supernatant was pipetted into another falcon tube without disturbing the pellet and used as exo-metabolome samples. These samples were diluted in 1:1 ratio with CMW extraction solvent in a pre-chilled Eppendorf tubes and placed on a shaker set at a maximum speed and temperature of 4^0C for an hour. Subsequently, the Eppendorf tubes were centrifuged at 16000 g, 10 min at 4^0C. The supernatants each at 90µL were put into an MS glass vial under argon gas. Then, 5µL was taken from each individual sample and mixed together into one Eppendorf (pre-chilled) used as quality control (QC). Samples were placed on dry ice during the transfer to Glasgow Polyomics building and the samples were stored in -80^0C until processed by LC-MS and analysed as elaborated in section 2.10, 2.11 and 2.12.

2.14 Biochemical assays

The objective for these assays was to determine the impact of small molecules in the exo-metabolome on the host cells with THP1 differentiated macrophage cells as an infection model. Aromatic pyruvates significantly enriched in the exometabolome were further investigated using pure compounds following the results from Chapter 4. Since the objective for these assays was to determine the role of small molecules during infection with host cells, the samples were prepared accordingly to enrich the small molecules without interference with bigger molecules such as proteins and ribonucleic acids.

2.15 Sample preparation for biochemical assays of aromatic pyruvates

The samples prepared for metabolomics foot-printing experiments were used for biochemical assays with few modifications as follows: *Leishmania mexicana* promastigotes were inoculated at 1×10^6 cells/ml in triplicates. Parasite concentration was recorded using the haemocytometer on day 1, 2, 3, 6, and 9 from the day of culture initiation. Then, 4×10^7 cells were pipetted out from each flask individually from the three different flasks to a 50 ml pre chilled falcon tubes and centrifuged at 1000 g, 10 min at 4^0C. The supernatant was carefully pipetted out into new tubes without disturbing the cell pellet. The supernatant was filter sterilised using 3kDa filter to remove traces of large molecules such as proteins/peptides which would, in turn, enrich the small molecules within the samples without the interference of bigger molecules whilst testing their impact on THP1 differentiated macrophage cells as an infection model.

2.16 Effect of parasite exometabolome on host cell viability

The host cells considered would be THP1 cells (human monocytic cell line) as a model system. Here, the assays investigated the role of aromatic pyruvates released by the promastigotes during the dynamic growth cycle. Alamar blue assay would be carried out to measure the effect of aromatic pyruvates (Indole lactate, sodium phenyl pyruvate, para-hydroxy phenyl pyruvate at 1 mM each) on the viability of THP1 cells with phenyl arsine oxide as a control.
The monocytes were maintained in RPMI 1640 medium containing 2 mM Glutamine with 10% FBS, 1% penicillin/streptomycin at 37^{o}C, 5% CO_2 in liquid suspension. The growth of the cells monitored by trypan blue exclusion method to check for cell viability and recorded using haemocytometer. 5 x10^6 cells/mL of THP1 cells were plated on chamber slides at 37^{o}C at 5% CO_2 and differentiated using 100nM PMA (phorbol myristate acetate). After 24 hours, the differentiated macrophages were treated with fresh RPMI medium, DM, incubated with exo-metabolome (DM (D6S)), or pure compounds of ascorbic acid, indole lactate, phenyl pyruvate, 4-hydroxy phenyl pyruvate at 1mM concentration each were taken in triplicates repeats (n=6) and phenyl arsine oxide at 10µM for 72 hours. On Day 4 from the start of culture initiation, alamar blue reagent, 0.49mM resazurin (Sigma) in 1 X PBS, pH 7.4 and incubated for another 48 hours. Fluorescence was measured on a Pherastar spectrometer (BMG Labtech), with excitation wavelength= 544 nm and emission wavelength= 590 nm. Viability was expressed in percentage with an optical density of wells containing THP1 cells in RPMI medium considered as 100% viable.

2.17 Reducing power determination for antioxidant activity

The reducing power of the spent medium would be determined using modified protocol from (Lee et al., 2014). Briefly, this assay measures the property of the compounds to act as electron donor using potassium ferricyanide reduction. Here the Fe3+/ferricyanide complex is reduced to ferrous form. Colour change from yellow to the blue and green range. Ascorbic acid (control) at a range of different concentrations from 0.001 mM-100mM was tested, as it is well known for its antioxidant activity. Aromatic pyruvates were also tested in the same manner from 0.001 mM-100mM. For this, 10 µl of 1% potassium ferricyanide was added. The plate was incubated at 50^{o}C for 30 min. The plate was cooled and 10 µl of 1% trichloro acetic acid and 10 µl of 0.1% $FeCl_3$ were added and left for 20 min. Absorbance was read at 700 nm to determine the amount of ferric ferrocyanide (Prussian blue) formed. The higher absorbance of the reaction mixture indicates the higher reducing power of the compounds tested.

2.18 Determination of phenolic nature of spent medium

Parasites secreted low molecular weight metabolites were observed to have characteristic enone moiety from structural analysis of metabolomics spent medium analysis (Chapter 5). In order to analyse their chemical nature over time, phenolic content of spent medium was assessed. Aromatic compounds with hydroxyl groups react with the phosphomolybdic acid in Folin-Ciocalteu reagent in an alkaline medium to produce a blue coloured complex. An aliquot of 20 µl of spent medium from each day of the culture (D1S, D2S, D3S, D6S and D9S) was compared to medium only without cells incubated for similar time lengths. 500 µl of Folin Ciocalteu reagent and 1000 µl of distilled water were added. Tubes left for 3 minutes at room temperature and 1000 µl of 20 % Sodium carbonate (Na_2CO_3) added. Tubes placed at 37°C in a water bath for 30 minutes. 50 µl transferred to the plate in triplicates and samples from eppendorf tubes transferred to a flat bottom plate and the absorbance was measured at 600 nm using a model PHERAstar FS microplate reader (BMG Labtech). Catechol was used as the reference standard with different concentration from 2mg/ml-10 mg/ml (18mM-90mM), and the results expressed as mg of catechol equivalents/µl.

2.19 Effect of exometabolome on nitric oxide radical scavenging assay

The experimental set up of the assay was similar to that followed by Hassani et al, 2011 (Hassani et al., 2011), with a few modifications. About, 5 $x10^6$ cells/mL of THP1 cells differentiated using 5ng/mL PMA for 24 hours. Differentiated macrophages infected with *L. mexicana* or incubated with exo-metabolome (Day 6 supernatant collected as described in experimental procedures after filtration using 3kDa-cut off centrifugal column (example supplier-Amicon Ultra) or pure compounds of ascorbic acid, indole lactate, phenyl pyruvate, 4-hydroxy phenyl pyruvate at 1mM concentration each were taken in triplicates (n=9) for 24 hours. After incubation for 24 hours under different conditions, the macrophages were washed with defined medium and 200µL of DM was added to all the wells. Subsequently, each of the wells was treated and untreated (Control) with 10ng/mL of LPS for 24 hours. LPS stimulated macrophages released nitric oxide which on reaction with Griess's reagent (50µL) (1% sulphanilamide, 2% phosphoric acid and 0.1% naphthylene diamine dihydrochloride) formed stable complex proportional to the amount of nitrite in the sample. The amount of nitrite measured was compared to standard curve ranging from 0-100µM of nitrite and analysed using linear regression analysis at 540 nm.

2.20 Estimation of phenolic nature of parasite secreted low molecular weight metabolites.

The principle of the assay: Phenolic assay was carried out according to the procedure (Lee et al., 2014). Aromatic compounds with hydroxyl groups react with the phosphomolybdic acid in Folin-Ciocalteu reagent in an alkaline medium to produce a blue coloured complex. Catechol was used as the reference standard with different concentration from 0-10 mg/ml, and the results expressed as mg of catechol equivalents/µL. An aliquot of 20 µL of defined medium supernatant from Day 0,1,2,3,6 and 9 of culture initiation taken in triplicates (n=6) in Eppendorf tubes. Similarly, an aliquot of 20 µL pure compounds of ascorbic acid, indole lactate, phenyl pyruvate, 4-hydroxy phenyl pyruvate each at 1mM concentration each was taken in triplicates (n=6) in Eppendorf tubes. Subsequently, 500 µL of Folin ciocalteu (Sigma) reagent and 1000 µL of distilled water were added and tubes incubated for 3 minutes at room temperature and 1000 µL of 20 % Sodium carbonate (Na_2CO_3) added. Tubes placed at 37°C in a water bath for 30 minutes. Then 50 µL transferred to the 96-well microtitre plate (Corning) and the absorbance was measured at 600 nm using a model PHERAstar FS microplate reader (BMG Labtech).

2.21 Determination of antioxidant activity of aromatic pyruvates by reducing power measurement

The principle of the assay: The reducing power of the spent medium would be determined using modified protocol from (Lee et al., 2014). This assay briefly measures the property of the compounds to act as electron donor using potassium ferricyanide reduction. Here, the $Fe^{3+/}$ferricyanide complex is reduced to ferrous form with colour changing from yellow to the blue and green range. Ascorbic acid, well known anti-oxidant was used as control at a range of concentrations from 0.001 mM-100mM. Aromatic pyruvates such as indole lactate, phenyl pyruvate, 4-hydroxy phenyl pyruvate at 1mM concentration each were taken in triplicates (n=6) for 24 hours. Acetate was also tested in the same manner from 0.001 mM-100mM. Potassium ferricyanide (1%) of 10 µL was added. The plate was incubated at 50°C for 30 min. The plate was cooled and 10 µL of trichloro acetic acid (1%) and 10 µL of $FeCl_3$ (0.1%) were added, and further incubated for 20 min at room temperature. Absorbance was read at 700 nm and the amount of ferric ferrocyanide (Prussian blue) formed was determined. The higher absorbance of the reaction mixture indicates the higher reducing power of the supernatant sample.

2.23 Estimation of chemical reducing activity of exo-metabolome at different growth stages of promastigotes

Parasites secreted several low molecular weight metabolites bearing an enone moiety, as observed from metabolomics spent medium analysis. In order to analyse their chemical nature over time, the phenolic content of spent medium was assessed. Aromatic compounds with hydroxyl groups react with the phosphomolybdic acid in Folin-Ciocalteu reagent in an alkaline medium to produce a blue coloured complex(Lee et al., 2014). An aliquot of 20 µL of spent medium from each day of the culture (D1S, D2S, D3S, D6S and D9S) was compared to medium only without cells incubated for similar time lengths. To this, 500 µl of Folin-Ciocalteu reagent and 1000 µL of distilled water were added. Tubes left for 3 minutes at room temperature and 1000 µL of 20 % Sodium carbonate (Na_2CO_3) added. Tubes placed at 37 °C in a water bath for 30 minutes. From this, 50 µL transferred to the plate in triplicates and samples from eppendorf tubes transferred to a flat bottom plate and the absorbance was measured at 600 nm using a model PHERAstar FS microplate reader (BMG Labtech). Catechol was used as the reference standard with different concentration from 2mg/mL-10 mg/mL (18mM-90mM), and the results expressed as mg of catechol equivalents/µL.

Chapter 3 Establishment of defined minimal medium for axenic culture

3.1 Introduction

Parasitic protozoa belonging to the order Kinetoplastida such as *Leishmania* are pleomorphic with different stages expressed during the course of their life cycle (Kaye and Scott, 2011) with complex biochemistry. Understanding the biochemical nature of parasites has been a priority for drug target discovery (Vincent and Barrett, 2015; Creek and Barrett, 2014; Landfear, 2011). This has been facilitated by robust *in vitro* culture techniques that allow studying these organisms in controlled environmental conditions which mimic the biological conditions.

3.1.1 Brief overview of the development of *in vitro* medium culture.

Formulation of *in vitro* culture medium for parasitic protists began at the start of the 20th century with the development of Novy-McNeal medium for cultivation of *Trypanosoma brucei brucei* (Novy and Mac Neal, 1904). This was later modified by Nicolle as blood agar slants inoculated with infected tissue, referred to as Novy-McNeal Nicolle (NNN) medium (Nicolle, 1908), and used to culture certain species of *Leishmania* (Limoncu et al., 1997). Subsequently, the formulation of the diphasic media, comprising of a solid agar phase containing a mixture of organic substances composed of diverse components including peptone, beef infusion, glucose, tryptose, liver extract, brain heart infusion, individual amino acids and Trypticase soy agars (Cross and Manning, 1973) and the liquid phase comprising water condensate or Locke's solution forming on the agar surface (Novy and Mac Neal, 1904) or rabbit blood at a concentration ranging from 2.5-50%. Many reports suggested that the diphasic media posed two major issues, by limiting the isolation of a large number of parasites and contamination from the constituents of the solid phase, which posed the need for liquid media (Chang and Hendricks, 1985).

Liquid media evolved from many variations of diphasic media composed of peptone and yeast extract with 10% foetal calf serum used for cultivation of *L. infantum* and *L. tropica* with cell yields (about 10^6 cells/mL) that was comparable to NNN medium (Limoncu et al., 1997). Kar et al 1997 have shown that *L. donovani* isolates from Kala-azar patients could be cultivated with a high concentration of folic acid (100 mg/mL) with the base medium of brain heart infusions (Kar, 1997).

3.1.2 Comparison of *in vitro* media for the culture of *Leishmania* promastigotes.

There are many other medium formulations reported in the literature, however, use of undefined components was prevalent until 1970. Medium HOMEM formulated by Berens, Brun and Krassner (Berens et al., 1976) in 1976 developed the culture of *L. donovani* promastigotes that has been routinely used with the addition of 10% foetal calf serum. Other media used for *in vitro* culture of *Leishmania* research involves HOMEM (Berens et al., 1976) and commercially available tissue culture media such as RPMI (Moore et al., 1967) or M199 with 10% foetal calf serum (FCS) adopted for the culture of certain *Leishmania* strains (Hassani et al., 2011, Moreno et al., 2014b) as listed in Table 3-1.

Table 3-1 Compilation of media formulations used for *Leishmania* culture.

Media name	Authors	Composition

M199	(Morgan et al,1950)	With 5% serum
RPMI 1640	(Moore. G.E. et al, 1967)	With 10% serum
HOMEM	(Berens RL 1976)	With 20% serum
Grace medium	(Childs, 1978)	With 15% serum
LITR9	(Sadigursky M, Brodskyn CI., 1986)	Elaborate with liver infusion and tryptose.
REIII	(Steiger and Steiger, 1976)	Chemically defined media with minimal components but only includes 17 amino acids
Semi defined	(Ali et al., 1998)	Casein hydrolysates and urine
Serum free	(Armstrong and Patterson, 1994)	Urine
Serum free	(Steiger and Steiger, 1977)	Includes BSA
REIX	(Steiger and Black, 1980)	Chemically defined media with minimal components but only includes 11 amino acids for the growth of L. *donovani* species
REX	(Steiger and Black, 1980)	Chemically defined media with minimal components without glucose.
MD29	(Melo et al., 1985)	Chemically defined media with many purines and pyrimidines sources
CDM	(Merlen, 1999)	Chemically defined media with complex fatty acids and amino acid intermediates

Some of the media compositions with the addition of serum poses significant disadvantages as listed below:

Undefined composition- Although the major constituents of serum include proteins, amino acids, glucose, minerals, fatty acids and other growth factors, their functions for *in vitro* culture remain obscure. The concentrations of the nutrient components vary with type and age of the serum. The effect of the undefined components on the cells has not been fully determined.

Batch variability- Serum varies from batch to batch, deteriorating over time. Although similarity could be maintained, the identical composition of serum as tested in the first batch cannot be met between experimental repeats. Hence, eliminating FCS will reduce batch variability and reproducibility between laboratories.
Contamination-FCS obtained from animal slaughter might have the risk of contamination with other infectious agents.
Downstream processing- Procedures such as heat inactivation of sera needs to be carried out before use to prevent complement induced cell lysis. With the use of serum free media, these procedures could be avoided altogether.
Cost-Serum free medium would eliminate the high cost of purchase, transport and storage of Foetal Calf Serum/ Foetal Bovine Serum (FCS/FBS).
The availability-increasing problem of global warming and other environmental conditions, such as drought in the cattle rearing areas, could restrict the amount of serum available. The economic and logistic regulations of individual regions are also factors that dictate the availability of serum. Hence, there is a need for a paradigm shift to be able to adopt serum-free media for routine laboratory research.

3.1.3 Importance of chemically defined media for the culture of *Leishmania* promastigotes.

Baltz et al showed that serum compatibility for the culture of specific organisms differed depending upon the source (Baltz et al., 1985), certain species of Kinetoplastida parasites showed preference to rabbit serum over the horse or pig sera; since there were additional requirements of external purines, growth factors and vitamins. Baltz et al also highlighted that human serum was found toxic for the culture of specific strains of Kinetoplastida which required cattle as a host system to complete their developmental cycle. Thus, undefined nature of the serum poses a significant issue for standardisation across multiple experiments.

Thus, the addition of various undefined components such as serum (FCS), yeast extract or albumin fractions adds to the complexity and variability of the culture media. These factors might lead to variable growth responses of parasites in culture, affecting hypothesis testing. Therefore, medium preparation without a serum component represents an imperative goal for hemoflagellate cultivation. Serum derived components such as fatty acid free bovine serum albumin, bovine alpha-2 macroglobulin and bovine beta-lipoprotein have been used as serum replacing components (Steiger and Steiger, 1977).

A study by Merlen et al (1999) formulated the completely defined medium (CDM/LP) composition for *Leishmania* which showed similar proteinase and antigenic profiles compared to parasites cultured in serum containing medium (Merlen et al., 1999). The medium components included glucose, amino acids and organic salts, ATP, many nucleosides and nucleotides, guanine and hypoxanthine, several vitamins, cholesterol, glutathione, Tween 80, five carbon ribose sugars. Some of these components in the medium were thought to be dispensable; since evidence from gene and protein expression studies have highlighted that promastigotes encode for several biosynthetic pathways, for example, exogenous sources of glutathione or cholesterol could be dispensable (Beach et al., 1979, Romao et al., 1999). Hence, CDM/LP composition has been considered very elaborate and the development of minimal media required for *in vitro* culture of *Leishmania* promastigotes was carried out in this study.

Detailed analysis of another defined medium termed MD-29 compared the cell densities of 19 different stocks of *Leishmania* promastigotes from the New world species and showed that incorporation of metal salts such as ferric nitrate allowed for cell yields in the order of 10^7promastigotes/mL over 9-day period at 25^{o}C. The base composition of MD-29 was based on modified *T. cruzi* medium AR-103 with the omission of nucleotides and nucleosides such as ATP and AMP but the inclusion of many purines and pyrimidines sources (Melo et al., 1985). However, *Leishmania* has the enzymatic potential to inter-convert purine sources and pyrimidine biosynthesis de novo; without the need for exogenous pyrimidine sources (Lafon et al., 1982).

Simplified medium reported by Steiger and Steiger termed RE I medium formulated to support the growth of *L. donovani* and *L. braziliensis* which contained 17 amino acids in addition to glucose, adenosine, vitamin mix, lipoic acid and bovine albumin (Steiger and Steiger, 1977). It was also reported that bovine albumin was not essential for *in vitro* culture conditions and thus modified composition termed as RE III had 14 amino acids and (Steiger and Steiger, 1976); subsequent modifications included medium with and without glucose termed, RE IX composition contained 11 amino acids with growth experiments optimised for the culture of *L. donovani* promastigotes (Steiger and Black, 1980).

In this chapter, different medium compositions were compared and only those components essential for the viability and growth promoting were included in development of defined medium for the growth of *L. mexicana* promastigotes in culture. Defined medium for *in vitro* culture would then allow reproducibility and standardisation between experiments and laboratories. Isolation of antigens would be more efficient than in serum containing media, cost and diagnosis could also be greatly benefitted to describe some of the potential applications further elaborated in the discussion section of this chapter.

3.1.4 Research aims

- Comparsion of different defined medium compositions for the culture of *Leishmania*.
- Growth analysis of individual components for the growth of *L. mexicana* promastigotes.
- Evaluation of newly developed defined medium by:
    - Morphological examination
    - Infectivity analysis
    - Drug sensitivity

3.2 Results

3.2.1 Development of serum and protein free defined medium for *in vitro* culture of *Leishmania* promastigotes

Two defined media reported for the culture of *Leishmania*, namely CDM/LP (Merlen et al., 1999) were compared to REIX medium (Steiger and Black, 1980) as listed in Table 3-2. CDM/LP contained an elaborate composition with protein complex whilst REIX developed for *L.donovani* promastigotes has a simpler composition but with only 11 amino acids. The REIX medium was used as a starting reference and systematic modification by the omission of certain undefined components provisionally referred to as base medium (BM) was tested for the growth of *L. mexicana* promastigotes for the addition of co-factors and metals as shown in results section of this chapter. Detailed comparisons of the three medium compositions have been explained in Table 3-2.

Table 3-2 Comparison of medium compositions.

Components	CDM/LP (mM)	REIX (mM)	BM (mM)
Salts			
NaCl	139	136.8	136.8
KCl	7.00	5.36	5.36
NaH_2PO_4	6.22	0.33	0.33
KH_2PO_4	0.09		
Sodium Pyruvate		0.99	0.99

NaHCO3	24.00	3.57	3.57
HEPES	20.00	25.01	25.01
Hemin	7.70	0.0077	0.0077
Vitamins			
Choline chloride	0.024	0.007	0.007
D-Calcium pantothenate	0.0009	0.002	0.002
Nicotinamide	0.0094	0.008	0.008
Pyridoxal hydrochloride	0.001	0.004	0.004
Thiamine hydrochloride	0.00034	0.002	0.002
I-Inositol	0.00025	0.01	0.01
L-Ascorbic acid	0.00006		
Nicotinic acid	0.00004		
Pyridoxine hydrochloride	0.0054		
Cyanocobalamine	0.004		
Calciferol	0.00005		
Menadione 3H2O	0.00001		
L-α-Tocopherol	0.00001		
Retinol	0.00007		
Co-factors			
PABA	0.009		
Riboflavin	0.00056	0.002	
folic acid	0.003	0.002	
Biopterin			
Lipoic Acid			
D-Biotin	0.0015		
Components	CDM/LP (mM)	REIX (mM)	BM (mM)
Metals			
MgSO4.7H2O	0.61	0.81	
CaCl2	0.72		
Zinc Chloride			
Fe(No3)3.9H20	0.00036		
Manganese chloride			
Copper			

Cobalt chloride			
Amino Acids			
L-Tryptophan	0.046	0.245	0.5
L-Phenylalanine	0.16	0.606	0.5
L-Lysine hydrochloride	0.32	1.366	0.5
L-Arginine hydrochloride	1.90		0.5
L-Leucine	0.60	2.29	0.5
L-Valine	0.27	0.854	0.5
L-Aspartic acid	0.26		0.5
L-Serine	0.42		0.5
L-Glutamic Acid	0.34		0.5
L-Glutamine	2.30	2.05	0.5
L-Histidine hydrochloride-H2O	0.13	0.476	0.5
L-Isoleucine	0.48	0.763	0.5
L-Threonine	0.29	3.361	0.5
L-Methionine	0.14	0.335	0.5
L-Cysteine	0.60		0.5
L-Tyrosine	0.17	0.191	0.5
L-Proline	0.20		0.5
L-Alanine	0.11*		0.5
Components	CDM concentrations (mM)	REIX concentrations (mM)	BM concentrations (mM)
L-Asparagine	0.36		0.5
L-Glycine	0.00028		0.5
Other components			
Adenosine	0.0086	0.074	0.074
D-Glucose	13.3	11.11	16.6
Cholesterol	0.0001		

Glutathione	0.0036		
Hydroxyproline	0.17		
D-Ribose	0.66		
2-Deoxyribose	0.74		
Na acetate	0.12		
$ATP(Na_2)$	0.0036		
Guanine.HCL	0.00032		
Hypoxanthine	0.00052		
Xanthine(Na)	0.0005		
Uracil	0.00062		
Thymine	0.00048		
Tween80 4mg/L			

3.2.2 Experimental design

The overall work flow involved the development of defined medium has been depicted in Figure 3.1. Briefly, the REIX (Steiger et al, 1980) was used as starting composition referred to as BM with the omission of undefined components and addition of all amino acids at equimolar concentrations instead of only 11 amino acids as specified in REIX. Addition of cofactors and metal salts were tested and together referred to as Nayak medium. Stock solutions of individual components were prepared and added to make the different media as specified in Table 3-2.

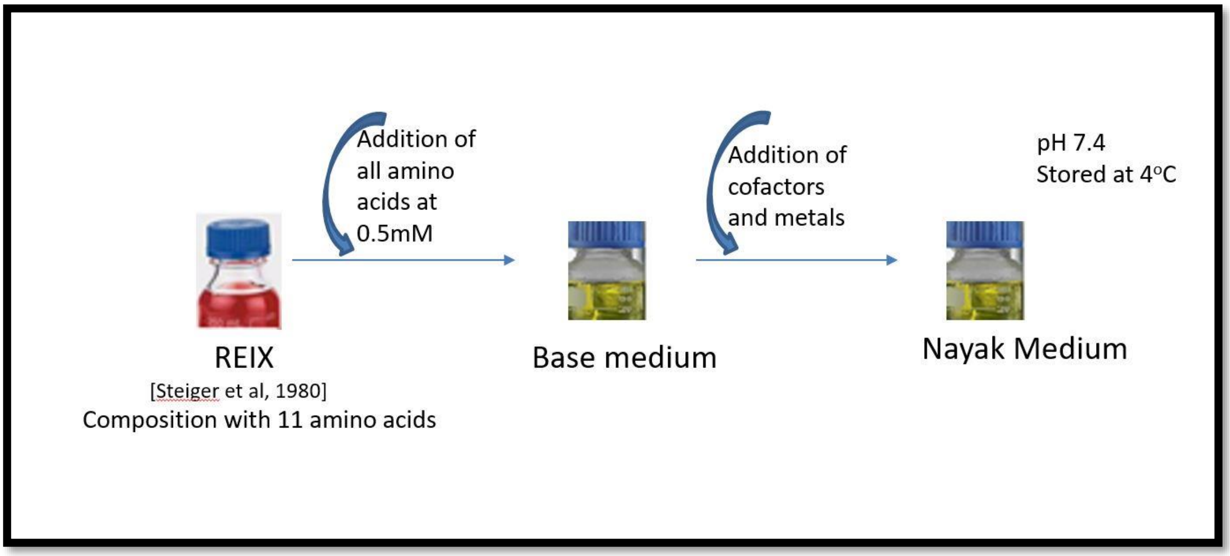

Figure 3.1 Workflow summary

Pictorial depiction of workflow strategy followed during the development and establishment of defined medium referred to as Nayak medium for *in vitro* culture of *Leishmania* promastigotes.

3.2.1. Growth analysis for the development of defined medium in the presence of all amino acids

As an experimental control for growth analysis, an established and routinely used method in our laboratory for the culture of *L. mexicana* promastigotes (strain MNYC/BZ/62/M379) using HOMEM medium (Berens et al., 1976) was used. HOMEM medium was prepared according to Berens et al, 1976 with 10% (v/v) heat-inactivated fetal calf serum (FCS) (Appendix table). Growth analysis was monitored for a period of 9 days in HOMEM, REIX and BM media in triplicate flasks and cell count recorded as shown in Figure **3.2**. Growth analysis was carried out under identical conditions from one set of inoculated cells, temperature and pH at 27^{0}C and pH 7.4 respectively.

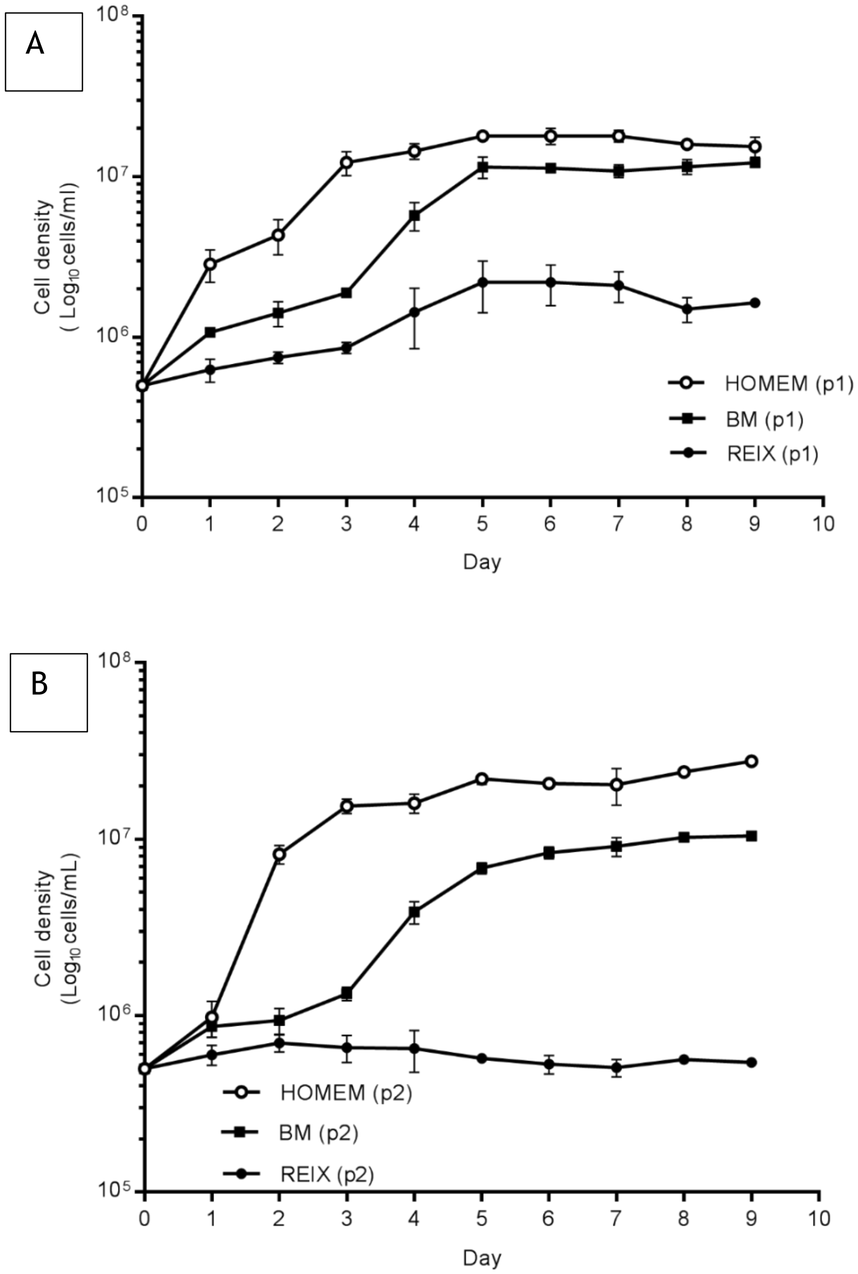

Figure 3.2 Cell count of *L. mexicana* promastigotes in BM (closed squares), REIX (closed circles) compared to serum containing HOMEM (open circles) shown over the 9day period in (A) passage 1 (p1) and (B) passage 2 (p2).

Parasites were inoculated at a density of 5 x10^5 cells/ml and aliquots of triplicate culture flasks were counted every 24 hours thereafter as described in experimental procedures. Representative data from biological triplicates each in independent experiments set up in parallel on multiple days. (Error bars = mean ± SD, n=9).

The viability of cells cultured in REIX medium was below 98% and the cells formed clumps as recorded in Figure 3.2 (A) and showed no growth when transferred to fresh batch REIX medium for the second passage as shown in Figure **3.2** (B). REIX optimised for the growth of *L.donovani* promastigotes had only 11 amino acids namely; L-Tryptophan, L-Phenylalanine, L-Lysine hydrochloride, L-Leucine, L-Valine, L-Glutamine, L-Histidine, L-Isoleucine, L-Threonine, L-Methionine and L-Tyrosine. It was observed that BM containing all 20 proteogenic amino acids those in REIX along with addition of L-Arginine hydrochloride, L-Aspartic acid, L-Serine, L-Glutamic Acid, L-Cysteine, L-Proline, L-Alanine, L-Asparagine and L-Glycine instead of only 11 amino acids in REIX significantly improved the viability of the *L. mexicana* promastigotes as measured by trypan blue exclusion dye reaching a cell density of more than 1 x 10^7 cells/mL over 9 day growth period with active motility. Also, the addition of equimolar concentration of all amino acids significantly improved the doubling time measured to be approximately 18 hours under conditions tested at pH 7.4 at 27^{o}C; whilst it was calculated as 14 hours in HOMEM and more than 25 hours for REIX.

3.2.1.2 Growth in the presence of cofactors

Although the addition of all amino acids caused a significant increase in viability, the cells in culture exhibited increased lag period. To overcome these issues, a combination of co-factors were tested individually and in conjunction as shown in Figure 3.3 to Figure 3.8.

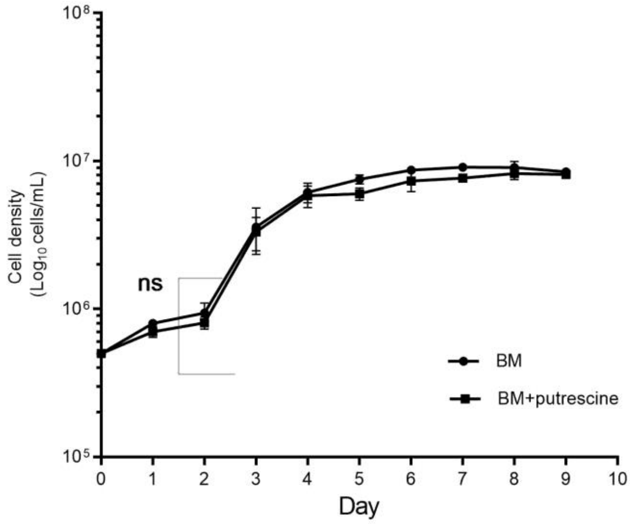

Figure 3.3 Cell count of *L. mexicana* promastigotes in Base medium (BM) in the presence and absence of putrescine (10μM).

(Error bars = mean ± SD, n=9)

From Figure 3.3, it was observed that addition of putrescine had a no significant effect on the growth of *L. mexicana* promastigotes under conditions tested.

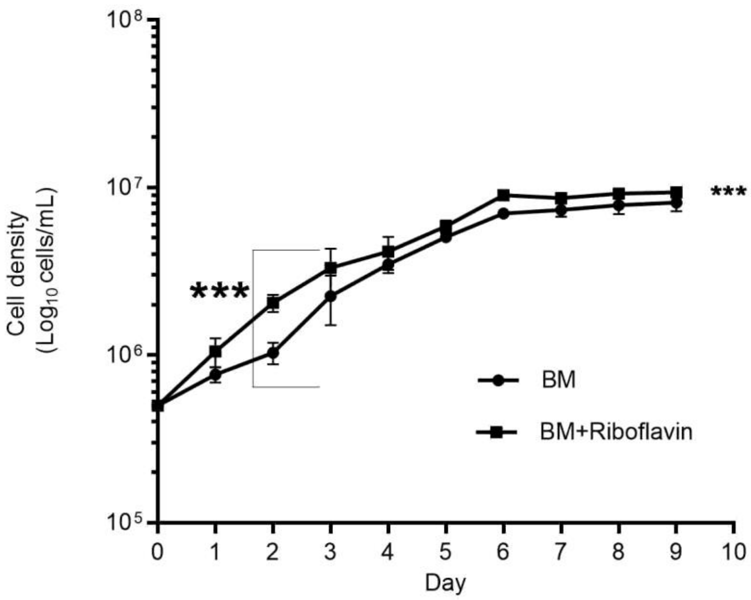

Figure 3.4 Cell count of *L. mexicana* promastigotes in Base medium (BM) in the presence and absence of riboflavin (10μM).

(Error bars = mean ± SD, n=9)

From Figure 3.4, it was observed that riboflavin had a positive effect in independent experimental repeats with a decrease in lag time during the 9 day, growth period tested.

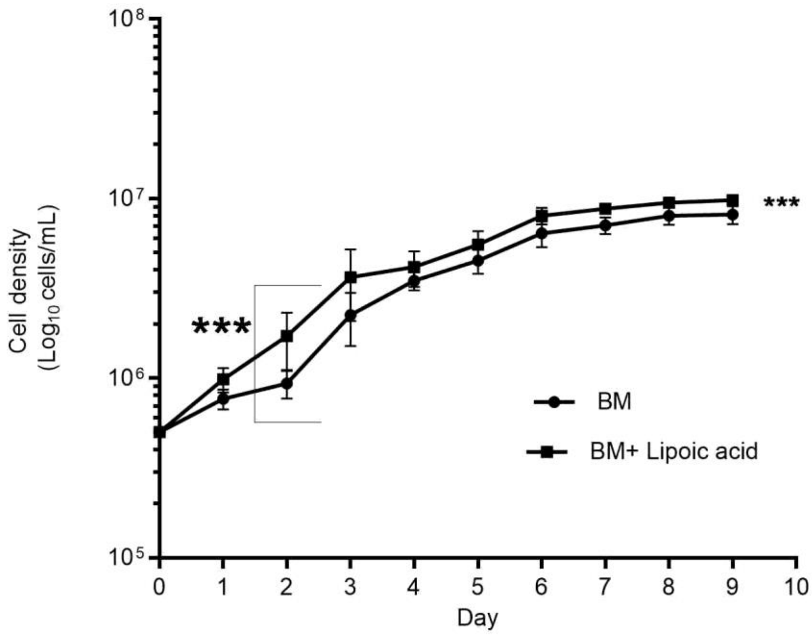

Figure 3.5 Cell count of *L. mexicana* promastigotes in Base medium (BM) in the presence and absence of Lipoic acid (10µM).

(Error bars = mean ± SD, *** $p<0.001$, n=9)

From Figure 3.5, it was observed that addition of lipoic acid shows distinct positive effect (*** $p<0.001$) to decrease the lag time in growth compared to the absence of it.

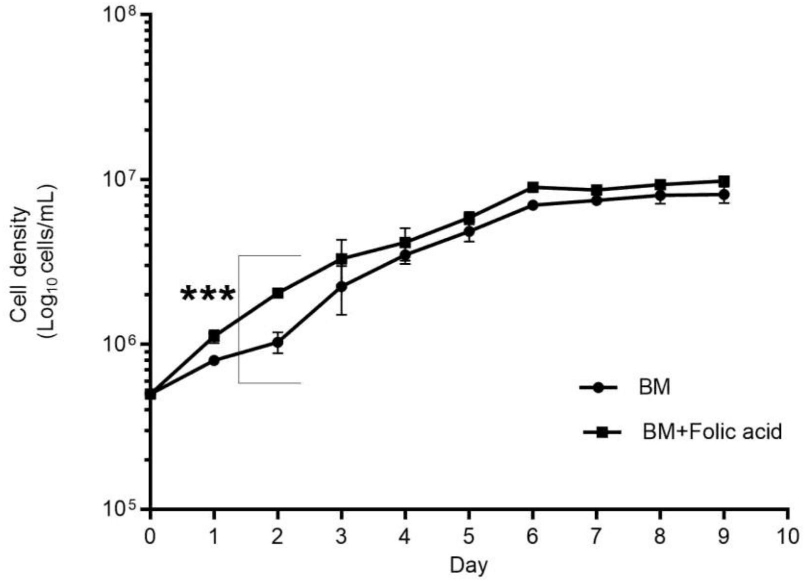

Figure 3.6 Cell count of *L. mexicana* promastigotes in Base medium (BM) in the presence and absence of Folic acid (10μM).

(Error bars = mean ± SD, *** $p<0.001$, $n=9$)

From Figure 3.6, it was observed that addition of folic acid have a positive growth effect with an increase in cell density observed over 9 day period.

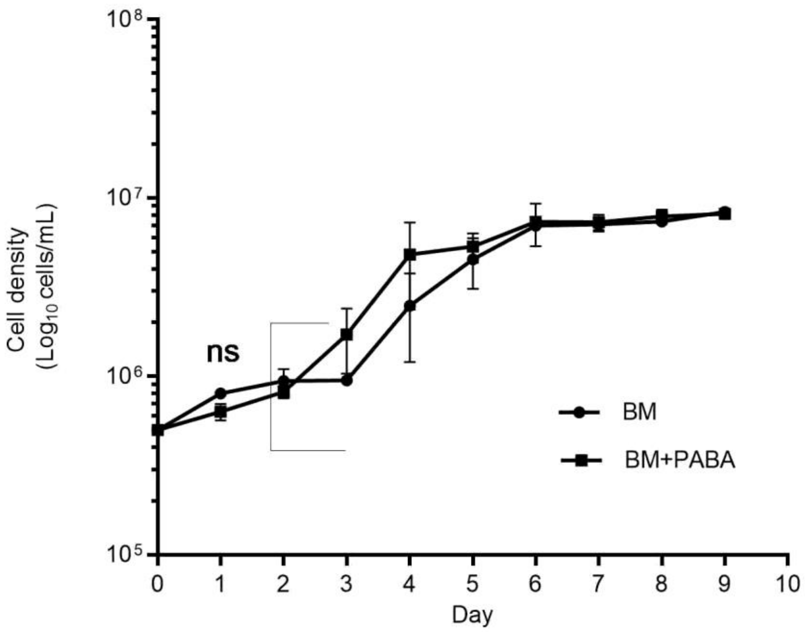

Figure 3.7 Cell count of *L. mexicana* promastigotes in Base medium (BM) in the presence and absence of PABA (10μM).

(Error bars = mean ± SD, n=9)

From Figure 3.7, it was observed that addition of PABA had no significant effect on the growth as observed over 9 day period.

Promastigotes were inoculated at a starting density of 5 X 10^5 cells/mL with various concentrations of biopterin ranging from 0μM to 160μM as shown in Figure 3.8. Stationary cell density was measured after 96 hours. Representative data from several independent experiments with an average of three determinations for each biopterin concentration.

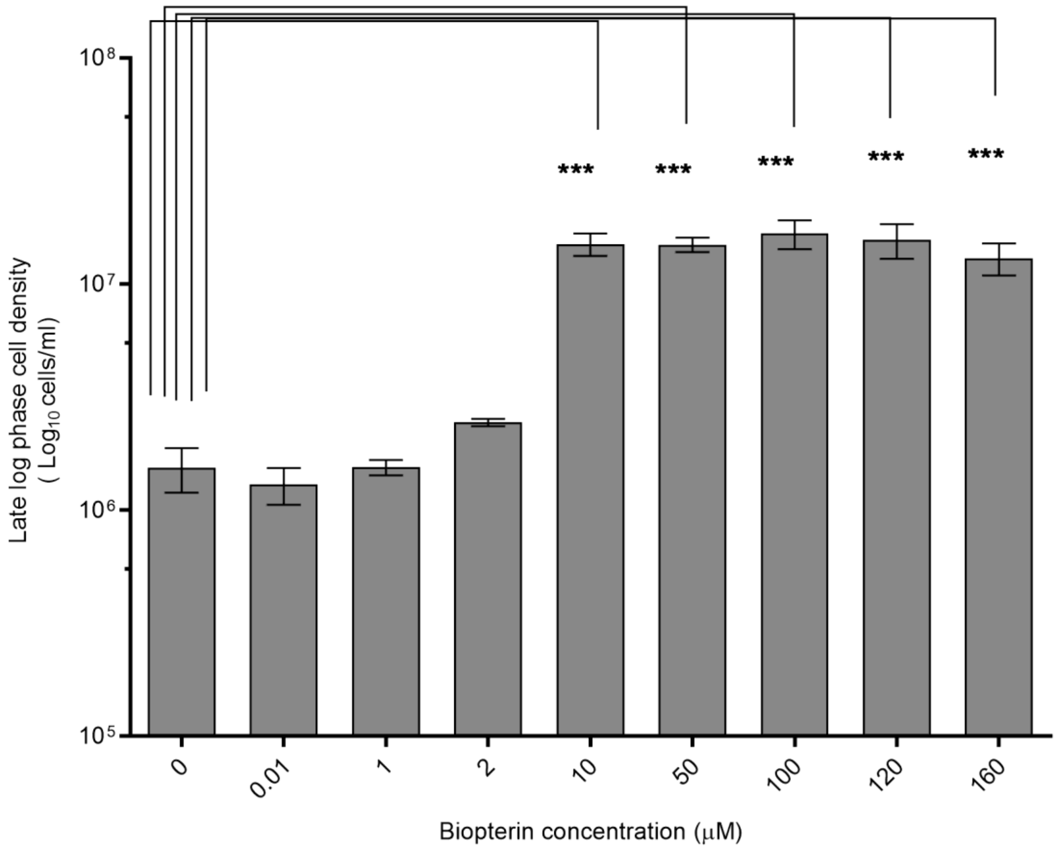

Figure 3.8 Addition of Biopterin (μM) stimulated the growth of *L. mexicana* in BM medium.

(Error bars = mean ± SD, n=9)

From Figure 3.8, it was observed that addition of Biopterin at 10-100μM have a constant positive growth effect with an increase in cell density observed over 96 hours from the start of the culture. *** Asterisks indicate significant growth with Biopterin above 10μM with $p<0.0005$ in comparison to medium without Biopterin (0 μM), one way ANOVA with Dunnett's multiple comparison test.

To test the comparative growth promoting of individual co-factors; with a starting cell density of 1 x 10^6 cells/mL were tested under different conditions of 10μM co-factor each and final cell density recorded after Day 6 in late log phase of the growth cycle as shown in Figure 3.9.

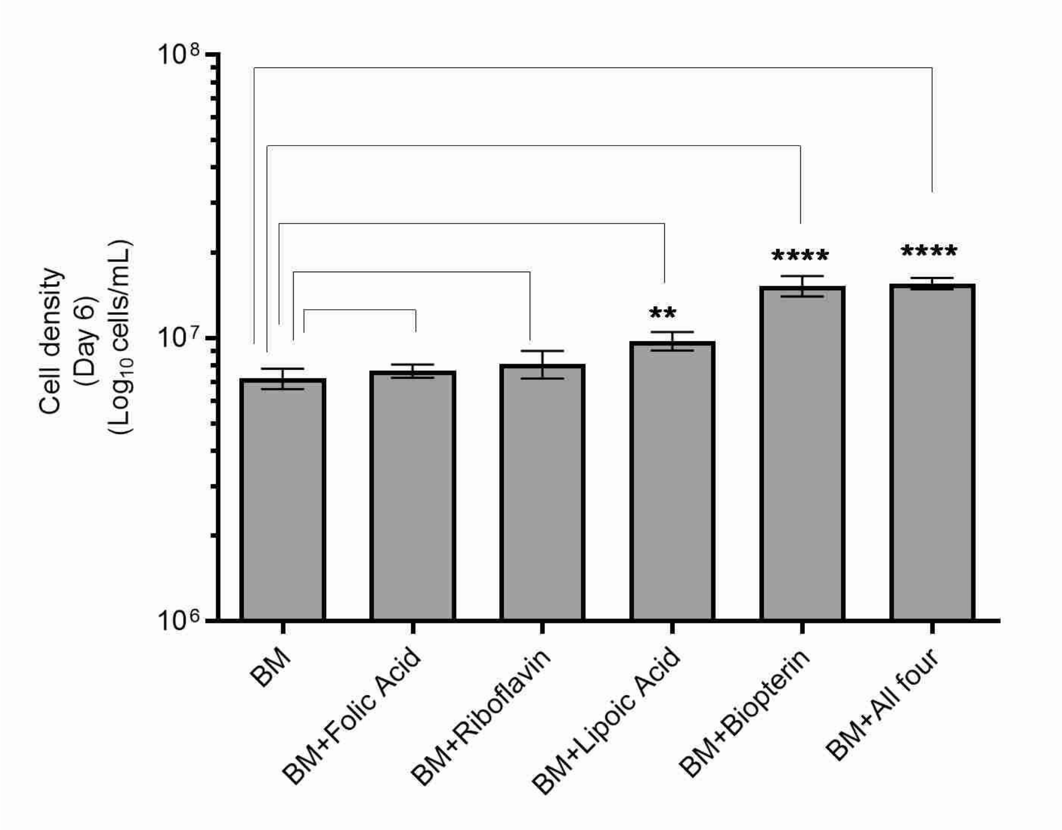

Figure 3.9 Growth of L. mexicana promastigotes in BM with and without folic acid (10 μM), riboflavin (10 μM), Lipoic acid (10 μM), Biopterin (10 μM).

(Error bars = mean ± SD, n=9)

From Figure 3.9, it was observed that among the co-factors tested biopterin had significant growth promoting activity compared to folic acid, riboflavin and lipoic acid. Asterisks indicate significant difference with **** p<0.0001; ** p<0.001 in BM plus cofactors comparison to BM, one way ANOVA with Dunnett's multiple comparison test.

The additive comparative effect of growth factors were tested by addition of all co-factors bar one. With starting density of 5 x 10^5 cells/mL, cell density estimated on Day 6 at late log phase of the growth cycle from the start of culture initiation as shown in Figure 3.10.

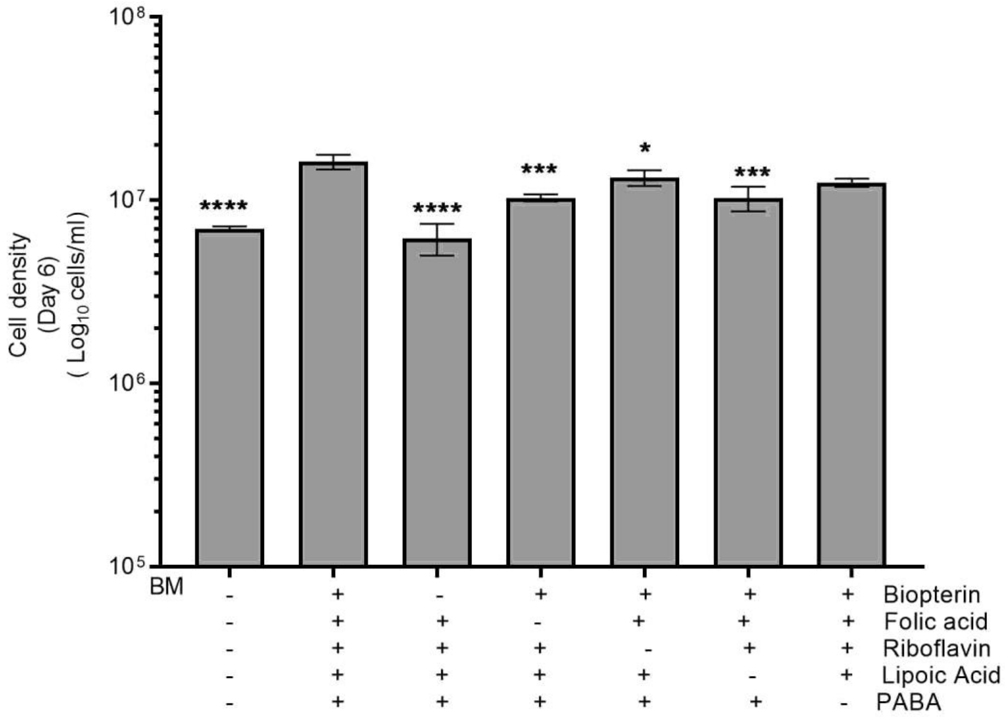

Figure 3.10 Growth of *L. mexicana* promastigotes in BM with and without folic acid, riboflavin, lipoic acid, biopterin and PABA (10μM) each.

(Error bars = mean ± SD, n=9)

From Figure 3.10, it was observed that upon single omission of each co-factors, biopterin > folic acid> lipoic acid > riboflavin > PABA had an increasing order of impact on *in vitro* growth of promastigotes. Asterisks indicate significant difference with **** $p<0.0001$; ***$p<0.0005$, *$p<0.05$ in BM plus individual cofactor in comparison to BM plus all cofactors, one way ANOVA with Dunnett's multiple comparison test,

3.2.1.3 Trace metals formulation by maximum growth in the presence/absence of metals mixture.

In this attempt to optimise the defined medium composition, mixture of metals was tested individually and together with other co-factors stated in section 3.2.1.2. Metal mixture of magnesium, calcium, zinc, iron, copper, manganese and cobalt were tested at various orders of magnitude each at 0.5mM, 0.05mM and 0.005mM as shown in Figure 3.11

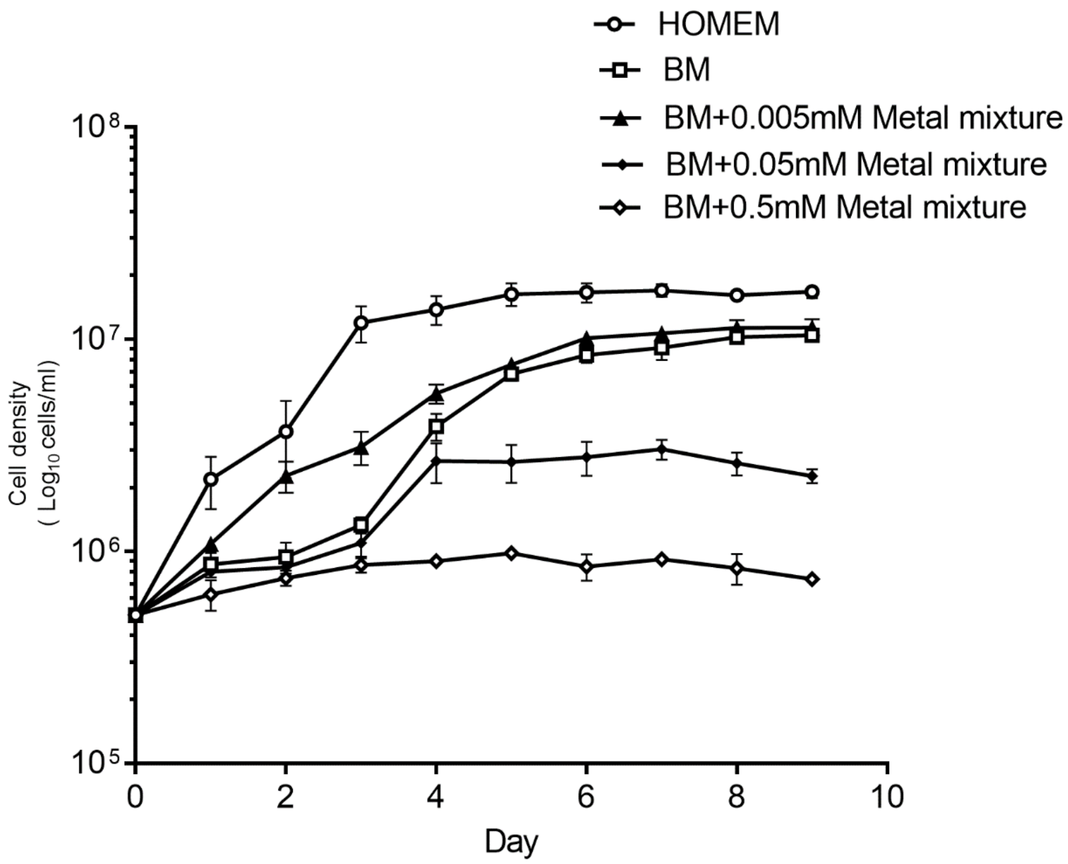

Figure 3.11 Comparative growth of *L. mexicana* promastigotes in HOMEM (open circles), BM (open squares) in the presence of equimolar metal mixture at 0.005 (closed triangles), 0.05 (closed diamonds) and 0.5 mM (open diamonds).

(Error bars = mean ± SD, n=9)

Parasites were inoculated at a density of 5 x10^5 cells/ml and aliquots of culture were counted every 24 hours thereafter until Day 9. It was found that equimolar metal mixture at a high concentration of 0.5mM and 0.05mM proved to be toxic which decreased cell viability by more than 50%; compared to 10-fold lesser concentration at 0.005mM. The addition of 0.005mM metals mixture resulted in decreased lag phase with growth in BM and improved growth reaching similar growth rate of promastigotes cultured in HOMEM as shown in Figure 3.11.

3.2.1.4 Optimisation of individual metal concentrations

Metals salts of $MgS0_4.7H_20$ at 0.81 mM, $CaCl_2$ at 0.72mM, $ZnCl_2$ at 0.03 mM, Fe $(NO_3)_3.9H_2O$ at 0.009 mM, $CoCl_2$ at 0.000032 mM, $CuSO_4$ at 0.0005mM and $MnCl_2$ at 0.000045 mM were tested individually as shown in Figure 3.12.

BM supplemented with cofactors and metals all together hereby, has been referred to as NM with complete composition stated in Table 3-3. The total density recorded in NM was much higher compared cells in BM as shown in result Figure 3.14.

Table 3-3 Compositions of BM (doubling time = ~25 hours) and NM medium (doubling time = ~18 hours) for axenic culture of *L. mexicana* promastigotes

Components	BM	NM
Salts	Concentration (mM)	Concentration (mM)
NaCl	136.8	136.8
KCl	5.36	5.36
NaH_2PO_4	0.33	0.33
Sodium Pyruvate	0.99	0.99
NaHCO3	3.57	3.57
HEPES	25.01	25.01
Vitamins		
Choline chloride	0.007	0.007
D-Calcium pantothenate	0.002	0.002
Nicotinamide	0.008	0.008
Pyridoxal hydrochloride	0.004	0.004
Thiamine hydrochloride	0.002	0.002
Myo-Inositol	0.01	0.01
D-Biotin	0.01	0.01
Co-factors		
Riboflavin		0.05
folic acid		0.05
Biopterin		0.1
Lipoic Acid		0.05
p-amino benzoic acid		0.01
Metals		
$MgS0_4.7H_20$		0.81
Calcium chloride		0.72
Zinc Chloride		0.03
$Fe(NO_3)_3.9H_20$		0.009
Manganese chloride		0.000045
Copper sulphate		0.000030
Cobalt chloride		0.000032

Components	BM concentrations (mM)	NM concentrations (mM)
Amino Acids		
L-Tryptophan	0.5	0.5
L-Phenylalanine	0.5	0.5
L-Lysine hydrochloride	0.5	0.5
L-Arginine hydrochloride	0.5	0.5
L-Leucine	0.5	0.5
L-Valine	0.5	0.5
L-Aspartic acid	0.5	0.5
L-Serine	0.5	0.5
L-Glutamic Acid	0.5	0.5
L-Glutamine	0.5	0.5
L-Histidine hydrochloride-H2O	0.5	0.5
L-Isoleucine	0.5	0.5
L-Threonine	0.5	0.5
L-Methionine	0.5	0.5
L-Cysteine	0.5	0.5
L-Tyrosine	0.5	0.5
L-Proline	0.5	0.5
L-Alanine	0.5	0.5
L-Asparagine	0.5	0.5
Glycine	0.5	0.5
Other components	BM concentrations (mM)	NM concentrations (mM)
Adenosine	0.074	0.074
D-Glucose	16.6	16.6
Hemin	0.0077	0.0077

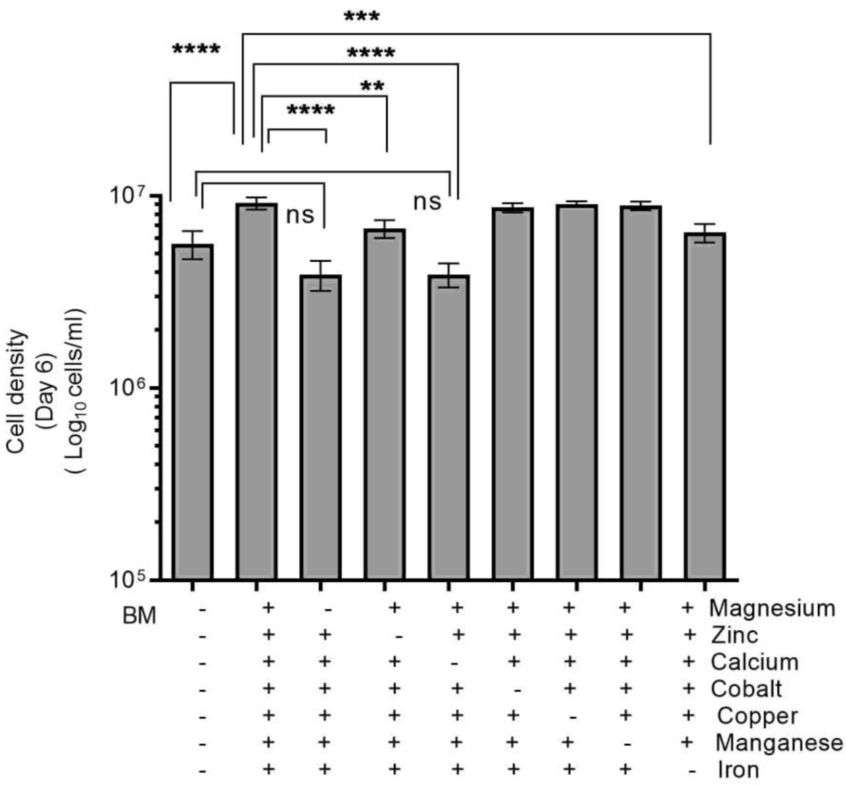

Figure 3.12 Effect of single omission of metals in defined medium.

(Error bars = mean ± SD, n=9)

Growth of *L. mexicana* promastigotes with starting density of 5 x 10^5 cells/mL in BM with and without the presence of individual metals. Cell density estimated after Day 6 from the start of culture initiation in late log phase of the growth cycle, independent experimental repeats in triplicates each time. Asterisks indicate significant difference with **** $p<0.0001$; ***$p<0.0005$, **$p<0.001$, ns non-significant with BM plus all metals except one in comparison to BM plus all metals, one-way ANOVA with Dunnett' s multiple comparison test.

Metals salts containing Iron (Fe), Cobalt (Co), Zinc (Zn), Copper (Cu), Manganese (Mn), Magnesium (Mg) and Calcium (Ca) were tested all together except one supplemented with BM as shown in Figure 3.12. Absence of manganese ($MnCl_2$, 0.000045 mM), cobalt ($CoCl_2$, 0.000032 mM), and copper ($CuSO_4$, 0.0005mM), had minor effect on the growth rate. Lack of magnesium ($MgS0_4.7H_20$, 0.81 mM), and calcium ($CaCl_2$, 0.72mM) exhibited the significant negative phenotype of growth with 75% and 60% decrease in cell viability respectively. Whilst, the absence of exogenous zinc ($ZnCl_2$, 0.03 mM), and iron ($Fe(NO_3)_3.9H_2O$, 0.009 mM) decreased total cell density by 35% and 45% respectively.

3.2.1.5 Evaluation of growth potential in the presence of both metals and cofactors

The growth of *L. mexicana* promastigotes was monitored in the presence of a combination of co-factors and metals and expressed as total cell density recorded on Day 6 from the start of culture initiation and doubling time (hours) as shown in Figure 3.13 and Figure 3.14.

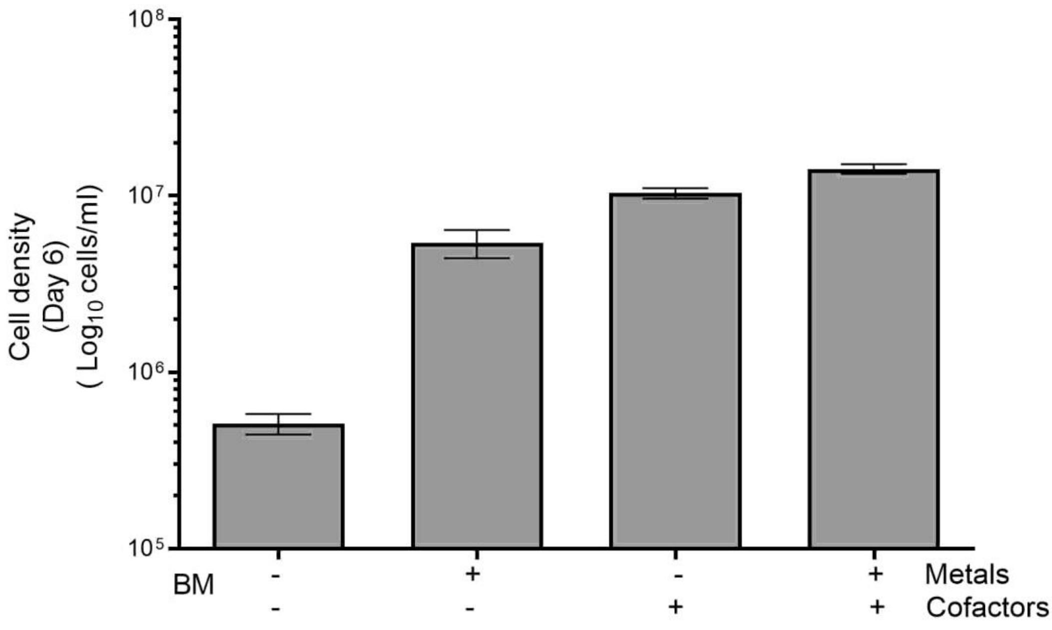

Figure 3.13 Cell density of *L. mexicana* promastigotes grown in BM with and without cofactors and metal salts individually and in combination.

(Error bars= mean ± SD, n=9)

Parasites were inoculated at a density of 5 x10^5cells/mL and aliquots of culture were counted in independent experimental repeats with triplicates each time on Day 6 of culture initiation.

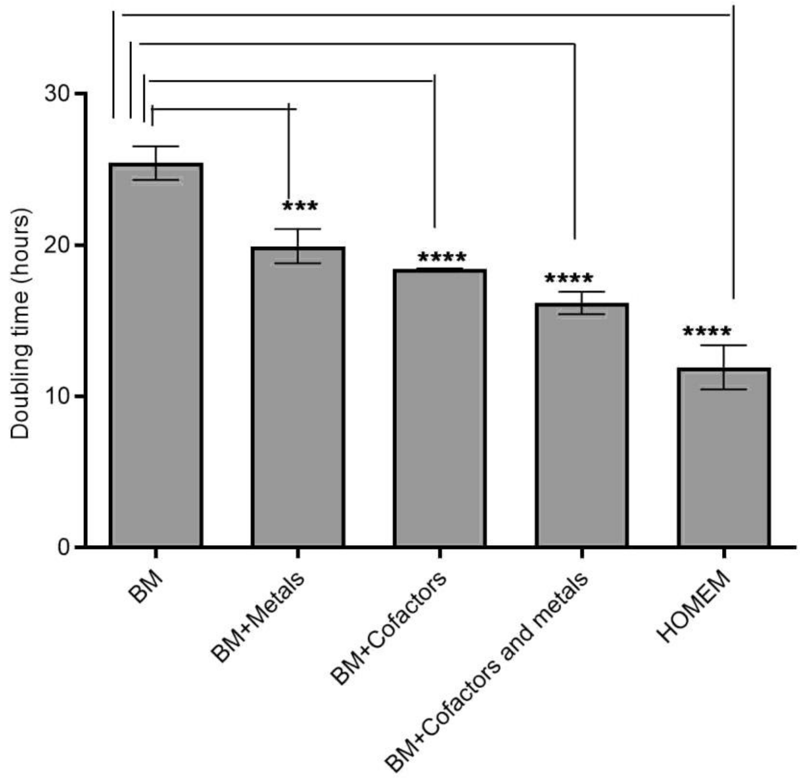

Figure 3.14 Effect of cofactors and metals on doubling time of *L. mexicana* promastigotes grown in BM with and without cofactors and metal salts individually and in combination.

(Error bars= mean ± SD, n=9)

Parasites were inoculated at a density of 5 x 10^5cells/ml and aliquots of culture were counted in triplicates at every 24 hours thereafter; up to day 6 from the start of culture initiation as described in experimental procedures. Doubling time calculated from growth curves conducted each time in sets of triplicates, repeated independently thrice. Number of Asterisks indicate significant p values with **** $P<0.0001$ and *** $p<0.005$, one way ANOVA with Dunnett's multiple comparison test.

From Figure 3.13 and Figure 3.14, the addition of co-factors such as biopterin, riboflavin, lipoic acid and folic acid at 10µM together with metals salts such as magnesium, calcium, zinc, iron, manganese and cobalt at respective concentrations ($MgSO_4.7H_2O$, 0.81 mM, $CaCl_2$, 0.72mM, $ZnCl_2$, 0.03 mM, Fe $(NO_3)_3.9H_2O$, 0.009 mM, $MnCl_2$, 0.000045 mM, $CoCl_2$, 0.000032 mM and $CuSO_4$, 0.0005mM) resulted in a total increase in cell density. Also, the addition of these supplements increased the growth rate of promastigotes in culture expressed as doubling time during the growth period at under conditions tested.

3.2.1.6 Evaluation of continuous culture of *L. mexicana* promastigotes

Optimised serum and protein free medium with the addition of all amino acids, cofactors and metals is henceforth referred to as Nayak medium (NM) with growth analysis shown in Figure 3.15. Continuous culture with serial passages within the medium was evaluated up until passage 15 as shown in Figure 3.16.

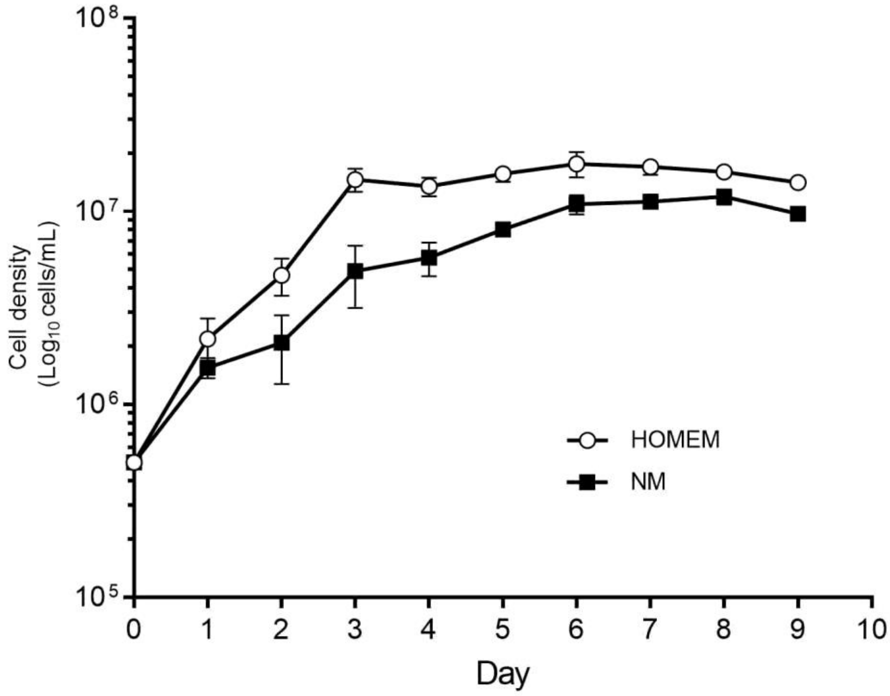

Figure 3.15 Growth of *L. mexicana* promastigotes in NM (closed squares) compared to growth in HOMEM with10%FCS (open circles).

(n=9, Error bars = mean ± SD).

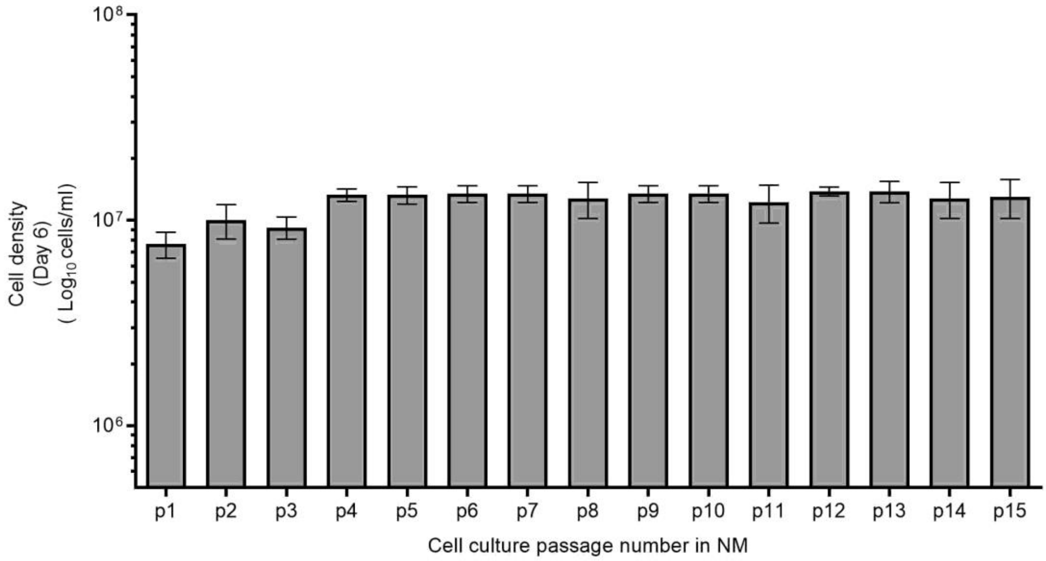

Figure 3.16 Growth of *L. mexicana* promastigotes in NM evaluated for the potential to support in continuous culture with passage numbered (p) accordingly.

Parasites were inoculated at a density of 5 x10^5 cells/mL and aliquots of culture were counted (n=9, mean ± SD) on Day 6 with sub passage carried out on Day 3 from the start of culture initiation as described in experimental procedures.

3.2.2 Evaluation of defined medium

3.2.2.1 Evaluation of growth potential of components in the presence of respective inhibitors

The growth promoting action of biopterin in the culture media was validated in the presence of methotrexate (MTX), a known competitive inhibitor for biopterin activity (Kumar et al., 2008) by alamar blue assay as shown in Figure 3.17.

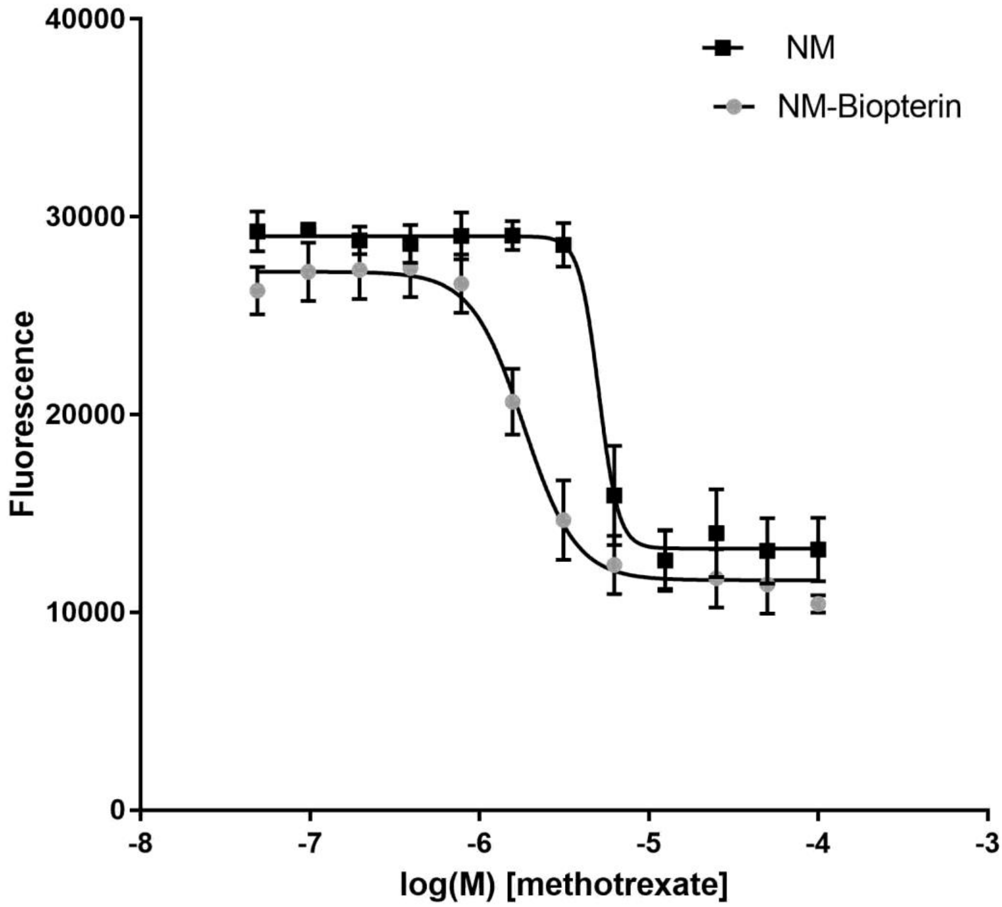

Figure 3.17 Alamar blue assay for *in vitro* drug sensitivity of Methotrexate (MTX) for *L. mexicana* grown in media NM with and NM without biopterin.

Experimental procedures described in methods for the alamar blue assay showed IC_{50} value = 1.1 µM for NM and IC_{50} value = 0.7 µM for NM without Biopterin. *L.mexicana* promastigotes were cultured in these two conditions two independent experimental repeats in triplicates each, n=6.

The absence of biopterin in the medium increases the susceptibility of promastigotes to the drug activity of MTX as shown by low inhibitory concentration (IC50 value) in NM-biopterin (grey circles) compared to higher IC_{50} value in the presence of biopterin in the media (black closed squares). Thus, biopterin serves an important constituent of the culture media composition of *L. mexicana* promastigotes as shown in Figure 3.17.

3.2.1.7 Growth in the presence of metal chelators

It was found that magnesium and calcium had substantial growth prompting action compared to other metals such as zinc, manganese, copper and cobalt as shown in Figure 3.12. To validate these results, alamar blue assay was carried out with competitive inhibitors of metal activity such as metal chelators- {ethylenediamine-tetraacetic acid} EDTA and {ethylene glycol-bis (β-aminoethyl ether)-N, N, N', N'-tetraacetic acid} EGTA for magnesium and calcium individually to adjust the composition of defined medium accordingly as shown in Figure 3.18 and Figure 3.19.

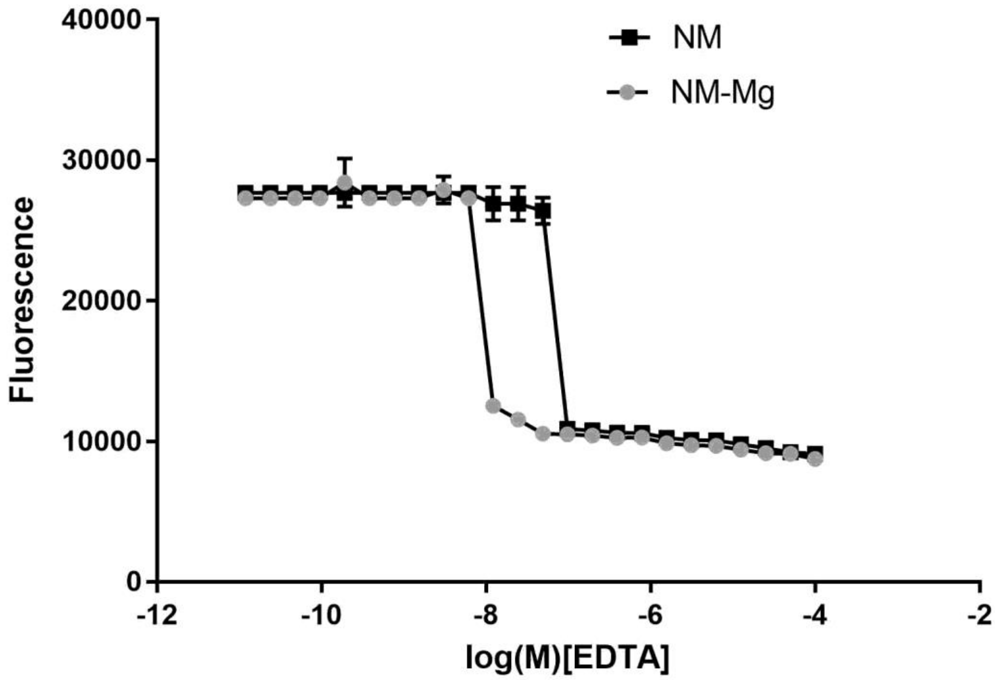

Figure 3.18 Alamar blue assay for *in vitro* drug sensitivity of EDTA for *L. mexicana* promastigotes grown in NM with and NM without Mg (0.81mM)

Experimental procedures described in methods for the alamar blue with EDTA was tested between 0-100μM to represents the range of concentrations that might have an inhibitory growth effect on promastigotes. It was found that the IC_{50} value = 30 μM with magnesium containing medium (NM) compared to modified NM without magnesium with IC_{50} value = 1 μM between the two conditions (n=6, two independent experiments).

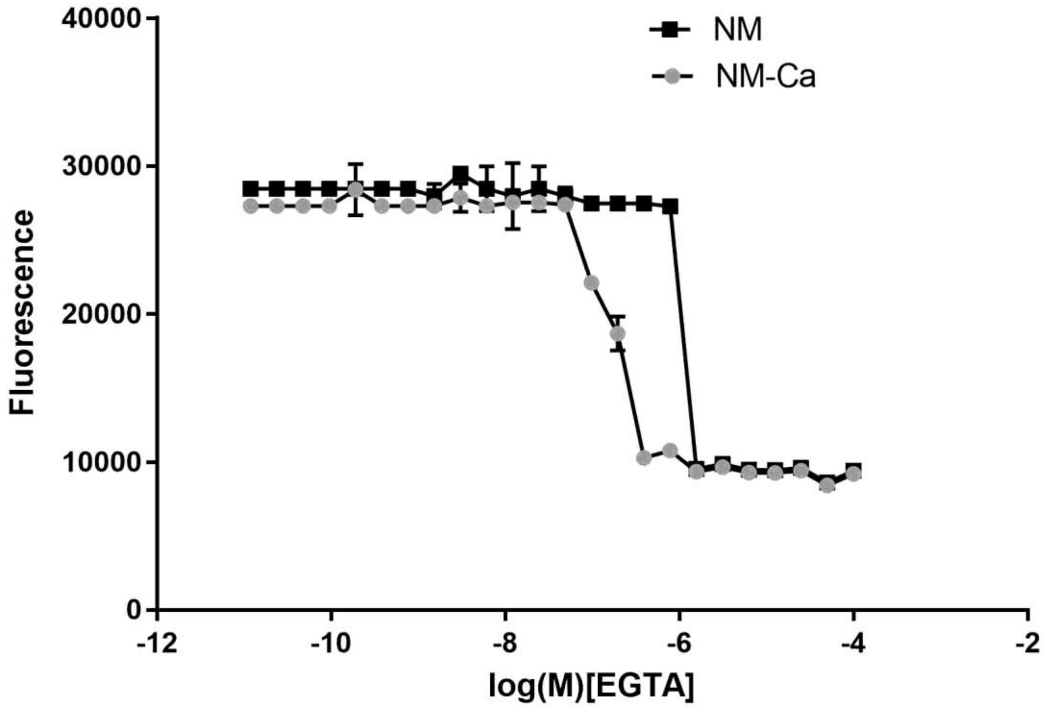

Figure 3.19 Alamar blue assay for *in vitro* drug sensitivity of EGTA for *L. mexicana* promastigotes grown in NM with and without metal mixture containing Ca (0.72mM).

Experimental procedures described in methods for the alamar blue with EGTA was tested between 0-100μM to represents the range of concentrations that might have an inhibitory growth effect on promastigotes. It was found that the IC_{50} value = 10 μM with NM (Nayak medium containing calcium) compared to NM-Ca (modified medium without added calcium) with IC_{50} value = 0.5 μM (n=6, two independent experiments).

The sensitivity of chelators determined by the concentration of the chelators needed to reduce cell yield by half during growth of *L. mexicana* promastigotes in NM for 5 days has been represented by the IC_{50} values. The cells grown with EGTA and EDTA exhibited decreased sensitivity in the presence of metals mixture. These chelators selectively compete with magnesium and calcium respectively. The presence of other individual metals did not significantly alter the sensitivity pattern compared to magnesium and calcium alone. The IC_{50} value of EDTA and EGTA was increased in the presence of magnesium or calcium in the medium.

These results validated the growth promoting action of magnesium and calcium on the growth of *L. mexicana* promastigotes in culture, hence inclusion in the medium composition.

3.2.1.7 Growth in the presence of adenosine

Adenosine was tested at different concentration in NM required to support the growth of *L. mexicana* promastigotes as shown in Figure 3.20.

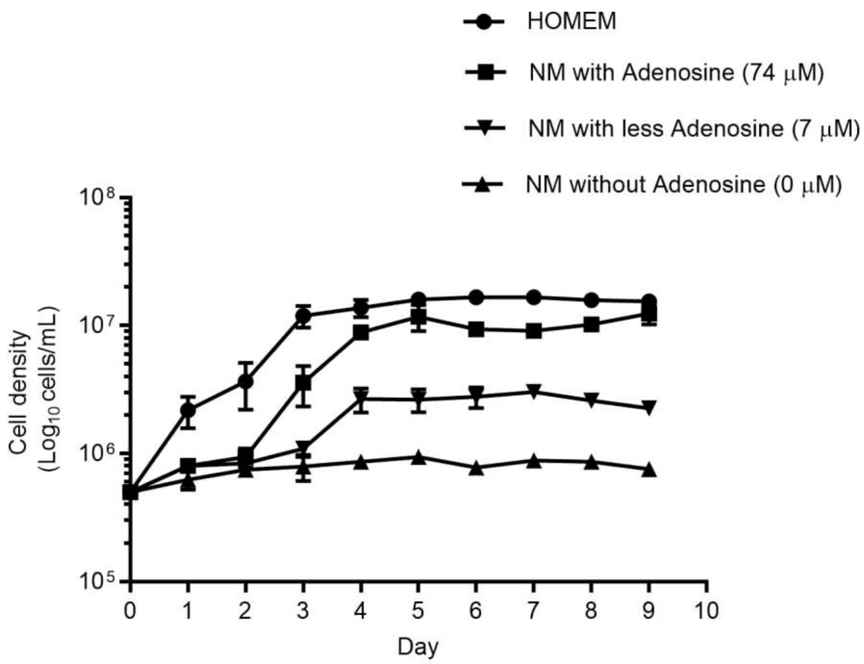

Figure 3.20 Growth of *L. mexicana* promastigotes with starting density of 5 x10^5 cells/mL in serum containing HOMEM (closed circles), NM with adenosine (74 μM, closed squares) or less adenosine (7 μM, inverted triangles) or no adenosine (0 μM, closed triangles).

Cell density estimated every 24 hours in 9-day growth period (Error bars = mean ± SD, n=9).

NM composition was tested under three different conditions with no adenosine, 7 μM adenosine (equivalent to adenosine concentrations in the serum) and 10-fold higher concentration of 74 μM adenosine. It was observed that adenosine serves as a major growth limiting nutrient, thus 74 μM adenosine was included in the final NM composition (Table 3-3).

3.2.1.8 Growth in the presence of glucose

It was of interest to check the growth of *L. mexicana* promastigotes with and without glucose in defined medium as shown in Figure 3.21.

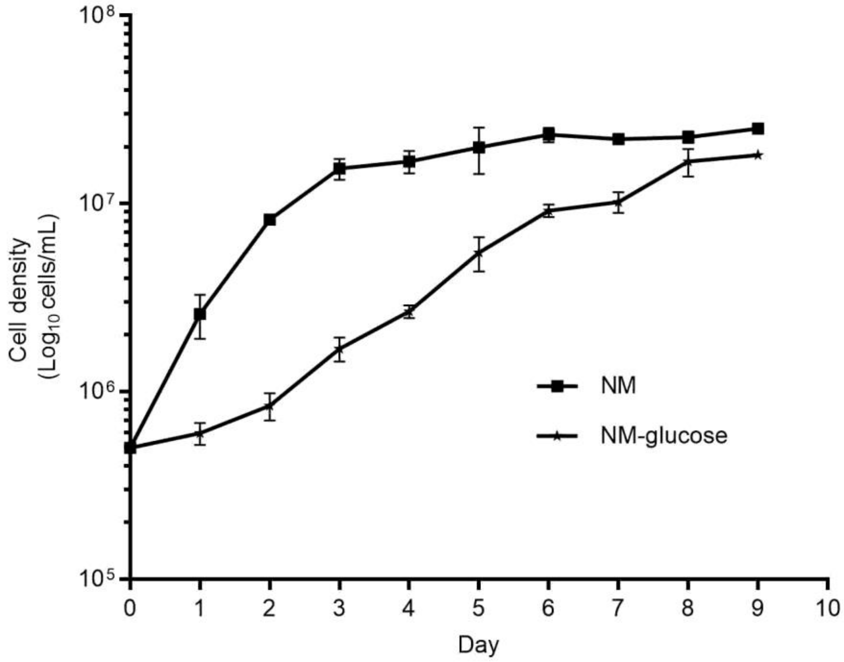

Figure 3.21 Growth of *L. mexicana* promastigotes in NM (closed squares) and NM minus glucose (closed triangles).

(Error bars = mean ± SD, n=9 with $p<0.0001$ in both comparisons, representative data from three independent experiments).

Omission of sugar (glucose 16mM) increased the lag phase with decreased cell density at stationary stages. The percentage of metacylics (~80% on Day 6) decreased two fold in the absence of glucose (~ 40%) with mixed populations of promastigotes of variable length.

3.2.2.1 Morphological evaluation of promastigotes growth

L. mexicana promastigotes were inoculated at a density of 5 x10^5cells/ml and visualised by giemsa staining on day 3 (log phase) and day 6 (metacylics phase) from the start of culture initiation in both the mediums (NM and HOMEM) as shown in Figure 3.22 and Figure 3.23.

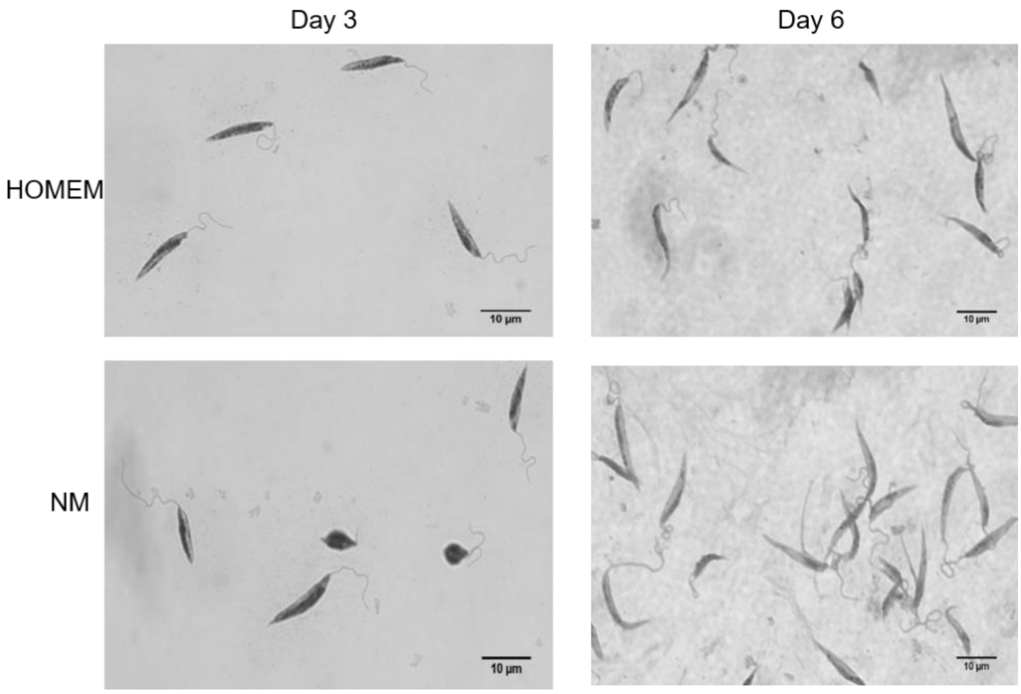

Figure 3.22 Cell morphology of *L. mexicana* promastigotes examined using Giemsa staining in HOMEM+10%FCS (top row) and NM (bottom row).

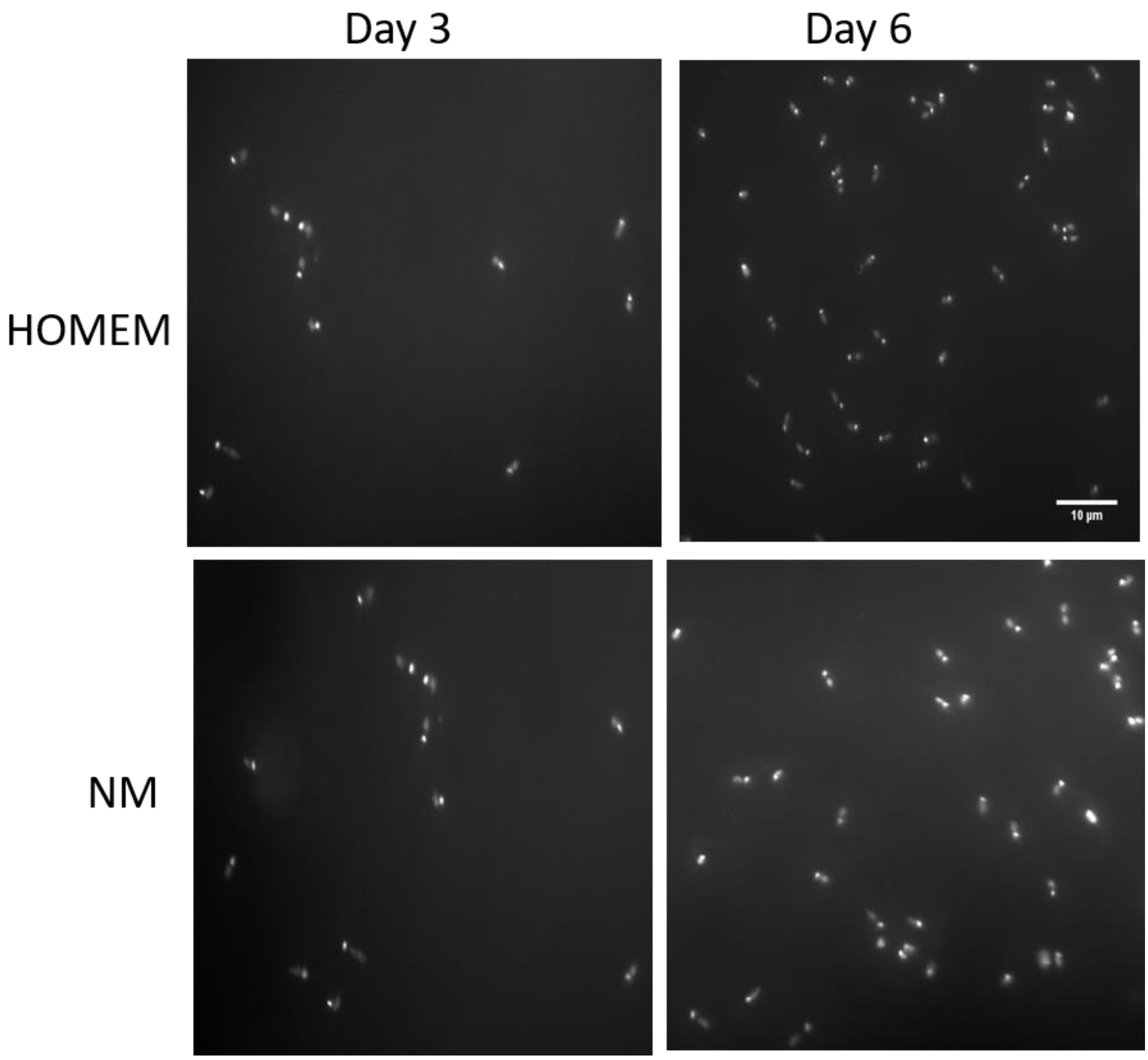

Figure 3.23 Nucleus and Kinetoplast position of *L. mexicana* promastigotes examined using DAPI staining in Homem+10%FCS and NM. From Figure 3.22, it was observed that promastigotes at log phase were shorter compared to elongated forms at stationary phase (Day 6). Also, cells at log phase procyclics promastigotes contained higher mean cell volume than at metacyclics stationary phase. This morphological pattern during the parasite life cycle could be visualised in NM owing to support normal cell growth as observed in HOMEM.

From Figure 3.23, with DAPI staining, the nucleus appeared ellipsoidal with the bar shaped deeply stained kinetoplast seen at the base of the flagellum.

3.2.2.2 Morphometric evaluation of promastigotes.

Cell body length of *L. mexicana* promastigotes stained and visualised at day 3 and day 6 of the growth cycle was measured as shown in Figure 3.24.

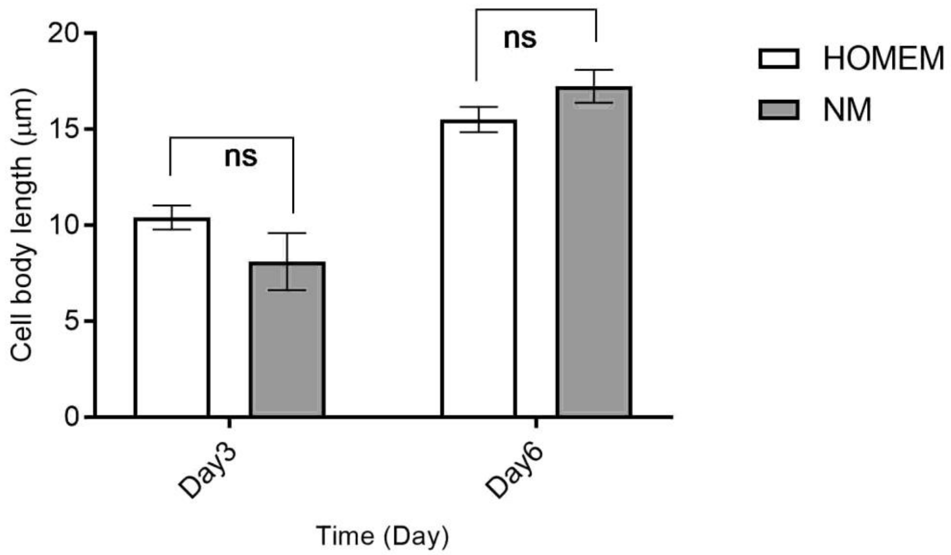

Figure 3.24 Morphometric evaluation of cell body length of *L. mexicana* promastigotes in NM compared to growth in HOMEM with 10%FCS (n=50, Error bars = mean ± SD).

1 x10^6 cells/ml from day 3 and day 6 of culture were counted stained using giemsa dye. Average of more than 50 images were taken using the camera on Zeiss Axiovision upright light microscope and analysed using Image J software for the measurement of cell body length of the parasites. Comparative evaluation of growth between the two media showed no statistically significant differences indicating promastigotes cultured in NM were the same length as HOMEM as shown in Figure 3.24.

3.2.2.3 Infectivity test of promastigotes.

The infective potential of promastigotes compared using differentiated monocytic cell line THP1 as a model between cells cultured in NM and HOMEM as shown in Figure 3.25, Figure 3.26, Figure 3.27 and Figure 3.28.

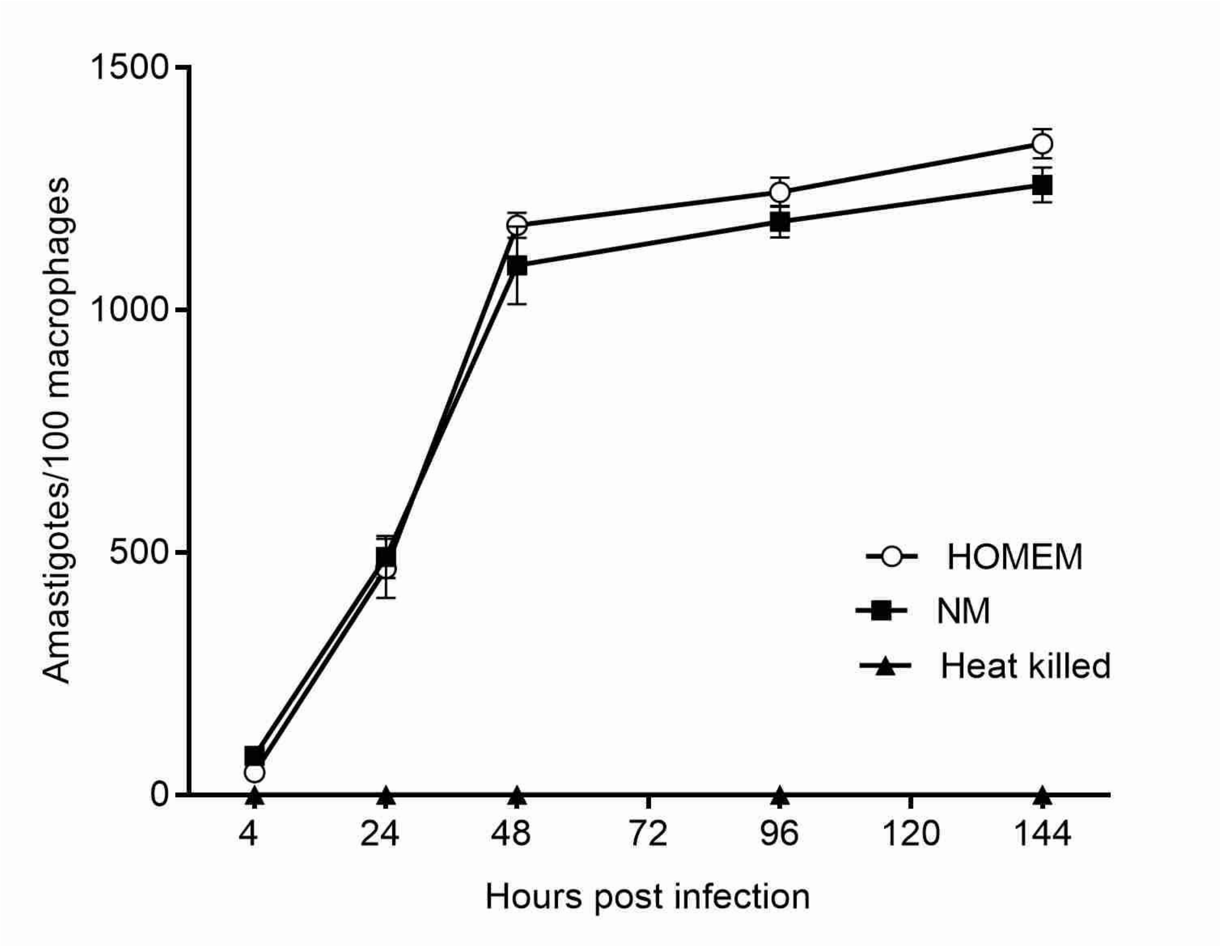

Figure 3.25 Total number of amastigotes per hundred macrophages measured to determine the infectivity of promastigotes cultured in medium containing either HOMEM (open circles) or NM (closed squares), heat killed promastigotes in NM (closed triangles).

(Error bars= mean ± SD, n=9 with independent experimental repeats with 1 x 10^5 cells/mL promastigotes grown in either media upon infection in 1:10 ratio with 1 x 10^6 cells/ml macrophages counted as number of amastigotes per 100 macrophages. Heat killed promastigotes in NM served as a negative control).

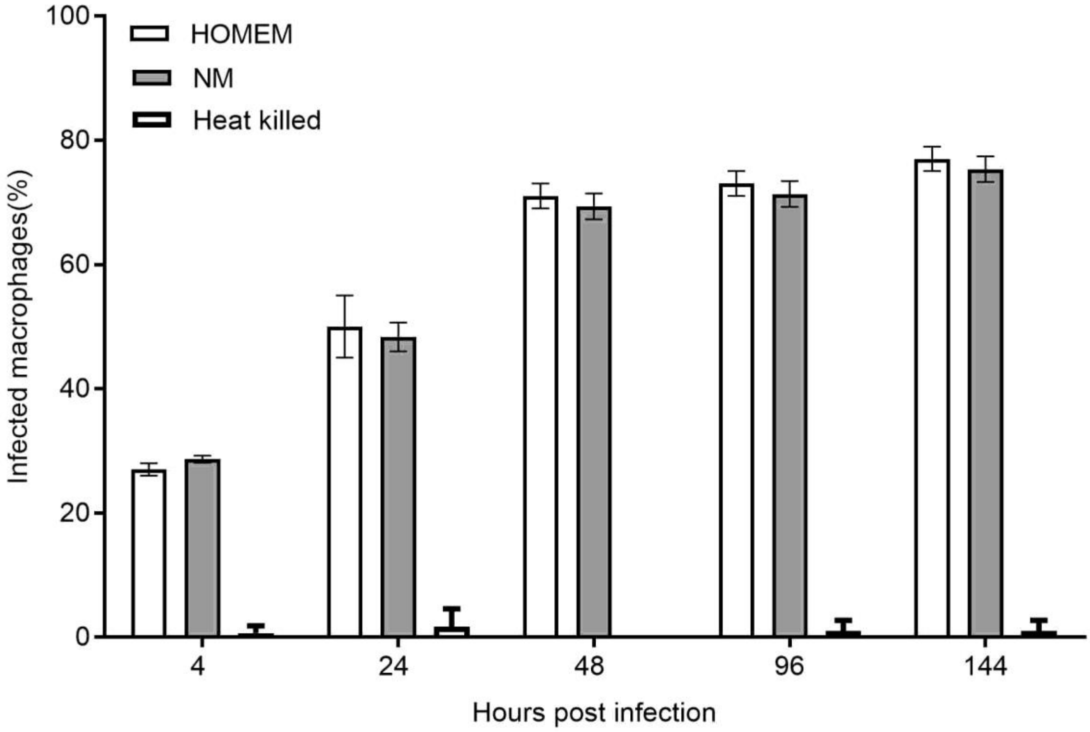

Figure 3.26 Percentage of infected THP1 differentiated macrophages with *L. mexicana* promastigotes grown in medium containing either HOMEM (open bars) or NM (closed bars) (n=9, mean ± SD) with heat killed promastigotes as a negative control.

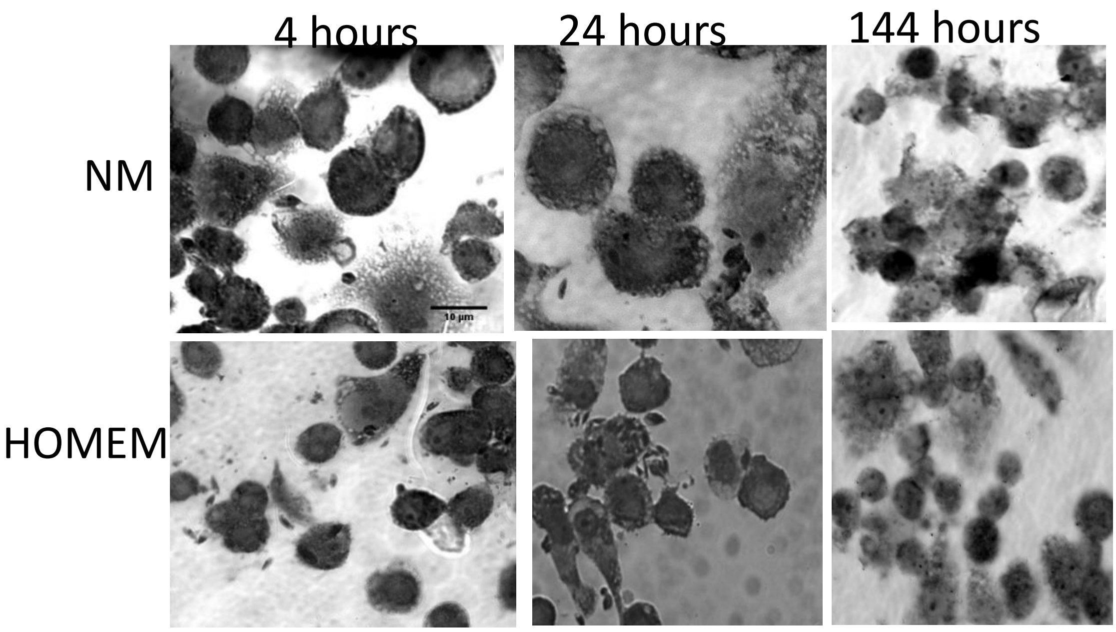

Figure 3.27 Giemsa stained images of infected THP1 cells with at 4 hours, 24 hours and 144 hours post infection as described in experimental procedures.

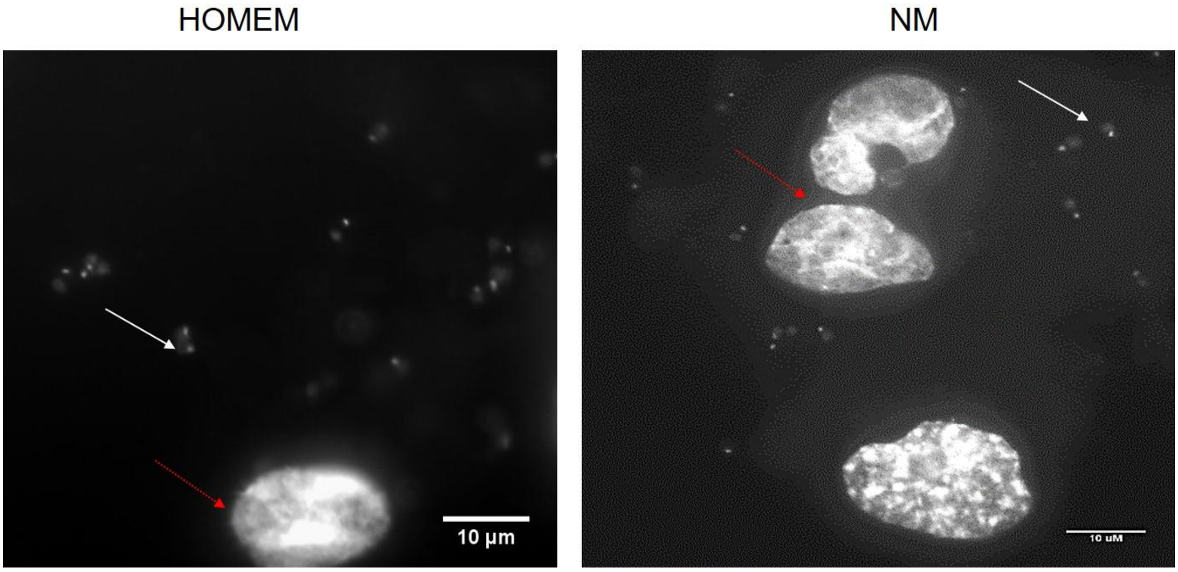

Figure 3.28 Nucleus and kinetoplast position of *L. mexicana* promastigotes (white arrow head) and macrophages nucleus (red arrow head) examined using DAPI staining in Homem+10%FCS and NM.

From Figure 3.25, the infective potential of the promastigotes was comparable between cells cultured in NM and HOMEM with the slight proportion of lysis in serum containing HOMEM at 4 hour time point with the lesser attachment of promastigotes established within the macrophages at that stage. However, similar proportion of metacylics were recorded in both HOMEM and NM and showed similar infectivity profiles as shown in Figure 3.26

The percentage of infected macrophages were similar between 60-80% in both medium conditions evaluated at 4 hours, 24 hours and 144 hours post infection as shown in Figure 3.26.

The infected macrophages were visualised using giemsa and Dapi staining as shown in Figure 3.27 and Figure 3.28 analysed by image analysis as described in the experimental procedures.

3.2.2.4 Drug sensitivity assay

Drug sensitivity assays were carried out using leishmanicidal drugs (Tiuman et al., 2011) with amphotericin B, pentamidine and methotrexate to evaluate their activity in NM and HOMEM as shown in Figure 3.29.

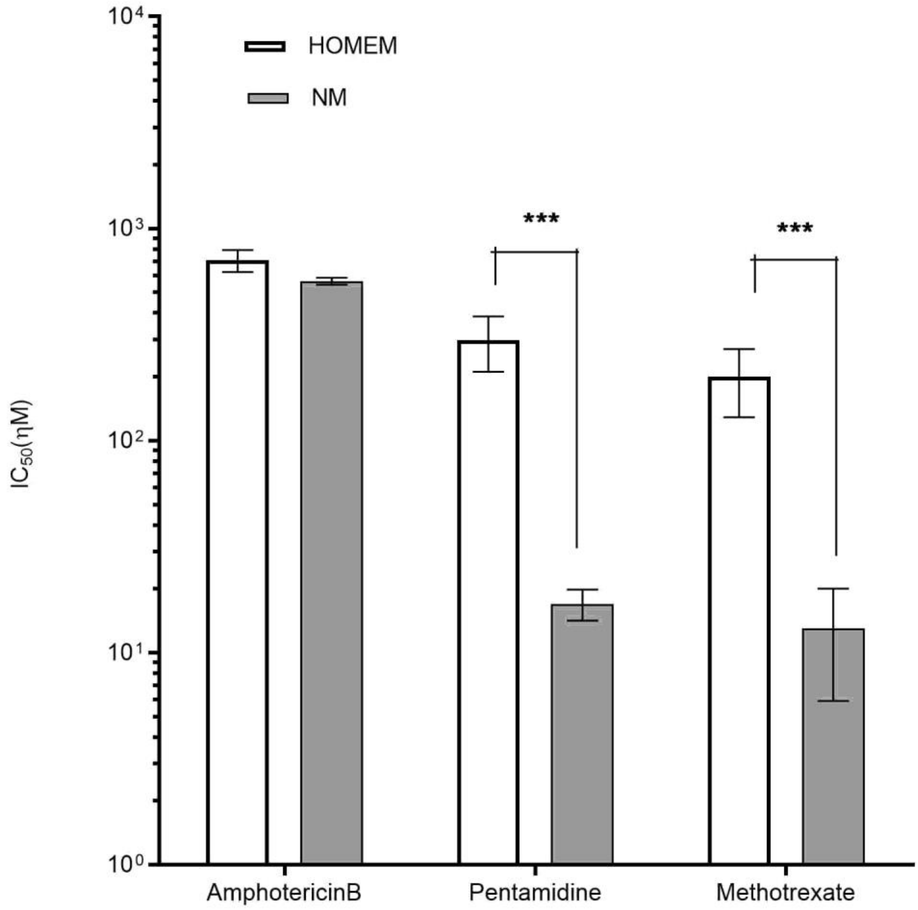

Figure 3.29 Alamar blue assay for *in vitro* drug sensitivity of Amphotericin B, Pentamidine and Methotrexate for *L. mexicana* promastigotes grown in media containing either HOMEM or NM.

Error bars = mean±SD, n = 6, two independent experimental repeats in triplicates each, asterisks indicate significant differences in drug activity with ***, p<0.0005 and **p < 0.001 in NM comparison to serum rich HOMEM, one way ANOVA with Dunnett’s multiple comparison test).

The IC_{50s} obtained in NM in comparison to those obtained in HOMEM showed one compound with no significant effect of the media on the IC_{50} value, whilst the differences observed with other two compounds were 2-fold in magnitude. The differences in the susceptibility between the drugs could be partly be explained because of different mode of action of each of these drugs explained in more detail by Basselin et al, 2002. Briefly, the activity of amphotericin B (average IC_{50} 710 nM and 554 nM) result in similar IC_{50} values between the two media; possibly owing to the fact that amphotericinB affect the intracellular metabolism of the cells especially in lipid biosynthesis [Roy Ph.D. thesis, III, UofG, 2016] not directly be affected by culture composition alone.

On the other hand, pentamidine (PTM), inhibitor of anionic amino acid channel showed increased leishmanicidal activity in NM (IC_{50} 14 nM) compared to HOMEM (IC_{50} 390 nM) which might be because of different concentrations of amino acids in serum containing HOMEM media compared to NM. Variable compositions between serum batches contributes to variable action of drugs such as PTM. Methotrexate (MTX), inhibitor of dihydrofolate reductase has higher leishmanicidal activity in NM (IC_{50} 10 nM) than HOMEM (IC_{50} 200 nM). Dihydrofolate reductase contributes to pyrimidine biosynthesis but increased concentration of folate in serum containing media might alleviate MTX action in HOMEM compared to MTX action in NM described in the discussion section of this chapter. Also, addition of biopterin to defined medium inhibits the activity of methotrexate; which might partly explain the increased leishmanicidal activity of methotrexate in NM compared to HOMEM (Beverley et al., 1986).

3.2.2.5 Optimisation of the colorimetric assay for growth monitoring in NM

Growth analysis of *Leishmania* promastigotes in culture was conducted by optimisation of colorimetric assay as shown in Figure 3.30 and Figure 3.31.

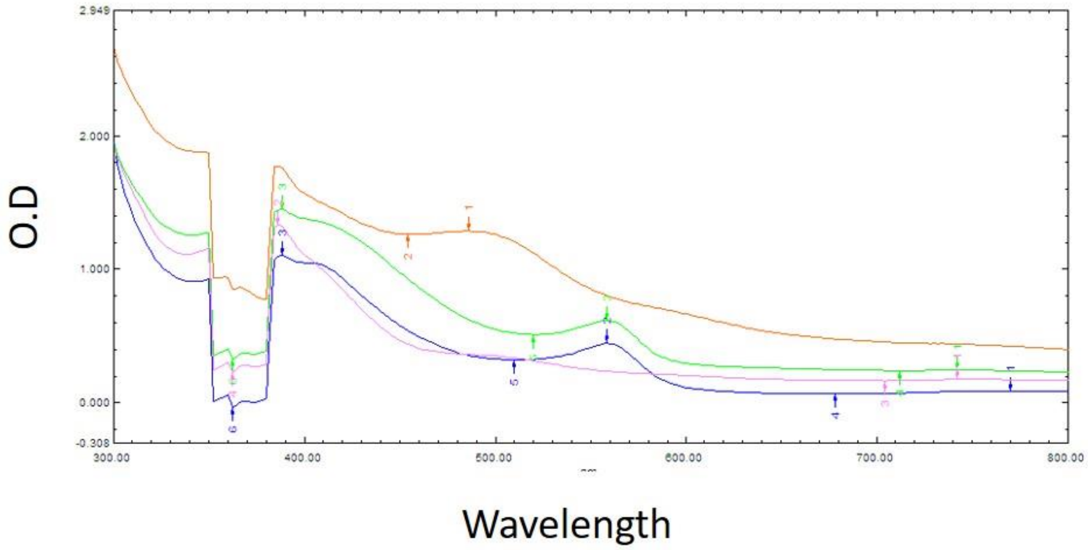

Figure 3.30 Optimisation of MTS colorimetric assay in NM with O.D (optical density) on Y axis and range of wavelength (300nm to 800 nm).

2 x 10^5 cells/mL of *L. mexicana* promastigotes in NM and absorption spectrum measured at 24 (blue), 48 (pink), 72 (green), 96 (orange) hours with tetrazolium compound MTS ([3-(4,5-dimethylthiazol-2-yl)-5-(3carboxymethoxyphenyl)-2-(4-sulfophenyl)-2H-tetrazolium) reagent (Promega).

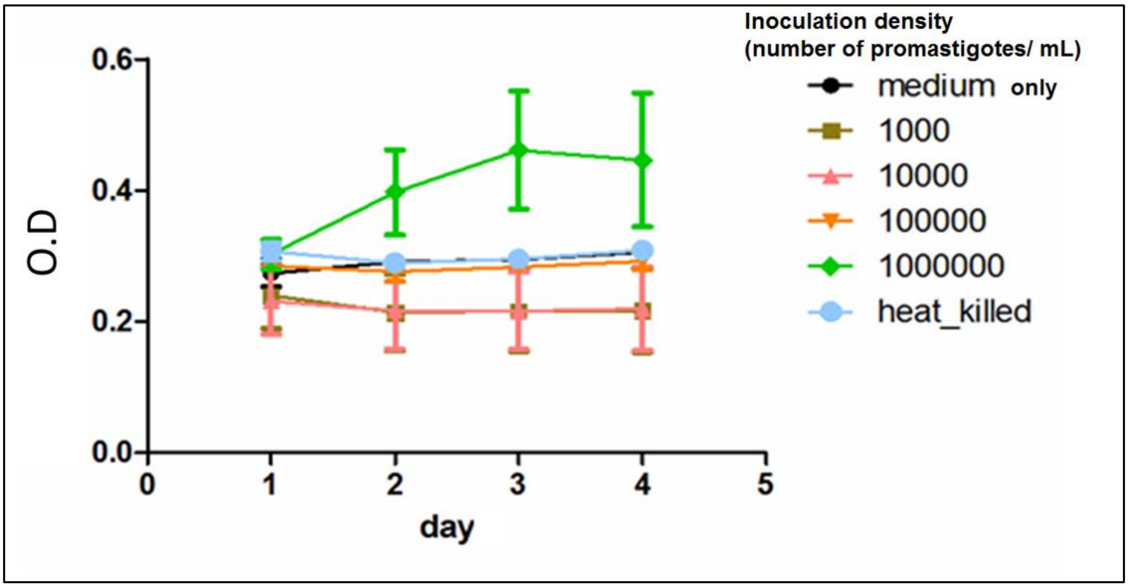

Figure 3.31 Optimisation of colorimetric assay to determine appropriate inoculation density with O.D (optical density) on Y axis and Day 0 from the start of culture initiation to Day 5 on the X axis.

L. mexicana promastigotes with inoculation densities between 1 x 10^3 cells/mL (brown), 1 x 10^4 cells/mL (pink), 1 x 10^5 cells/mL (orange), 1 x 10^6 cells/mL (green) cultured in NM with tetrazolium compound MTS ([3-(4,5-dimethythiazol-2-yl)-5-(3carboxymethoxyphenyl)-2-(4-sulfophenyl)-2H-tetrazolium) reagent (Promega) were aliquoted to measure the optical density at 395 nm on Day 1, 2, 3 and 4 from the start of culture initiation. Naïve medium samples (black) without cells and heat killed cells (blue) in the medium were also tested at similar times as positive and negative controls.

There was an increase in overall value of optical density with the MTS/PMS dye at 37ºC, however, manual morphological examination of parasites showed increased percentage of metacyclics with long slender cell body; not expected at day 3 of the culture compared to incubation at 27ºC. An important inference meant the appearance of the coloured product alone cannot be considered as a direct measure of growth; since temperature could accelerate the formation of the coloured product and not because of metabolically active cells. Hence, the shift in OD at a steady temperature owing to the change in reduction of MTS dye alone reflects the metabolic activity to accurately reflect the fold difference in cell density.

From Figure 3.30, it was also noted that wells with MTS alone without cells had a significant increase in OD readings after 24-hour incubation period. Hence, the optimal incubation time was up-to 3 hours which correlated linearly with the total count of the parasite. Any further increase in OD after this point of incubation was observed due to auto-oxidation. Hence, it was not possible for repeated use of same culture plates and variable OD values made control subtraction difficult to exclude from background values with the maximum peak activity of optical density (O.D) at 395 nm respectively.

From Figure 3.31, the increase in optical density throughout the growth cycle of promastigotes in NM was measured under different incubation density with optimised at 1 x 10^6 cells/mL. There was an increase in the OD observed with 1 x 10^6 cells/200 µL/well, there was no linear correlation between the shift in OD and manual growth counts at further time points. Also, the effect of the cofactors which could variously modify the mitochondrial dehydrogenase enzyme activity could not be ignored. Thus, a shift in OD due to the conversion rate of the MTS/PMS dye into coloured formazan product could not be directly accounted for the effect of cofactors on growth. Possibly, OD measured at 380 nm might show better visual measurement with MTS reagent; if colorimetric optimisations were to be repeated. In summary, these results indicated that evaluation of growth kinetics in the presence/absence of additional components was best carried out using manual counting and morphological examination as elaborated earlier in section 3.2.1.

3.3 Discussion

An undefined component such as serum leads to difficulty in purifying parasite antigens for vaccine development, variable metabolic response between different batches of serum, contamination of the source serum with other organisms. For example, advanced filtration techniques have been adopted to avoid mycoplasma infection screening, however, these filters have not yet surpassed to remove viruses as explained in Section 1.1. Serum from cattle from particular countries has been reported to contain a higher percentage of prions associated with the risk of bovine spongiform encephalitis amongst the cattle in Europe and North

America [Book on culture of animal cells, Freshney]. To achieve purified cultures of *Leishmania* antigens, metabolic profiles, drug testing and reproducible results between experimental repeats under identical experimental conditions, we set out to develop a serum and protein free medium. The key features for consideration for medium composition was based on the rationale that medium has minimal buffer base with only HEPES adjusted to pH 7.4 and the medium has purified ingredients to substitute for any non-defined components such as bovine serum albumin, casein, urine extracts or Tween80 and thirdly, only minimal components required to support growth of *L. mexicana* promastigotes *in vitro*. Initially, the proportions of components in (Steiger and Black, 1980) were adapted.

As shown in Table 3-1, the components of Steiger medium were compared to components from the Merlen medium and new base medium with minimum components was selected based on the impact of the growth of *Leishmania* promastigotes. REIX medium composition has only 11 amino acids but amino acids such as L-Arginine, L-Cysteine, L-Aspartate, L-serine, L-Glutamic Acid, L-Glutamine, L-Proline, L-Alanine, L-Asparagine and L-Glycine were missing in REIX composition. The reason these amino acids were not included in the medium could partially be because the REIX medium was optimised for *L. donovani* species. Individual nutritional requirements of *L. mexicana* promastigotes during the growth cycle has not been reported before.

Bioinformatics analysis of amino acid essentiality by comparison of genome sequences have shown that L-Arginine biosynthesis pathway is missing in *L. major* [52]. L-Arginine has shown to be subverted from the host cells to support and maintain parasite viability and proliferation leading to a high infection rate of *Leishmania* within macrophages (Colotti and Ilari, 2011). Thus, efforts in this chapter have been focused on designing medium composition with components required for the growth of *L. mexicana* promastigotes in *in vitro* culture conditions. Since individual requirements of amino acids will vary from one species to another, the base medium (BM) was supplemented with equimolar concentration at 0.5 mM of all amino acids (Figure **3.2**) resulted in higher growth rate and viability on sub-passage of *L. mexicana* promastigotes than REIX.

HOMEM media supplemented with 10% FCS has been reported elsewhere that amino acids between a range of 0.01-1.0 μM (Wishart et al., 2007). The range of amino acid concentrations are approximate and the order of magnitude varies with the type/source of serum used in specific experiments. Direct comparison of a range of amino acid concentrations affecting the growth of *L. mexicana* without the influence of undefined components such as serum or serum derived macromolecules have not been reported earlier. In this study, 0.5 mM of all amino acids was used in the base medium as starting point to test the viability of cells in multiple passages for continuous culture. The presence of all amino acids in BM supports better growth *L. mexicana* promastigotes compared to REIX with only 11 amino acids (Figure **3.2**).

Further efforts were made to optimise the growth rate in the defined medium by addition of co-factors and metals as appropriate. Results from Figure 3.3 to Figure 3.14, the results showed that the medium composition was improved by the addition of co-factor mixture containing biopterin, lipoic acid, riboflavin and folic acid supports increasing cell density and required to be added fresh for continued passage. To ensure that only minimal components are present in the medium, we tested the effect of replacing folic acid with an equimolar mixture of para-aminobenzoic acid (PABA) and biopterin, which mammals can readily convert to folic acid. The presence of PABA in the culture medium did not lead to increase in cell density, confirming that absence of either folic acid or biopterin reduced mean cell density ($P<0.0001$ in both comparisons, n=9, representative data from more than five independent experiments, one way ANOVA with Dunnett's multiple comparison test). The addition of cofactors combination containing lipoic acid, riboflavin, folic acid and biopterin together decreased the doubling time from 30 hours to 16 hours along with the addition of metals and all amino acids.

Early studies in *Leishmania* species report higher requirements of vitamins, thiamine, nicotinic acid, pantothenate, riboflavin, biotin, heme, high levels of folic acid, 6-hydroxymethylpterine and related pteridines for kinetoplastid assemblage (Chang and Hendricks, 1985). Hence, individual co-factors were tested based on differences in cell densities by manual counting and colorimetric assays to optimise the concentrations required to formulate the composition of Defined Medium as shown in Figure 3.3 to Figure 3.14.

Extensive literature search for medium compositions including Walkinshaw et al, Beverly (Lima et al., 2014, Papadopoulou et al., 2002) served as reference for optimising the concentrations of putrescine, p-Aminobenzoic acid, Riboflavin, Biotin, DL-α-Lipoic acid (oxidised form), Folic acid, 6-Biopterin to be included in the Defined medium. For the purposes of a minimal medium, the rationale was to include only those exogenous sources which are required for chemical energy generation, precursors and co-factors that have growth promoting action for *in vitro* culture of the parasites.

Putrescine has been recently shown to have substantial growth promoting activity for *T. cruzi*, belonging to the same order of Kinetoplastida (Lima et al., 2014). Under the conditions of DM in the presence of all amino acids including L-Arginine, we observed there was no significant increase in growth with 10 µM of putrescine for *L. mexicana* promastigotes. Putrescine biosynthesis requires ornithine decarboxylase/ L-Arginine decarboxylase (ODC/ ADC) enzyme to convert L-Arginine to putrescine via ornithine. JM Boitz et al have shown that ODC mutant is unable to infect host macrophages and is indispensable for survival within a host system(Boitz et al., 2009). Hence, these results re-confirm that *Leishmania* depends upon de-novo biosynthesis of putrescine via L-Arginine metabolism and an exogenous source of putrescine does not have additional growth promoting effect (Figure 3.3).

Initially, vitamins included in DM were added from commercial stock solution. Different manufacturers have various compositions in their mixture, with certain commercial solutions not containing riboflavin, biotin or folic acid in their vitamin mixture. Riboflavin is an important co-factor required for NADH biosynthesis and energy generation (Opperdoes and Coombs, 2007, Castro and Tomas, 2008); hence, it was speculated that addition of this precursor molecule could decrease the lag period of growth. The addition of riboflavin had a positive effect ($P<0.001$ in both comparisons, $n=9$ several independent experiments, one way ANOVA with Dunnett's multiple comparison test) with a small increase in cell density with riboflavin alone (Figure 3.4); but pronounced growth promoting effect in the presence of biopterin.

Biotin also had a small positive effect ($p<0.001$) on the growth of *Leishmania* promastigotes, hence was included in the medium composition as shown in Table 3-3. Biotin acts as an important cofactor for the enzyme carboxylyases required for the fatty acid synthesis. Search for *Leishmania* specific genes in Genebank database returned no accession numbers for enzymes involved in the synthesis of most vitamins such as biotin, pantothenate, thiamine, folic acid, etc. Bioinformatics analysis by CC Klein, et al 2013 using genomic sequences comparing trypanosomatid species indicated a lack of enzymes for the biosynthesis of these vitamins (Klein et al., 2013).

The addition of Lipoic acid to BM showed distinct positive effect ($p<0.001$) with a decrease in the lag time of *L. mexicana* promastigotes in culture compared to the absence of it (Figure 3.5). However, the growth promoting ability of lipoic acid is less than folic acid or biopterin. Lipoic acid serves as co-factor for enzymes such as pyruvate dehydrogenase, branched chain dehydrogenase and other enzymes. It has been previously shown that *Leishmania* has both de-novo biosynthesis pathway for lipoic acid and also, *Leishmania* genome encodes specific transporters to uptake lipoic acid from the environment (Bissett Ph.D. thesis, III, UofG, 2009).

Folic acid is another important co-factor tested for growth promoting activity using *L. mexciana* promastigotes. In mammals, a complex compound of folic acid in the form of tetrahydrofolate (THF) is required for purine synthesis along with serine, glycine and formate(Rowe and Lewis, 1973). THF also serves as an important catalyst for reactions in L-Methionine recycling and pyrimidine biosynthesis. Folate in *Leishmania* is metabolised by bifunctional DHFR (dihydrofolate reductase) TS-thymidylate synthase to further metabolic intermediates such as 5, 10-methylene-tetrahydrofolate (required for pyrimidine synthesis); 10-formyltetrahydrofolate required for methionyl-tRNA(Met) formylation for protein synthesis (Beck and Ullman, 1990). It was observed that increasing concentration of folic acid have a positive growth effect with an increase in cell density observed over 9-day period (Figure 3.10). This is in agreement with previous data about lack of PABA transporters in *Leishmania*; hence more external dependence for folate and biopterin supplementation in defined medium culture (Kar, 1997, Beck and Ullman, 1990); also, when tested with *L. donovani* promastigotes and Vickers et al (Scott et al., 1987, Vickers and Beverley, 2011) with *L. infantum* species.

In higher eukaryotic organisms, folic acid biosynthesis occurs in the presence of PABA with the addition of pterin component and glutamic acid by the enzyme DHPS (dihydropteorate synthase)(Rowe and Lewis, 1973). Results as shown Figure 3.3 to Figure 3.9 demonstrated that addition of PABA did not significantly increase cell density. Irrespective of the presence of PABA, only folic acid in conjunction with biopterin made a significant increase in cell density. Genome search for DHPS in TritrypDB.org returned no hits for the enzyme in *L. mexicana*. Hence, these results confirm that *Leishmania* relies on the uptake of exogenous folic acid, rather than de novo folic acid biosynthesis of the same.

This is in agreement with previous radio labelled studies, no uptake of exogenous PABA reported in *L. major* promastigotes (Beck and Ullman, 1990). Antibiotics such as sulphonamides, structural analogs of PABA are reported as ineffective against *Leishmania* (Kumar et al., 2008). It has been confirmed in lizard parasite *L. tarentolae* that folic acid biosynthesis does not proceed through DHPS pathway, with speculations of an alternative pathway (Papadopoulou et al., 2002).

In mammals there are two pathways for biopterin biosynthesis, one pathway involves GTP as a precursor and other from sepiapterin to tetrahydrobiopterin catalysed by dihydrofolate reductase (Crabtree et al., 2009). There have been many studies highlighting the importance of biopterin for *Leishmania* and why it deserves further investigation as a drug target (Kaur et al., 1988, Ouellette et al., 2002). *Leishmania* might obtain their folate from biopterin; whilst mammals bypass this pathway as the pterins are recycled by GTPs and in bacteria, GTP contributes to folate. The functional roles of biopterin in trypanosomatids are not known. In mammals, it acts as co-factor for L-Phenylalanine hydroxylase, L-Tyrosine hydroxylase, L-Tryptophan hydroxylase for neurotransmitter biosynthesis, but in single celled protozoan parasites there is no neurotransmitter biosynthesis, and hence the exact role of pterin is still unclear.

Growth promoting activity of folic acid was increased in the presence of biopterin (Figure 3.8). Amongst the co-factors tested, it was observed that addition of biopterin had a significant increase in cell density above 10^7 cells/mL. Serum concentration of biopterin ranges from 1-10 µM (Wishart et al., 2007). It was speculated that serum free condition might pose a greater need for biopterin. Hence, a range starting from 0-200 µM of biopterin was tested in increasing concentration. It was observed that the growth promoting activity of biopterin was linear up-until 0-10 µM ($p<0.0001$) and saturated after that concentration. However, supplementation of 100 µM biopterin was required for first axenic culture. For example, *Leishmania* promastigotes from stabilates exhibited a significant decrease in the lag period of growth with supplementation of 100 µM biopterin directly into the flask.

Growth promoting activity has been checked in two approaches; firstly, the addition of each component at a time was tested to determine the impact of the cofactors on total cell density achieved on Day 6 of the culture. In this case, the concentrations adopted were from other medium formulations (Ouellette et al., 2002, Moore et al., 1967). Among the co-factors, biopterin alone had significant growth promoting activity ($p<0.0001$, multiple comparison, ANOVA). An alternative approach used to validate these results was by single omission of a co-factor in the culture medium at a time. This showed that biopterin > lipoic acid > folic acid > riboflavin followed an increasing order of impact on the *in vitro* growth of promastigotes.

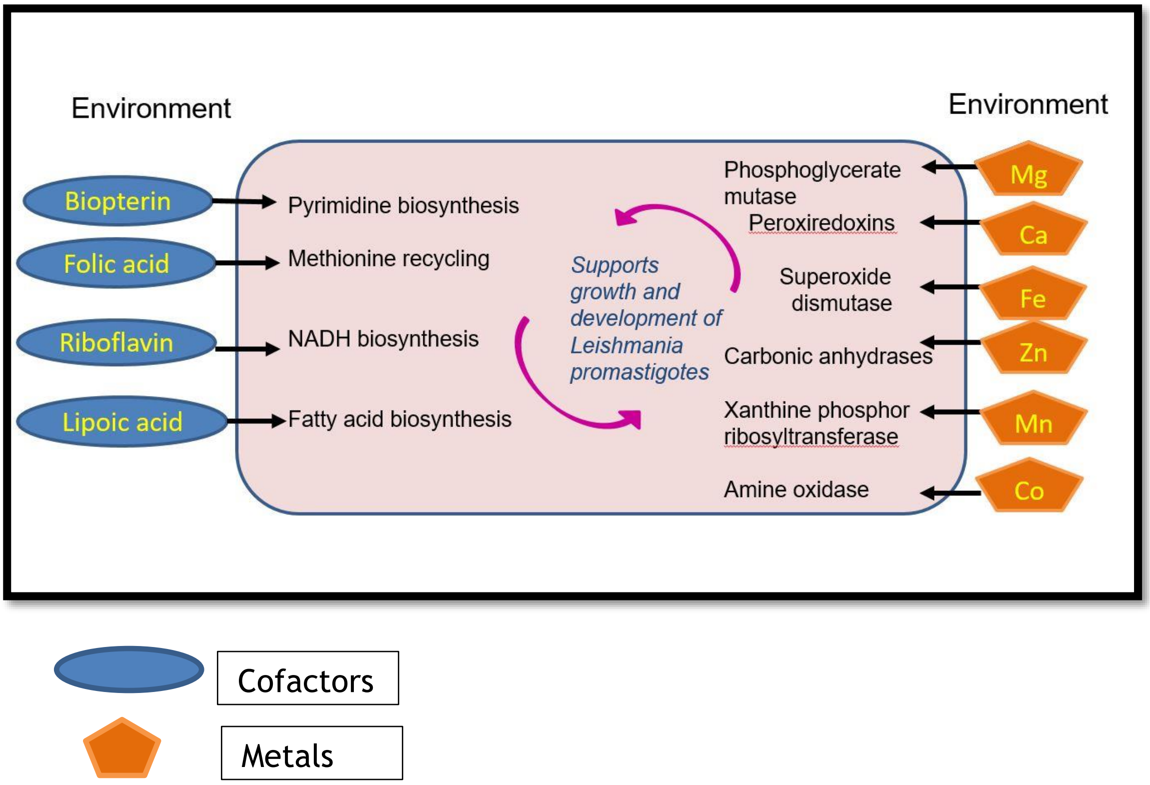

Figure 3.32 Pictorial summary of cofactors and metals used in NM composition for the growth of *L. mexicana* promastigotes in culture.

Abbreviations: Mg- magnesium, Ca-calcium, Fe-iron, Zn-zinc, Mn-manganese, Co-cobalt

Metal ions serve as co-factors for a variety of biochemical reactions and are present in critical sites in many proteins. As a result of their incomplete electron shells, metals can shift between different oxidation states. Thus, metals help in activation and stabilisation of enzymes depending upon the redox states (Andreini et al., 2008). Recent studies have shown that concertation of intracellular metals such as Magnesium, Zinc, Iron, Nickel, Cobalt, Copper and Manganese in *T. brucei* played an important role in activation of phosphoglycerate mutase, a novel drug target in the glycolytic pathway (Fuad et al., 2011).

In this study, it was of interest to test whether the metals concentration from the environment would affect the growth of promastigotes, hence be included to improvise growth rate in the defined medium. Under the conditions tested, growth was diminished in the absence of magnesium, zinc, calcium and iron compared to other metals. Various combinations of the test metals were tried in BM at different concentrations. The absence of manganese, cobalt and copper had a minor effect on the growth rate. Lack of magnesium and calcium exhibited significant negative phenotype of growth with 75% and 60% decrease in cell viability respectively (Figure 3.12 and Figure 3.13). Similarly, absence of exogenous zinc and iron decreased total cell density by 35% and 45% respectively.

Iron is an important co-factor for various enzymes, especially iron superoxide dismutases as protection against oxidative damage resulting from activation of NADPH oxidase. Iron uptake has been an extensively regulated process in prokaryotes and eukaryotes. At neutral pH, iron exits as oxidised ferric ($Fe^{3+)}$ form complexed with ferritin, one of the important factors controlling high iron load in hematophagous insect (Valenzuela, 2014). Free form of Fe^{3+} is reduced to Fe^{+2}; however, increased accumulation of ferrous iron ($Fe^{2+)}$ in the presence of oxygen undergoes Fenton reaction to form highly toxic hydroxy radicals. There are evidences for certain metals such as iron is required to support the growth of *Leishmania*. Wilson et al have assessed the knockout of L1T1, an iron transporter, to be essential for infecting macrophages (Wilson et al., 2002). It is also known that macrophages control the infection progression via restriction of iron to the parasites by secreting lipocalin 2, an antimicrobial peptide that captures proteins for internalisation (Flo et al, 2004). Lack of iron decreased the total yield of cells obtained on Day 6 of the culture, hence, iron (9 µM) was included in the trace metals supplement of BM to support optimal growth *of L. mexicana* promastigotes.

Except for cobalt, copper, manganese; other metals showed increased viability with increasing concentration of metals as shown in Figure 3.12 to Figure 3.19. However, it has been shown that cobalt and manganese (Fuad et al., 2011) responsible for enzyme activation, hence included in the composition. Zinc has been shown to exhibit toxic effects at high concentrations against *Leishmania*, however, absence of zinc at 30 µM as tested showed decreased cell density in

Figure 3.12, thus included in the composition. A linear relationship was observed between the metal concentration and growth for calcium and magnesium; but less for zinc and iron. Magnesium and calcium are required at higher concentrations and support growth of promastigotes *in vitro*. Magnesium at 81 μM and calcium at 72 μM was included in the medium composition. Iron concentration above 50 μM was found to toxic range; hence, low concentration as reported from other medium [27] at 9 μM was included in the DM composition. The addition of metals to the base medium during culture were tested using standard alamar blue assay [48] to study its effect on the growth of the first passage of BM inoculum. Individual metal salts were tested with growth monitored in the presence and absence of metal chelator. The parasites were seeded at 10^6 cells/mL. The alamar blue reagent was added after 72 hours in culture, thus, growth observed based on the reduction potential of reazurin from blue to pink accordingly.

To further validate the medium, inhibition studies were carried out in the presence and absence of metal chelators as shown in Figure 3.18 and Figure 3.19. Metal chelators such as EDTA and EGTA had growth inhibitory action on *Leishmania* promastigotes. Addition of metals competitively inhibited the growth inhibition by these chelators decreased due to competitive inhibition by the addition of metals in defined medium composition for the growth of *L. mexicana* promastigotes showed improved growth in presence of metals for growth.

Furthermore, growth experiment in the presence and absence of co-factors inhibitors serves to validate the inclusion of co-factors in medium that biopterin have growth promoting action on *L. mexicana* promastigotes in culture as shown in Figure 3.17. Biopterin in the medium increases the viability of promastigotes even under the influence of the MTX drug.

The IC_{50} value with biopterin in the medium was higher, indicating compensatory biosynthesis pathway activation. The synergistic effect of increased substrate concentration of folic acid and biopterin on *de-novo* thymidine biosynthesis overcomes the blockage caused by MTX on the activity of DHFR-TS, the bi-functional single protein exclusively found in *Leishmania* cells. These results agree with literature on the role of biopterin involved in thymidine biosynthesis (Beverley et al., 1986).

The addition of haemin for *in vitro* culture of *Leishmania* has been elaborated in most studies. The requirement of free metal salts for the growth of *L. mexicana* has not been noted before; probably because of the presence of trace metals as contaminants from organic solvents. The addition of metals to the medium composition was tested individually and in conjunction with biopterin. The addition of magnesium, zinc, calcium significantly improved doubling time ($p<0.01$) and iron, copper, manganese, cobalt ($p<0.001$) with significant effect observed in the presence of biopterin in the medium as observed from Figure 3.12. Thus, in summary, the cofactors and metals included in the improvisation of the growth rate of *Leishmania* promastigotes in Nayak medium were as shown in Table 3-4.

Table 3-4 Summary of co-factors and metals included in NM

Co-factors	Metal salts
Folic acid	Magnesium septa-hydrate
Riboflavin	Calcium chloride
PABA	Zinc Chloride
Biopterin	Iron (III) nitrate nona-hydrate
Lipoic Acid	Manganese chloride
Biotin	Cobalt chloride

Adenosine serves a purine source for increased demand of nucleotides for DNA and RNA synthesis required for rapid proliferation in host cells (Ortiz et al., 2010). *Leishmania* genome encodes for enzymes catalysing the interconversion of purines; hence, increasing adenosine might cater for the production of other purines and pyrimidines. *Leishmania* genome encode for *de novo* bio-synthesis of pyrimidines, hence, not essential to be salvaged from the environment (Marr et al., 1978).

Amongst the purines, it has been reported that adenosine is preferential purine source interconvertible to other purines such as hypoxanthine, inositol and pyrimidines with enzymes encoded in *Leishmania* genome (Lafon et al., 1982, Carter et al., 2001). Adenosine serves as important co-factor for L-Methionine recycling pathway. Adenosine combines with L-Methionine to form S-adenosyl L-Methionine which acts proton carrier intermediate for various metabolic pathways (Crabtree et al., 2009). Adenosine was tested at various orders of magnitude at 0 µM, 7 µM, and 74 µM on the growth of *L. mexicana* promastigotes.

Growth in NM with no adenosine and at 7 µM adenosine equivalent to serum adenosine concentration was slow with a low yield of cells compared to cell density in the presence of adenosine at 74 µM measured from the growth curves as shown in Figure 3.20. Increased adenosine concentration played a major role in increased cell density, thus serving as a major growth-limiting nutrient.
Promastigotes thrive within the mid gut of the insect sand-fly rich in various sugars such as glucose, fructose, galactose, ribose and mannose (Leslie et al., 2002). It has been previously shown that *Leishmania* have transporter proteins that facilitate the uptake hexose and pentose sugars for carbon and energy purposes (Naula et al., 2010). In fact, Steiger et al reported that RE X formulation without glucose for the culture of *L. donovani* promastigotes did not affect the growth of promastigotes.

Figure 3.21 indicated that the growth of *L. mexicana* promastigotes in defined medium was not significantly decreased. However, there was 33% increase in doubling time in conditions without glucose; with a prolonged lag phase. The total number of promastigotes in metacyclics phase were significantly decreased than in the culture medium with glucose.

The IC_{50s} of AmpB obtained in NM were comparable to those obtained in HOMEM.AmpB showed no significant effect of the medium on the IC_{50} value; however, the differences observed with other two compounds were 2 fold magnitude. Methotrexate, inhibitor of dihydrofolate reductase shows poor activity in HOMEM (average IC_{50} 200 nM) owing to increased concentration of folate; however there was higher activity observed in NM (IC_{50} 14 nM). We have previously observed that addition of biopterin to defined medium improves growth and inhibits the activity of methotrexate as shown in Figure 3.17; which might partly explain the increasing activity of methotrexate in NM and not in HOMEM. Defined medium was evaluated for drug sensitivity testing using standard alamar blue assay of clinically used drugs against leishmaniasis. Pentamindine and Methotrexate showed increased activity in NM than in serum containing HOMEM medium; increased bioavailability of these drugs cost effective for multiple drugs. The activity of amphotericin B (average IC_{50} 710 nM and 554 nM) result in similar IC_{50} values between the two media; possibly owing to the fact that AmpB drugs affect the intracellular metabolism of the cells especially in lipid biosynthesis which might not directly be affected by culture composition alone as shown in Figure 3.29

The need for serum free medium for the culture of *L. mexicana* compelled the need to take the more laborious approach by the systematic omission of single components and then concentrations of those components with growth promoting activity was optimised. Defined medium was developed by individually testing each component including amino acids, co-factors and metals at a time and in conjunction to map the minimum requirements to support parasite growth for *in vitro* culture conditions. Purification of parasite specific antigens, free of contaminants could be better accomplished in the absence of undefined serum component; hence useful for generation of parasite specific antibodies and vaccine development. Drug sensitivity assays carried out using standard leishmanicidal drugs, Amphotericin B and Pentamidine showed increased activity in DM than in serum containing medium; increased bioavailability of these drugs allowed cost advantages since smaller concentrations were sufficient for inhibitory effect tested over multiple trails. Hence, given the morphological and nutritional response of promastigotes; we note that defined medium would offer a more stable platform for drug sensitivity assays.

Also, since all the components of the defined medium are chemically known; the variability between experiments are significantly minimised under similar *in vitro* culture conditions. Thus, defined medium offers stable platform compared to batch variability in compositions of serum containing media. This is especially important for high throughput methods such as metabolomics and proteomics involving analytical instruments such as mass spectrometers which generate vast amount of data (Kell et al., 2005). The quality of the data relies on the ratio between the signals to noise of the individual chemical compounds. There is a significant decrease in background signals in the absence of serum and protein molecules free in the defined medium conditions; hence leading to better validation of peaks of the spectrum and compound identification. Stage specific differences during *L. mexicana* promastigotes growth were mapped using defined medium for the discovery of novel metabolic pathways unique to the insect stages of the parasite addressed in Chapter 5.

A large part of the work for the development of defined medium has been based on growth analysis of *L. mexicana* promastigotes. This was done using manual examination of the parasite morphology using trypan blue exclusion test (Chapter 2, Methods) and viable cell counts using the haemocytometer for growth evaluation, a standard technique used routinely in most laboratories. Although morphological examination of the promastigotes in different medium compositions have been evaluated, it was very laborious and time consuming method. Therefore, efforts were made to adopt colorimetric assays.

Three different types of colorimetric assays were evaluated as stated. Alamar blue assay routinely used for growth evaluation in the presence/absence of drugs (Raz et al., 1997). The reazurin dye (blue) is reduced by mitochondrial NADH dehyrogenase enzyme into resorufin (pink) coloured product, measured spectrophometrically at 570 nm.

MTT assay involves conversion of tetrazolium salt, 3-(4, 5- dimethylthiazol-2-yl)-2, 5, -diphenyltetrazolium bromide into coloured product. Cells lysis needed to be carried out before OD measurement served as major limitation; since the entire reaction relied on the principle of conversion of soluble colourless formazan into insoluble formazan by mitochondrial dehyrogenase. Measurement of formazan was possible only after harsh treatment with chemical reagents such as alcohols and dimethylsulfoxide (DMSO) (Henriques et al., 2011).

MTS assay was carried out according to (Berg et al., 1994) but modified for various steps of optimisation as stated. 50 µl PMS stock solution was added to 1 mL MTS stock solution immediately before use. Mid log phase promastigotes (1 x 10^5 cells/ml) per 100 µl/well were seeded in 96 well plates. Heat killed parasites were prepared by incubating the parasites at 99°C for 30 min which served as negative control. MTS/PMS was diluted to 5:1 with PBS and 20 µl was added to each well and incubated at 37°C for 3 hours. Absorbance was measured at 490 nm using plate reader. The optical density of the medium minus the background OD was considered as the corrected absorbance value plotted against each parameter tested.

The advantages and disadvantages of the different colorimetric methods such as Alamar blue, MTT and MTS/PMS dye, were evaluated as shown in Table 3-5.

Table 3-5 Comparison of colorimetric assays for monitoring growth of *Leishmania* promastigotes

Name of the compound	Advantages	Disadvantages
MTT-3-(4, 5-dimethylthiazol-2-yl)-2, 5, -diphenyltetrazolium bromide	Enzymatic method	Insoluble dye not released into the system
Alamar blue	Reliable and optimised for *L. mexicana* drug sensitivity assays.	Lengthy incubation time required for the complete metabolism of the reazurin salt; hence not very suitable for monitoring subtle changes in growth kinetics.
MTS/PMS dye 3-(4, 5-dimethylthiazol-2-yl)-5-(3-carboxymethoxyphenyl)-2(4 –sulphonyl)-2H-tetrazolium	Soluble end product rapidly released into the system Lesser incubation time	Needed to be optimised for *L. mexicana* promastigotes growth conditions.

Extensive optimisation of the assays for the cells of interest, *L. mexicana* promastigotes, was conducted for the parameters involving different inoculation densities, different lengths of incubation, temperature and range of wavelength for optical density measurement as follows:

a) **Evaluation of optimal inoculation cell density**-Different densities of cells containing 1 x 10^5, 5 x 10^5, 1 x 10^6, and 5 x 10^6 in 96 well flat bottom plates were tested in triplicates as shown in Figure 3.31.
b) **Evaluation of optimal temperature for the assay-**The 96 well plates were incubated at different temperature of 27^{oC} and 37^{oC}
c) **Evaluation of optimal incubation time-***L. mexicana* promastigotes with or without MTS/PMS dye in 96 well plates were incubated for several time points at 3, 24, 48, 72, 96, 120 and 144 hours as shown in Figure 3.30.
d) **Evaluation of optimal wavelength-** Scanning spectrophotometer was used to measure the absorbance spectrum of the formazan product resulting from the reduction of MTS at various incubation times as stated above. This was mainly carried out to evaluate the background change in optical density due to cell debris, fingerprints and other non-specific absorbance as shown in Figure 3.31. However, the fold change between the optical densities (O.D) is minimal, therefore it could not infer as an accurate measure of the growth of *L. mexicana* promastigotes.

The linear range of the MTS assay was measured for 1 x 10^5 to 5 x 10^6 /well/200 µL. The corrected absorbance was plotted against the starting inoculation density (X axis). For cell density above 5 x 10^5, the increase in cell density showed a positive correlation with the corresponding increase in O.D value; however, the opposite was observed for cell densities above 5 x 10^6 cells/mL with dye saturation. Results as shown in Figure 3.31; that there was no shift in the optical density in wells with cell density below 10^5 cells/ml. The values were linear only for wells with starting density with 1 x 10^6; however, the fold difference between the OD values was not as significant as observed from manual counting.

Also, there were speculations about any minor toxic role of MTS/PMS reagent on the parasites growth. Cell numbers in the presence of MTS/PMS reagent. *L. mexicana* promastigotes cultured in HOMEM and defined medium with and without

MTS/PMS reagent in culture wells were also examined for density effect on motility. The percent motility of cells was reduced and hence manual analysis was chosen as adapted method for analysis of cell viability.

In summary, the development and establishment of defined medium would enable design of novel experimental protocol customised to the question of interest. Amino acids have been tested for their impact on viability and growth of *L. mexicana* promastigotes as shown in Chapter 4.

Chapter 4 Determination of amino acid requirement for parasite viability

4.1 Introduction

Amino acids have varied functions ranging from protein synthesis, energy production to maintaining homeostasis. In general, amino acids classification has been broadly described based on nutrition or chemical nature. The term essential and non-essential amino acids as coined by W.C Rose was based on nutrition value of individual amino acids (Womack and Rose, 1947, Womack and Rose, 1934, Mccoy et al., 1935). However, the essentiality of amino acids has been subject to debate depending upon various factors about the metabolic, dietary and functional capabilities of a particular organism (Reeds, 2000, Millward and Rivers, 1988, Boutry et al., 2008).

Much of the knowledge on amino acid essentiality in *Leishmania* parasites relies on early biochemistry work on related species of Kinetoplastida with different hosts (Cross et al., 1975, Cross and Manning, 1973). Silber et al in *Trypanosoma cruzi* demonstrated that the insect stage exhibited higher dependence on amino acid metabolism (Silber et al., 2005). Especially, L-Proline has been shown as carbon source consumed from the host and serves as a major osmolyte during the differentiation process from the replicative, non-infective epimastigote to the infective, non-replicative trypomastigote stages (Silber et al., 2002). In *T. brucei*, it was observed that the procylic forms depend on amino acids for energy metabolism compared to the bloodstream forms, exclusively on glycolysis (Michels et al., 2000). Though genetically similar, *Leishmania* encounters different nutritional host environments as compared to related *Trypanosoma* species (Burchmore and Barrett, 2001).

In human infecting *Leishmania* promastigotes, it has been shown to utilise amino acids as both carbon and energy sources (Burchmore and Barrett, 2001, Saunders et al., 2010). Promastigotes are known to undergo a complex developmental cycle in the alimentary tract of the insect, sand-fly (Kamhawi, 2006). It has been previously shown that parasites have the metabolic capability to utilise L-Proline as their preferred carbon source in the absence of glucose (Burchmore et al., 2003). Radio labelled studies have shown that L-Proline contributes to the carbon skeleton of several other metabolites including other amino acids through the transamination process via L-Glutamine (Mukkada, 1985). Amino acids serve as precursors for metabolites leading to energy production for growth, regulation of oxidative stress (Colotti and Ilari, 2011) and for osomo-regulation (Blum, 1996). However, the role of individual amino acids in parasite viability without extraneous supplements such as serum and protein is unexplored.

4.1.1 Determination of impact of amino acids on parasite viability

Krassner and Flory (1971) conducted experiments to determine amino acid essentiality in *Leishmania tarentolae* (Krassner and Flory, 1971). Parasite growth was monitored for six successive sub-cultures (each 5-7 days long) and reported that L-Arginine, L-Histidine, L-Tryptophan, DL-Phenylalanine, DL-serine, L-L-Tyrosine, L-Threonine, L-Valine, L-Leucine and L-Lysine were found essential. It can be argued that amino acids essentiality during six sub cultures might allow for adaptive prototrophic growth and also, *L. tertentole* is a lizard infecting parasite. Early work by Steiger et al determined the effect of amino acids on growth of *L. donovani* with variable amino acid concentrations (Steiger and Steiger, 1977). Recent studies show that *Leishmania* species largely differ in amino acid metabolism (Westrop et al., 2015), but as in most other studies, was conducted in the presence of extraneous supplements such as serum (modified) or proteins and other intermediates (Saunders et al., 2011). Because of the paucity of data on amino acid essentiality in human infecting *L. mexicana* species in minimal defined media conditions, this study represents the first step towards this direction. Here, systematic analysis of amino acid essentiality for the growth of *L. mexicana* promastigotes was carried out by the creation of a novel equimolar single amino acid knock out media, modified from serum and protein free Defined medium as described in Chapter3.

4.1.3 Research aims

- The design of novel equimolar amino acid knock out media for the culture of *L. mexicana* promastigotes.
- The impact of individual amino acids on parasite viability was examined in novel single amino acid knock out media by:
    - Growth analysis
    - Protein production
    - Acetate overflow quantification
- Growth analysis in presence of selected amino acid analogues as drugs.

4.2 Results

4.2.1 Preparation of novel single amino acid knock out media

Single amino acid knock out media were prepared by modification of Nayak medium composition (Chapter 1) as elaborated in Chapter 2 methods section as shown in Figure 4.1. Individual bottles were then adjusted to pH 7.4 and stored at 4^{o}C.

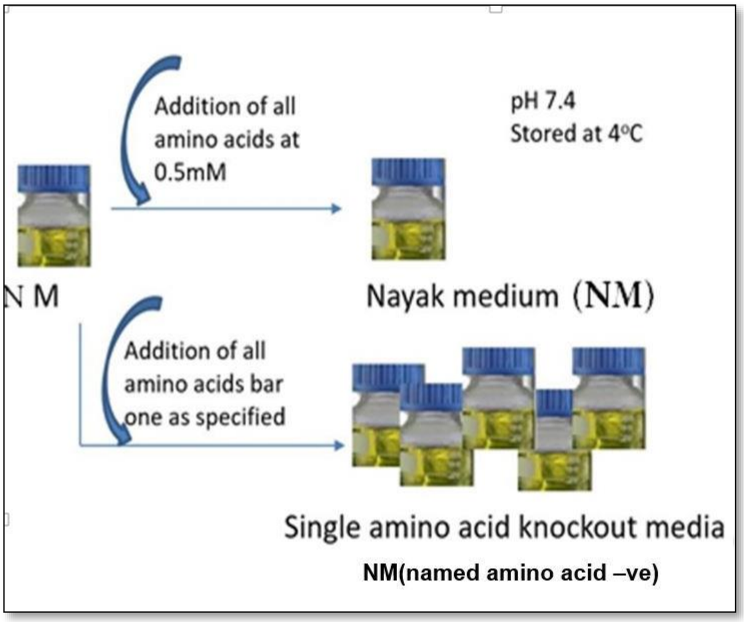

Figure 4.1: Workflow for preparation of single amino acid knock out media

Briefly, Nayak medium minus all amino acids media (NM-AA) were aliquoted into 21 different autoclaved bottles. To the first medium, each of the 20 proteogenic amino acids were added at 0.5 mM, this equimolar amino acid medium is hereby referred to as Nayak medium (NM) and to subsequent bottles, all amino acids bar one were added to make the single amino acid knock out media referred to as Nayak medium minus each amino acid as specified (NM-specified AA) were used for subsequent growth and biochemical analysis.

4.2.2 Growth analysis in single amino acid knock out media

The growth of *L. mexicana* promastigotes was monitored in defined media containing all but one of the 20 standard proteogenic amino acids, hereafter referred to as single amino acid knock out media as described in methods section of Chapter 2. Growth curves were compared and doubling time was calculated by least square fitting of the growth curve (Steel, 1967) as shown in Figure 4.2. Regression analysis was used to find the portion of the curve which is linear during exponential phase mostly between 48 and 120 hours in single amino acid knock out media. The resulting slope obtained was used to find the growth rate (K), substituted in the equation as K = log (2)/ Doubling time which corresponds to order the importance of individual amino acids as highlighted in Figure 4.3.

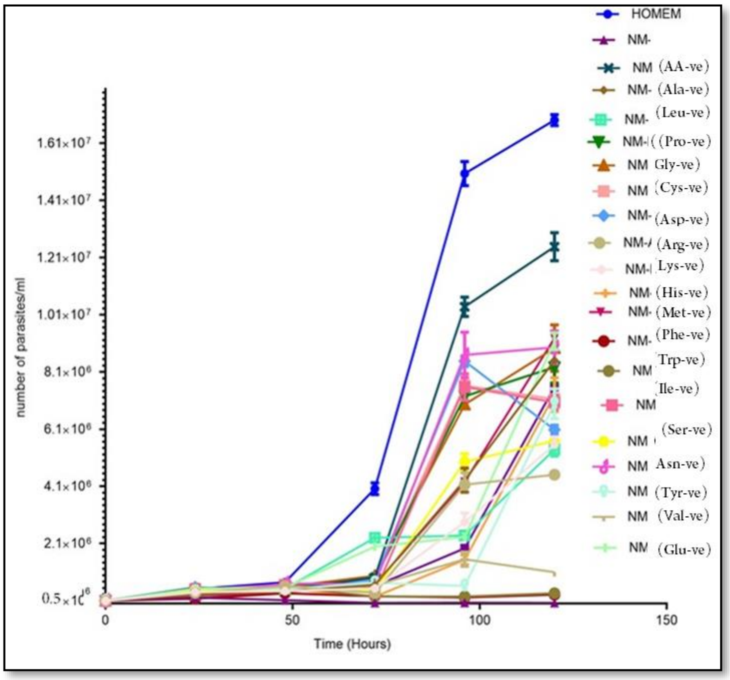

Figure 4.2: Growth curve of *L. mexicana* promastigotes in single amino acid knock out media.

5×10^5 cells/mL of *L. mexicana* promastigotes in single amino acid knock out media containing 0.5mM of all standard proteogenic amino acids bar one, specified with 3 letter abbreviations for 9-day growth period at pH 7.4 at 27°C, n=9, Error bars = mean ± SD, as described in experimental procedure. HOMEM is a standard semi-defined hemoflagellate culture medium with 10% FCS (Berens et al., 1976). NM (Table 3-3) is a defined medium containing all 20 proteogenic amino acids and negative control, NM-AA media, NM (named amino acid -ve).

It was observed that in absence of exogenous source of L-Tryptophan or L-Phenylalanine, the promastigotes were not viable for more than 4 hours in culture. Whilst absence of L-Arginine, L-Lysine, L-Leucine there was no viable promastigotes in culture beyond Day 3. The absence of L-Valine pronounced lag phase and stunted morphology as demonstrated through measurement of cell body length explained in Figure 4.3. Thus, the exogenous presence of individual amino acids such as L-Tryptophan, L-Phenylalanine, L-Arginine, L-Lysine, L-Leucine and L-Valine were noted as important for the viability of promastigotes in culture. Growth rate expressed as doubling time was used to calculate the order of amino acid importance for the growth of the *L. mexicana* promastigotes under conditions tested were as follows L-Tryptophan > L-Phenylalanine> L-Lysine> L-Arginine> L-Leucine> L-Valine> L-Aspartate> L-serine> L-Histidine> L-isoleucine> L-Threonine> L-Glutamate> L-Methionine> L-Glutamine> L-cysteine> L-L-Tyrosine> L-Proline> L-Asparagine > L-Alanine> L-glycine in Figure 4.3.

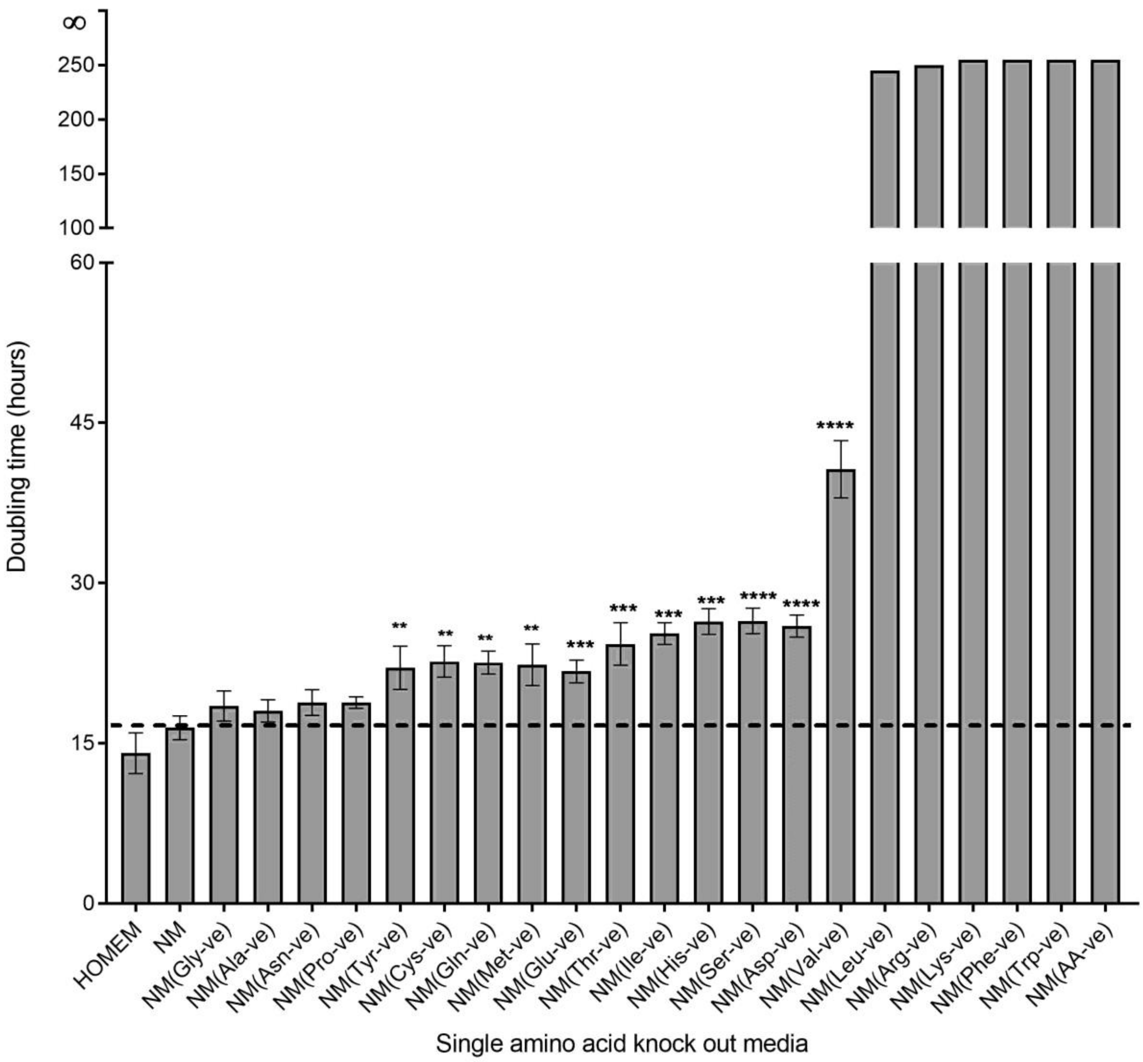

Figure 4.3: Doubling time of *L. mexicana* promastigotes in single amino acid knock out media.

(Single amino acid knock out media contains 0.5mM of all standard proteogenic amino acids bar one, as specified in 3 letter abbreviation. HOMEM is a standard semi-defined hemoflagellate culture medium with 10% FCS (Berens et al., 1976). NM (Table 3-3) is a defined medium containing all 20 proteogenic amino acids and NM-AA contains no amino acids. Dashed line to show comparison with doubling time in NM. For all samples, doubling time was calculated by least square fitting of the growth curve (Steel, 1967). (n=9, Error bars = mean ± SD) The number of asterisks indicate significant p values with **** P<0.0001, *** p<0.0005, ** p<0.001 and * p<0.05 one way ANOVA with Dunnett's multiple comparison test to NM). Statistical significance calculated independently for experimental repeats conducted in triplicates each time.

4.2.3 Growth analysis in minimal amino acid media

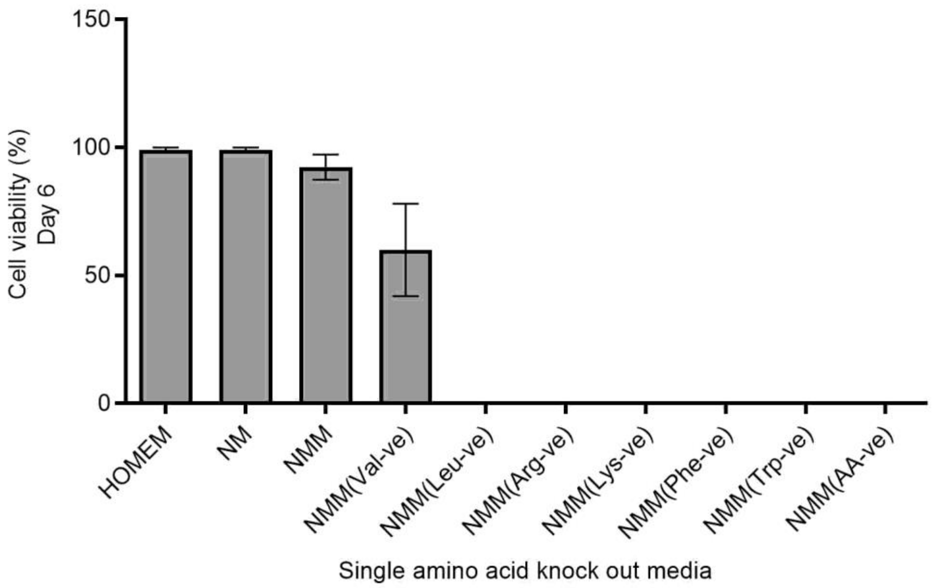

Figure 4.4: Cell viability expressed as percentage of *L. mexicana* promastigotes

Cell viability of *L. mexicana* promastigotes in HOMEM and NM compared to NMM (Nayak minimal medium, minimal amino acid media composed of 6 amino acids) and in NMM individually lacking component 6 amino acids each condition with n=9, Error bars = mean ± SD and statistical significance calculated independently for experimental repeats conducted in triplicates each time.

Growth analysis from single amino acid knock out media was further confirmed by the preparation of minimal amino acid media referred to as Nayak Minimal Medium (NMM). NMM composed of only 6 important amino acids of 0.5 mM of L-Leucine, L-Arginine, L-Lysine, L-Valine, L-Phenylalanine and L-Tryptophan. It was observed that about 80% of *L. mexicana* promastigotes were viable in NMM compared to 100% viability in NM and HOMEM plus 10% FCS. However, NMM lacking individual component amino acid such as L-Tryptophan, L-Phenylalanine, L-Leucine, L-Arginine and L-Lysine were non-viable and absence of L-Valine showed more than 50% decrease in cell viability as shown in Figure 4.4.

4.2.4 Growth analysis at different concentrations of amino acids

The six amino acids, L-Tryptophan, L-Phenylalanine, L-Lysine, L-Arginine, L-Leucine and L-Valine identified as most important exogenous sources required for the viability of promastigotes were further investigated in dose dependent manner as shown in Figure 4.5.

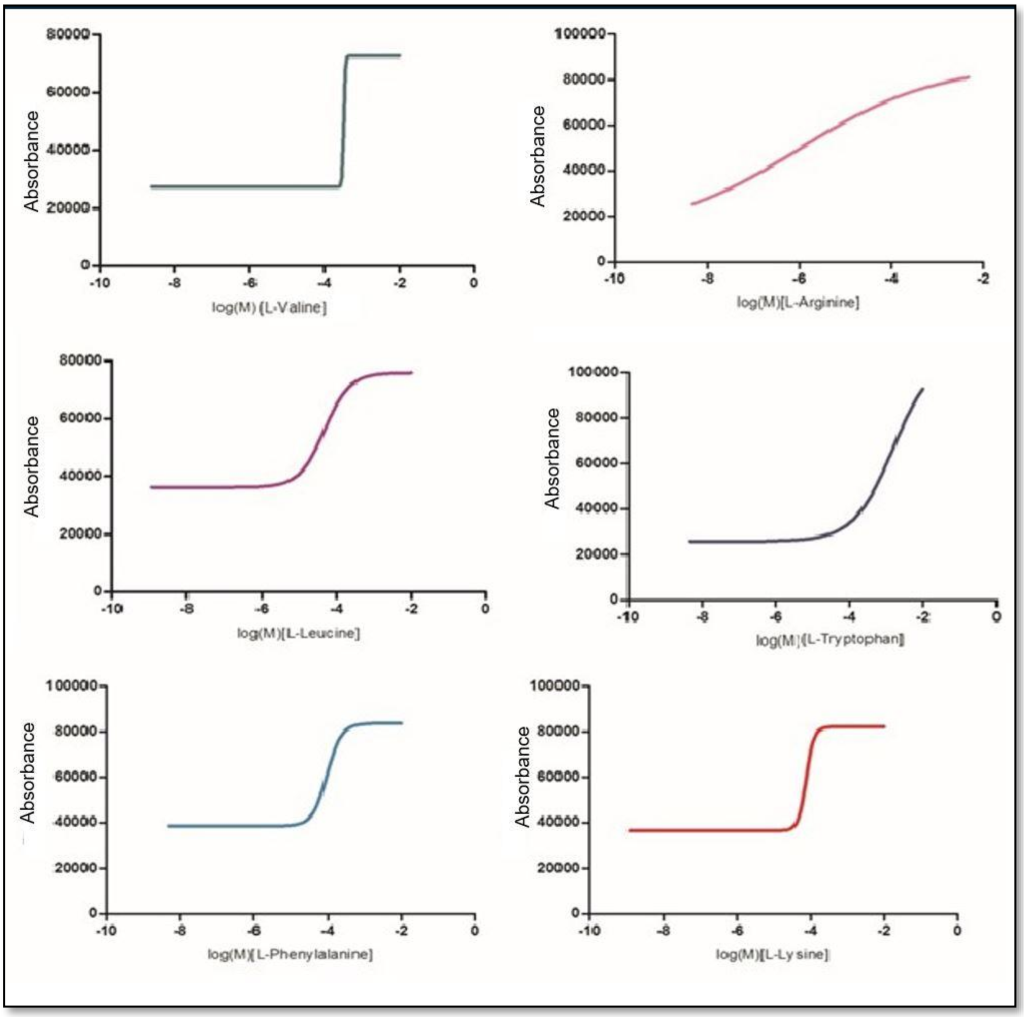

Figure 4.5: Growth response *of L. mexicana promastigotes* in the presence of 0-10mM of individual amino acids as specified in appendix table-1.

5 x 10^5 cells/mL of *L. mexicana* promastigotes in single amino acid knockout media containing 0.5mM of all standard proteogenic amino acids bar one as specified for 6 day growth period at pH 7.4 at 27^{o}C, n=6. Experiment was carried out using alamar blue assay (Raz et al., 1997) in 96 well plate as described in

experimental procedure with each amino acid specified in 24 concentrations by serial dilution from 10 mM-0 mM depicted in log(M) values as described in appendix table 1. All wells were set at same starting cell density as inoculum and absorbance values measured on Day 6 and plotted using Graph pad Prism software. The IC_{50} values for all these six amino acids was found to be in the range between 0.156 mM and 0.625mM; thus equimolar supplementation of amino acids at 0.5mM was considered for Nayak medium composition.

The six critical amino acids, L-Tryptophan, L-Phenylalanine, L-Lysine, L-Arginine, L-Leucine and L-Valine identified as most important exogenous sources were further investigated and growth of *L. mexicana* promastigotes tested in the presence of increasing concentration of individual amino acid as specified at 10mM-0mM in serial dilutions with other amino acids constant at 0.5mM each in modified NM as shown in Figure 4.5. There were no viable cells in wells between 0 mM and 0.1 mM (log (M) with constant absorbance values similar to base line in wells containing medium only samples. There was an increase in absorbance between 0.1 mM and 0.5 mM concentrations of individual amino acids as specified. It was observed that presence of increased amino acid concentration of above 0.5mM showed an improved growth response, especially for L-Tryptophan and L-Arginine.

4.2.5 Growth analysis in modified minimal amino acid media

To further investigate the importance of the other 14 amino acids on parasite growth, *L. mexicana* promastigotes were monitored in minimal medium with and without the addition of each of the 14 amino acids individually as shown in Figure 4.6 and doubling time calculated from linear regression analysis from the exponential phase according to Steel et al, 1967.

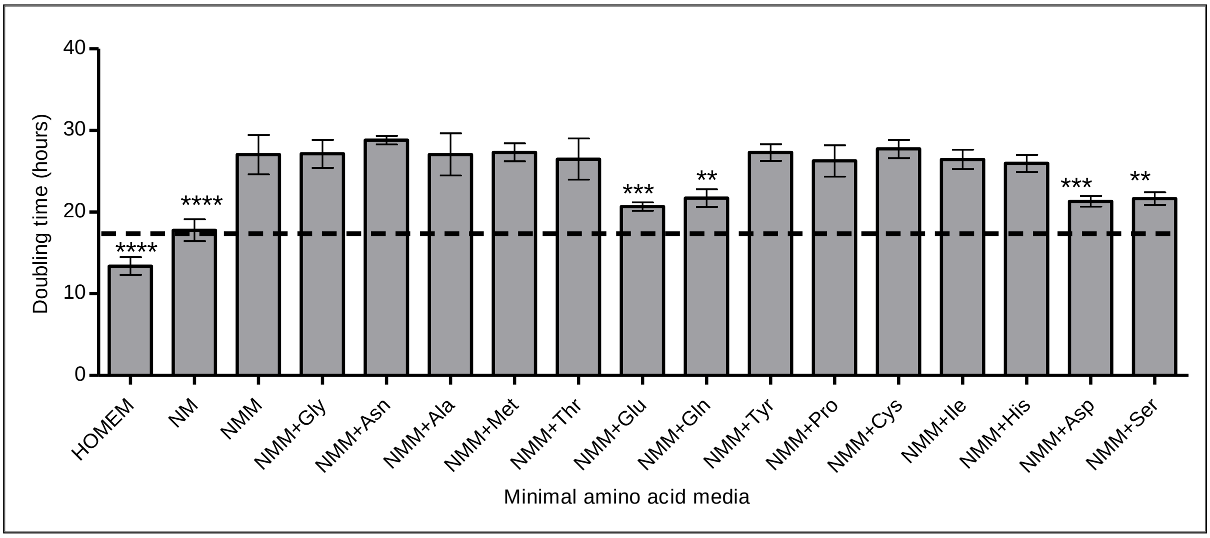

Figure 4.6 Growth rate expressed in doubling time for *L. mexicana* promastigotes in minimal amino acid media.

5 x 10^5 cells/mL of *L. mexicana* promastigotes cultured in HOMEM, NM, NMM and NMM plus specified amino acid indicated with their respective 3 letter abbreviation for 9-day growth period at pH 7.4 at 27^{o}C, n=9, error bars = mean ± SD, as described in methods chapter 2. HOMEM is a standard semi-defined hemoflagellate culture medium with 10% FCS (Berens et al., 1976). NM (Table 3-3) is a defined medium containing all 20 proteogenic amino acids at 0.5mM each, NMM is a minimal media with 6 amino acid and NMM plus individual amino acid as specified at 0.5mM. The number of asterisks indicate significant p values with **** P<0.0001, *** p<0.0005, ** p<0.001 and * p<0.05 one way ANOVA with Dunnett's multiple comparison test to NMM. Statistical significance calculated independently for experimental repeats conducted in triplicates each time.

Compared to the six amino acids as found in NMM, addition of all amino acids in NM significantly reduced the doubling time as shown in Figure 4.6. Especially, the exogenous presence of L-Aspartate and L-Glutamate had growth promoting effect on *L. mexicana* promastigotes, followed by L-Glutamine and L-serine compared to the other remaining amino acids.

4.2.6 Morphological analysis in single amino acid knock out media

To investigate the influence of individual amino acids on the morphology of the parasites, average cell body length per 50 *L. mexicana* promastigotes in single amino acid knock out media were assessed by giemsa stain and ImageJ analysis as shown in Figure 4.7.

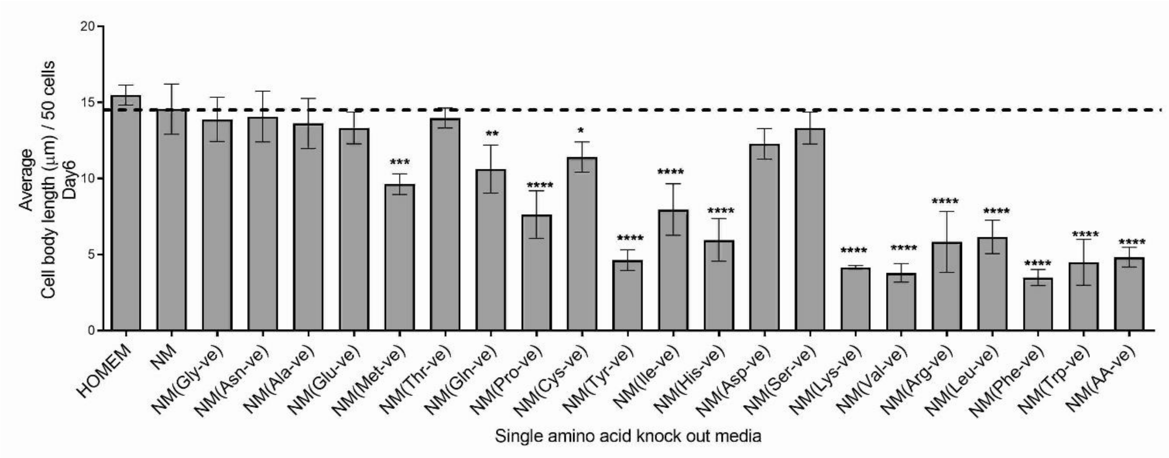

Figure 4.7 Average cell body length in single amino acid knock out media.

(5 x 10^5 cells/mL of *L. mexicana* promastigotes cultured in HOMEM, NM, single amino acid media of NM bar one amino acid as specified with their respective 3 letter abbreviation at pH 7.4 at 27ºC, n=9, Error bars = mean ± SD, as described in experimental procedure. HOMEM is a standard semi-defined hemoflagellate culture medium with 10% FCS (Berens et al., 1976). NM (Table 3-3) is a defined medium containing all 20 proteogenic amino acids at 0.5mM each. The number of asterisks indicate significant p values with **** P<0.0001, *** p<0.0005, ** p<0.001 and * p<0.05 one way ANOVA with Dunnett's multiple comparison test to NMM. Statistical significance calculated independently for experimental repeats conducted in triplicates each time. Dashed line indicates cell body length in NM. For all samples, giemsa stained images were analysed using ImageJ software on Day 6 from the start of the culture initiation and represented as their frequency distribution.)

The average cell body length of *L. mexicana* promastigotes in NM containing all amino acids was measured to be ~12µm which was not statistically different to ~15 µm in serum containing HOMEM medium. Omission of six amino acids including L-Tryptophan, L-Phenylalanine, L-Lysine, L-Arginine, L-Leucine and L-Valine individually or also L-isoleucine, L-Methionine, L-Histidine and L-Threonine individually as shown in Figure 4.7 showed stunted morphology and ~50% decrease in cell body length.

However, it was recorded that absence of L-Aspartate, L-serine, L-Glutamate, L-Methionine, L-Glutamine, L-cysteine, L-L-Tyrosine, L-Proline, L-Asparagine, L-Alanine and L-glycine did not show significant negative phenotype measured by cell body length of metacyclic promastigotes on Day 6 from the start of culture initiation as shown in Figure 4.7.

4.2.7 Protein determination in amino acid drop out media and bioinformatics approach

Amino acids serve as primary building blocks in proteins synthesis. In order to understand relative influence of individual amino acids on protein synthesis, whole cell lysates from single amino acid knock out media were analysed for total protein concentration as shown in Figure 4.8.

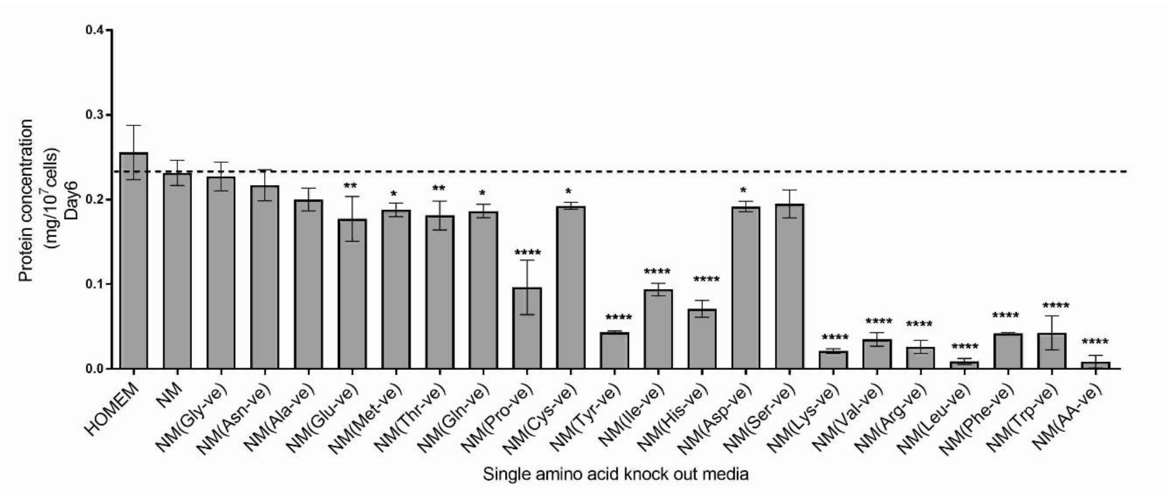

Figure 4.8 Protein quantification in single amino acid knock out media.

Dashed line indicates protein concentration (mg) in single amino acid knock out media compared to NM on Day 6. About 1 x 10^7 cells were inoculated on Day 0 as the start of culture initiation in different single amino acid knock out conditions with NM (named amino acid-ve) and on Day 6 total protein estimated from all samples. 1 x 10^7 cells/mL of *L. mexicana* promastigotes were cultured in HOMEM, NM as controls at pH 7.4 at 27ºC, n=9, Error bars = mean ± SD, as described in experimental procedure. HOMEM is a standard semi-defined hemoflagellate culture medium with 10% FCS (Berens et al., 1976). NM (Table 3-3) is a defined medium containing all 20 proteogenic amino acids at 0.5mM each. The number of asterisks indicate significant p values with **** P<0.0001, *** p<0.0005, ** p<0.001 and * p<0.05 one way ANOVA with Dunnett's multiple comparison test to NM. Statistical significance calculated independently for experimental repeats conducted in triplicates each time.

From these results as shown in Figure 4.8, the omission of L-Lysine has the most significant impact on protein production followed by L-Leucine, L-Valine, L-Arginine, L-Tryptophan and L-Phenylalanine compared to other amino acids under identical conditions. Interestingly, promastigotes cultured in media without L-Threonine, L-Histidine, L-isoleucine and L-Methionine were much smaller in size and showed significantly less protein production. These results indicate that limiting individual amino acids *in vitro* induces differential nutritional stress leading to decrease of global protein synthesis.

To further investigate the relative incorporation of individual amino acids into the global proteome, a bioinformatics approach was undertaken. The protein sequence files of *L. mexicana* proteome from TritrypDB database was collected and processed using in house script (appendix) to decipher codon usage of individual amino acids to calculate the occurrence of individual amino acid expressed as relative amino acid frequency per amino acid residues in the global proteome as shown in Figure 4.8.

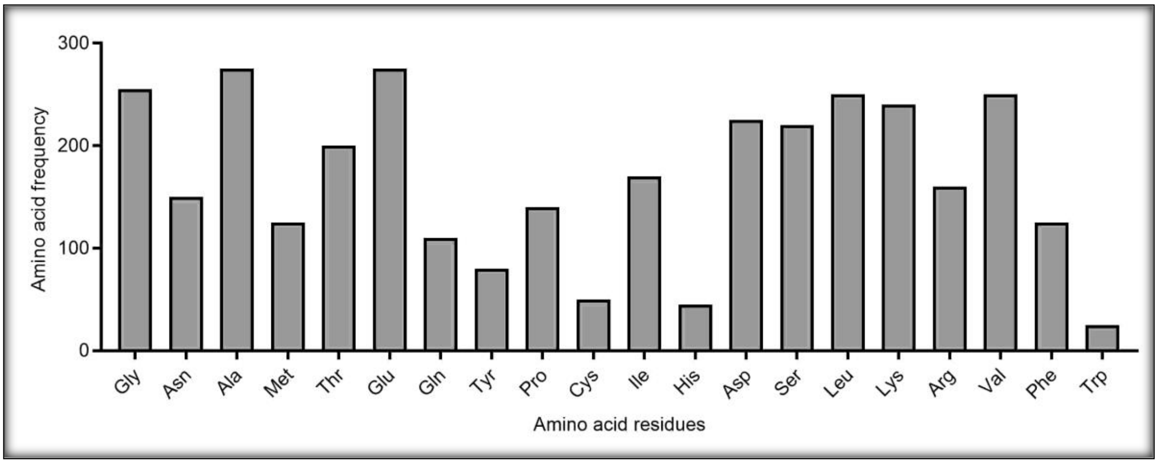

Figure 4.9 Amino acid distribution in the global proteome of *L. mexicana* promastigotes.

From Figure 4.9, the number of individual L-Lysine incorporation into proteins was found to be high, which is in agreement with the results from Figure 4.8 on the importance of exogenous L-Lysine source for protein synthesis. However, the number of L-Tryptophan incorporated into proteins was found to be less compared other amino acids. These results highlight the differential roles of these amino acids and their influence on global protein synthesis in correlation to the growth cycle of the organism.

4.2.8 Energy determination in amino acid knock out media via acetate quantification

Acetate is major high energy intermediate at the crossroads between glucose and amino acid catabolism. Acetate concentration in the extracellular environment has been used as an indicator of the intracellular activities to understand the relative contribution of amino acid to energy production as shown in Figure 4.10, Figure 4.11 and Figure 4.12.

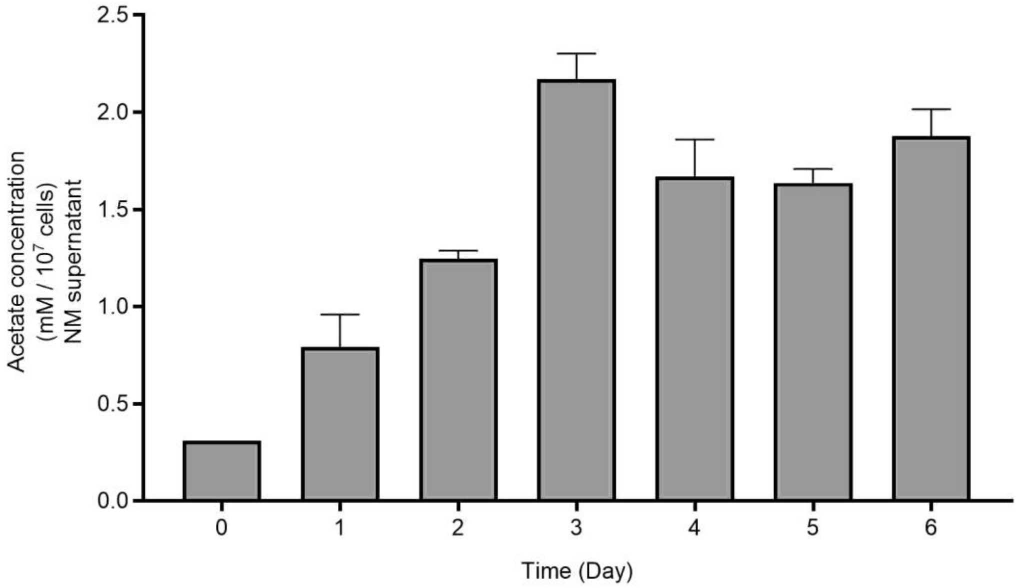

Figure 4.10 Acetate concentration (mM /10^7 cells) of *L. mexicana* promastigotes in NM supernatant samples from Day 0 to Day 6 from the start of culture initiation.

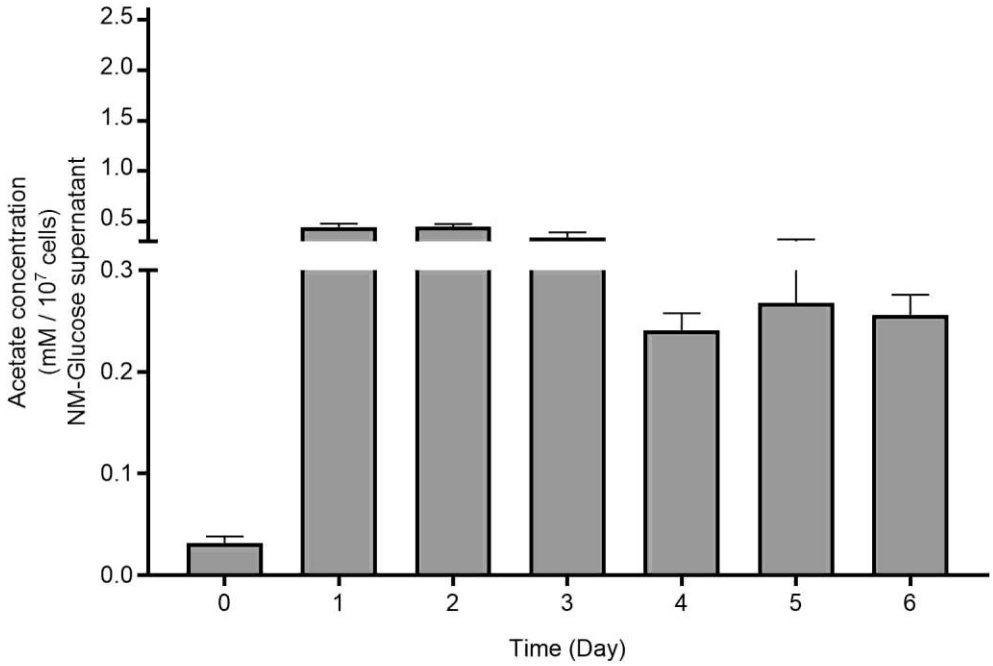

Figure 4.11 Acetate concentration (mM /10^7 cells) of *L. mexicana* promastigotes in NM-Glucose supernatant samples from Day 0 to Day 6 from the start of culture initiation.

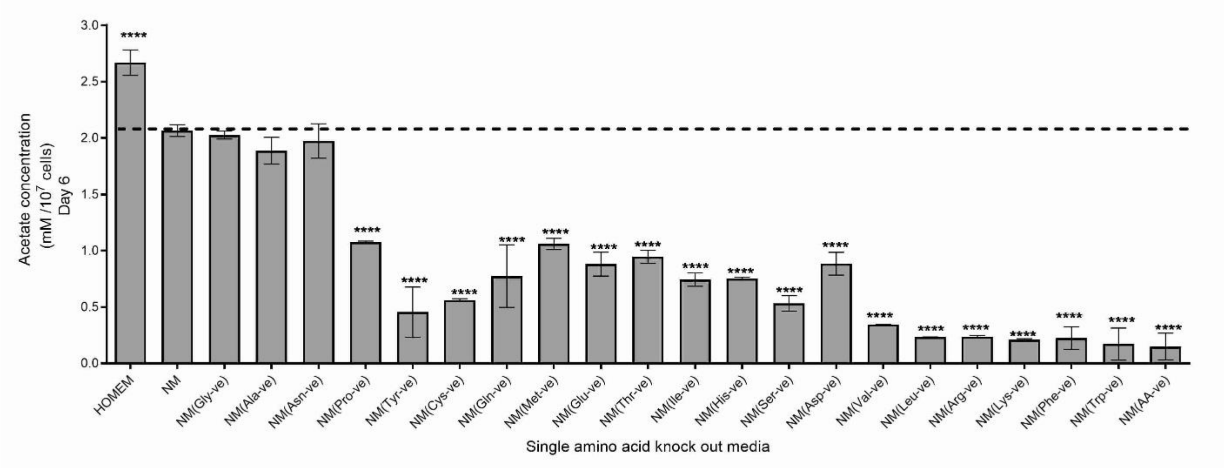

Figure 4.12 Acetate concentration (mM/10^7 cells) in supernatant samples of single amino acid knock out media.

(Dashed line indicates acetate concentration (mM) per 1 x 10^7 cells in single amino acid knock out media compared to NM on Day 6 from the start of culture initiation. 5 x 10^5 cells/mL of *L. mexicana* promastigotes cultured in HOMEM, NM, single amino acid media of NM bar one amino acid as specified with their respective 3 letter abbreviation at pH 7.4 at 27ºC, n=9, Error bars = mean ± SD, as described in experimental procedure. HOMEM is a standard semi-defined hemoflagellate culture medium with 10% FCS(Berens et al., 1976). NM (Table 3-3) is a defined medium containing all 20 proteogenic amino acids at 0.5mM each. The number of asterisks indicate significant p values with **** P<0.0001, *** p<0.0005, ** p<0.001 and * p<0.05 one way ANOVA with Dunnett's multiple comparison test to NM. Statistical significance calculated independently for experimental repeats conducted in triplicates each time).

Here, in Figure 4.10, it was found that acetate overflow increased in the 9 day growth period tested. From Figure 4.11, it was found that without glucose, the amino acids contributed less to overall acetate overflow. And from Figure 4.12 it was understood that with the exception of L-glycine, L-Asparagine and L-Alanine, the supernatant of single amino acid knock out media of other amino acids were found to contain less acetate concentration. These results are in agreement with growth analysis that absence of specific amino acids resulted in decreased growth leading to decreased metabolism, hence decreased acetate overflow in the supernatant samples.

4.2.9 Amino acid analogues as drugs

The aromatic amino acid analogues for L-Phenylalanine (p-fluro-L-Phenylalanine), L-Methionine (Norleucine), L-Tyrosine (3-Fluro-L-Tyrosine) and L-Tryptophan (5-fluro-L-Tryptophan) were tested. 12 different concentrations were serially diluted starting from 100 μM to 49 nM depicted as log of molar concentration described in appendix table 2. The drug activity on the parasites was measured 120 hours using alamar blue assay described in methods section of chapter 2.

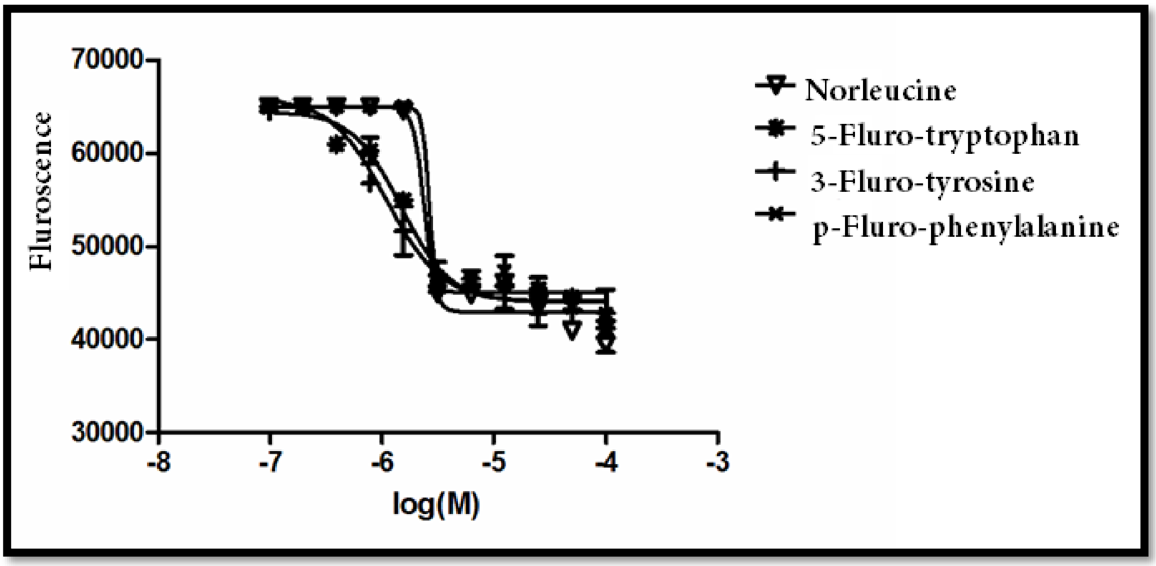

Figure 4.13 Differential inhibition by amino acid analogues on the growth of *L. mexicana* promastigotes in NM with Norleucine (inverted triangle), 5-fluro-L-Tryptophan (asterisk), p-fluro-L-Phenylalanine (inverted cross) and 3-Fluro-L-Tyrosine (cross).

Table 4-1 Table of IC_{50} of amino acid analogues

Amino acid	Analogues	IC_{50} (μM)
L-Methionine	Norleucine	2.39
L-Phenylalanine	P-fluro-L-Phenylalanine	2.62
L-Tyrosine	3-fluro-L-Tyrosine	1.47
L-Tryptophan	5-fluro-L-Tryptophan	1.09

From the alamar blue assay, it was observed that the growth of promastigotes is considerably affected by increasing concentration of the amino acid analogues. The presence of even small concentration (IC_{50} 1.09 μM) of 5-fluro-L-Tryptophan, L-Tryptophan analogue proved detrimental for the viability of the *Leishmania* promastigotes. The IC_{50} values for amino acid analogues for L-Tyrosine (IC_{50} 1.47 μM) followed a similar pattern as L-Tryptophan. The results for both p-fluro-L-Phenylalanine and nor-L-Leucine showed a similar pattern of inhibition of growth, but at a higher concentration than the former two; as specified in Table 4-1 described in more details in discussion section.

4.3 Discussion

4.3.1 Growth analysis in single amino acid knock out media

Amino acids play a fundamental role in many biological processes such as protein synthesis, alternative energy production and homeostasis. Studies about amino acids required to maintain osmoregulation within the host system (Blum, 1996), and unique metabolism of amino acids leading to antioxidant-polyamine biosynthesis (Colotti and Ilari, 2011) within *Leishmania* has been reported. However, amino acid requirements of *Leishmania* had been mostly based on early biochemistry research on related species of kinetoplastida with different hosts (Krassner and Flory, 1971, Coombs et al., 1982, Steiger and Steiger, 1977, Steiger and Steiger, 1976, Steiger and Black, 1980). Lack of missing enzymes within metabolic pathways might highlight alternative routes of metabolism that could be targeted for potential drugs. A thorough understanding of amino acid utilisation and metabolic pathways in *Leishmania* would aid in the discovery of novel drug targets (Zilberstein, 1993, Goldman-Pinkovich et al., 2011).

Here, our aim was to identify amino acids in their order of importance required to support growth for *L. mexicana* promastigotes. Single amino acid knock out media were prepared by methods elaborated in Chapter 2 and growth and biochemical analysis were monitored by culturing of *L.mexicana* promastigotes lacking each individual amino acid at a time. Our experiment allowed us to study the comparative effect of each amino acid on growth and determine their physiological importance.

Growth analysis from single amino acid knock out media demonstrated the order of importance of amino acids as L-Tryptophan > L-Phenylalanine> L-Lysine> L-Arginine> L-Leucine> L-Valine> L-Aspartate> L-serine> L-Histidine> L-isoleucine> L-Threonine> L-Glutamate> L-Methionine> L-Glutamine> L-cysteine> L-L-Tyrosine> L-Proline> L-Asparagine > L-Alanine> L-glycine under identical conditions of starting inoculum, temperature and pH.

The viability of *L. mexicana* promastigotes in the absence of L-Tryptophan or L-Phenylalanine decreased significantly in as less as four hours in culture Figure 4.2. Lack of L-Tyrosine showed sustained growth, yet small increase (** $p<0.001$) in doubling time compared to growth observed in defined medium with an equimolar mixture of all amino acids. These results are in agreement with Beverly et al that PAH knock out *Leishmania major* promastigotes showed viability in L-Tyrosine deficient media but unable to survive in L-Phenylalanine or L-Tryptophan deficient media (Lye et al., 2011). But the fact that our study compared all amino acids at the same time and highlights L-Tryptophan and L-Phenylalanine as most important for viability indicates an additional role in supporting parasite viability. It has been shown that L-Phenylalanine acts as an important regulator of starvation signalling in mammalian systems via mtor pathway (Vendelbo et al., 2014). Phenylalanine might act similarly in *Leishmania* with signalling role *in* gene expression and regulation required to support growth in these parasites. *Leishmania* genome encodes for L-Phenylalanine hydroxylase (PAH) responsible for L-Tyrosine biosynthesis from L-Phenylalanine, but knock out of this particular gene proved that the gene was not essential for viability, further emphasising the fact that exogenous L-Phenylalanine may be involved in multiple roles required to sustain the viability of *L. mexicana* promastigotes.

The absence of L-Arginine, L-Lysine, L-Leucine showed no proliferation, hence no doubling time of promastigotes as shown in Figure 4.3. However, the absence of L-Valine showed sustained viability, albeit, less efficiently with significantly increased doubling time ($P<0.0001$) and distorted morphology. The importance of L-Arginine for viability could be attributed to many roles of L-Arginine in the production of antioxidants such as spermidine and putrescine in the polyamine biosynthesis, trypanosomatid-specific antioxidant molecule, trypanothione has been reported extensively (Colotti and Ilari, 2011, Wanasen and Soong, 2008). L-Arginine is also reported to be converted to phosphoarginine, high energy phosphagen, in peroxisome like organelles, known as glycosomes (Voncken et al., 2013). The presence of exogenous L-Lysine was observed important for the viability of *L. mexicana* promastigotes which was observed primarily due to its contribution to protein production. Amongst the branch chain amino acids, L-Leucine proved to have a significant effect compared to L-Valine and L-isoleucine. It has been previously shown that L-Leucine in *Leishmania* is catabolised into 3-hydroxy-3-methylglutaryl coenzyme A (HMG-CoA) which is incorporated into sterols (Ginger et al., 2001, Ginger et al., 1999) with unique enzyme HMG-CoA synthase not found in mammals. The absence of L-Valine had pronounced lag phase with distorted morphology as observed through giemsa staining. Hence, an exogenous source of six amino acids namely L-Tryptophan, L-Phenylalanine, L-Lysine, L-Arginine, L-Leucine and L-Valine were found to be most important for the viability of *L. mexicana* promastigotes.

To further confirm the impact of other amino acids, provisional medium referred to as NMM (Nayak minimal medium) with and without each of the other amino acids were tested. From these experiments, the growth rate of promastigotes significantly improved in the presence of L-Aspartate, L-Glutamate, L-serine and

L-Glutamine. L-Aspartate has shown to contribute its carbon skeleton for the formation of various TCA cycle intermediates, including oxaloacetate, succinate and fumarate confirmed by heavy stable isotope in targeted metabolomics (Saunders et al., 2011), and also been shown in production of glucose and contribution to storage molecule mannonogen (Rodriguez-Contreras and Landfear, 2006). Thus, L-Aspartate serves as fuel for oxidative phosphorylation and gluconeogenesis might contribute to the growth promoting action of L-Aspartate.

In the presence of both L-Glutamate and L-Glutamine in the medium, parasites showed a significant decrease in doubling time. This indicates that *L. mexicana* promastigotes prefer an exogenous source of L-Glutamate and L-Glutamine, despite the metabolic capability for L-Glutamate and L-Glutamine biosynthetic pathways. It has been shown that labelled carbon from glucose converted to pyruvate undergoes transamination reaction with alpha-ketobutyrate leading to L-Glutamate production catalysed by L-Glutamate dehydrogenase (GDH) (Opperdoes, 2008). L-Glutamate fuels the TCA cycle either by conversion primary intermediate alpha-ketobutyrate or by conversion to succinate via 4-aminobutanoate pathway. L-Glutamate also serves as a major source for L-Glutamine synthesis via the L-Glutamine synthetase. L-Glutamine reported being the key player for regulation of nitrogen metabolism (Manhas et al., 2014) and nitro group donor for pyrimidine biosynthesis (Carter et al., 2008) and amino sugar production (Naderer et al., 2008).

From the growth analysis of, the addition of L-serine to minimal medium significantly improved doubling time $p<0.01$. The presence of exogenous serine improves the growth rate of *L. mexicana* promastigotes, which is in agreement with results from bioinformatics approach in *Leishmania major* genomes predict not all enzymes for serine biosynthesis are present in the genome (Payne and Loomis, 2006). Serine serves as an important precursor for sphingolipid, glycerolipid and phospholipid biosynthesis(Hanada, 2004) apart from cysteine synthesis. Lack of lipids in the NM composition (Chapter1) might further add to the need of exogenous serine source. Serine is metabolised by three different routes via serine dehydratase, serine amino transferase and serine hydroxyl-methyl transferase to pyruvate, hydroxy-pyruvate and glycine production respectively. Thus, supplementation of equal amounts of all 20 proteinogeneic amino acids referred to as NM including L-Aspartate, L-Glutamate, L-Glutamine and L-serine recorded as higher cell density from day 4 to day 6 in 9 day growth period as shown in Figure 4.6 with similar doubling time to serum containing HOMEM medium compared to NMM. These results indicate that growth and development of *L. mexicana* promastigotes vastly depend upon the exogenous supply of amino acids from the extracellular environment or the host system, rather than de novo biosynthesis with dynamic regulation. Thus proteins involved in uptake and metabolism of these important amino acids and their analogues/inhibitors serve as for drug targets.

Amino acids play vital roles in protein synthesis and as carbon or energy source. Amino acids influence protein synthesis two fold, either absence of amino acid for the required synthesis of protein macromolecule or downstream regulation on gene expression controlling protein synthesis. Hence the availability of amino acids influences a variety of regulatory processes including mRNA activation, transcription, translation, protein maturation, turnover, and autophagy. Thus, amino acids impose a cumulative effect on cellular metabolism as a whole. It has been shown in other species that activation of amino acid response pathway might occur in time dependent manner through expression of Atf3, Chop and Asns genes during amino acid deprivation (Anderson et al, 2014). Hence, amino acid deprivation has been suggested to induce restriction in protein production from DNA.

It has been observed from single amino acid knock out media, absence of amino acids in the following order had decreasing order of impact on protein production as follows: L-Lysine > L-Leucine > L-Valine > L-Arginine > L-Tryptophan > L-Phenylalanine > L-Threonine > L-Histidine > L-isoleucine > L-Methionine > L-Aspartate > L-Glutamate > L-serine > L-Glutamine > L-Proline > L-Tyrosine > L-cysteine > L-Asparagine > L-Alanine > L-glycine as shown in Figure 4.8. These results clearly demonstrated that presence or absence of exogenous amino acids determines the nutritional stress encountered by the parasites affecting the global protein production. Especially, the absence of L-Methionine, L-Threonine, L-Isoleucine, and L-Histidine from the exogenous supply caused no negative effect on growth rate observed during of *in vitro* culture period but significant decrease in protein production as shown in Figure 4.8. In 2007, Opperdoes and Coombs suggested that all genes for the de novo biosynthesis of L-Methionine and L-Threonine are present, but experimental evidence for these four metabolic pathways involving L-Methionine, L-Threonine, isoleucine and L-Histidine have not been tracked before.

To understand this, further investigation was carried out using untargeted metabolomics from the intracellular data to map individual amino acid pathways as shown in section 4.2.9. Thus, amino acids were classified into 4 categories as shown in Table 4-2 based on the impact of each amino acid on parasite viability, growth and protein production. Viability of promastigotes in this context indicates that parasites were alive. However, slightly motile when examined under the microscope and exhibited more like a dormant state, with lack of growth and doubling; whilst supplementation of additional amino acids allowed to clearly decrease the lag phase with decrease in doubling time and protein synthesis.

Table 4-2 Classification of amino acids based on exogenous requirements for the growth of *L. mexicana* promastigotes

Exogenous supply critical for viability	Exogenous supply critical for increased growth rate	Exogenous supply critical for protein synthesis	Exogenous supply not important
L-Tryptophan	L-Aspartate	L-Threonine	L-Alanine
L-Phenylalanine	L-Glutamate	L-Histidine	L-Glycine

L-Arginine	L-Serine	L-Isoleucine	L-Cysteine
L-Lysine	L-Glutamine	L-Methionine	L-Aspargine
L-Leucine			L-Proline
L-Valine			L-Tyrosine

4.3.2 Energy quantification in amino acid knock out media using acetate as indirect measure of amino acid catabolism.

Amino acids are involved in acetate and ATP production via the ASCT pathway. Trypanosomatids encode for Acetate-Succinate CoA transferase (ASCT) enzyme involved in acetate and ATP production, not found in mammals (Hellemond et al., 2005). This particular pathway occurs with direction conversion of certain amino acids such as L-Methionine, L-Valine and L-Leucine to succinyl-CoA, metabolised by the enzyme ASCT for acetate and ATP production. Also, metabolism of amino acids to intermediates of TCA cycle leading to succinyl CoA production also leads to acetate production via reversible reaction from acetyl CoA to acetate and ATP formation as illustrated in Figure 4.14.

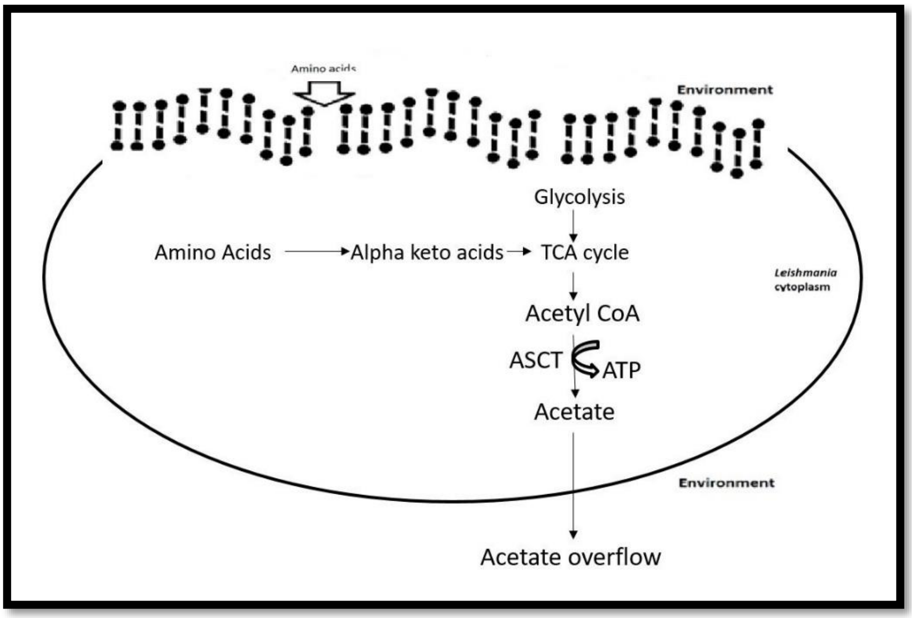

Figure 4.14 Schematic illustration of amino acids utilisation for acetate production in *Leishmania*.

(Unique amino acid metabolism in *Leishmania* promastigotes with direct route of amino acids to energy generation in the form of ATP by the enzyme acetate succinate CoA transferase (ASCT) leads to acetate production and overflow which has been quantified under different experimental conditions).

Acetate overflow has been well demonstrated pathway reported in trypanosomatids due to aerobic fermentation. Acetate concentration in the supernatant serves as an indicator of internal metabolic activity. To understand the relative contribution of individual amino acids to energy production, acetate was used as an indirect measure of amino acid catabolism. Acetate in the supernatant of defined medium under different experimental conditions was quantified by using bioassay kit as described in experimental methods. Acetate concentration in the medium supernatant increased from Day 0 to Day 6 of the culture from the start of culture initiation secreted by *L. mexicana* promastigotes development from procyclics to pre-infective metacyclic stages as shown in Figure 4.10. It was also found that the acetate concentration in the supernatant of culture media containing glucose was 80 fold higher than medium without glucose, indicating that glucose metabolism contributes to higher acetate production than amino acids alone as shown in Figure 4.11.

Further, acetate determination in the supernatant of single amino acid knock out analysis showed that absence of L-Tryptophan, L-Phenylalanine, L-Lysine, L-Arginine, L-Leucine and L-Valine significantly decreased acetate in the spent media compared to absence of L-Aspartate, L-serine, L-Histidine, L-isoleucine, L-Threonine, L-Glutamate, L-Methionine, L-Glutamine, L-cysteine, L-L-Tyrosine, L-Proline, L-Asparagine, L-Alanine and L-glycine as shown in Figure 4.12. These results validate the observations from growth analysis that exogenous supply of amino acids, especially L-Tryptophan and L-Phenylalanine as most important for viability and normal metabolic functioning of *L. mexicana* promastigotes summarised in
Figure 4.15.

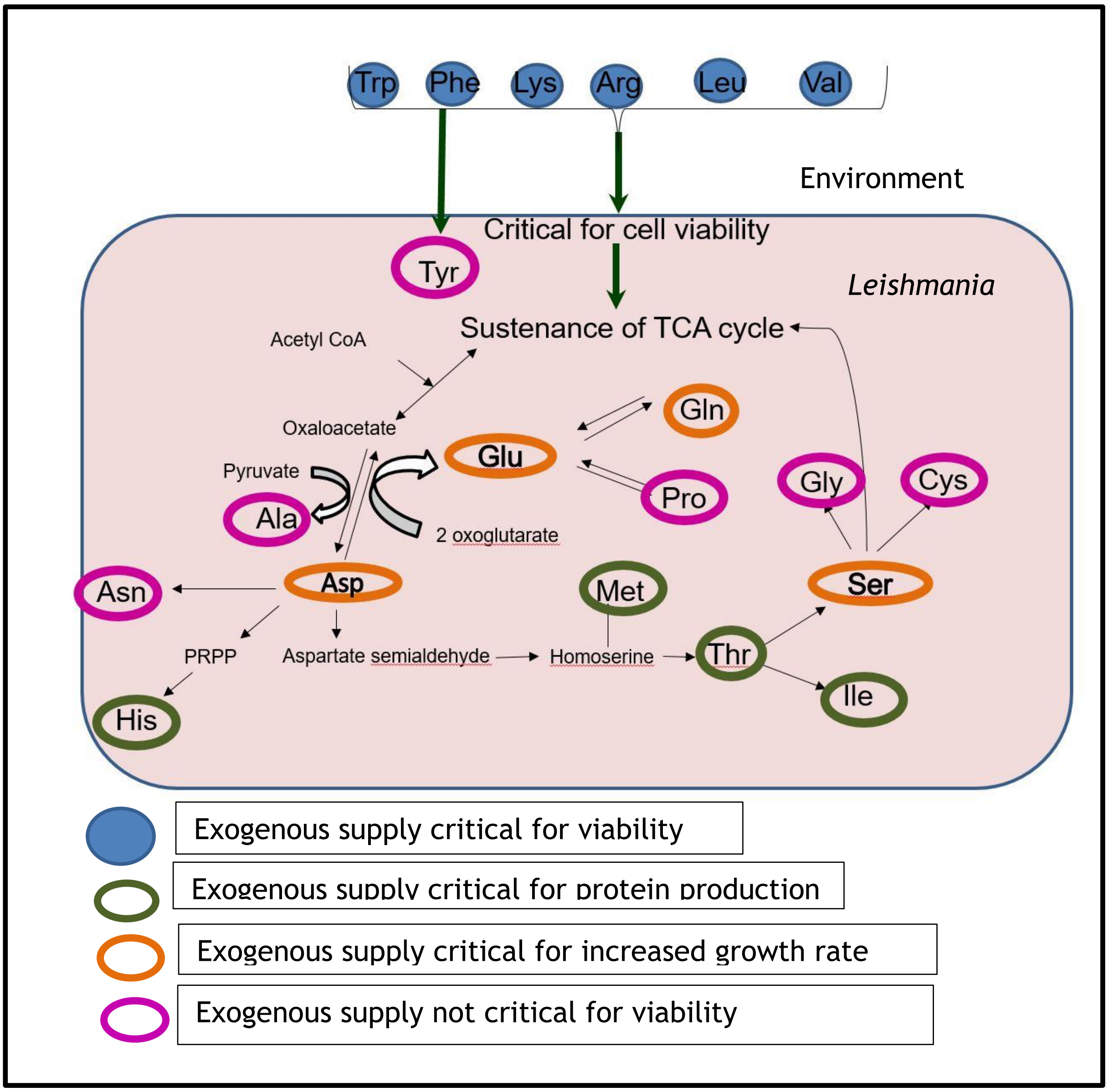

Figure 4.15 Proposed model of amino acids requirements and interconversion in *L. mexicana* promastigotes

(Amino acids classified based on their requirement for the growth of *L. mexicana* promastigotes. Exogenous supply of amino acids critical for viability are shown in blue circles, (Abbreviations: Trp - L-Tryptophan, Phe – L-Phenylalanine, Lys - L-Lysine, Arg – L-Arginine, Leu - L-Leucine and Val – L-Valine) Orange circles denotes those required for increased growth rate (Asp - L-Aspartate, Glu – L-Glutamate, Gln - L-Glutamine, Ser – L-Serine) Green circles denotes those required for increased protein production (Thr - L-Threonine, Met – L-Methionine, His - L-

Histidine, Ile – L-Isoleucine) Pink circles denotes not critically important as exogenous sources (Ala - L-Alanine, Pro – L-Proline, Gly - L-Glycine, Asn – L-Asparagine, Tyr- L-Tyrosine, Cys-L-L-Cysteine). Amino acids interconversion specified using arrow heads.

4.3.3 Amino acid analogues as drug targets

It has been shown in other organisms that amino acid analogues could compete with natural amino acids occurring in proteins and serve as biological inhibitors (Richmond, 1962). The extent of inhibition depends upon various effects on the active sites of enzymes and degree of substitution caused and also the relative level of the intracellular pool of free amino acids available to compete differs at different growth stages(Simon et al., 1983). Amino acid analogues might effect growth and general metabolism via decreased enzyme activities or unknown mechanisms.

Traditionally, drug target strategies have involved structural analogues, inhibitors of uptake of nutrients, antagonists/agonists of receptors, fluorine substitutions, etc. Woods et al in 1940 have shown that structural analogues such as sulphonamides competitively inhibit p-amino benzoic acid reaction to form dihydro-folic acid required for purine synthesis(Woods, 1962). Imatinib used to treat leukemia is chemically known to be 2-phenyl amino pyrimidine which occupies the active site of L-Tyrosine kinases specific to oncogenes, inhibits subsequent phosphorylation and downstream signalling cascades to block proliferation of cancerous cells (Druker et al., 2001).

Analysis from single amino acid knock out media indicated that the exogenous source of aromatic amino acids, especially L-Phenylalanine and L-Tryptophan are most important to support parasite viability followed by other amino acids as shown in Figure 4.2. From other the previous results, it was observed that absence of aromatic amino acids L-Tryptophan and L-Phenylalanine from the exogenous supply also has the most significant negative effect on protein and energy production as shown in Figure 4.8 and Figure 4.12. Hence, in this experiment, amino acid analogues of L-Tryptophan, L-Phenylalanine, L-Tyrosine and L-

Methionine i.e. 5-fluoro L-Tryptophan, p-flourophenylalnine, 3-Fluorotyrosine and norleucine respectively were tested.

From the alamar blue assay, it was observed that the growth of promastigotes was considerably affected with increasing concentration of the amino acid analogues as shown in Figure 4.13. Especially, the presence of an even small concentration of 5-fluro-L-Tryptophan competes with naturally occurring extracellular L-Tryptophan and proved detrimental to the viability of the *Leishmania* promastigotes with the IC_{50} found to be 1.09 μM under conditions tested. Followed by L-Tyrosine analogue, 3-Fluro L-Tyrosine was found to have an IC_{50} of 1.47 μM with the growth inhibition pattern for L-Tryptophan and L-Tyrosine analogues were similar; potentially indicating competitive substrate binding to a single protein transporter for the two amino acids or affecting fresh protein synthesis in a similar way. Also, it was found that L-Phenylalanine and L-Methionine analogues i.e. p-fluro-L-Phenylalanine and norleucine were found to have an IC_{50} of 2.62 μM and 2.39 μM respectively and exhibited similar inhibition pattern potentially competitive substrate for same transporter protein. This is in agreement with Hasne et al (Hasne and Barrett, 2000), demonstrated that in *T. brucei* procyclics encode for the same transporter protein involved in the transportation of both L-Phenylalanine and L-Methionine.

Thus, amino acid analogues especially of L-Tryptophan could be most effective as drug target against the growth of *L. mexicana* promastigotes within the insect vector. Effects of L-Tryptophan analogues such as 5-fluro-trytophan, 7-azaL-Tryptophan have been shown to result in defective protein formation, growth inhibition and blockage of heterocycst differentiation (Mitchison and Wilcox 1973). Blocking L-Tryptophan uptake and metabolism might serve as preferential drug candidate compared to other amino acids because of dual inhibition on viability and protein synthesis required for developmental cycle of parasites within the insect vector. The knowledge from these results could facilitate the design of effective insecticides and better vector control methods, which are often less elaborated. However, understanding the amino acid metabolic pathways in an unbiased manner would allow identification of unique parasite routes to be designated as a potential drug target as elucidated using intracellular metabolomics in Chapter 5.

Chapter 5 Determination of intracellular amino acids metabolic pathways by unbiased network mapping.

5.1 Introduction

In this chapter, unbiased mapping of amino acid metabolic pathways has been elucidated using intracellular metabolomics. Early studies on tracing amino acid metabolic pathways involved incorporation of radiolabelled precursors into the system of interest (Sporn et al., 1959). For example, uptake kinetics of radiolabelled amino acids such as L-Proline, L-Arginine, L-Lysine and L-Glutamate in *Leishmania* have been reported (Burchmore et al., 2003, Shaked-Mishan et al., 2006, Inbar et al., 2012, Paes et al., 2008, Colotti and Ilari, 2011). Previously, metabolic pathways have been characterised using enzyme activity assays in promastigotes and amastigotes stages of *Leishmania* (Hart and Coombs, 1982, Coombs et al., 1982*)*. Also, descriptions of metabolic pathways in *Leishmania* has been based on whole genome annotation (Opperdoes and Coombs, 2007) and bioinformatics approaches (Payne and Loomis, 2006). These methods allow only partial understanding of metabolic pathways of the parasite; without taking into effect the niche environmental impact on metabolism.

5.1.1 Intracellular amino acid utilisation using untargeted metabolomics

Metabolomics holds great promise to the field of tracing metabolic pathways in any level within the system of interest (Creek et al., 2012a). The activities of the underlying enzymes at multiple steps in individual metabolic pathways determine the varied effects of amino acids on the viability of the parasites. Thus, complete elucidation of global unbiased mapping of metabolites by untargeted metabolomics especially in complete defined media would allow for novel biomarker discovery unreported before. Deeper insights about the parasite metabolism could aid in accelerating drug development and to unravel the unique metabolic routes that play crucial roles required for the survival of parasites within the host system.

Kindt et al reported *Leishmania* metabolome cultured in serum rich medium with sample preparation methods for LC-MS study (Scheltema et al., 2010, T'kindt et al., 2011). Silva et al (Silva et al., 2011) demonstrated that promastigotes cultured in serum rich medium underwent significant changes of glycerophospholipids which correlated to the parasite development and rapid lipid turn-over using untargeted metabolomics in *Leishmania donovani* promastigotes. Saunders et al (Saunders et al., 2011) showed the potential of targeted metabolomics using heavy stable isotopes with emphasis on tri-carboxylic acid cycle and carbohydrate metabolism. Recently, Westrop et al reported untargeted metabolomics to highlight differences between species of *Leishmania* using semi defined medium which contained dialysed serum (Westrop et al., 2015).

5.1.2 Research aims

Untargeted metabolic finger-printing of the intracellular metabolome were carried out as follows:

- Defined medium was used to culture *L. mexicana* promastigotes with optimisation of sample preparation method for maximum coverage of metabolites.
- Multivariate data analysis and data exploration.
- Novel unbiased mapping of amino acid metabolites to highlight metabolic differences from mammalian host as drug targets.

5.2 Results

5.2.1 Study objectives

The results from previous section of single amino acid knock out media (Chapter 4) highlighted that exogenous supply of only six amino acids are critical for the viability of promastigotes. Thus, in the following sections of the chapter, untargeted metabolomics of *L. mexicana* promastigotes cultured in defined media allowed new insights into the metabolic routes of amino acids by network mapping. Relative levels of amino acids maintained in the intracellular metabolome of the parasites have also provided information about the activation of certain alternative pathways; not found in mammalian host. In this chapter, aspects about the optimisation of sample preparation steps has been described; including analysis of the intracellular metabolome data of promastigotes cultured in defined medium, mapping of individual metabolites leading to amino acid pathways construction, relative abundance of metabolites within the intracellular metabolome has allowed to highlight alternate metabolic pathways as suitable drug targets.

5.2.2 Experimental design

Here, defined medium composed of commercial solution of non-essential (2X) and essential (1X) amino acids have been used (Table 5-1) to understand the nature of amino acids uptake and intracellular metabolism. Equimolar composition of amino acids in NM proved useful to understand the order of importance of amino acids under identical conditions of inoculation, temperature and pH (Chapter 4) required to support the viability of promastigotes. However, it was thought that amino acids at variable concentrations might better mimic the environment of promastigotes development *in vivo* within sand-fly mid gut. Nayak medium (NM) with equimolar amino acids have been modified and provisionally termed as modified Nayak medium (mNM) for metabolomics experiments. It was not within the time limit of this project for testing metabolomics profiles at different amino acid concentrations. The amino acids pathways constructed using intracellular metabolome for tracing parasite specific metabolic pathways have been highlighted as drug targets.

Table 5-1 Composition of NM and mNM for axenic culture of *Leishmania* promastigotes

Components	NM concentrations (mM)	mNM concentrations (mM)
Salts		
NaCl	136.8	136.8
KCl	5.36	5.36
NaH_2PO_4	0.33	0.33
Sodium Pyruvate	0.99	0.99
NaHCO3	3.57	3.57
HEPES	25.01	25.01
Hemin	0.0077	0.0077
Vitamins		
Choline chloride	0.007	0.007
D-Calcium pantothenate	0.002	0.002
Nicotinamide	0.008	0.008
Pyridoxal hydrochloride	0.004	0.004
Thiamine hydrochloride	0.002	0.002
I-Inositol	0.01	0.01
Co-factors		
Riboflavin	0.05	0.05
folic acid	0.05	0.05
Biopterin	0.1	0.1
Lipoic Acid	0.05	0.05
D-Biotin	0.1	0.1
Metals		
MgSO4.7H2O	0.81	0.81
CaCl2	0.72	0.72
Zinc Chloride	0.03	0.03
Fe(No3)3.9H20	0.009	0.009
Manganese chloride	0.000045	0.000045
Copper sulphate	0.000030	0.000030
Cobalt chloride	0.000032	0.000032
(continued)		

Components	NM concentrations (mM)	mNM concentrations (mM)
Amino Acids		
L-Tryptophan	0.5	0.05
L-Phenylalanine	0.5	0.2
L-Lysine hydrochloride	0.5	0.39
L-Arginine hydrochloride	0.5	0.59
L-Leucine	0.5	0.4
L-Valine	0.5	0.4
L-Aspartic acid	0.5	0.2
L-Serine	0.5	0.2
L-Glutamic Acid	0.5	0.2
L-Glutamine	0.5	2.048
L-Histidine hydrochloride-H2O	0.5	0.2
L-Isoleucine	0.5	0.4
L-Threonine	0.5	0.4
L-Methionine	0.5	0.1
L-L-Cysteine	0.5	0.1
L-Tyrosine	0.5	0.19
L-Proline	0.5	0.2
L-Alanine	0.5	0.2
L-Asparagine	0.5	0.2
Glycine	0.5	0.2
Other components		
Adenosine	0.074	0.074
D-Glucose	16.6	16.6

5.2.3 Protocol optimisation steps of sample preparation for untargeted metabolomics

Early methods reported in literature for *Leishmania* parasites involved rapid quenching of *Leishmania* cultures and washing cells with ice cold PBS to remove the serum rich extracellular medium. Here, sample preparation was optimised for cells cultured in defined medium by omission of washing step and centrifugation speed at 1000 g with slow acceleration and slow deceleration to avoid cell lysis. Results from LC-MS experiment were visualised using principal component analysis to compare intracellular samples of *L. mexicana* promastigotes cultured in Defined medium with naïve medium (without parasites) and culture supernatant on Day 3 by untargeted metabolomics as shown in Figure 5.1.

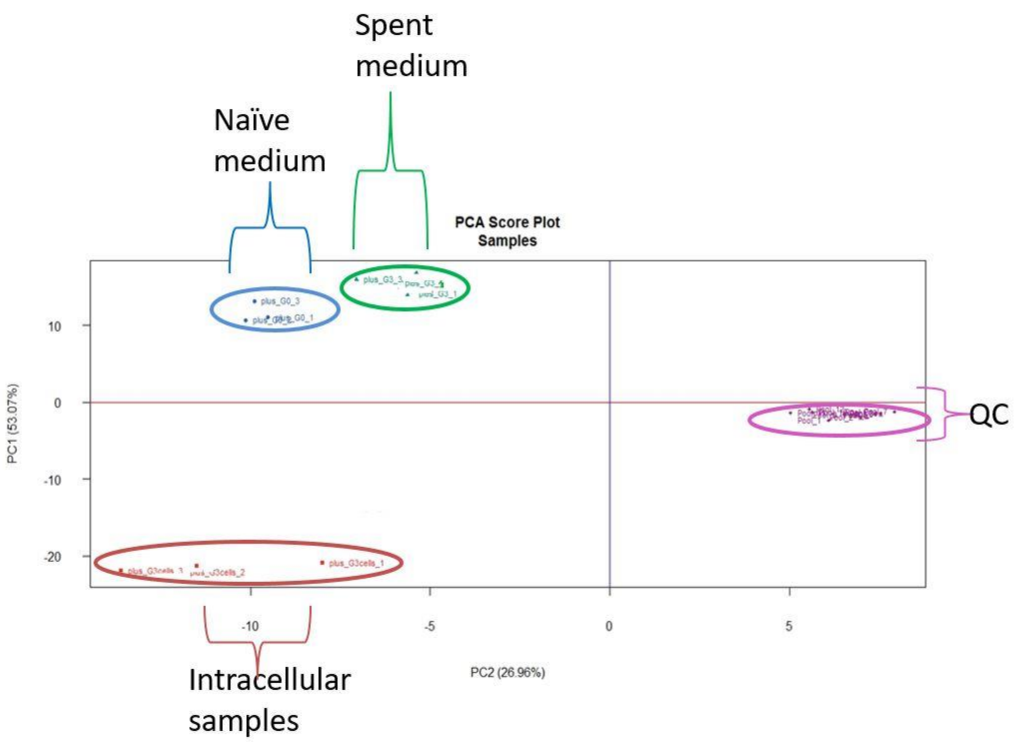

Figure 5.1 Principal component analysis of intracellular data

(21 samples from *L. mexicana* promastigotes (4 x 10^7 cells/mL) in log phase Day 3 from the start of culture initiation in defined medium processed and analysed LC-MS metabolite finger-printing data. Individual groups shown by different colours: Red- Intracellular samples (plus_G3 cells 1, 2, 3 in triplicates), Green -Spent samples (plus_G3 spent 1, 2, 3 in triplicates) and Blue-Naïve medium samples

(plus_G0 1, 2, 3 in triplicates) are clearly separated from each other and from Pink-Quality controls (Pool samples 1-12)).

Here, the pooled samples forming the quality control QC forms a cluster separated from the intracellular, spent and medium samples probably indicating increased salts in pooled samples compared to others. However, principal component analysis accounts for 80% of variance that could be explained in two components as shown amongst the data points projected in Figure 5.1. The clusters showed distinct separation between the intracellular samples, spent medium samples and naïve medium from each other. Furthermore, the robustness between the replicates has been visualised using hierarchical cluster analysis (HCA) as shown in Figure 5.2.

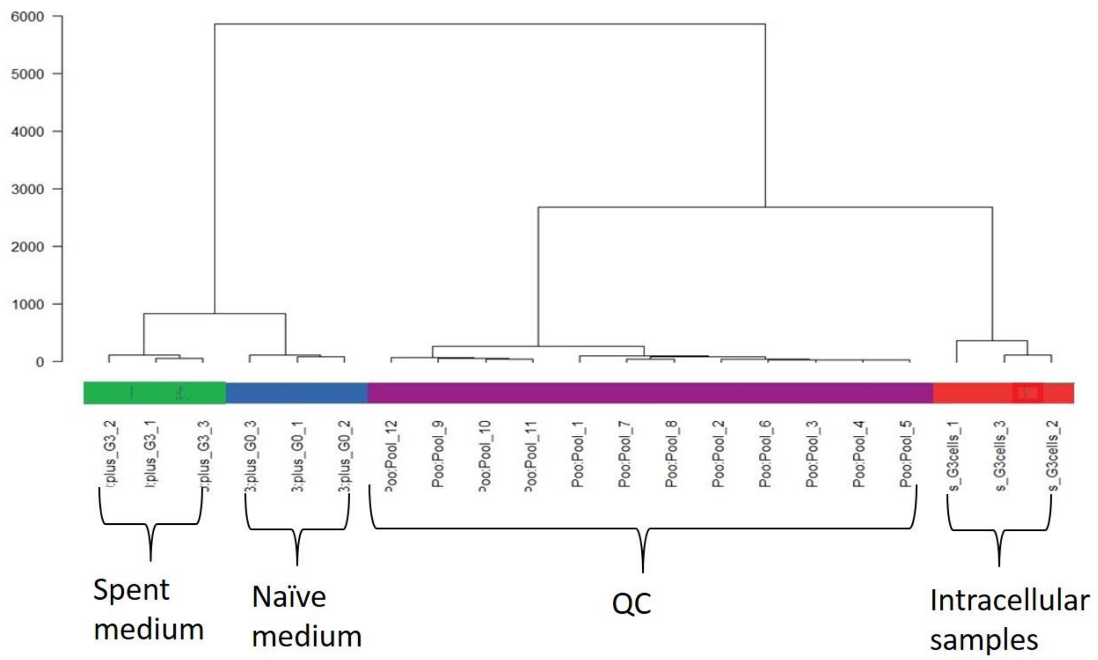

Figure 5.2 Hierarchical cluster analysis of intracellular data

Individual groups shown by different colours: Red- Intracellular samples (plus_G3 cells 1, 2, 3 in triplicates), Green -Spent samples (plus_G3 spent 1, 2, and 3 in triplicates) and Blue-Naïve medium samples (plus_G0 1, 2, 3 in triplicates) and Pink- Quality controls (Pool samples 1-12) are clearly separated from each other.

HCA analysis showed that triplicates within each group clustered together indicating reproducibility amongst the samples and validation of the sample preparation step.

Spectral analysis of intracellular metabolome was simplified by subtraction of background signals of the *in vitro* defined medium used for culture, known composition allowed for easier data interpretation of the spectral peaks not crowded by undefined serum molecules. Mass accuracy (ppm error) as observed from LC-MS (Thermo Orbitrap) and peak shapes verified for inclusion of metabolites below confidence score 7-10 using the Thermo software Quant browser and PeakML software from the total ion chromatogram as shown in Figure 5.3.

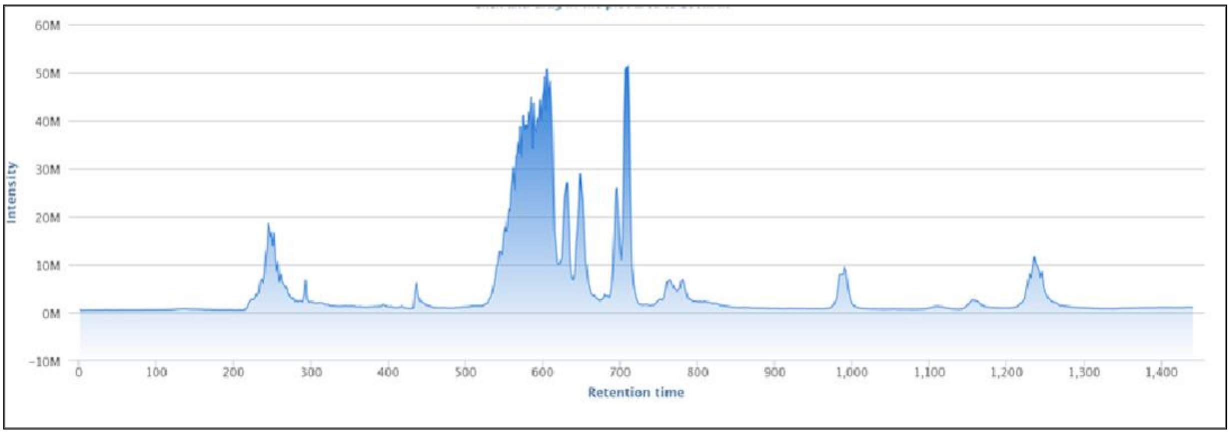

Figure 5.3 Total ion chromatogram of intracellular metabolite pool in *L. mexicana* promastigotes.

Extensive data processing steps allowed identification of 402 putatively identified metabolites peaks with mass and retention time (RT) as shown in Figure 5.4 with approximately 23 out of 45 components of the defined medium.

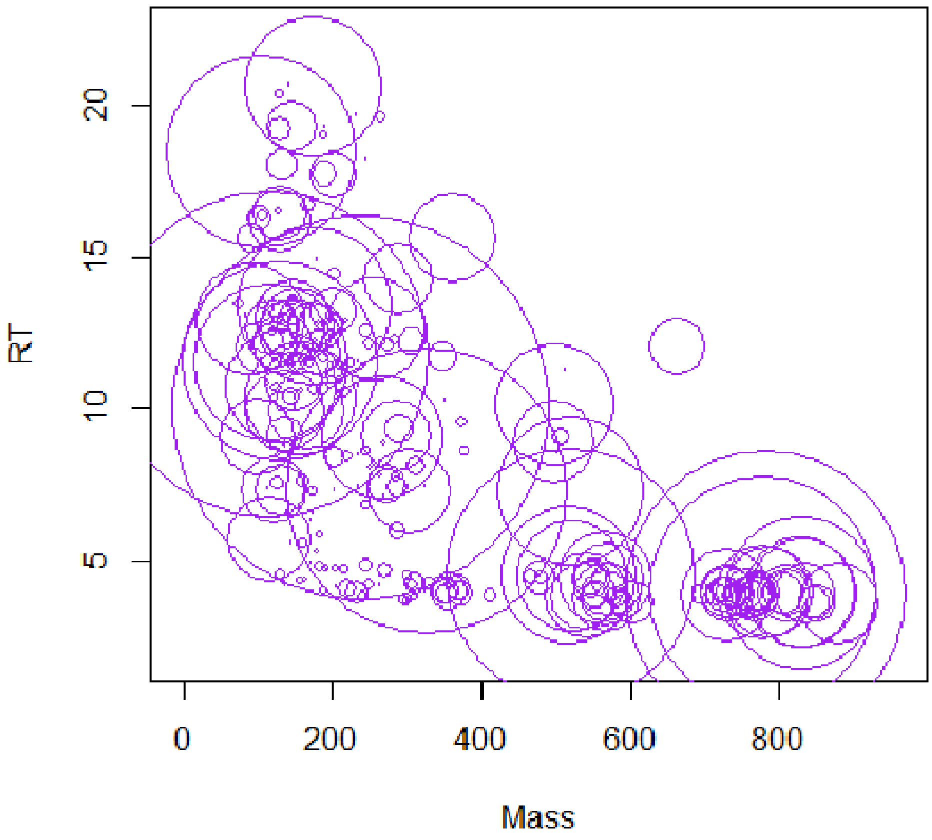

Figure 5.4 Bubble plot of all metabolites detected in the intracellular dataset

(Mean peak intensity of metabolites expressed as relative radius of the circles).

Amongst the 402 metabolites recovered from the intracellular dataset; ~252 metabolites are depicted as circles relative to their abundance in the intracellular metabolome as shown in Figure 5.4. These 252 metabolites could be assigned to metabolic pathways as specified by IDEOM software (Creek et al; 2012b). Hence, only ~60% of metabolites found either in the intracellular extract, spent sample or fresh medium could be assigned to metabolic pathways. The putatively identified metabolites could then be divided between the different pathways expressed as bar graph shown in Figure 5.5. The remaining 150 metabolites were assigned as class 2 identifications not matched with authentic standard; and subjected as putatively identified by the instrument.

Since, the sample preparation method was focused on extraction of polar metabolites such as amino acids; authentic standards included during the sample preparation were mostly polar compounds too. Amongst the 252 metabolites, 64 metabolites were associated with amino acid metabolic pathways within the intracellular metabolome as shown in Figure 5.5.

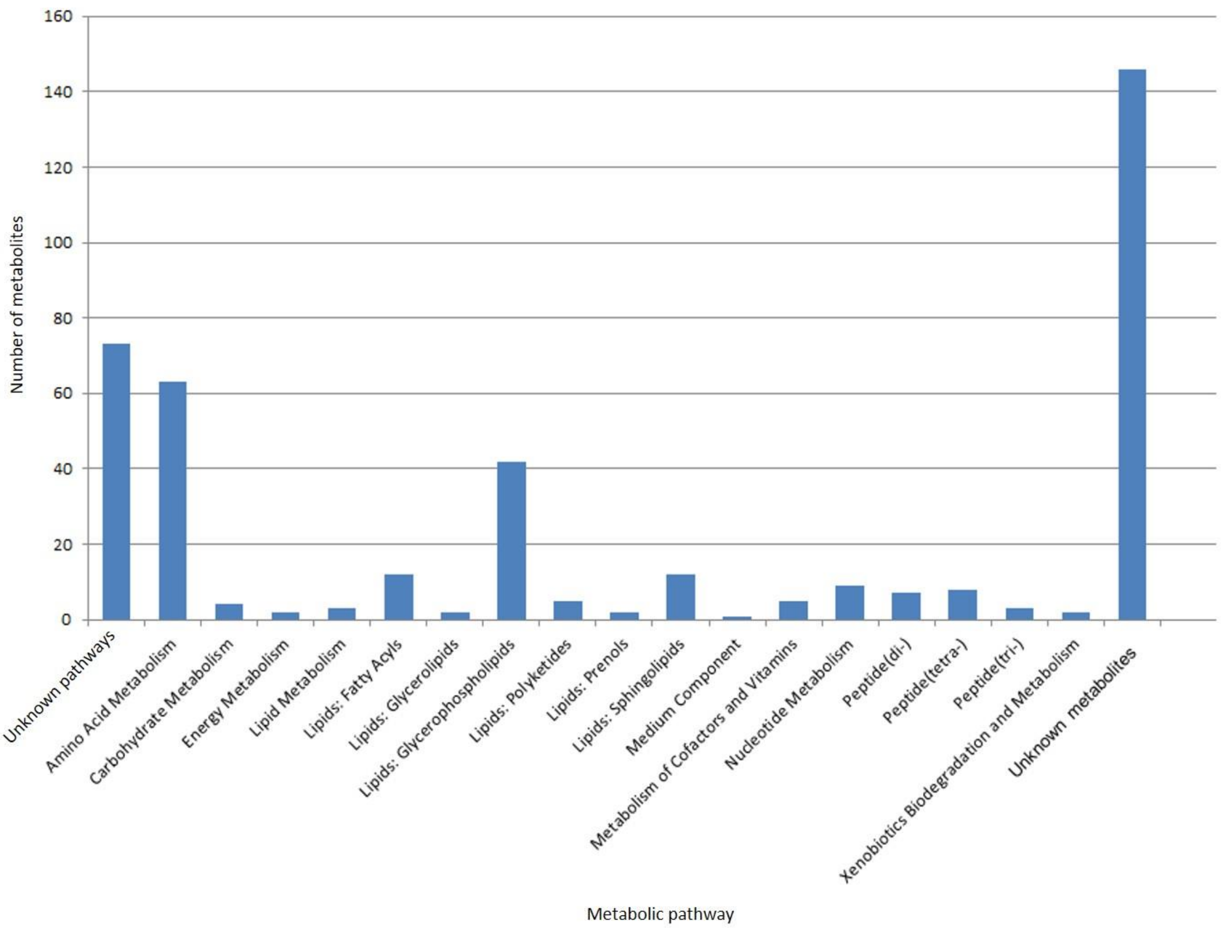

Figure 5.5 Pathways identified within the intracellular metabolome of *L. mexicana* promastigotes

The number of metabolites in individual pathways from the intracellular metabolome of log phase *L. mexicana* promastigotes on day 3 from the start of culture initiation have been depicted in Figure 5.5. Pathway names depicted as annotations represented in KEGG database (Kanehisa and Goto, 2000).

Amongst the 64 metabolites related to amino acid metabolism, only 44 could be identified with authentic standards, whilst the remaining have been validated using mass, retention time and chemical identity using databases such as chemspider, Metacyc, KEGG, etc.

The rate of depletion of the amino acids have been expressed as relative ratio of amino acids level in spent medium compared to naïve medium incubated to similar time as shown in Figure 5.6.

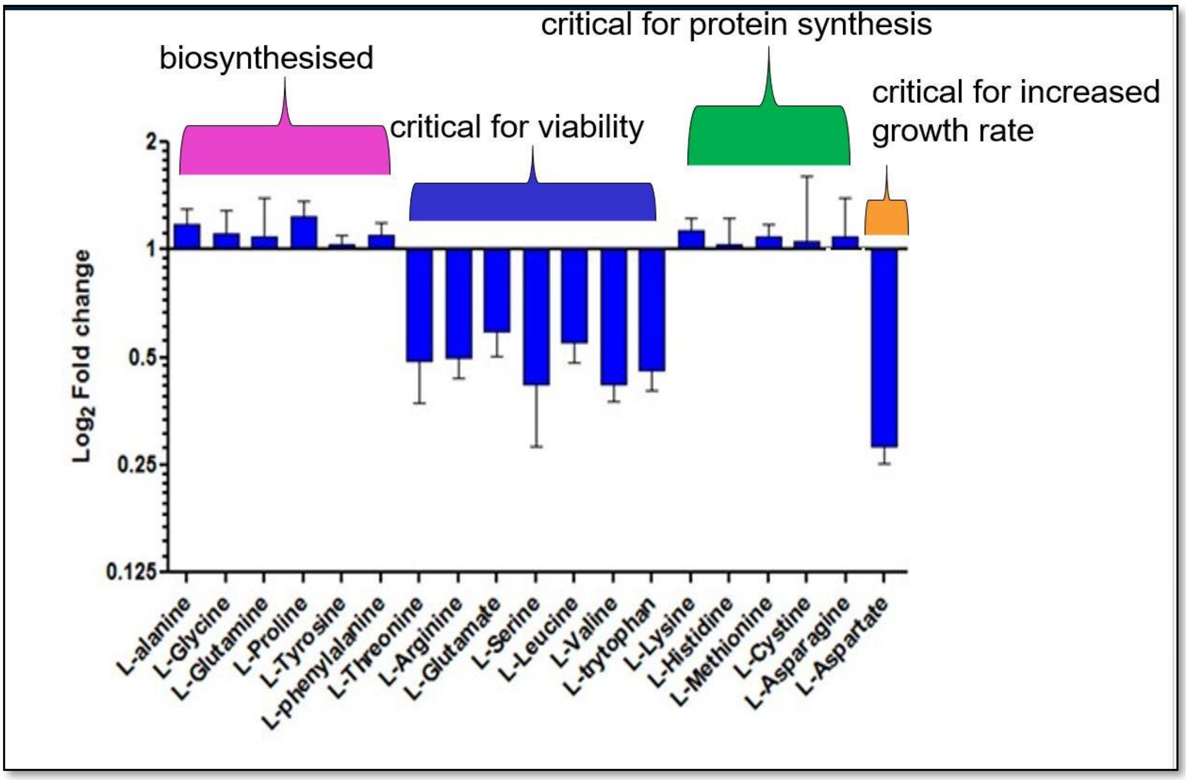

Figure 5.6 Relative quantification of amino acids in spent medium (culture supernatant) on day 3 from the start of culture initiation.

The height of the bar (n=3, Error bars = mean ± SD) is proportional to the log 2 fold change of amino acid levels in the spent medium (culture supernatant day 3 from the start of culture initiation) compared to naïve medium shown in Figure 5.6. The amino acids levels are further annotated according to the classification shown in

Table 4-2 to highlight correlation between amino acid essentiality based on growth data of Chapter 4 and intracellular metabolome.

The amino acids depleted from the spent medium on Day 3 culture supernatant of the log phase *L. mexicana* promastigotes were found to be L-Threonine, L-Arginine, L-Glutamate, L-serine, L-Leucine, L-Valine, L-Tryptophan and L-Aspartate as shown in Figure 5.6.

The metabolites and the instrument response recorded in the form of their peak intensity are as shown in Table 5-2.

Table 5-2 Index of bubble number and corresponding metabolite names as per KEGG annotation

Bubble number	Putative metabolite	Instrument response recorded as peak intensity
1	L-Citrulline	6437385
2	Indole-3-acetaldehyde	6345
3	L-Pipecolate	2454765
4	4-Imidazolone-5-propanoate	1126898
5	Urocanate	4320
6	Creatine	5664
7	L-Ornithine	13664
8	5-Guanidino-2-oxopentanoate	53601
9	N6,N6,N6-Trimethyl-L-Lysine	968
10	Indolelactate	1071576
11	N2-(D-1-Carboxyethyl)-L-Arginine	8197
12	Trypanothione disulfide	302976
13	N6-Acetyl-L-Lysine	980627
14	Choline	45479
15	4-Guanidinobutanoate	158854
16	L-Alanine	118701
17	[FA oxo,amino(6:0)] 3-oxo-5S-amino-hexanoic acid	5193
18	N-Acetylputrescine	3560
19	D-Lysine	8504

20	L-Leucine	902516
21	4-Imidazolone-5-acetate	752
22	4-Guanidinobutanamide	18005
23	L-Proline	235
24	indole-3-glycol	2590
25	L-Methionine	345
26	8-[(aminomethyl)sulfanyl]-6-sulfanyloctanoic acid	622636
27	L-Kynurenine	11967
28	L-Threonine	30644
29	Pantothenate	503
30	N-Acetyl-D-glucosamine	325
31	L-Histidine	1200
32	L-Glutamate 5-semialdehyde	6197
33	L-Arginine	8771
34	L-Formylkynurenine	2607825
35	L-Lysine 1,6-lactam	14532
36	N,N-Dimethylglycine	12980
37	O-Acetyl-L-homoserine	1046
38	L-Valine	2052950
39	LL-2,6-Diaminoheptanedioate	1586564
40	L-Tyrosine	917
41	L-Phenylalanine	9384
42	Imidazole-4-acetate	16989
43	L-Methionine S-oxide	4854
44	L-Asparagine	7727
45	N-gamma-Acetyldiaminobutyrate	28492
46	L-Cystine	56851
47	L-Glutamine	53456
48	Glycine	1144
49	L-Tryptophan	2430
50	L-Serine	57402
51	Indole-3-acetamide	1416
52	L-Glutamate	2180
53	L-Aspartate	100046
54	indole-3-glyoxal	628288

55	Indole-3-acetate	61894
56	(S)-1-Pyrroline-5-carboxylate	548
57	N4-Acetylaminobutanal	2367
58	Homoarginine	6786333
59	Spermidine	5429
60	Glutathione	16002
61	gamma-Glutamyl-gamma-aminobutyraldehyde	173108
62	gamma-L-Glutamyl-L-cysteine	179084
63	N(pi)-Methyl-L-Histidine	190815
64	Methyl-L-Histidine	1256

Visual analysis of the 64 metabolites as shown in Table 5.5 which were associated with amino acid metabolism within the intracellular metabolome were considered for further analysis using bubble plots as shown in Figure 5.7 and 5.8.

The relative abundance of all the amino acid intermediates are shown in Figure 5.7 (A) and amino acids shown as sub set in Figure 5.7(B) for more clear data exploration.

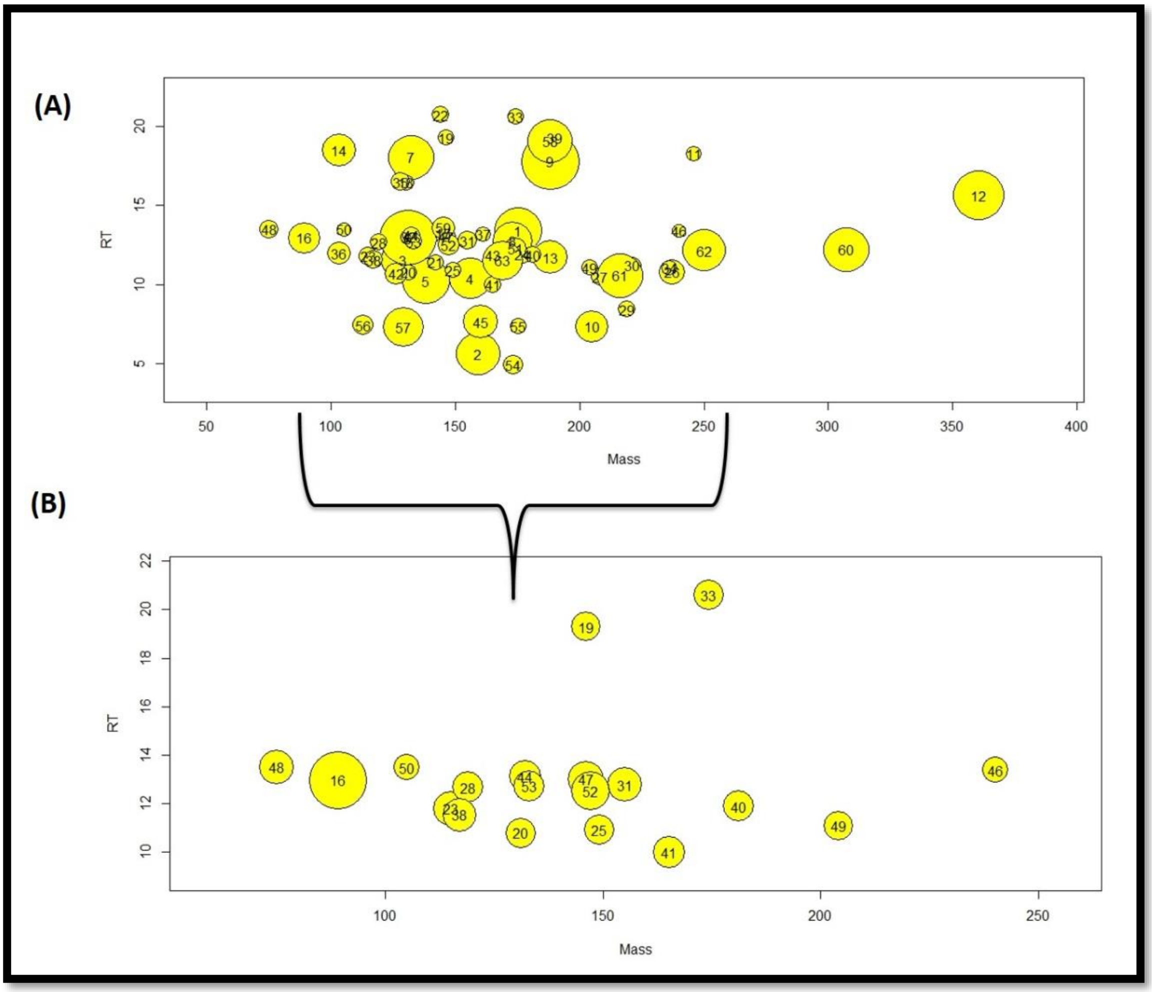

Figure 5.7 Intracellular metabolome of *L. mexicana* promastigotes

Bubble plot of (A) all amino acid intermediates and (B) amino acids. Peak intensity of metabolites proportional to the relative radii of circles. The metabolites were identified as belonging to amino acid pathway as annotated from Kegg database (Kanehisa and Goto, 2000).

The order of increasing peak intensities of amino acids in the intracellular samples of *L. mexicana* promastigotes in log phase, Day 3 from the start of culture initiation as observed from Figure 5.7 (B) were found as follows L-Alanine > L-Glutamate > L-Glutamine > L-Glycine > L-Proline > L-Histidine > L-Valine > L-Asparagine > L-Phenylalanine > L-Threonine > L-Tyrosine > L-Aspartate > L-Leucine > L-Arginine > L-Methionine > L-Tryptophan > L-Lysine > L-Serine and L-Cysteine.

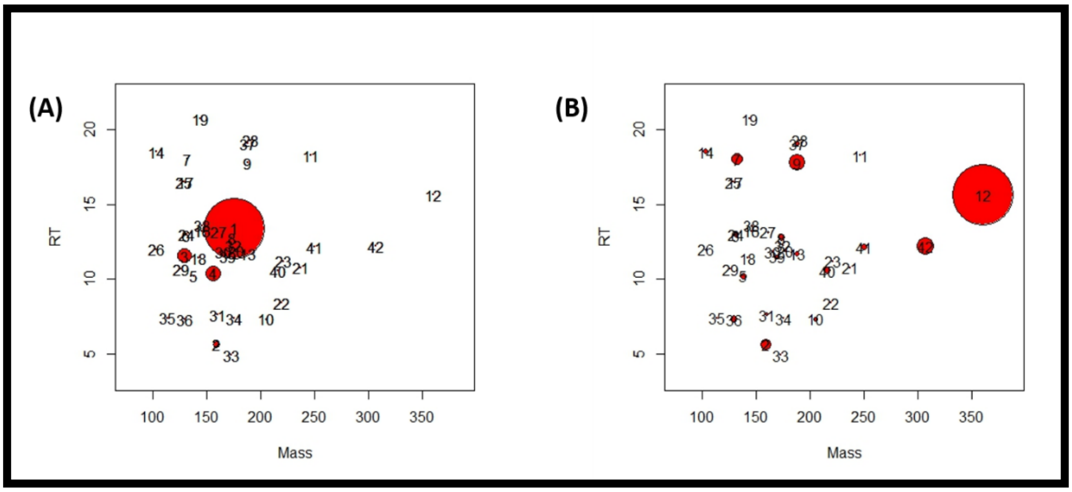

Figure 5.8 Bubble plot of amino acid intermediates

Further data exploration of amino acid intermediates was done plotting individual subsets of data as represented in Figure 5.8 (A) and (B). This showed that certain amino acid intermediates highlighted in Figure 5.8 (A) such as L-Citrulline (Bubble plot number 1), L-Indole-3-acetaldehyde (Bubble plot number 4) and L-Pipecolate (Bubble plot number 3) were significantly accumulated in the intracellular metabolome. A sub-set was plotted to understand which other metabolites accumulated in the intracellular metabolome by masking the above mentioned first three abundant metabolites showed that trypanothione (Bubble plot number 12), imidazole acetate (Bubble plot number 42) and N6-N6-N6 tri-methyl L-Lysine (Bubble plot number 9) were found to be accumulated within the intracellular metabolome shown in Figure 5.8(B).

Most of the metabolites detected in the intracellular samples were not present in the naïve medium. Furthermore, the efficiency of cell disruption during sample preparation were checked by comparing the peak intensities in naïve medium and supernatant samples versus the intracellular metabolome. Metabolic intermediates such as gamma-Glutamyl-gamma-amino-butyraldehyde, gamma-L-Glutamyl-L-cysteine and trypanothione biosynthesised exclusively in *Leishmania* were considered as key markers as shown in Table 5-3. There was no metabolite leakage due to cell disruption during sample preparation as observed from Table 5-3.

Table 5-3 shows relative mean peak intensity values compared between the intracellular, spent medium and naïve medium.

Bubble number	Putative metabolite	Mass	RT	Pea
				Day 3
12	Trypanothione disulfide	360.644	15.635	302
40	gamma-Glutamyl-gamma-amino-butyraldehyde	216.110	10.571	173
41	gamma-L-Glutamyl-L-cysteine	250.062	12.138	179
42	Glutathione	307.083	12.226	160

Intracellular metabolites exclusive to *Leishmania* metabolism such as gamma-glutamyl-cysteine and, trypanothione were not detected in the spent medium. This result validated the protocol optimisation steps of ensuring minimum shear physical stress with slow centrifugation method during sample preparation and avoiding the washing step allowed to capture the metabolic snapshot without delays. Absence of leakage of intracellular metabolites also highlighted the separation efficiency of intracellular metabolites between cells extracts, supernatants and naïve medium treated under similar conditions.

Table 5-4 Number of metabolites per pathway detected in the intracellular dataset.

Name of the pathway	No. of metabolites detected in the intracellular dataset	No. of total metabolites annotated in Kegg pathway databases
Alanine, L-Aspartate and L-Glutamate metabolism	7	25
L-Arginine biosynthesis	5	19
Tyrosine metabolism	4	75
Cysteine and L-Methionine metabolism	3	54
Glycine, serine and L-Threonine metabolism	6	45

Sulfur metabolism	4	22
L-Tryptophan metabolism	3	80
L-Arginine and L-Proline metabolism	8	67
Lysine degradation	3	42
Phenylalanine metabolism	4	64
Phenylalanine, L-Tyrosine and L-Tryptophan biosynthesis	6	31
Valine, L-Leucine and isoleucine biosynthesis	4	23
Valine, L-Leucine and isoleucine degradation	2	32

Comparison of metabolites detected to number of total metabolites annotated in KEGG pathway database KEGG (Kanehisa, Goto et al. 2006) charted using Pathos (A metabolomics tool from Glasgow Polyomics accessible at http://motif.gla.ac.uk/Pathos/) (Leader, Burgess et al. 2011), and MetaCyc, accessible at http://metacyc.org/))

The metabolites from the amino acid pathway were variously populated as shown in Table 5-4 to calculate the number of metabolites detected per pathway. Pathos software was used to compare the different metabolites detected in this study of *L. mexicana* intracellular data set compared to total number of metabolites annotated in KEGG pathway database (Leader et al., 2011) in a non-organism specific manner. Thus Table 5-4 highlights the specific differences of particular pathway metabolism in *Leishmania* compared to standard annotated pathway in public database such as KEGG (Kanehisa, Goto et al. 2006). These metabolites were of interest since network mapping in an unbiased manner would allow new insights to be gained from the data as shown in section 5.2.4.

5.2.4 Metabolite levels of individual amino acid pathways in *L. mexicana* promastigotes

Intracellular metabolites of *L. mexicana* promastigotes at Day 3 in defined medium from the start of culture initiation are measured using the values of peak intensities specific to instrument response at conditions as specified in the methods section of chapter 2. The metabolites of individual amino acids in metabolic pathways are shown below in the order of importance of proteogenic amino acids as reported in section 4.1.

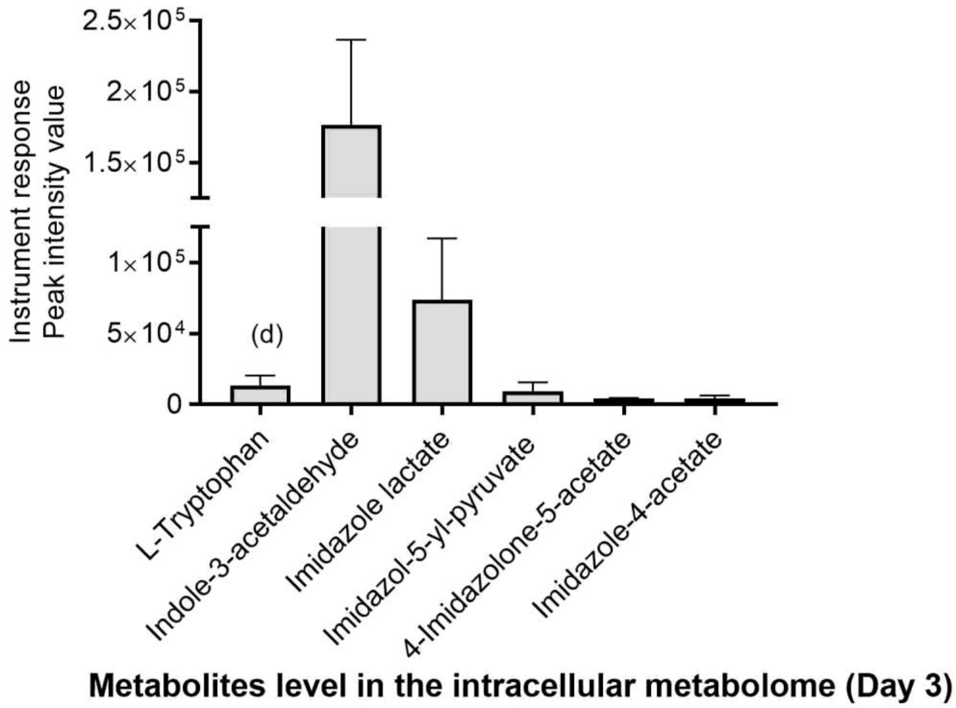

Figure 5.9 L-Tryptophan metabolism

Metabolites shown in Figure 5.9 were intracellular samples of 4e+10^7 cells of *L. mexicana* promastigotes from Day 3 from the start of culture initiation in DM in triplicates as described in experimental procedures. Instrument response of peak intensity of metabolites recorded for the intracellular samples with n=3, Error bars = mean ± SD. Those metabolites detected in the naïve medium (incubated for similar time) are represented as (d).

L-Tryptophan is metabolised with major flux directed to indole acetaldehyde and indole lactate as shown in Figure 5.9. Other intracellular intermediates include indole-3-glycol, indole 3 acetate, indole 3 glyoxal, indole acetamide, L-kynurenine, L-formylkynurenine are found in lesser abundance.

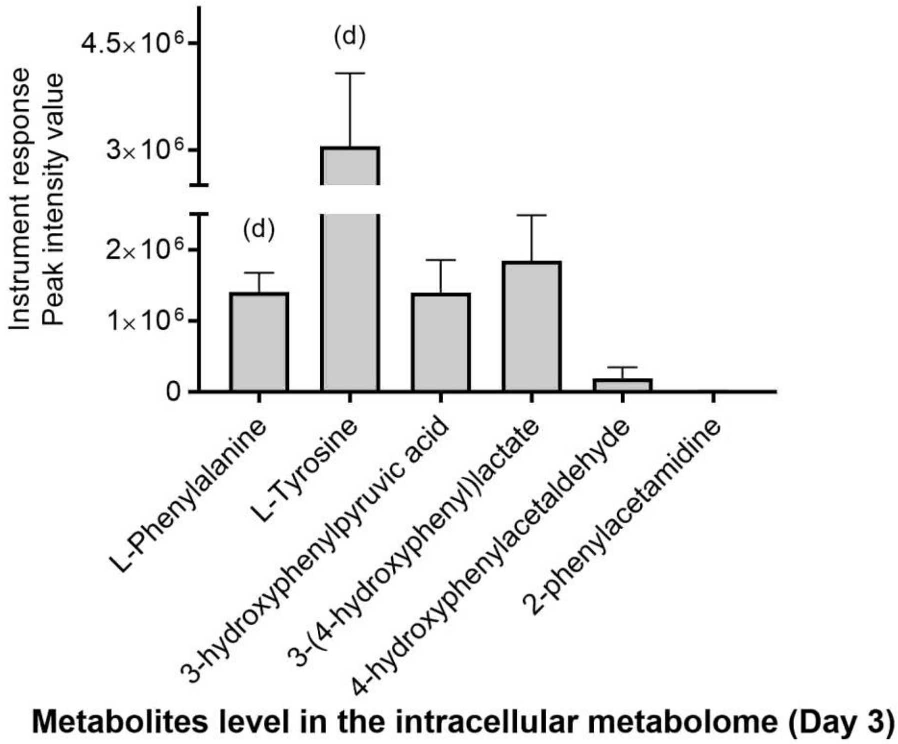

Figure 5.10 L-Phenylalanine metabolism

Metabolites shown in Figure 5.10 were intracellular samples of 4e+10^7 cells of *L. mexicana* promastigotes from Day 3 from the start of culture initiation in DM in triplicates as described in experimental procedures. Instrument response of peak intensity of metabolites recorded for the intracellular samples with n=3, Error bars = mean ± SD. Those metabolites detected in the naïve medium (incubated for similar time) are represented as (d).

Intracellular metabolites of L-Phenylalanine metabolism detected and putatively identified in this study through the LC-MS data were L-Phenylalanine, L-Tyrosine metabolised to relatively abundant concentration of 3-Hydroxyphenyl-pyruvic acid (also called as phenylpyruvate), and 3-(4-Hydroxyphenyl) lactate (also called as phenyllactate) compared to 4-Hydroxyphenylacetaldehyde (also called phenylacetaldehyde) and 2-phenylacetamidine (also called phenylacetate) as shown in Figure 5.10

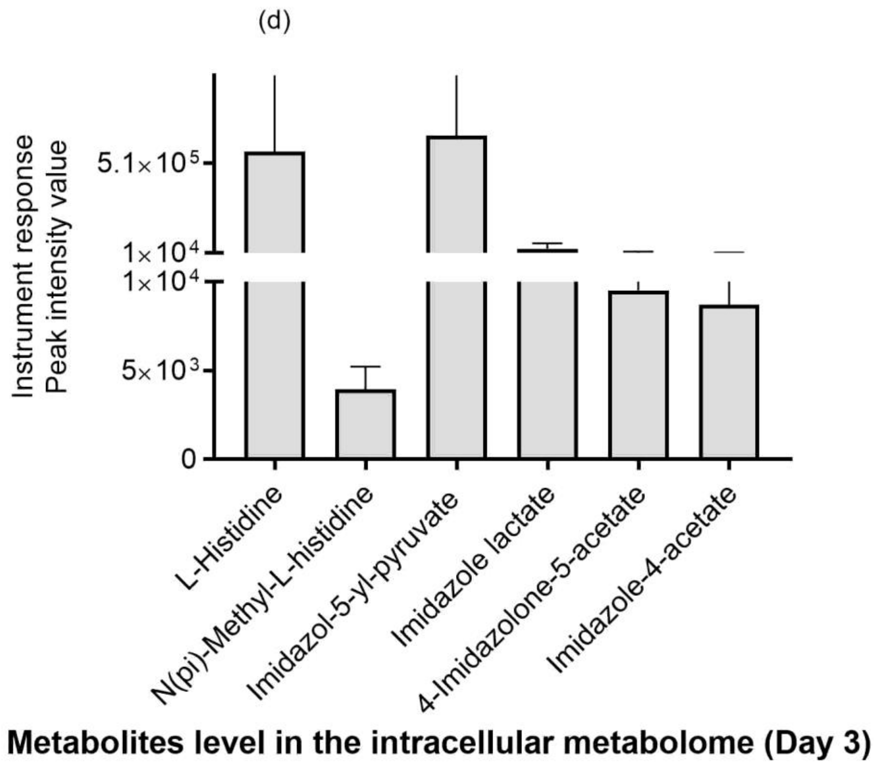

Figure 5.11 L-Histidine metabolism

Metabolites shown in Figure 5.11 were intracellular samples of 4e+10^7 cells of *L. mexicana* promastigotes from Day 3 from the start of culture initiation in DM in triplicates as described in experimental procedures. Instrument response of peak intensity of metabolites recorded for the intracellular samples with n=3, Error bars

= mean ± SD. Those metabolites detected in the naïve medium (incubated for similar time) are represented as (d).

It has been observed that Imidazol-5-yl-pyruvate followed by Imidazole lactate were found in relatively more abundance compared to 4-Imidazolone-5-acetate and Imidazole-4-acetate. Also, methylated L-Histidine in the form of N-(pi)-Methyl-L-Histidine was observed in the intracellular metabolome linked to L-Histidine metabolism as represented in Figure 5.11.

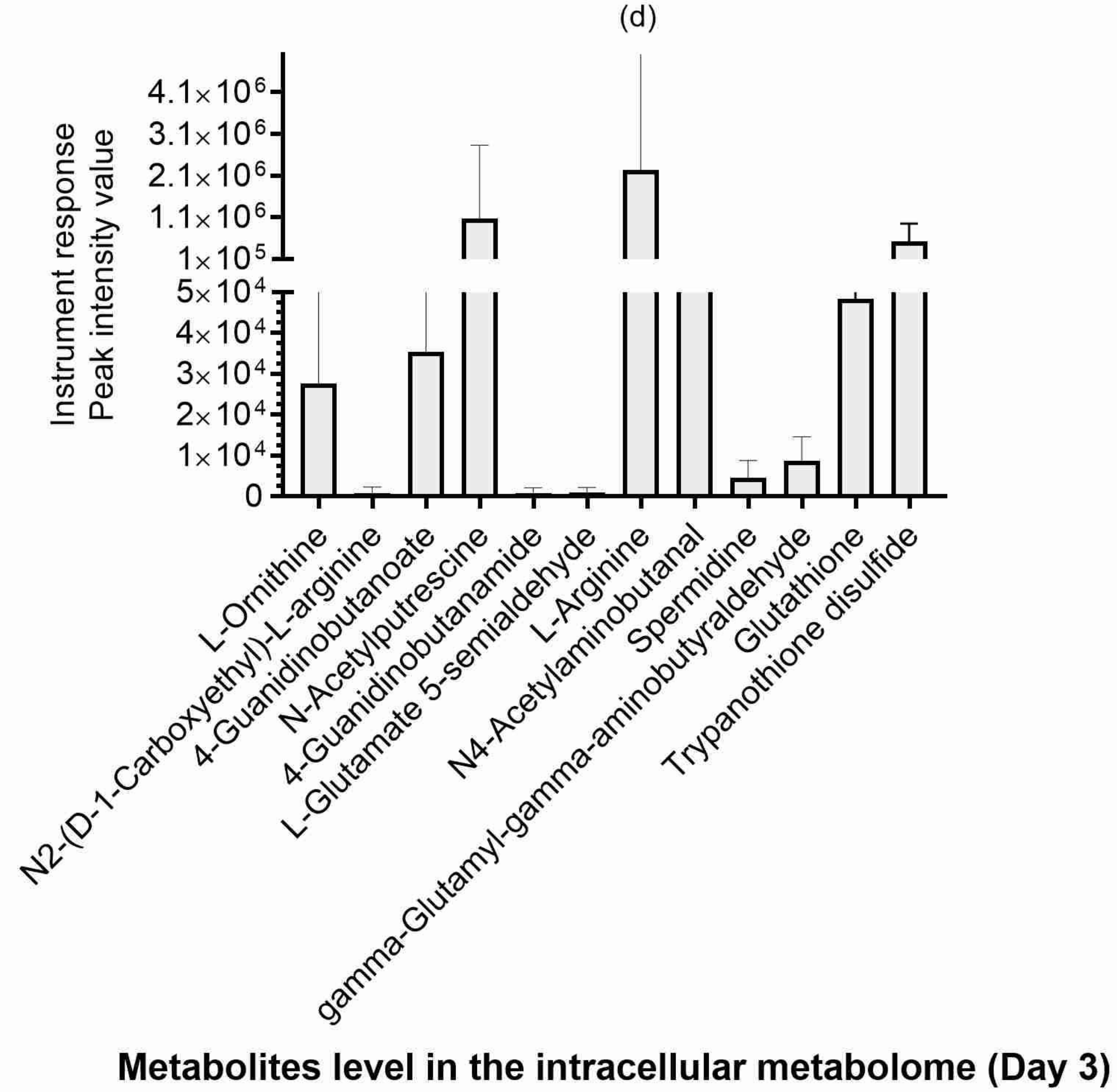

Figure 5.12 L-Arginine metabolism

Metabolites shown in Figure 5.12 were intracellular samples of 4e+10^7 cells of *L. mexicana* promastigotes from Day 3 from the start of culture initiation in DM in triplicates as described in experimental procedures. Instrument response of peak intensity of metabolites recorded for the intracellular samples with n=3, Error bars

= mean ± SD. Those metabolites detected in the naïve medium (incubated for similar time) are represented as (d).

Putative identifications of metabolites from the L-Arginine metabolism are as follows: L-Arginine, L-Glutamate 5-semialdehyde, (S)-1-Pyrroline-5-carboxylate, Spermidine, gamma-Glutamyl-gamma-aminobutyraldehyde, N4-Acetylaminobutanal, L-Citrulline, L-Ornithine, 4-Guanidinobutanamide and Creatine as shown in Figure 5.12.

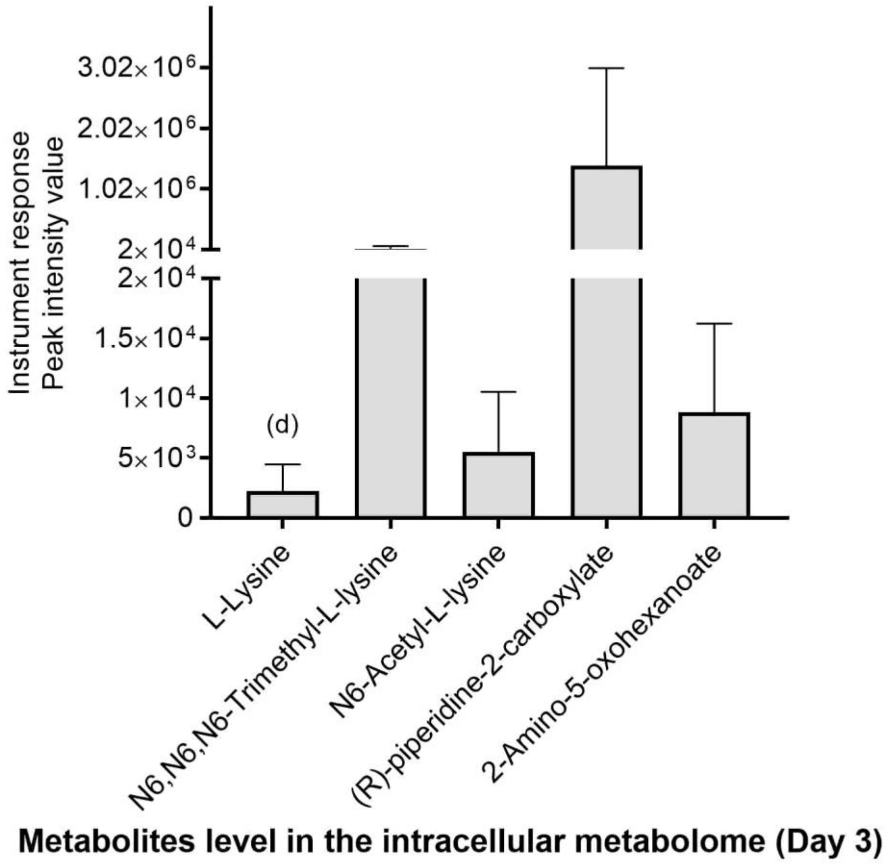

Figure 5.13 L-Lysine metabolism

Metabolites shown in Figure 5.13 were intracellular samples of 4e+10^7 cells of *L. mexicana* promastigotes from Day 3 from the start of culture initiation in DM in triplicates as described in experimental procedures. Instrument response of peak intensity of metabolites recorded for the intracellular samples with n=3, Error bars

= mean ± SD. Those metabolites detected in the naïve medium (incubated for similar time) are represented as (d).

Putative identifications of metabolites from the L-Lysine metabolism are shown in Figure 5.13 increased relative abundance of intermediates such as N6,N6,N6-Trimethyl-L-Lysine, N6-Acetyl-L-Lysine, (R)-piperidine-2-carboxylate and 2-Amino-5-oxohexanoate and L-Lysine.

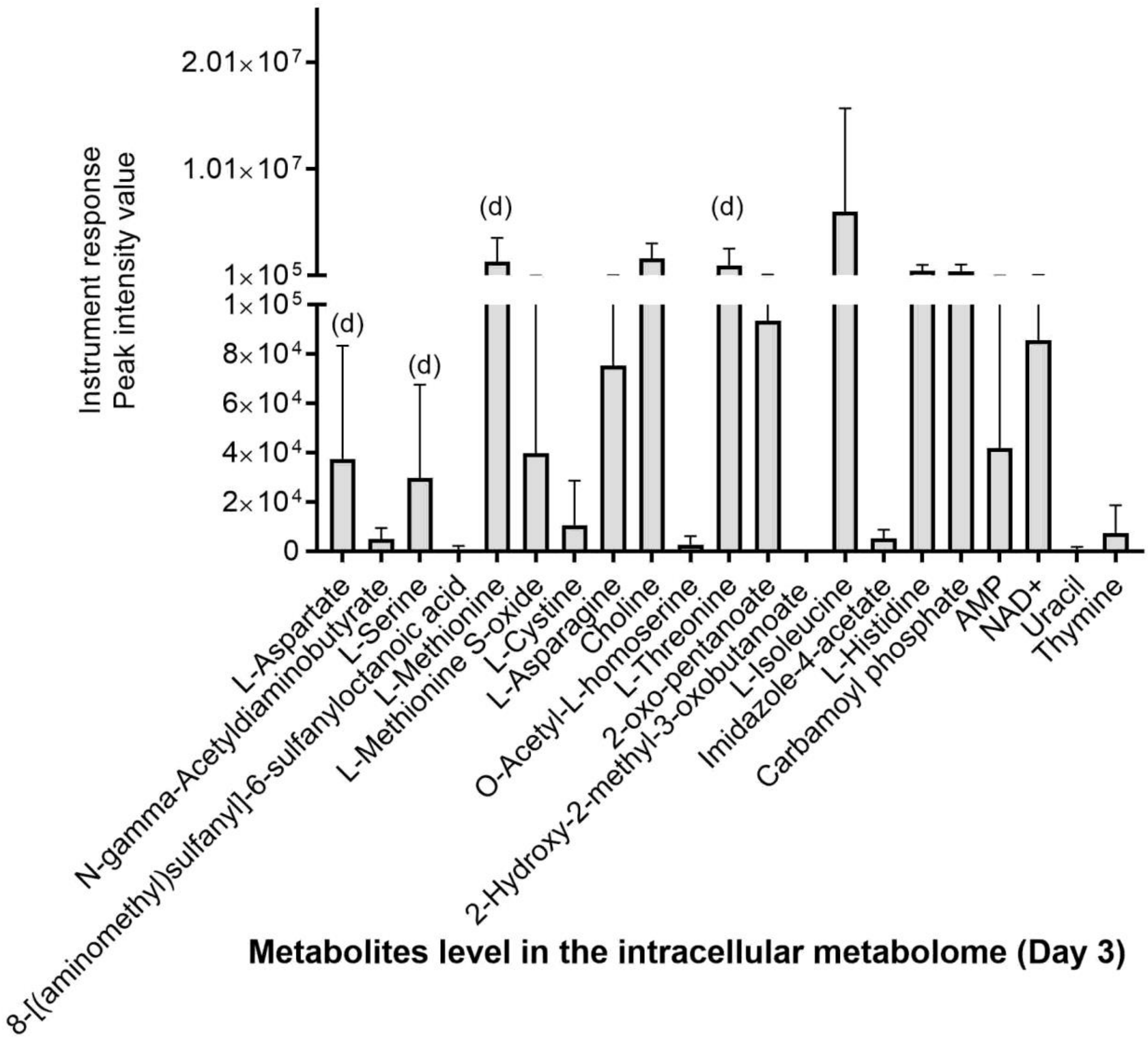

Figure 5.14 L-Aspartate metabolism

Metabolites shown in Figure 5.14 were intracellular samples of 4e+10^7 cells of *L. mexicana* promastigotes from Day 3 from the start of culture initiation in DM in triplicates as described in experimental procedures. Instrument response of peak intensity of metabolites recorded for the intracellular samples with n=3, Error bars = mean ± SD. Those metabolites detected in the naïve medium (incubated for similar time) are represented as (d).

Metabolites associated with L-Aspartate metabolism as shown in Figure 5.14 were found as follows N-gamma-acetyl-di-amino-butyrate, O-acetyl-L-homo-serine, 8-[(amino-methyl)-sulphonyl]-6-sulphanyloctanoic acid, 2-oxo-pentanoate, 2-Hydroxy-2-methyl-3-oxobutanoate, AMP and NAD+, were found to be more abundant than L-Serine, L-Methionine, L-Methionine S-oxide, L-L-Cysteine, L-Asparagine, L-Threonine, L-isoleucine, Imidazole-4-acetate, L-Histidine, Carbamoyl phosphate, Uracil and Thymine.

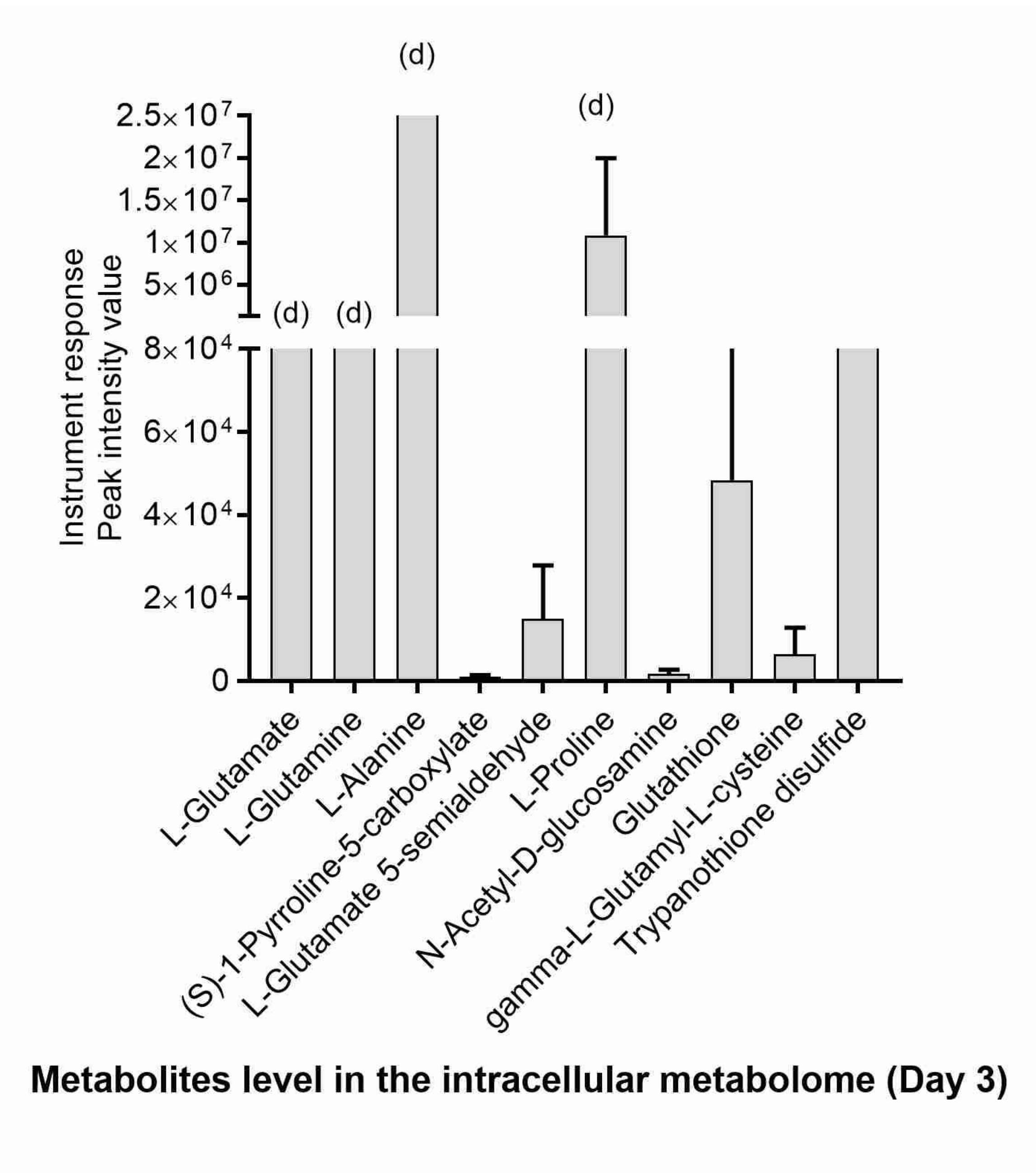

Figure 5.15 L-Glutamate metabolism

Metabolites shown in Figure 5.15 were intracellular samples of 4e+10^7 cells of *L. mexicana* promastigotes from Day 3 from the start of culture initiation in DM in triplicates as described in experimental procedures. Instrument response of peak intensity of metabolites recorded for the intracellular samples with n=3, Error bars

= mean ± SD. Those metabolites detected in the naïve medium (incubated for similar time) are represented as (d).

Metabolites linked to L-Glutamate in the intracellular metabolome in the decreasing order of relative abundance at log phase of growth were L-Glutathione, gamma-L-Glutamyl-L-cysteine, L-Alanine, (S)-1-pyrroline-5-carboxylate, L-Proline, L-Glutamate 5-semialdehyde, N-Acetyl-D-glucosamine, L-Glutamine and L-Glutamate as shown in Figure 5.15.

The relative levels of metabolites associated with individual amino acid pathways within the intracellular metabolome shown above has been visualised by novel network mapping of the metabolites in an unbiased manner without limitations from genome annotations, but purely on the metabolic snapshot data; as elaborated in the next section 5.2.5.

5.2.5 Novel unbiased mapping of amino acid metabolites

Here, unbiased mapping of amino acid metabolic pathways were constructed to using intracellular metabolome data. Metabolites for each individual amino acid pathway have been separately analysed and non-homologous differences between *Leishmania* and mammals were highlighted to indicate the presence of alternative routes and novel metabolic enzymes/pathways as potential drug targets.

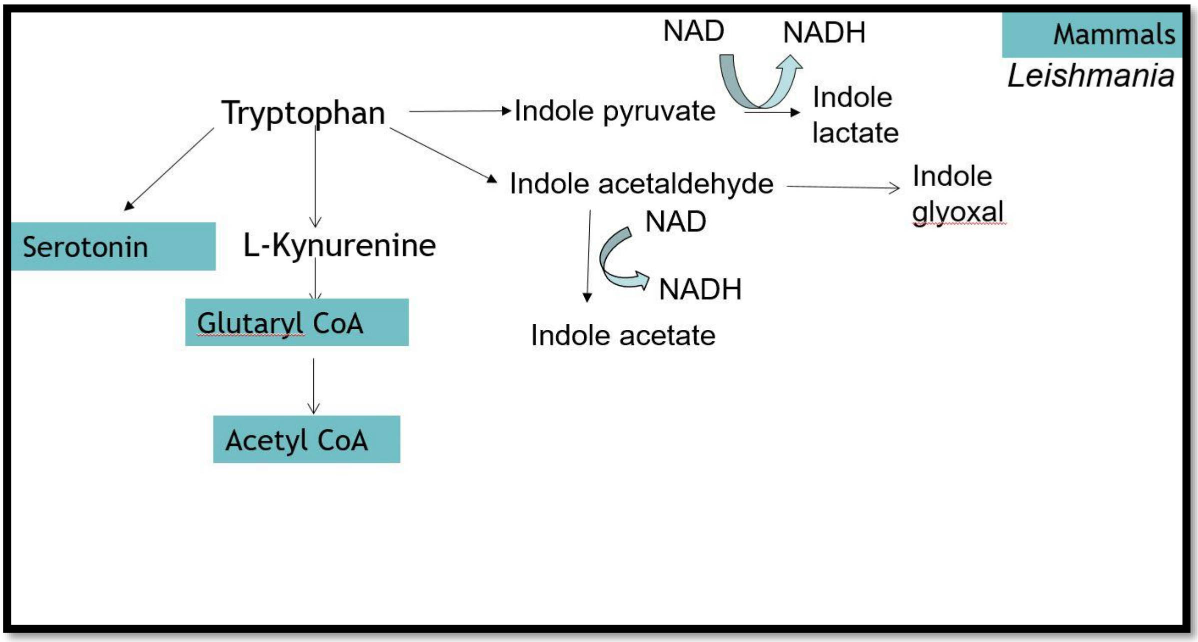

Figure 5.16 Schematic representation of L-TL-Tryptophan metabolism

L-Tryptophan utilisation in *L. mexicana* promastigotes using intracellular metabolomics data shown with the step for NADH regeneration compared to metabolic routes in mammals (*Homo sapiens*) is highlighted.

As observed from Figure 5.9, L-Tryptophan is metabolised with major flux directed to indole acetaldehyde and indole lactate. Other intracellular intermediates includes indole-3-glycol, indole 3 acetate, indole 3 glyoxal, indole acetamide, L-kynurenine, L-formylkynurenine are found to lesser abundance, indicating low activities of these enzymes described in discussion section

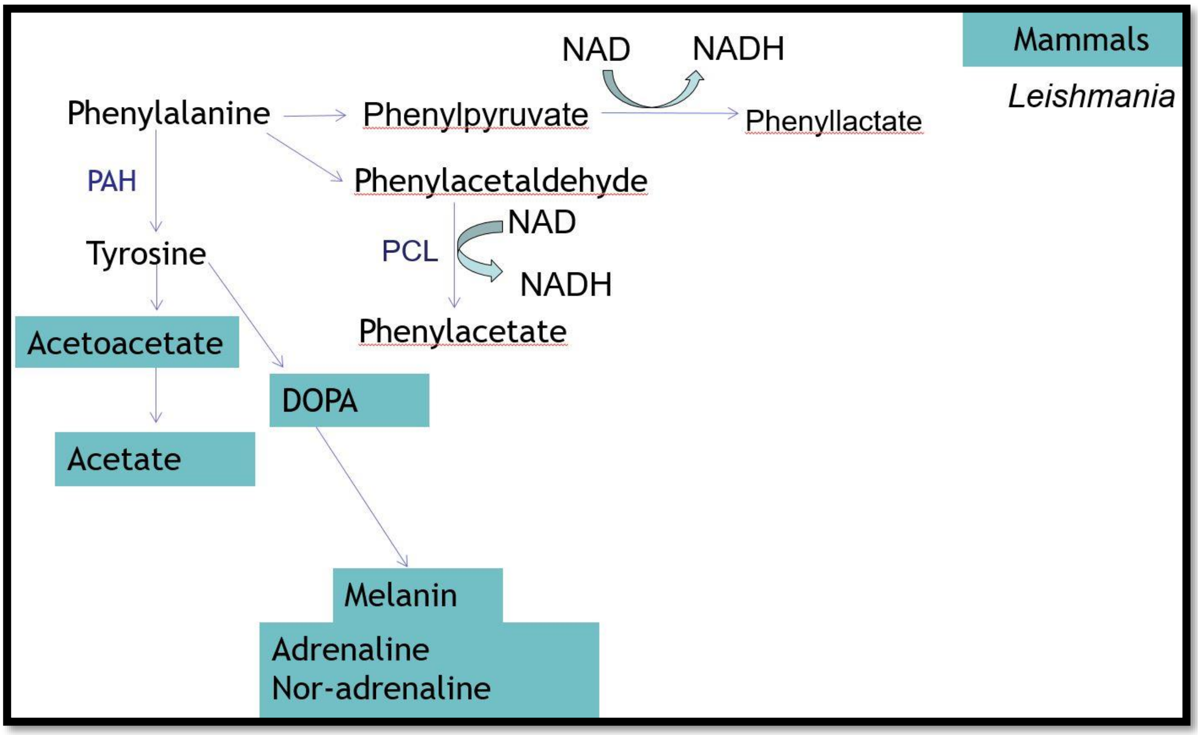

Figure 5.17 Schematic representation of L-Phenylalanine metabolism

L-Phenylalanine utilisation by *L. mexicana* promastigotes using intracellular metabolomics data shown with the step for NADH regeneration compared to in mammals (*Homo sapiens*) is highlighted.

Intracellular metabolites of L-Phenylalanine metabolism detected and putatively identified in this study through the LC-MS data as shown in Figure 5.10 has been used for network mapping to show L-Phenylalanine is metabolised to L-Tyrosine by the enzyme L-Phenylalanine hydroxlase (PAH) present in *Leishmania* and mammals. However, an additional step forming phenyllactate is responsible for NADH generation and detection of metabolites such as phenylacetaldehyde *and* phenylacetate gave insights that new enzyme involved in L-Phenylalanine metabolism called L-Phenylalanine carboxylase (PCL) converts phenyl-acetaldehyde to phenylacetate for NADH regeneration as an alternative route not reported before.

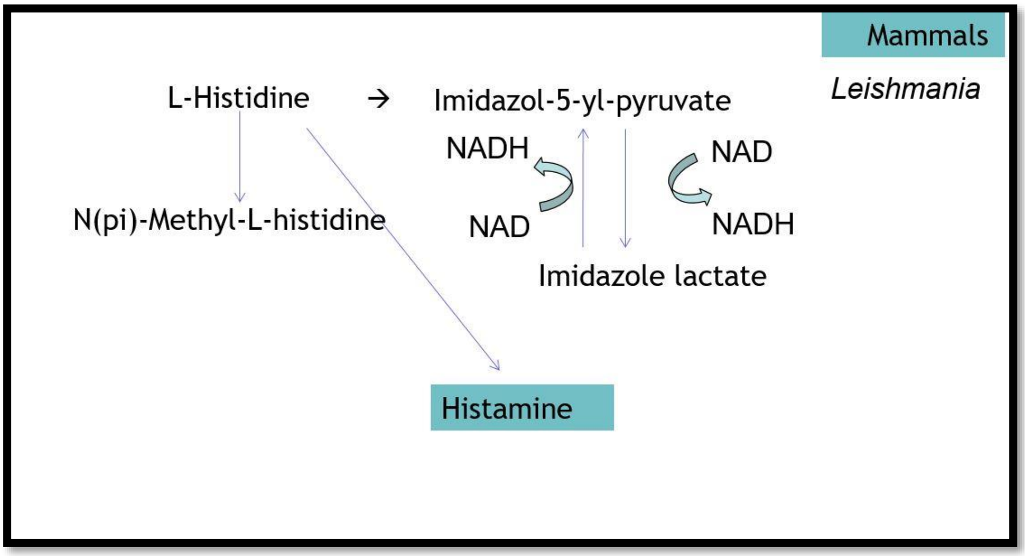

Figure 5.18 Schematic representation of L-Histidine metabolism

Histidine utilisation by *L. mexicana* promastigotes using intracellular metabolomics data shown with the step for NADH regeneration compared to in mammals (*Homo sapiens*) is highlighted.

Metabolomics data was examined for metabolites of the L-Histidine pathway as shown in Figure 5.11, such as imidazol-5-yl-pyruvate, imidazole lactate, 4-imidazolone-5-acetate, imidazole-4-acetate has been putatively detected and verified using Chemspider for chemical synonyms. These metabolites indicate that L-Histidine could potentially be degraded by alternative pathway not found in mammals. Instead, from network mapping of these metabolites as shown in Figure 5.18, L-Histidine catabolised to yield Imidazol-5-yl-pyruvate /1H-Imidazole-5-propanoic acid by the broad spectrum L-Histidine-pyruvate aminotransferase. However, it is the detection of the downstream metabolites of imidazole lactate, 4-imidazolone-5-acetate and imidazole-4-acetate are metabolites which participate in NADH regeneration. These enzymes are not present in the mammalian systems, hence serve as potential drug targets.

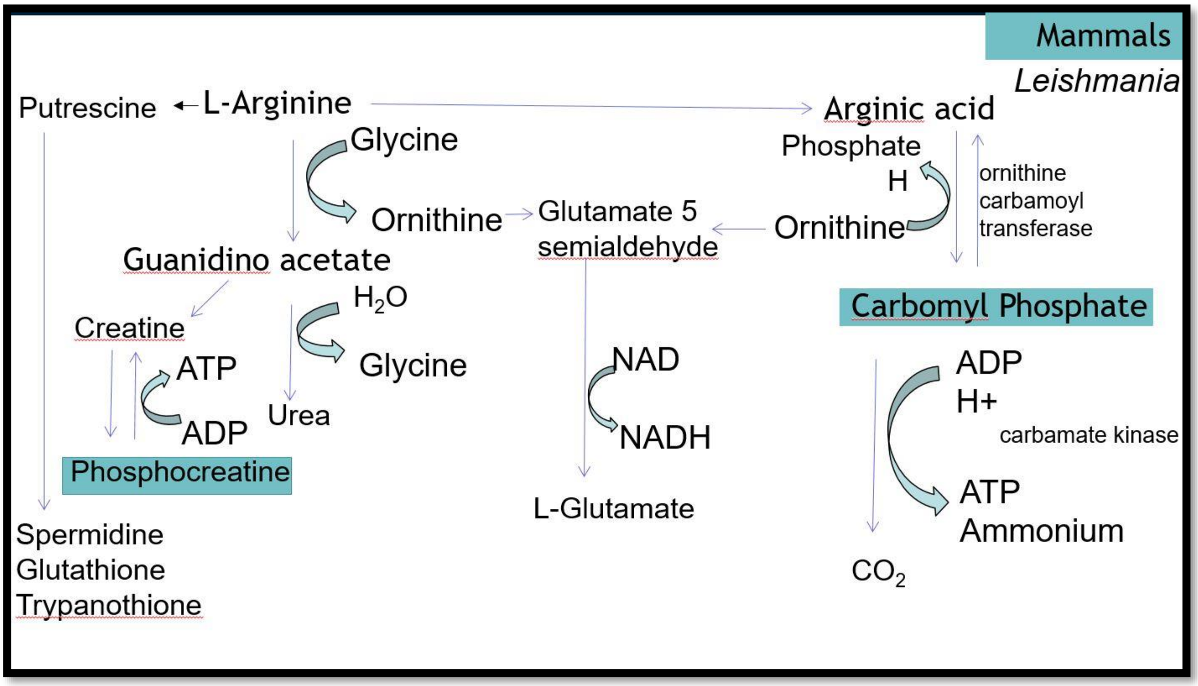

Figure 5.19 Schematic representation of L-Arginine metabolism

L-Arginine utilisation in *L. mexicana* promastigotes using intracellular metabolomics data shown with the step for NADH regeneration compared to in mammals (*Homo sapiens*) is highlighted.

L-Arginine metabolism reported as unique for *Leishmania* not present in mammals due to polyamines production. Polyamines are required for defence and oxidative stress regulation within the intracellular metabolism (Colotti and Ilari, 2011). Putative identifications of metabolites from the L-Arginine metabolism are as follows: L-Arginine, L-Glutamate 5-semialdehyde, (S)-1-Pyrroline-5-carboxylate, Spermidine, gamma-glutamyl-gamma-aminobutyraldehyde, N4-Acetylaminobutanal, L-Citrulline, L-Ornithine, 4-Guanidinobutanamide and creatine as shown in Figure 5.12.

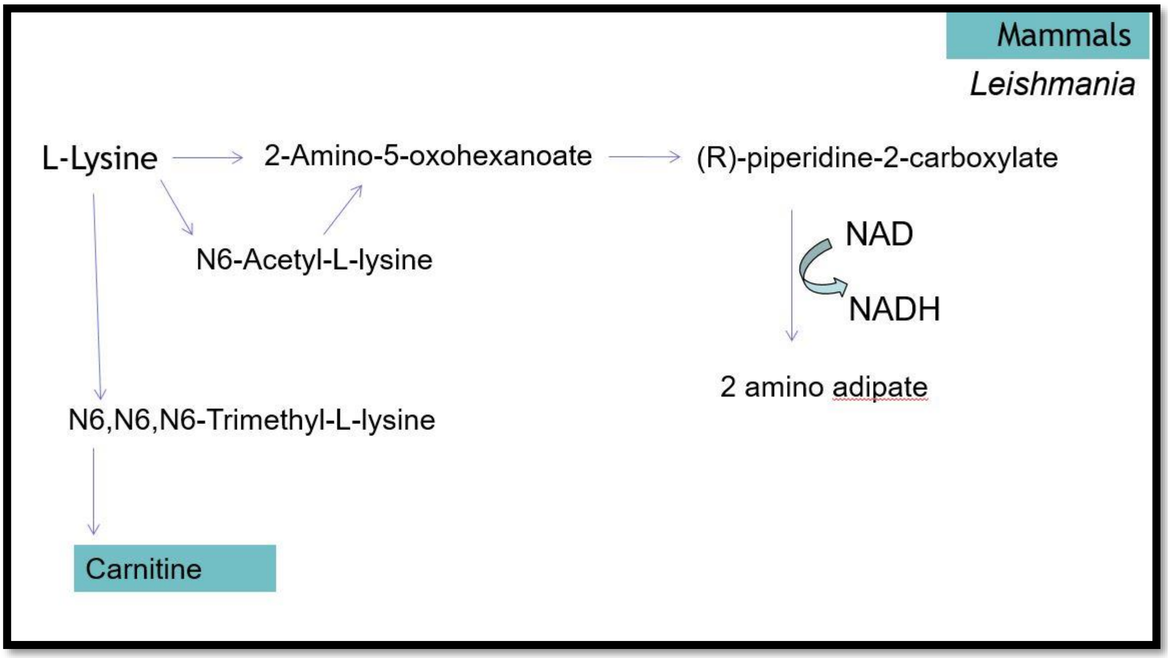

Figure 5.20 Schematic representation of L-Lysine metabolism

L-Lysine utilisation in *L. mexicana* promastigotes using intracellular metabolomics data shown with the step for NADH regeneration compared to in mammals (*Homo sapiens*) is highlighted.

The intermediates shown in Figure 5.13 were schematically represented as N6-Acetyl-L-Lysine, 2-Amino-5-oxohexanoate found to oxidised forms of L-Lysine and subsequently (R)-piperidine-2-carboxylate is oxidised to form 2-amino-adipate which facilitates NADH regeneration as observed in degradation pathways of other amino acids in *L. mexicana* promastigotes as shown in Figure 5.20.

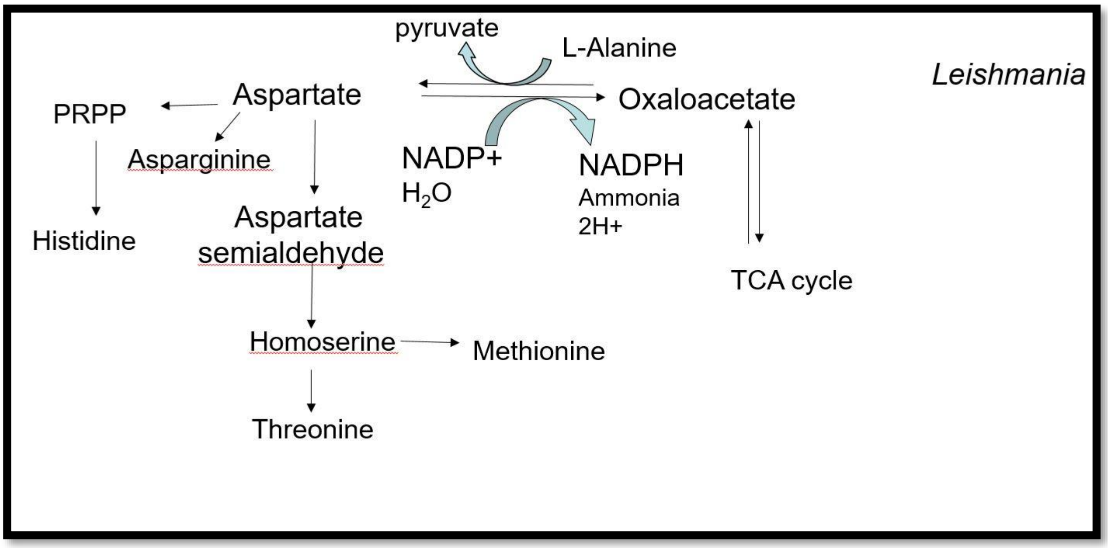

Figure 5.21 Schematic representation of L-Aspartate metabolism

Aspartate utilisation in *L. mexicana* promastigotes using intracellular metabolomics data shown with the step for NADPH regeneration described in discussion section.

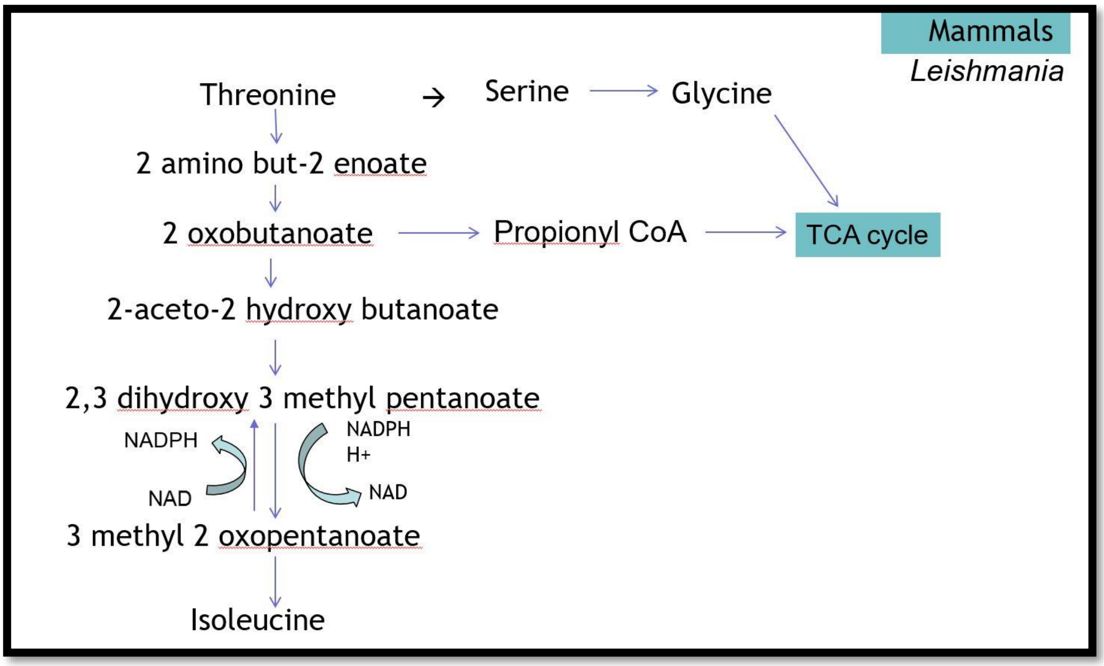

Figure 5.22 Schematic representation of L-Threonine metabolism

Threonine utilisation in *L. mexicana* promastigotes with enzymatic steps for isoleucine biosynthesis shown with the step for NADH regeneration.

Isoleucine biosynthesis described in discussion section verified using blast analysis against the genome from NCBI blast tool at https://blast.ncbi.nlm.nih.gov/Blast.cgi?PAGE=Proteins provided in Appendix Figure .

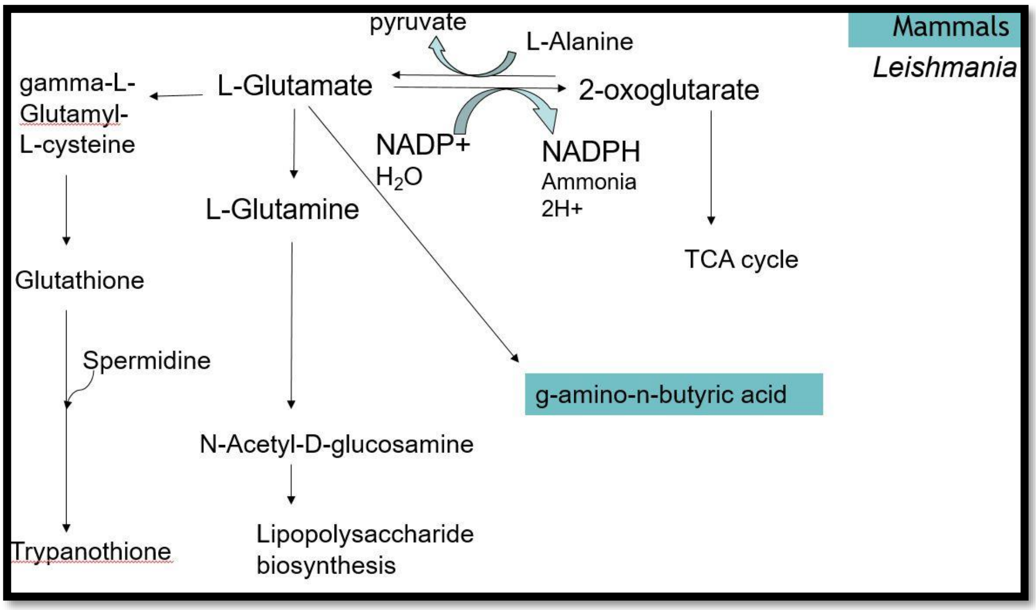

Figure 5.23 Schematic representation of L-Glutamate metabolism

L-Glutamate utilisation in *L. mexicana* promastigotes using intracellular metabolomics data shown with the step for NADH regeneration compared to in mammals (*Homo sapiens*) is highlighted with details in discussion section.

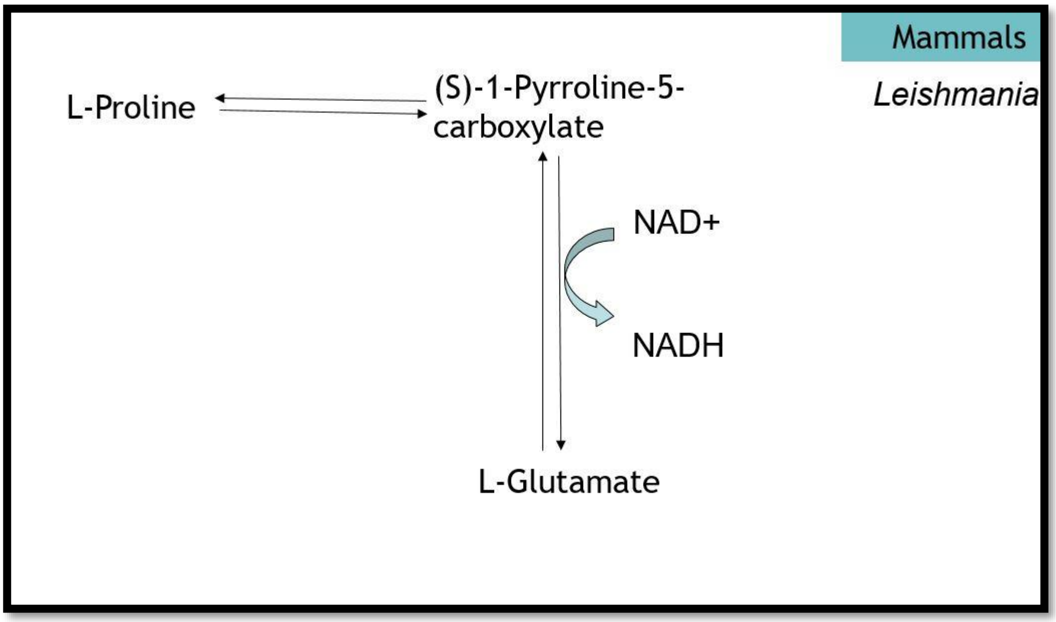

Figure 5.24 Schematic representation of L-Proline metabolism

Proline utilisation in *L. mexicana* promastigotes using intracellular metabolomics data shown with the step for NADH regeneration with details in discussion section.

5.3 Discussion

Use of Defined medium for untargeted metabolomics of *L. mexicana* promastigotes allowed for reproducible trends for compounds with similar behaviour as analysed by their mass and retention time; despite variations of instrument response of peak intensity values introduced by machine drifts compromising sensitivity and resolution. Huge biological variability due to background signals from serum molecules and variation between different serums batches are overruled by the use of the chemically defined medium for *in vitro* culture. The significant advantage of metabolomics is to be able to capture information at particular time point reflecting the appropriate phenotype (Fiehn, 2002). Previously, most metabolomics sample preparation has been optimised for *Leishmania* culture in rich medium containing 20% v/v foetal calf serum (De Souza et al., 2006, Kamleh et al., 2008, T'kindt et al., 2011). In the next section, results of optimisation for metabolome extraction of *L. mexicana* promastigotes in Defined medium carried out by modification of certain steps in the protocol has been discussed.

5.3.1 Protocol optimisation for quenching and washing *Leishmania* promastigotes

Intracellular metabolome of *L. mexicana* promastigotes cultured in Defined medium were compared between naïve medium (without parasites) and culture supernatant on Day 3 from the start of culture initiation by untargeted metabolomics. Sample preparation for untargeted metabolomics involves steps for immediate arrest of metabolism by quenching the cells (Dunn et al., 2012) and separating the intracellular metabolome. Early methods for *Leishmania* parasites involved rapid quenching of *Leishmania* cultures to 0ºC using a dry ice/ethanol bath and washing cells with ice cold PBS to remove the extracellular medium. These steps was mainly carried out to remove any contaminants surrounding the cells, since routine *Leishmania* culture involved rich medium containing (up to 20% v\v) foetal calf serum. This extensive washing procedure carried out to remove the growth medium using PBS as washing buffer causes additional stress and delays metabolic arrest (Dunn et al., 2012). Hence, protocol was optimised as described in experimental procedures and mass spectrum data analysed using IDEOM (Creek et al., 2012b) and mzMatch software (Scheltema et al., 2011). Data visualised using principal component analysis as shown in Figure 5.1.

Multivariate methods deals with separation of signal from the noise, reduces the dimensionality by removing the redundancy and provides more stability for further analysis. Principal component analysis allows for projection of data taking into consideration all variable features for explanation of the underlying correlation structure (Swartzla.Ee, 1974) with total of 80% variance explained in two components and distinct separation between the intracellular samples, spent medium samples and naïve medium was observed. The robustness between the triplicates were visualised using hierarchical cluster analysis as shown in Figure 5.2 which showed good reproducibility between samples.

Amongst the 252 metabolites, those from the medium include the 45 different chemical components, with changes in amino acids, glucose and adenosine matched with standards within the data set. Other remaining components such as vitamins, including biotin, thiamine, inositol, salts, cofactors and metals were only putatively identified as the signal intensities were low and features could not be distinguished by the software mzMatch (Scheltema et al., 2011) and IDEOM (Creek et al., 2012b). Most of these metabolites detected in the intracellular samples were not detected in the naïve medium only samples. Since, only 64 metabolites were matched with the authentic standards, most of these metabolites are represented as putative identifications with more emphasis on the pattern of change in metabolites with underlying biological context

5.3.2 Relative quantification of amino acids in *L. mexicana* promastigotes

To understand about the amino acids salvaged from the environment, the peak intensity calculated as ratio between intracellular metabolites and naïve medium. The extracellular metabolite concentration secreted by the cell is calculated as fold change of the metabolite in defined medium and the spent medium (Culture supernatant). Amino acids depleted on Day 3 from the start of culture initiation from the extracellular medium were found to be L-Threonine, L-Arginine, L-Glutamate, L-serine, L-Leucine, L-Valine, L-Tryptophan and L-Aspartate as shown in Figure 5.6.

The relative abundance of the amino acids has been represented as bubble plot as shown in Figure 5.8. Depending upon the experimental conditions tested in this study. The peak intensities as detected by the instrument response of free amino acids in the intracellular metabolome under experimental conditions used in this study showed the following order with L-Alanine > L-Glutamate > L-Glutamine > L-Glycine > L-Proline > L-Histidine > L-Valine > L-Asparagine > L-Phenylalanine > L-Threonine > L-Tyrosine > L-Aspartate > L-Leucine > L-Arginine > L-Methionine > L-Tryptophan > L-Lysine > L-Serine and L-L-Cysteine.

L-Alanine is abundantly detected in the intracellular metabolome which has been shown in previous studies (Inbar et al., 2013, Hart and Coombs, 1982, Coombs et al., 1982) as it is important for osomo-regulation, has active biosynthesis pathway in *Leishmania* and participates in transamination reactions, etc. L-Glutamate and L-Glutamine detected in the intracellular samples serve as amino group acceptor/donor in transamination reactions which is one of the reasons for high turn-over of these amino acids in the intracellular metabolome compared to others. Here, the defined medium used for *in vitro* culture have been composed of amino acids at concentrations as specified in Table 5-1. The concentrations of the amino acids might influence the level of salvage from the extracellular medium. It was not within the time limit of this project for testing under different amino acid concentrations; the results discussed were for observations under experimental conditions tested. However, unlike carbohydrates and lipids, amino acids cannot be converted to storage forms and hence, subjected to high metabolism. In the next section, untargeted metabolomics of the intracellular metabolome has been carried out to trace individual amino acid pathways. Emphasis in this study has been to trace trends and patterns of changes of metabolite levels in the biological context of parasite specific unique metabolic pathways. These alternative routes described have not been found in mammals and hence, are proposed as more promising potential drug targets.

Novel unbiased mapping of amino acid metabolites to highlight metabolic differences from mammalian host as drug targets.

Previously, certain studies have used radioactive compounds to trace metabolic pathways and gene knock out studies for validation of particular steps using reductionist approaches. Predictions from whole genome annotations and bioinformatics approaches have shown to accelerate biochemical pathway mapping (Payne and Loomis, 2006, Opperdoes and Coombs, 2007); however, these methods have limitations due to static data analysis. In this chapter, dynamic intracellular metabolome data are presented from Figure 5.9 to Figure 5.15. Unbiased mapping of metabolites of the amino acid intermediates were constructed from these data and also, the differences between *Leishmania* and mammals have been highlighted from Figure 5.16 to Figure 5.24 to propose the presence of alternative routes that could potentially serve as drug targets.

In-silico analysis for *Leishmania* have shown that a possibility of 1101 metabolites annotated from the genome (Chavali et al., 2008). In this study, 402 metabolites were putatively identified within the intracellular metabolism with defined medium as control and only 252 compounds were matched to mass/charge ratio (m/z) and retention time to KEGG chemical identifiers. Network mapping at structural, functional and empirical levels have also revealed new insights about alternative amino acid pathways based on metabolite detection that were not previously predicted using genome annotation or experimental evidence.

Here, amino acid pathways are studied using two approaches; firstly to collect the information of intracellular metabolites from untargeted metabolomics experiment and then, compare it to total number of metabolites as observed in KEGG database to construct amino acid pathways. A comparative overview of enzymes between *Leishmania* and mammals have been highlighted to propose specific parasite specific enzymes that could serve as drug targets. With metabolomics experiments, there can be varied number of metabolites which are fragments or adducts not identified as a particular metabolite. Thus,, unique metabolites with authentic standards and confident identifications detected reproducibly in the parasitic intracellular samples were being considered for further scrutiny.

5.3.2.1 Aromatic amino acid metabolism

As observed from Figure 5.9, L-Tryptophan is metabolised with major flux directed to indole acetaldehyde and indole lactate. Other intracellular intermediates includes indole-3-glycol, indole 3 acetate, indole 3 glyoxal, indole acetamide, L-kynurenine, L-formylkynurenine at lesser abundance. From the intracellular metabolomics data set, these metabolites were between the confidence score of 8-10, hence would be referred to as putative identifications compared to first 2 metabolites identified with authentic standards. Relative quantification of metabolites have been calculated and expressed as peak intensity as shown in Figure 5.9. Compared to static network of L-Tryptophan pathway from the KEGG pathway database; here, a more dynamic representative biological network of L-Tryptophan metabolism is shown in Figure 5.16 corresponding to log phase responsible for NADH generation.

Network mapping of metabolites found in the intracellular data set indicate that extracellular L-Tryptophan has been uniquely utilised by *L. mexicana* promastigotes for NADH regeneration. Berger et al argued that the amount of

NADH regenerated would be quantitatively lesser and stressed that these aromatic amino acids mainly act as preferential nitrogen source for L-Methionine recycling (Berger et al, 1996). However, particular enzymes involved in L-Tryptophan metabolism such as L-Tryptophan transaminase and indole pyruvate dehydrogenase with no homologs found in mammalian species deserves further attention as novel drug targets. From the growth analysis as shown in Chapter 4 and intracellular metabolome data in this chapter confirms that L-Tryptophan is salvaged from the environment and not biosynthesised by *L. mexicana*. The transport of L-Tryptophan is critical for the viability of the parasites. In mammalian systems, L-Tryptophan is utilised for production of neurotransmitters such as serotonin or metabolised via the glutaryl CoA pathway for acetyl CoA production.

Montemartini et al proposed that aromatic amino acids, L-Tryptophan, L-Phenylalanine and L-Tyrosine serve as important NADH regeneration in *Trypanosoma cruzi (*Montemartini et al., 1994). Database mining for *Leishmania* encoded enzymes was carried out, which indicated that L-Tryptophan/L-Phenylalanine carboxylyase (PCL) has putative Gene Id-LmjF.28.1580 unique to *L.mexicana*, not found in other trypanosomatids. Furthermore, this particular enzyme has no mammalian homologue, hence might prove novel drug target unreported before. This gene was found to be homologous to fungal species responsible for anaerobic utilisation of L-Phenylalanine to phenylacetate production (Prasuna et al., 2012) using the Ehrlich pathway. Ehrlich pathway involves a set of reactions for the conversion of certain amino acids especially L-Leucine, L-Valine, L-Methionine, L-Phenylalanine by transamination followed by a decarboxylation reaction. In glucose abundant batch cultures of *Saccharomyces cerevisiae* samples, Ehrlich pathway involved amino acids catabolism to aldehyde and then reduced to fusel alcohols. However, in glucose limited conditions, the aldehydes are majorly oxidised to fusel acids (Hazelwood et al., 2008). It has been suggested that Ehrlich pathway may have implications on the overall cellular redox metabolism. Excess NADH oxidised by glycerol-3-phosphate dehydrogenase during formation of glycerol from glucose requires ATP and thus is energetically unfavourable. Also, amino acids catabolised through the Ehrlich pathway provides an energy efficient alternative pathway for NADH regeneration. From the intracellular metabolomics network mapping as shown in Figure 5.17, *L. mexicana* promastigotes show evidence of an Ehrlich pathway for NADH regeneration.

Intracellular metabolites of L-Phenylalanine metabolism detected and putatively identified in this study through the LC-MS data as shown in Figure 5.10 were L-Phenylalanine, L-Tyrosine, 3-Hydroxyphenyl-pyruvicacid (also called phenylpyruvate), 3-(4-Hydroxyphenyl) lactate (also called phenyllactate), 4-Hydroxyphenylacetaldehyde, 2-phenylacetamidine. In mammalian systems, L-Phenylalanine is metabolised to L-Tyrosine by the enzyme L-Phenylalanine hydroxlase (PAH), which is present in *Leishmania;* and an additional step forming phenyllactate. However, *Leishmania* genome encodes for an additional enzyme involved in L-Phenylalanine metabolism called as L-Phenylalanine carboxylase (PCL) to form phenyl-acetaldehyde to phenylacetate for NADH regeneration.

In certain species of bacteria and fungi, this pathway has been determined in which phenylpyruvate is metabolised to phenylacetate through phenylacetaldehyde. The enzyme phenylpyruvate decarboxylase catalyses the non-oxidative decarboxylation of various substrates such as phenyl-pyruvate, indole pyruvate and other substrates with characteristic feature with more than 6 carbon atoms in a straight chain with Phenylacetaldehyde dehydrogenase requires NAD as cofactor and hence, allows for NADH regeneration.

Interestingly, belonging to the same class of aromatic amino acids, L-Histidine has received less attention in the past research in *Leishmania*. Metabolomics data was examined for metabolites of the L-Histidine pathway as shown in Figure 5.11, such as imidazol-5-yl-pyruvate, imidazole lactate, 4-imidazolone-5-acetate, imidazole-4-acetate has been putatively detected and verified using Chemspider for chemical synonyms. These metabolites indicate that L-Histidine could potentially be degraded by alternative pathway not found in mammals. Instead, from network mapping of these metabolites as shown in Figure 5.18, L-Histidine catabolised to yield Imidazol-5-yl-pyruvate /1H-Imidazole-5-propanoic acid by the broad spectrum L-Histidine-pyruvate aminotransferase. However, it is the detection of the downstream metabolites of imidazole lactate, 4-imidazolone-5-acetate and imidazole-4-acetate are metabolites which participate in NADH regeneration. These enzymes are not present in the mammalian systems, hence serve as potential drug targets. Berriman et al, 2005 from the *Leishmania* genome predicted that *Leishmania* have no enzymes for L-Histidine degradation (Berriman et al., 2005). This is the first report with experimental evidence for L-Histidine pathway for NADH regeneration not reported in *Leishmania* before.

5.3.2.2 L-Arginine metabolism

L-Arginine utilisation is primarily responsible for protein synthesis and contributes to high energy intermediates via the TCA cycle as observed in most organisms (Paselk, 1983). There had been considerable debate in *Leishmania* about L-Arginine biosynthesis, since genome annotation suggests that the parasites have incomplete urea cycle encoding for the formation of arginosuccinate from L-Aspartate; however, no further conversion to L-Arginine (Opperdoes and Coombs, 2007). From growth analysis as shown in Chapter 4, there was no growth recorded in the absence of exogenous L-Arginine. Thus L-Arginine serves as critical exogenous source required for the viability of promastigotes.

In mammals, L-Arginine has been used for energy generation in the cell by creatine production in muscles. Rapid interconversion of creatine and creatinine leads to ATP replenishment (Darlyuk et al., 2009). Using in vivo mouse models for nutritional studies, L-Arginine has been shown to be the major contributor of citrulline followed by L-Glutamine. It has been verified using tracer experiments that L-Arginine contributes to approximately 40% to citrulline synthesis followed by L-Proline (3.4%) and L-Glutamine (0.5%) negligible. L-Glutamine incorporates ureido group upon conversion to carbomyl phosphate, leading to citrulline synthesis (Marini et al., 2010). The main purpose of this pathway being ATP generation.

L-Arginine metabolism reported as unique for *Leishmania* not present in mammals due to polyamines production. Polyamines are required for defence and oxidative stress regulation within the intracellular metabolism (Colotti and Ilari, 2011). Putative identifications of metabolites from the L-Arginine metabolism are as follows: L-Arginine, L-Glutamate 5-semialdehyde, (S)-1-Pyrroline-5-carboxylate, Spermidine, gamma-glutamyl-gamma-aminobutyraldehyde, N4-

Acetylaminobutanal, L-Citrulline, L-Ornithine, 4-Guanidinobutanamide and creatine as shown in Figure 5.12. It has been reported by fragmentation analysis that L-citrulline annotated as arginic acid (Westrop et al., 2015). Apart from polyamines, it has been shown using genome analysis that there is no specific enzyme with creatine kinase activity; whilst, the phylogenetic analysis indicate similarity between sequences of creatine kinase activities with *Leishmani*a genome. Thus, it has been speculated that parasitic protozoa must have different type of enzyme with function similar to creatine kinase, leading to ATP production (Voncken et al., 2013). Hence, the schematic overview representation of L-Arginine utilisation in *L. mexicana* promastigotes is shown in Figure 5.19.

5.3.2.2 L-Lysine metabolism

Lysine metabolism intermediates in the intracellular metabolome as represented in Figure 5.13. Significant ($p<0.05$) levels of N6, N6, N6 tri-methyl L-Lysine found in the intracellular metabolome. The methyl groups could be obtained through the S-adenosyl L-Methionine cycle or intracellular proteolysis leads to release of methyl-lysines. In mammals, other than L-Lysine contribution towards protein production; L-Lysine to tri-methyl L-Lysine is also involved in carnitine biosynthesis. Carnitine is responsible to transport fatty acids to mitochondria for oxidation and energy production. Although, N6, N6, N6 tri-methyl L-Lysine, the precursor for synthesis of carnitine (Hulse et al., 1978) has been found in the intracellular metabolome, it is not clear whether *Leishmania* genome encode for carnitine biosynthesis. The different steps of carnitine biosynthesis including oxidation, release of glycine residue, dehydrogenation and re-oxidation of tri-methyl-L-Lysine to carnitine formation was individually analysed by bioinformatics approach using blast analysis but no gene annotations were found for the same (Appendix table for Lysine).

The intermediates shown in Figure 5.13 were schematically represented as N6-Acetyl-L-Lysine, 2-Amino-5-oxohexanoate found to oxidised forms of L-Lysine and subsequently (R)-piperidine-2-carboxylate is oxidised to form 2-amino-adipate which facilitates NADH regeneration as observed in degradation pathways of other amino acids in *L. mexicana* promastigotes as shown in Figure 5.20.

5.3.2.4 L-Leucine, L-Valine and L-Isoleucine metabolism

Leishmania genome encode for many enzymes involved in elaborate degradation pathway of branch chain amino acids of L-Leucine, L-Valine and L-Isoleucine according to KEGG pathway database. However, the extraction methods adopted in this study (Chapter 2, methods) was more suitable for polar metabolites and organic acids, whilst branch chain amino acids have shown to be incorporated into lipids and CoA molecules which are much less emphasised in this study. Radiolabelled studies in *L. mexicana* using labelled L-Leucine have indicated the carbon skeleton of L-Leucine are directly incorporated into sterol biosynthesis (Ginger et al., 2001). Isoleucine and L-Valine are degraded into pathways that lead to succinyl coenzyme A but analysis of CoA (coenzyme A) derivatives requires targeted extraction procedure as explained elsewhere (Basu and Blair, 2012).

5.3.2.5 L-Aspartate and related amino acids metabolism

The first step in L-Aspartate degradation is mediated by L-Aspartate aminotransferase (AAT) which has been shown to have broad spectrum substrate specificity unique to *Leishmania* (Leblancq and Lanham, 1984). AAT has been described to have multiple isoforms with localisation with both glycosome and mitochondrial specific. Aspartate converted to oxaloacetate which enters the TCA cycle by mitochondrial L-Aspartate aminotransferase, alternative route involves L-Aspartate conversion to fumarate by the purine-nucleotide cycle (Marciano et al., 2009). In the past L-Aspartate utilisation in *Leishmania* has been described with respect to TCA cycle and energy generation (Saunders et al, 2014). However, in other biological organisms, for example, in bacteria and fungi, it has been shown that L-Aspartate leads to production of various other amino acids including L-Threonine, L-Methionine, isoleucine, phosphoribosyl pyrophosphate, L-Histidine (Rees et al., 2009) and pyrimidines (Paselk, 1983).

Within the intracellular metabolome recovered from *L. mexicana* promastigotes in defined medium, the metabolites belonging to L-Aspartate metabolism have been shown in Figure 5.14. In this study, efforts have been made to schematically represent metabolites associated with L-Aspartate as important precursor supporting the biosynthesis of most of the amino acids following the metabolic pathway as shown in Figure 5.21. Absence of L-Aspartate significantly increased the doubling time (Chapter 4) indicating the importance of exogenous supply of L-Aspartate required during the growth cycle of promastigotes. Aspartate degradation via the asparatokinase enzyme is alternative route of action compared to L-Aspartate amino transferase leading to oxaloacetate contribution to oxidative phosphorylation via the TCA cycle. Aspartate broken down to aspartyl phosphate is energy consuming reaction with ATP to ADP conversion leading to aspartyl phosphate via asparatokinase. Further, L-Aspartate dehydrogenase leads to production of L-Aspartate semialdehyde formation with the conversion of NADPH to NADP. Aspartate semialdehyde leads to homoserine biosynthesis via the enzyme homoserine dehydrogenase (Flavin and Slaughte.C, 1967). O-acetyl L-Homoserine putatively identified in the intracellular dataset as shown in Figure 5.14.L-Homoserine biosynthesis is the first committed step before L-Methionine and L-Threonine biosynthesis. It has been shown in bacterial systems that homoserine biosynthesis could be negatively regulated by increased concentration of L-Threonine or L-Methionine within the cells (Vitreschak et al., 2004).

Threonine serves as an indispensable amino acid to mammals as no biosynthesis pathway encoded. Enzymes involved in both biosynthesis/degradation cycle of L-Threonine metabolism are proposed as important candidates to be considered for further investigation as drug target because these enzymes were found not encoded in the genome of *Homo sapien*s (Reeds, 2000).

L-Aspartate metabolism includes sub branch leading to L-Methionine biosynthesis as shown in Figure 5.14 is another Leishmania specific pathway needs further investigation. The enzymes encoded within *Leishmania* for specific L-Methionine metabolism pathway was found to have no mammalian homologs. From the results from single amino acid knock out experiments (Chapter 4) , growth in the absence of L-Methionine was comprised with increase in doubling time and cell body appear smaller in size with lesser protein production. From the untargeted metabolomics data, there were other metabolites putatively identified such as homoserine, cystathionine and homocysteine not highlighted before. In the intracellular metabolome, the relative abundance of homoserine at 0.44 < lesser than downstream metabolites from the pathway such as cystathionine and L-Methionine each at 0.46 and 0.52 as shown in Figure 5.14. This allows to map the pathway using metabolomics data as shown in Figure 5.21. In-order to survive within the insect vector, the parasites may modify their metabolic repertoire to meet the changes in nutrient availability and maximise the chance of survival by efficient use of resources. These results indicated that *Leishmania* encode residual L-Methionine biosynthetic pathway to maximise viability under nutrient deprived conditions as tested.

L-Methionine biosynthesis pathway has been well studied in *E .coli*, although not universal in all organisms, it has been considered as standard pathway for comparison (Flavin and Slaughte.C, 1967). The first step in L-Methionine synthesis starts from activated homoserine as shown in Figure 5.21. Met A gene encoding for the enzyme homoserine O-succinyltransferase transfers the succinyl group from succinyl-CoA to gamma-hydroxyl group resulting in O-succinylhomoserine. Met B encodes for cystathionine gamma synthase which catalyses the trans-sulfurlyation reaction by transfer of the thiol group from cysteine to homoserine forming cystathionine. This has been subjected to cleavage by cystathionine beta lyase encoded by Met C resulting in homocysteine, pyruvate and ammonia. Met H encodes cobalamin dependent L-Methionine synthase with cobalamin cofactor serving as acceptor or donor of methyl group from 5-methyl tetrahydrofolate to homocysteine (Koutmos et al., 2009). However, an alternative pathway in the absence of exogenous cobalamin with the aid of Met E encoded enzyme cobalamin-independent L-Methionine synthase which transfers the methyl group directly from the tri-L-Glutamate derivative of 5-methyl-tetrahydrofolate to homocysteine (Whitfiel.Cd et al., 1970).

It has been shown in *L. donovani* and *L. infantum* species (Berger et al., 1998) that there is evidence for L-Methionine recycling using inorganic keto-thio-butyrate and aromatic amino acids as nitrogen donor as alternative metabolic pathway for maintaining intracellular L-Methionine concentration. Thus, dependence on exogenous L-Methionine might depend upon the intracellular concentration of the promastigotes at particular stage in the life cycle. *L. tartentole* has been shown to assimilate inorganic sulphur for L-Methionine biosynthesis, and hence does not depend upon exogenous L-Methionine (Steeleda.F and Krassner, 1971). Methionine is an important amino acid with many functions: it is the first amino acid added during protein translation, essential for cysteine biosynthesis and acts as preferential methyl donor during most biochemical reactions. Methionine degraded to succinyl-CoA and succinate and feds into the TCA cycle. Methionine also converted to acetyl CoA by acetate succinyl CoA transferase to form acetate and ATP. Methionine has shown to have regulatory role in protein activation and inactivation owing to its chemical properties to undergo reversible oxidation (Drazic and Winter, 2014).

L-Aspartate metabolism contributes to the phosphoribosyl pyro phosphate (PRPP) via carbamoyl phosphate pathway. PRPP serves as precursor molecule for synthesis of pyrimidines and L-Histidine schematically represented in Figure 5.21. The pyrimidines and intermediates of L-Histidine biosynthesis pathway were as shown in Figure 5.14 within the intracellular metabolome. These results indicate that increased accumulation of L-Histidine or downstream intermediates supports parasite viability even in the absence of exogenous supply of L-Histidine during the first passage in culture.

Increased presence of pyrimidines such as uracil and thymine as shown in Figure 5.14 indicate high level of pyrimidines maintained within the intracellular metabolome. It has been previously reported that pyrimidines biosynthesis occurs within *Leishmania* by interconversion and purine source (Serafim et al., 2012). However, exogenous supply of purine such as adenosine is essential for the viability and growth of *Leishmania* as shown in growth analysis (Chapter 3).

In summary, results from unbiased mapping of intracellular metabolomics data have shown presence of compensatory biosynthetic metabolic pathways; highly conserved with dependence on the extracellular or the host environment required to support viability of promastigotes under conditions of absence of exogenous supply of L-Threonine, L-Methionine, L-isoleucine and L-Histidine as recorded during growth analysis shown in Figure 4.15 (Chapter 4). These evidences also suggest that amino acid utilisation pathways for NADH regeneration other than protein synthesis, cell structure maintenance amongst other functions within *L. mexicana* promastigotes.

5.3.2.6 Glutamate and related amino acids metabolism

According to genome annotation, L-Glutamate has been shown as primary source for L-Proline and L-Glutamine production in *Leishmania* (Berriman et al., 2005). All the intermediates of L-Glutamate metabolism as shown in Figure 5.15 with the relative intensity value as observed under experimental conditions of defined medium. Glutamate metabolism occurs in two different localisations, with the putative cytosolic NADPH dependent L-Glutamate dehydrogenase and mitochondrial NAD dependent isoenzyme. Glutamate on deamination forms alpha keto butyrate that feds into the TCA cycle as represented in Figure 5.23. The transamination reaction involving L-Glutamate to 2-oxoglutarate is coupled with L-Alanine degradation to form pyruvate. The intra-cellular pool of L-Alanine is maintained very high in *Leishmania* Figure 5.15 and has shown to play an important role to maintain osmoregulation (Inbar et al., 2013) with dynamic extracellular environment of the host system. Unlike in mammals where L-Glutamate utilised for production of neurotransmitters such as gamma amino n-butyric acid; in *Leishmania* promastigotes, L-Glutamate on reaction with cysteine forms gamma glutamyl cysteine, which contributes to the production of Kinetoplastida specific polyamines, trypanothione; important for redox homeostasis (Paes et al., 2008) as represented in Figure 5.23. Furthermore, Glutamate contributes to L-Glutamine by amidation (Figure 5.23) and L-Proline via L-Glutamate semi aldehyde (Saunders et al, 2014) . It was observed from the metabolomics data that L-Glutamine, L-Proline and L-Alanine are the most abundant amino acids in the intracellular pool of promastigotes as shown in Figure 5.8. The carbon skeletons of L-Alanine, L-Glutamine and L-Proline are shown to be incorporated to gluconeogenic intermediates (Saunders et al., 2011) leading to the production of glucose via the TCA cycle in *Leishmania* promastigotes as represented in Figure 5.23.

From growth analysis of promastigotes cultured in the single amino acid knock out media as shown in Chapter 4, it was observed that the parasites were viable even in the absence of exogenous supply of L-Threonine, L-Histidine, L-isoleucine and L-Methionine. This indicates that biosynthesis could be active in *Leishmania* promastigotes but negatively regulated because of high amino acid availability within the insect midgut. Thus, possible routes of biosynthesis have been discussed to highlight the enzymes involved in the biosynthesis of these amino acids as potential drug target not found in mammals.

Threonine biosynthesis pathway involves 2 enzymes, Homoserine kinase (HSK) is the enzyme involved in the first step of L-Threonine biosynthesis. It has been shown in related kinetoplastida, *Trypanosoma brucei*, that this particular step from the conversion of homoserine to L-Threonine biosynthesis occurs only in L-Threonine limited conditions (Ong et al., 2015). One of the peculiar feature of HSK exist as bifunctional enzyme with AK activity. They also explain the localisation of the enzyme in insect vector tsetse endosymbionts encode for the production of these unusual metabolites such as 3-oxohexanoylhomoserine lactone. Genetic and biochemical studies reported from the paper indicated that HSK null mutant were unable to compensate for the non-availability of L-Threonine compared to wild type *T. brucei*. They demonstrated that wild type parasites were able to grow with the homoserine. Wilson et al 1991. Similar studies in plants by Weisemann and Matthews, 1993 have reported HSK as bifunctional protein. Bioinformatics approach was used to comparative phylogeny mapping of the enzyme Homoserine kinase in *Leishmania* shows early branch point in evolution from eukaryotes and similar to *T. brucei* forms (Ong et al., 2015). Threonine synthase catalyses the second step with the conversion of O-phospho L-homoserine to L-Threonine with the addition of water moiety and release of the phosphate group as schematically represented in Figure 5.21. Thus, L-Aspartate could serve as major precursor molecule for many other amino acids as shown from schematic mapping in Figure 5.21

Threonine degradation involves 3 pathways. Threonine degradation I involves the enzyme THF-dependent serine hydroxymethyltransferase (SHMT) to form glycine, undergoes reversible reaction in serine production. Serine is converted to pyruvate. Threonine degradation II involves L-Threonine catabolism via the Ser/Thr dehydratase to alpha keto butyrate that feds to the TCA cycle to form succinyl CoA. From the intracellular data as shown in Figure 5.14, the relative abundance of 2-oxobutonate is high which indicates that the major flux of L-Threonine degradation to generate high energy TCA cycle intermediates. Thus, L-Threonine deaminase plays major role to form 2-oxobutonate from L-Threonine. Subsequent reaction of 2-oxobutonate into propionyl CoA has not be identified, which may be because of the analytical method used in this study is focused on polar metabolites and not CoA which might be cleaved off and small size of the ion was beyond detection of parameters chosen.

Earlier literature indicated the contribution of L-Threonine to TCA cycle via the propionyl pathway unique to species of *Leishmania* and *T. cruzi*, not found in *T. brucei* (Opperdoes, 2008). L-Threonine contributes to L-serine and subsequently to L-glycine (Opperdoes and Coombs, 2007) . Glycine is metabolised by the glycine cleavage system to form formic acid and CO_2. Glycine is also converted to serine and pyruvate by the THF-coupled serine hydroxyl-methyltransferase, and Thr/Ser dehydratase which is reversible reaction. Glycine can also be formed from the glyoxylate via the enzyme serine pyruvate aminotransferase which has not been completely characterised in *Leishmania* before. The third pathway of L-Threonine metabolism to L-Isoleucine biosynthesis has not been less explored. Threonine degradation through alternative pathway leading to isoleucine biosynthesis (Levinthal et al., 1973) as detailed in schematic representation in
Figure 5.22. The 4 enzymes involved in the **isoleucine biosynthetic reactions** involve:

Step 1: **Formation of acetolactate**: This intermediate has been putatively detected in the intracellular dataset as 2-Hydroxy-2-methyl-3-oxobutanoate validated by chemspider for synonym as acetolactate with molecular formula C5H7O4 and average mass 131.107 Da. The mass/charge was verified in the intracellular dataset and 4 compounds were identified with similar mass range of 131 Da. Further filtering of the data by molecular formulae indicate mass detected at 131.06 and retention time at 13 as 2-Hydroxy-2-methyl-3-oxobutanoate. Caution was exercised since it is only putative identification at this stage. Blast analysis using gene sequence from UNIPROT ID I6YEX6 from *Mycobacterium tuberculosis* were compared to *Leishmania* species. Homologous gene was identified as putative pyruvate/indole-pyruvate carboxylase, putative [*Leishmania mexicana* MHOM/GT/2001/U1103] with sequence id as XP_003878881.1 and corresponding E value of 6e-26. The gene activity has been well characterised in *Mycobacterium tuberculosis* which requires ascorbic acid as cofactor (Yin et al., 2011).

Step 2: **Formation of (S)-2-hydroxy-2-ethyl-3-oxopentanoate**: 2-oxobutanoate catalysed by ketol-acid reductoisomerase binds to Mg^{+2} in a metal-dependent reduction reaction by NADPH to yield (S)-2-hydroxy-2-ethyl-3-oxobutanoate with NADPH regeneration.

Step 3: **3-methyl-2-oxopentanoate formation**: Loss of water moiety of 2, 3-dihydroxy-3-methylpentanoate catalysed by di-hydroxy-acid dehydratase leads to formation of 3-methyl-2-oxopentanoate.

Step 4**: Formation of isoleucine**: This involves the enzyme branch chain amino transferase that catalyses the reversible reaction between the alpha keto acid, such as 3-methyl-2-oxopentanoate to yield L-isoleucine. Evidence of this enzyme was verified by blast analysis as shown in
Figure 5.22. As shown in Figure 5.14, some of putatively identified metabolite leads to isoleucine biosynthesis pathway have been detected. The first committed step encoded by acetolactate synthase and last step encoded by branch chain transaminase showed significant homology in *Leishmania* genome by blast analysis as shown in
Figure 5.22.

Proline is oxidised by L-Proline oxidase and delta 1 pyrroline 5 carboxylate dehydrogenase which enter the TCA cycle as represented in Figure 5.24. Proline serves as major energy contributor of energy through oxidative phosphorylation. This is in agreement with previous studies by Mukkada et al (Bringaud et al., 2012, Glaser and Mukkada, 1992) where L-Proline serves as major energy contributor especially found in high concentrations within the insect midgut. Proline has shown to be the major molecule of osmoregulation and co-transported by L-Proline-L-Alanine symporter (Zilberstein and Gepstein, 1993). It has shown that when promastigotes were subjected to osmotic stress, the Proline transporter gene LdAAP24 has been upregulated confirming their role in osomoregulation (Inbar et al., 2013).

From growth analysis as elaborated in Chapter 4, promastigotes cultured in the single amino acid drop out media in the absence of L-serine, L-Histidine, L-isoleucine, L-Threonine, L-Glutamate, L-Methionine, L-Glutamine, L-cysteine, L-

L-Tyrosine, L-Proline, L-Asparagine, L-Alanine, L-glycine causes no significant increase in doubling time during the growth cycle of promastigotes. From the unbiased network of amino acids as shown in Figure 5.21, biosynthesis of L-Glutamate, L-Methionine, L-Glutamine, L-cysteine, L-L-Tyrosine, L-Proline, L-Asparagine, L-Alanine, L-glycine, L-serine, L-Histidine, L-isoleucine, L-Threonine could be active in *Leishmania* promastigotes via L-Aspartate metabolism. These biosynthetic pathways could be intermittently active since increased availability within the insect midgut leads to negative regulation. However, these enzymes involved in the biosynthesis of these amino acids, especially for L-Threonine biosynthesis could serve as potential drug target not found in mammals.

This is first report using metabolomics data from defined medium with efforts being made to build unbiased networks of amino acid metabolism in *Leishmania* promastigotes. The dynamic information of change of intracellular metabolites has been captured from the log phase (Day 3) of the culture in defined medium with optimised protocol as described in the methods section. Moreover, the knowledge from this study has allowed for new insights of amino acid metabolic pathways in *Leishmania* promastigotes unreported before.

From the untargeted metabolomics of the intracellular metabolome, network mapping has highlighted that amino acids are metabolised by simplistic route in *Leishmania* promastigotes mostly for NADH regeneration as shown in Equation 1. Furthermore, metabolic route of the amino acid derived keto acids have been found unique to *L. mexicana* promastigotes.

$$Amino\ acid\ \rightarrow Amino\ acid\ derived\ keto\ acids\ + NADH$$

Equation 1 Unique metabolic route of amino acid catabolism in *Leishmania* promastigotes using enzyme amino acid carboxylases.

Hence, this unique metabolic pathway involving the enzymes, amino acid carboxylases could serve as drug targets specific for the parasite alone without affecting the host system. Furthermore, inhibition of this particular enzymatic step of amino acid metabolism could inhibit increased production and secretion of amino acid derived keto acids

It is still intriguing that these parasites follow different metabolic pathway follow much simpler metabolic degradation pathway compared to other organisms. To further verify the role of small molecules in infection, time resolved metabolic foot-printing of exometabolome samples and biochemical assays of aromatic pyruvates on activated host cells were carried out as reported in Chapter 5. Time course metabolomics of the exometabolome highlights keto acids play in role in supporting infection with host cells, especially from aromatic amino acids were found be enriched in the Defined medium supernatant over time indicating active secretion of these metabolites from procyclic to infective metacylic forms (i.e Day 0 to Day 9 during growth phase *in vitro* culture in Defined medium) that have shown novel role in supporting early stages of infection in mammalian cells as further elaborated in chapter 5).

Chapter 6 Determination of amino acids utilisation required for parasite development and infection.

6.1 Introduction

The human pathogenic *Leishmania* promastigotes colonise the sand-fly gut before infecting the macrophages in the mammalian host. As obligate parasites *Leishmania* promastigotes rely completely on host system for acquiring nutrients to complete their dynamic developmental life cycle (Burchmore and Barrett, 2001). Routes of nutrients uptake have been shown as drug targets discussed in the past (Shaked-Mishan et al., 2006, Inbar et al., 2012). However, mapping of all nutrients in global unbiased manner had been challenge due to the complex nature of the *in vitro* medium used for axenic culture of parasites. In this chapter, the use of metabolic foot-printing for nutrients uptake have been explored. This is the first report of data from time resolved metabolic foot-printing from in house developed chemically defined medium (composition Chapter 4) that would allow to decipher accurate information about substrate utilisation during the growth of *L. mexicana* promastigotes.

The true metabolome as described by Oliver (Oliver et al., 1998) as the complete set of all low molecular weight metabolites present in and around growing cells at a given time during their growth or production cycle cannot be captured using one single technique because of the diverse chemical nature and concentrations of metabolites. Studies on intracellular metabolomics optimised using different extraction procedures for comprehensive analysis of diverse nature of small molecules with a molecular weight of less than 1500Da known as metabolic finger-printing (Mashego et al., 2007, T'Kindt et al., 2011). Unlike genomics, changes in metabolites composition reflect the phenotype of the organism as a result of the complex interplay between various signalling and regulatory factors (Fiehn, 2002). Studies on *Leishmania* metabolome in the past has been carried out using complex media containing undefined serum component (Scheltema et al., 2010, Silva et al., 2011, Westrop et al., 2015). Few other studies (Saunders et al., 2011) have used chemically defined media containing many components (Merlen et al., 1999) which is not important for the viability and growth of *Leishmania* promastigotes (as shown from our results in chapter 3), thus the metabolomics studies in our defined medium allowed to derive further novel biological inferences unexplored in the past.

6.1.1 Time resolved metabolic foot-printing in defined medium

Metabolic foot-printing involves quantification of metabolite uptake and secretion from the culture media. Use of chemically defined media for metabolic foot-printing brings new insights into compound utilisation different from that observed in complex undefined medium and allows for standardised platform for comparison between laboratories (Kell et al., 2005, Aurich et al., 2015). Growth dependent changes of cellular metabolism can be captured using time-resolved metabolic foot-printing. In classic model organisms of the fungal and bacterial kingdoms, time resolved metabolic foot-printing have shown to be useful for various purposes including and not limited to taxonomic classifications of species, gene function identification by comparing profiles between mutated and wild-type forms and varied metabolic adaptations of clinical isolates (Behrends et al., 2009, Allen et al., 2003, Palmer et al., 2007).

Leishmania promastigotes undergo a complex developmental cycle within the insect vector before transition into amastigotes stages within macrophages in the mammalian host. Metabolic foot-printing approach was applied to study time resolved utilisation of multiple metabolites simultaneously at different growth stages of promastigotes. The physiochemical environment encountered by promastigotes within the insect vector changes depending upon the host species and nutritional status of the sand-fly vector (Pimenta et al., 1992). Broadly, it has been described elsewhere that promastigotes undergo dynamic transformation from procyclics 24-48 hours, nectomonands 48-72 hours, leptomonads 4-7 days, about 5-7 days termed as metacyclics which infect the host cells and about 7-9 days within the insect midgut referred to as haptomonads which forms the lining of the salivary duct (Walters, 1993). This transformation is associated with morphological changes from short procyclics to slender metacyclics with longer flagella and slender cell body (Gossage et al., 2003). Functional differences during the different growth stages have been illustrated by Bates et al, 1993 that metacyclics have increased resistance to complement mediated lysis, increased infectivity and varied ultrastructure of the surface membrane (Bates, 1994).

6.1.2 Research aims

Time resolved metabolic foot-printing by untargeted metabolomics approach was conducted by:

- Samples from different time points of promastigotes growth were analysed to understand metabolic requirements during the developmental cycle.
- Classification of metabolites those depleted and enriched were further investigated.
- Secreted small molecules especially aromatic pyruvates in defined media have been tested with pure compounds as standards in biochemical assays to elucidate their role in establishment of parasitism with THP1 cells as macrophage infection model.

6.2 Results

6.2.1 Study objectives for time course metabolomics data

L. mexicana promastigotes were cultured using serum and protein free, Defined medium (composition Chapter 4) and optimised experimental procedures for metabolomics as explained in chapter 2 and 4. In this study, time resolved metabolic foot-printing was carried out starting from early log (Day 1 and Day2), mid log (Day 3) and stationary phase (Day 6 and Day 9) to determine uptake and secretion of metabolites during promastigote growth. With an untargeted metabolomics approach, it was possible to differentiate the salvage and biosynthesis pathways of *Leishmania* promastigotes and highlight parasite specific metabolic pathways as potential drug targets. Furthermore, secreted small molecules enriched in the culture media throughout the growth of the promastigotes were tested to derive physiological inferences during the establishment of parasitism, with macrophage cells as *in vitro* experimental model.

6.2.2 Experimental design

Growth was monitored on day to day basis by manual cell counting using haemocytometer from Day 0 to Day 9 and six time points were chosen to represent the various stages of the promastigote life cycle as described in by Gossage et al (Gossage et al., 2003). Samples were collected from three different flasks set up independently from different inoculation flasks as elaborated in methods section (Chapter 2). From each flask, triplicates were collected at six different time points and analysed by Liquid chromatography Mass spectrometry (LC-MS) on pHILIC chromatographic column in both ionisation modes (positive and negative) as indicated in Figure 6.1. The samples were run in 2 ionisation modes from 3 independent cultures summing up to 36 data points of each compound.

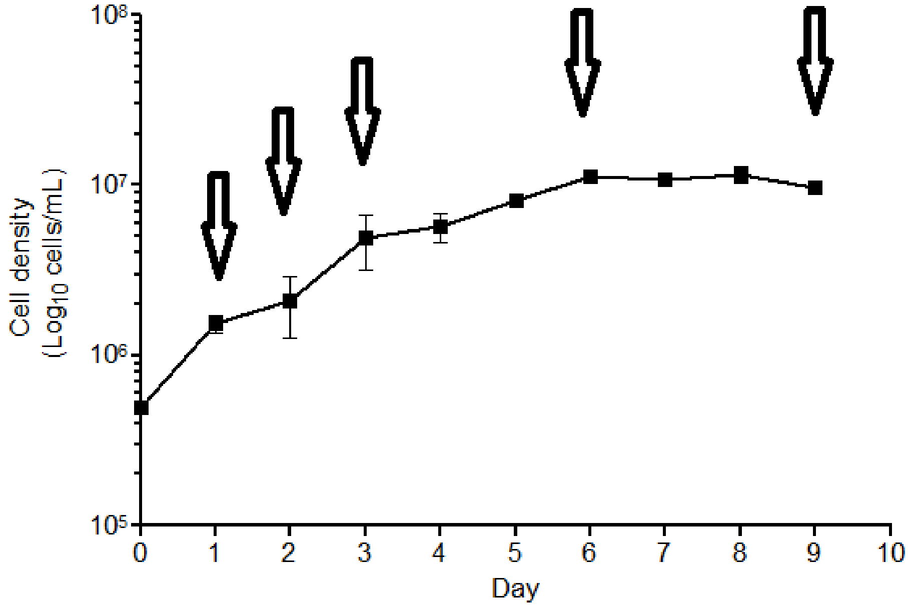

Figure 6.1 Growth of *L. mexicana* promastigotes

(Arrow heads to indicate of the time points of the growth curve from which supernatant were collected from 4 x 10^7 cells at 0, 1, 2, 3, 6, and 9 day from the culture initiation in total of 6 time points, (n=9, Error bars = mean ± SD), as described in experimental procedures).

6.2.3 Pre-processing and annotation

The raw files were processed using IDEOM software for spectral feature detection. Briefly, peaks matched with compound identifications with a filtration criteria such that those below $p < 0.05$ retained in the data set analysed by unpaired t-test between time course samples (treatments) and naïve medium without cells (controls). Hence, about 206 metabolites were putatively identified across replicates in positive and negative mode with 64 metabolites matched with authentic standards for individual mass/charge ratio and retention time comparison. Raw spectral files with peak intensity, m/z and retention time included in appendix file. Furthermore, the 206 putatively identified metabolites were analysed by multi-variant data analysis techniques such as principal component analysis (PCA), Partial Least-Squares regression and Discriminant Analysis (PLS-DA model) and hierarchical clustering analysis (HCA) across samples to derive deeper insights that would help reduce the dimensions in the data set and uncover changes of metabolites pattern within the data(Fiehn, 2002) and individual metabolites analysed.

6.2.4 Multi variant analysis

Partial Least-Squares regression and Discriminant Analysis (PLS-DA), a supervised machine learning method was conducted for the metabolic foot-printing data, especially useful for visualisation of time course samples. PLS-DA allows for easier interpretation of data patterns as the number of samples (18) were lesser than the total number of variables (spectral peaks) measured. PLS-DA model analysis was accompanied by unsupervised classification method such as principal component analysis (PCA), for visual interpretation of underlying groups within the high dimensional data as shown in Figure 6.2.

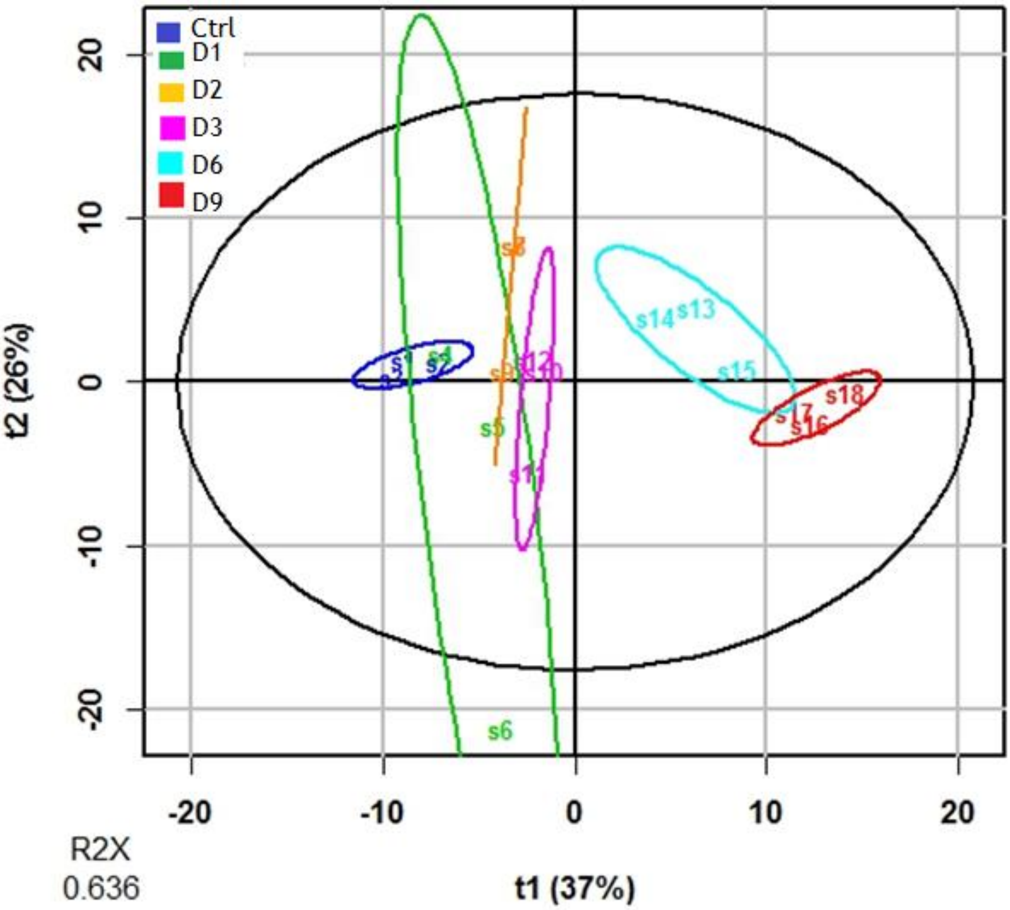

Figure 6.2 PLS-DA model of exo-metabolome at six different time points during the growth of *L. mexicana* promastigotes cultured in Defined medium.

PLS-DA model showed the variance plot with the first two components explaining the maximum variability within the data. Each sample of the mass spectrum has been mathematically represented as single point on the graph annotated by the respective sample number. The observation diagnostics shows the spread of the 18 samples across the orthogonal distance on the score plot. The score plot (Principal component analysis) indicates clusters amongst the 18 samples with outliners within the dataset. The Loadings plot shows the placement of different metabolites subdivided into four sections (+/+, +/-, -/+, -/-) based on the levels of their peak intensities. Principal component analysis (PCA) of time course samples shows each group of clustered separately. Individual groups shown by different colours each for Day 0 (Ctrl-dark blue), Day 1 (D1-green), Day 2 (D2-orange) and Day 3 (D3-pink) are clearly separated from Day 6 (D6-light-blue) and Day 9 (D9-red); indicating significant change in the media throughout the growth of promastigotes from early log to stationary stage). The variance plot shows the first two principal components accounts for 26% and 37% of the variation respectively present in the LC-MS dataset.

The colour coded ellipses as shown in Figure 6.2 shows that metabolic foot print of supernatant samples from day 1, day 2 and day 3 of the culture overlaps with each other (Fig 2) indicating that log phase (Day 1-3) promastigotes in culture are similar at the initial time points. Whilst, the samples from Day 6 and Day 9 form individual clusters which represent the metabolic profile during stationary phase of promastigotes, well separated from log phase promastigotes.

Hierarchical clustering analysis (HCA)

HCA used to depict the similarity between samples in the group from the total set of 18 samples as shown in Figure 6.3.

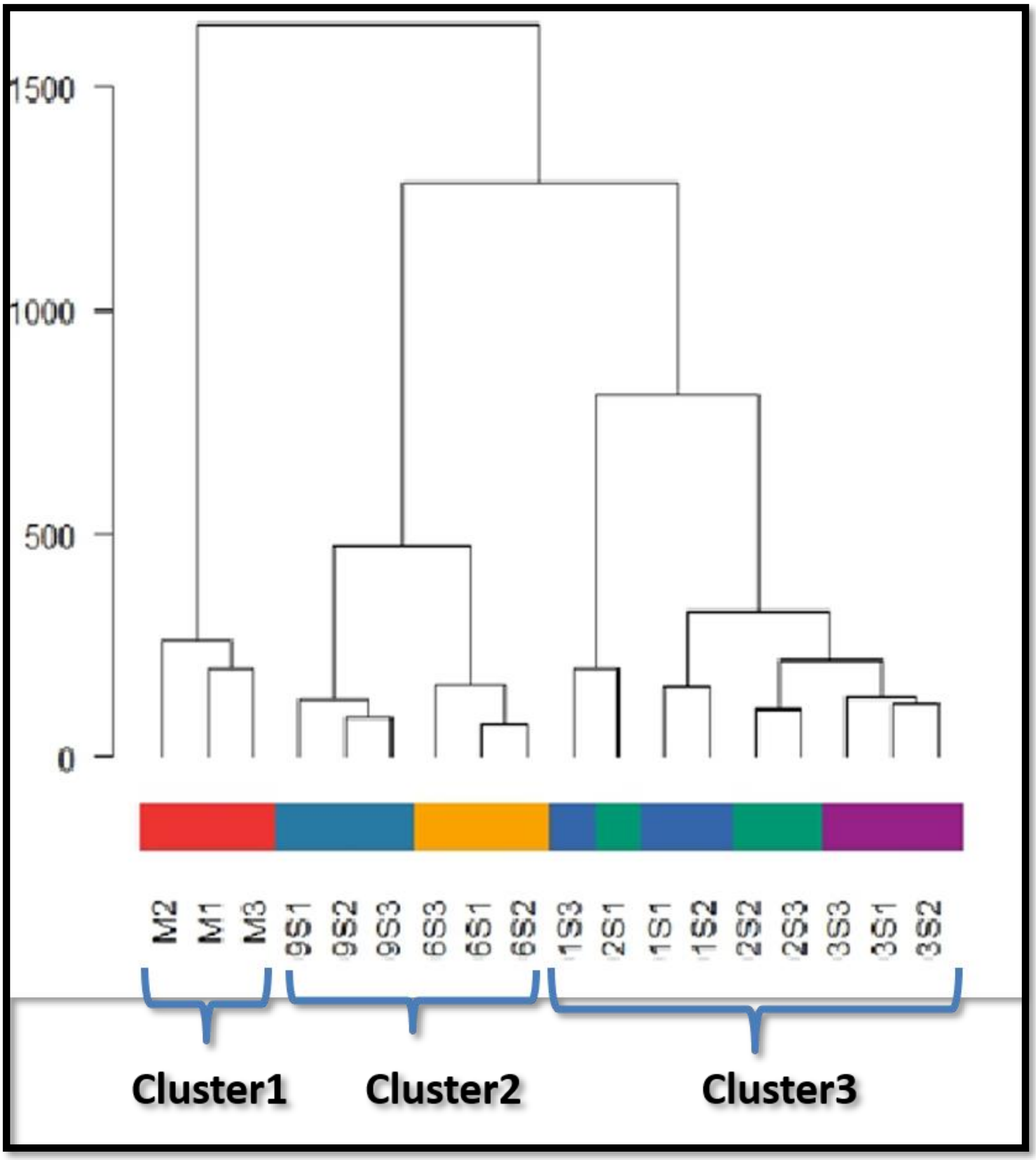

Figure 6.3 Hierarchical cluster analysis shows that the18 samples are sub divided into 3 main clusters.

(The naïve culture medium referred to as Cluster 1 with each sample abbreviated as M1, M2 and M3 are completely separated from other two sub clusters with Cluster 2 consisting of Day 6 (6S1, 6S2, 6S3) and Day 9 (9S1, 9S2, 9S3) sample triplicates and Cluster 3 consisting of Day 1 (1S1, 1S2, 1S3), Day 2 (2S1, 2S2, 2S3), and Day 3 (3S1, 3S2, 3S3) sample triplicates).

Hierarchical cluster analysis shows that the log phase promastigotes are clearly separated from stationary phase promastigotes with metabolic profiles significantly different from each other as shown in Figure 6.3. For this part of the analysis, metabolites with confidence score of 8-10 were selected based on matching peaks from a set of 250 authentic standards below 5% error window for individual mass/charge ratio and retention time. HCA show that samples are sub divided into 3 main clusters indicating different metabolic signatures for log, stationary and medium only samples.

6.2.5 Overview of distribution of metabolites in the exo-metabolome.

Overall changes of the medium that followed the growth of *L. mexicana* promastigotes in a period of 6 days from the start of culture initiation is as shown in Figure 6.4.

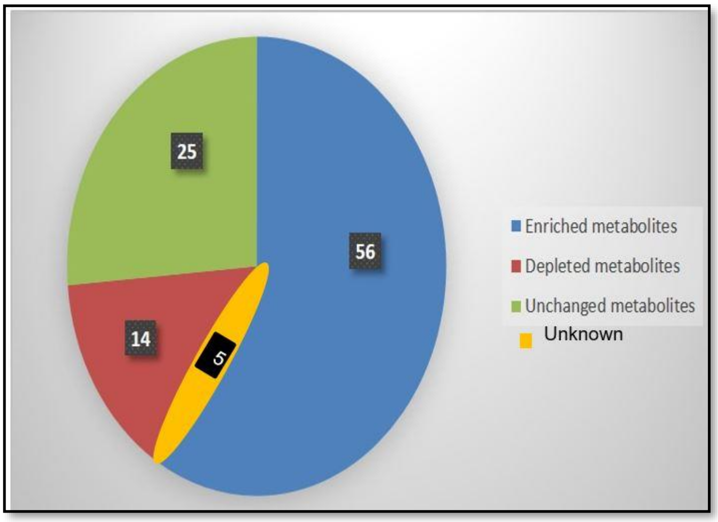

Figure 6.4 Overall distribution of metabolites in the spent medium of defined medium after the growth period of 6 days from the start of culture initiation.

Defined medium with known composition of 45 compounds in naïve condition without cells were subjected to similar incubation time, temperature and pH and analysed along with supernatant samples at different points from the culture. Of the 206 metabolites putatively identified across replicates in both positive and negative ionisation mode, 64 metabolites matched with authentic standards for individual mass/charge ratio and retention time comparison. Overall pattern indicated that approximately 25% metabolites depleted from the medium, 14% not changed significantly, 5% unknown and unassigned metabolites and 40% of overall metabolites significantly enriched in the medium. In terms of numbers of metabolites; , only approximately ~14 metabolites could be identified with authentic standard with confidence score of 10 that were depleted from the medium, and about ~56 metabolites were significantly enriched whose confidence score was between a range from 7-10.

6.2.6 Changes in individual metabolites levels

The amino acids present in defined medium were identified as putative metabolites with confidence score >10 that matched with authentic standards and expressed as change in fold intensity at Log2 scale. Here, they were compared between metabolite levels in supernatant medium and medium without cells incubated and treated for similar times as shown in Figure 6.5 to Figure 6.11.

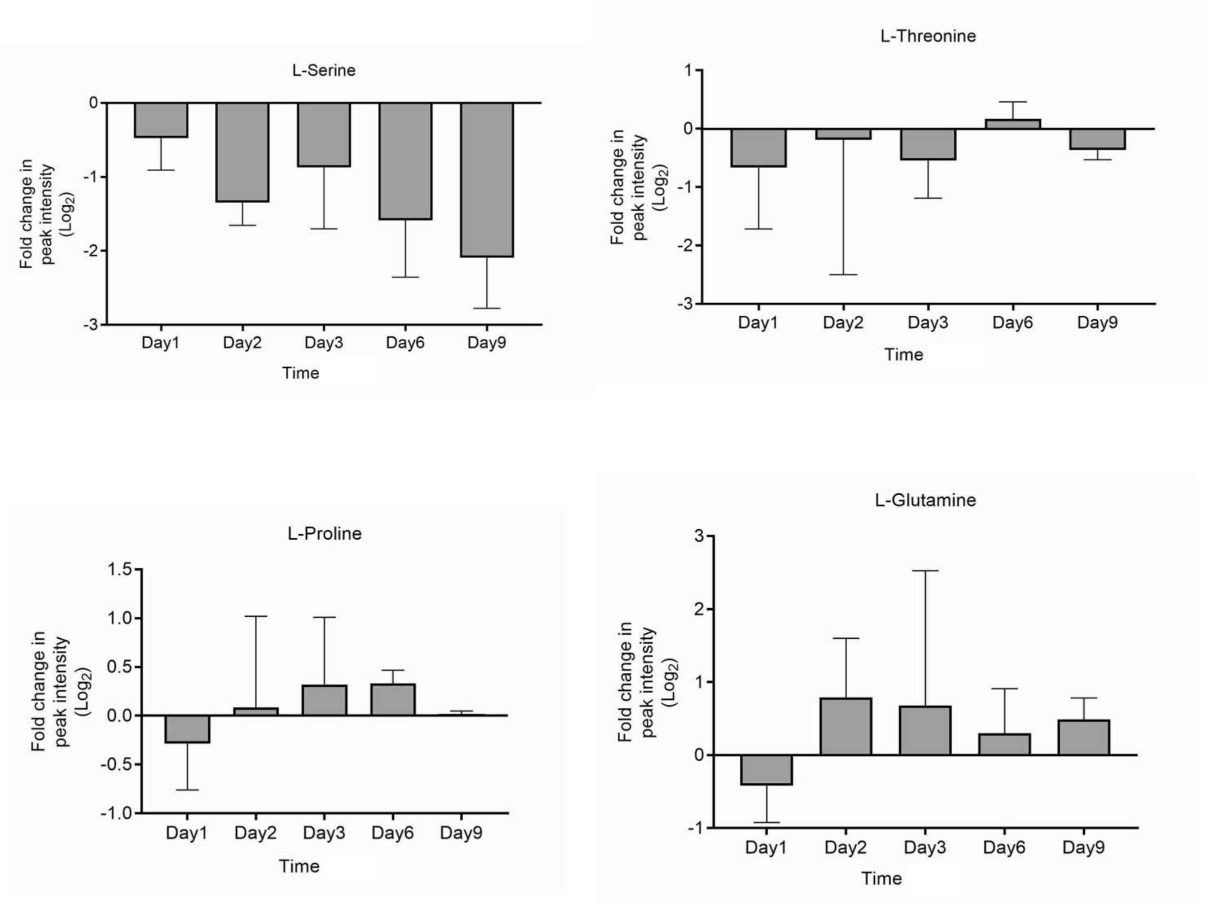

Figure 6.5 Changes of relative peak intensities of polar amino acids calculated from the exo-metabolome data.

Supernatant collected from 4 x 10^7 cells on Day 0, 1, 2, 3, 6, and 9 from the start of culture initiation n=3, Error bars = mean ± SD. Histograms expressed as log2 fold change from the baseline (medium only samples from fresh medium incubated to similar times) over the course of growth from Day 0 to Day 9 of *L. mexicana* promastigotes in defined medium).

Amongst the amino acids with polar uncharged side groups, L-Threonine and L-serine were depleted compared to L-Proline and L-Glutamine as shown in Figure 6.5.

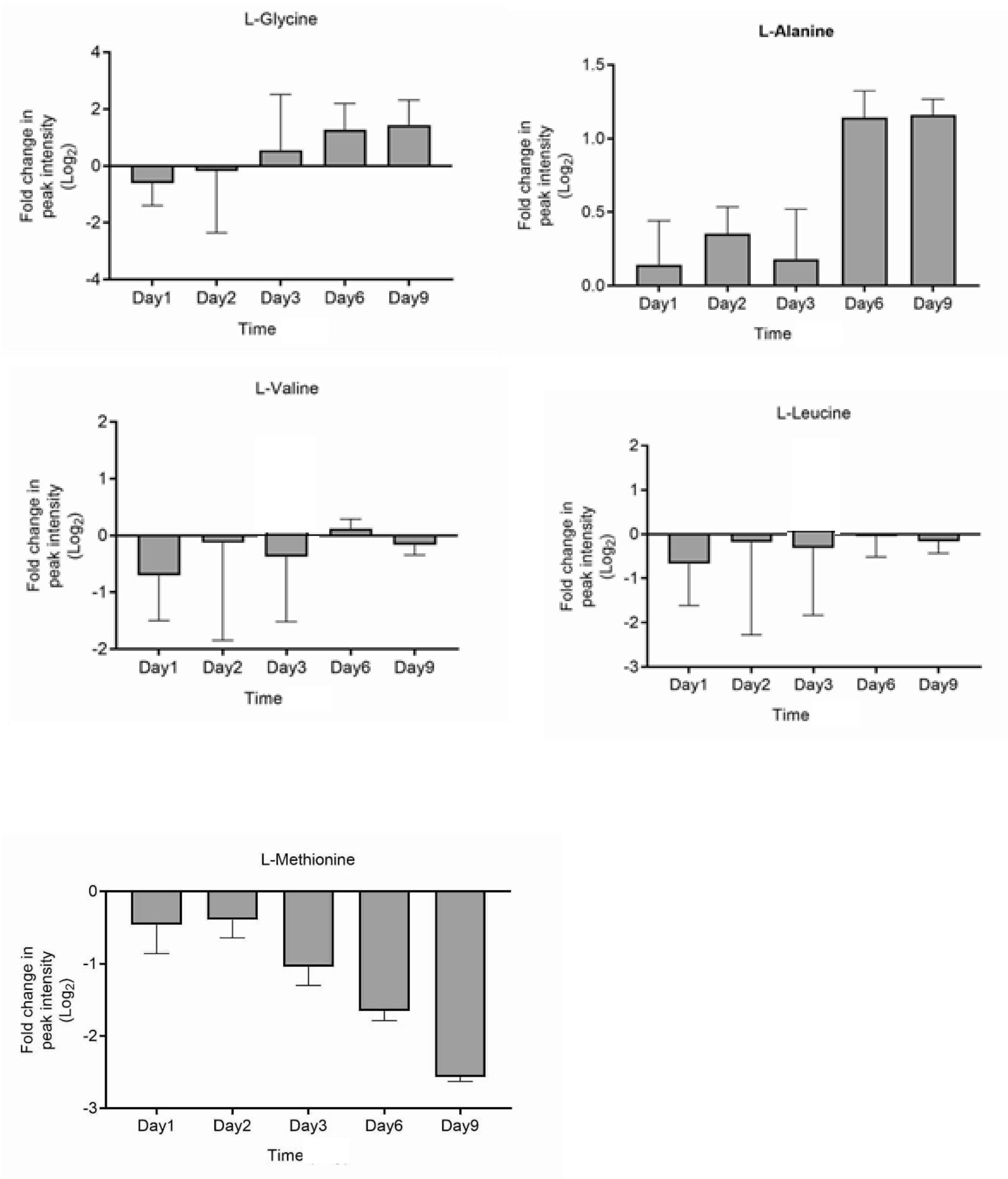

Figure 6.6 Changes of relative peak intensities of non-polar amino acids calculated from the exo-metabolome data.

Supernatant collected from 4 x 10^7 cells on Day 0, 1, 2, 3, 6, and 9 from the start of culture initiation n=3, Error bars = mean ± SD. Histograms expressed as log2 fold change from the baseline (medium only samples from fresh medium incubated to similar times) over the course of growth from Day 0 to Day 9 of *L. mexicana* promastigotes in Defined medium. Stereo isomers, L-Leucine and L-Isoleucine not differentiated in this study.

Those amino acids with non-polar aliphatic side groups, L-Leucine, L-Valine and L-Methionine were depleted compared to L-glycine and L-Alanine as shown in Figure 6.6.

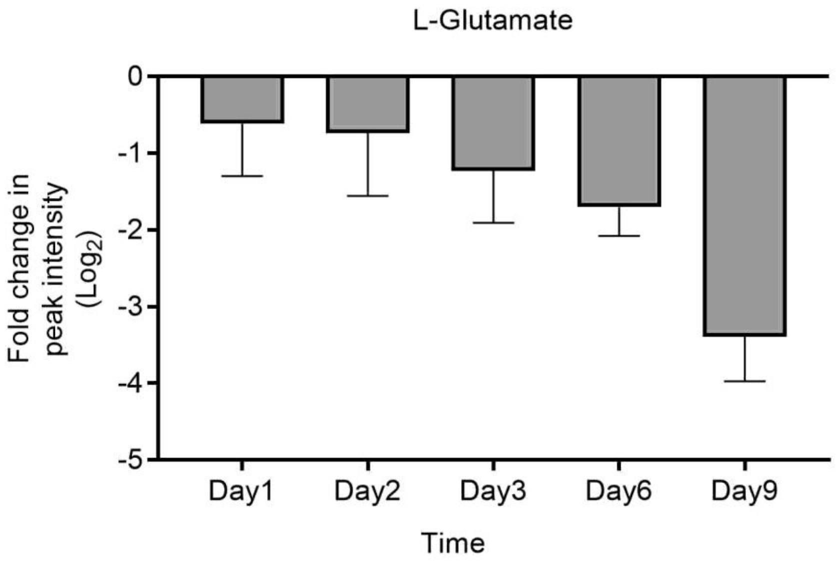

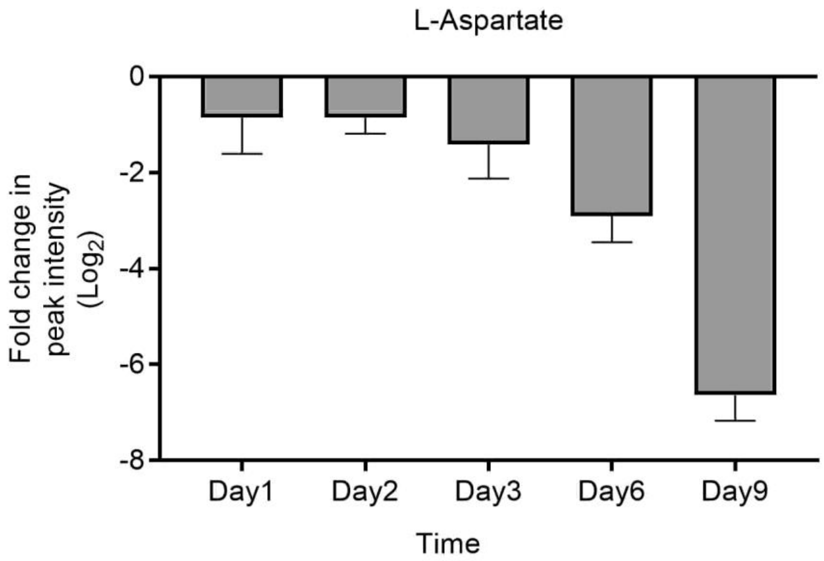

Figure 6.7 Changes of relative peak intensities of negatively charged amino acids calculated from the exo-metabolome data.

Supernatant collected from 4 x 10^7 cells on Day 0, 1, 2, 3, 6, and 9 from the start of culture initiation n=3, Error bars = mean ± SD. Histograms expressed as log2 fold change from the baseline (medium only samples from fresh medium incubated to similar times) over the course of growth from Day 0 to Day 9 of *L. mexicana* promastigotes in Defined medium.

Aspartate and L-Glutamate were consumed rapidly with less than 50% remaining by day 1 of growth period in defined medium as shown in Figure 6.7.

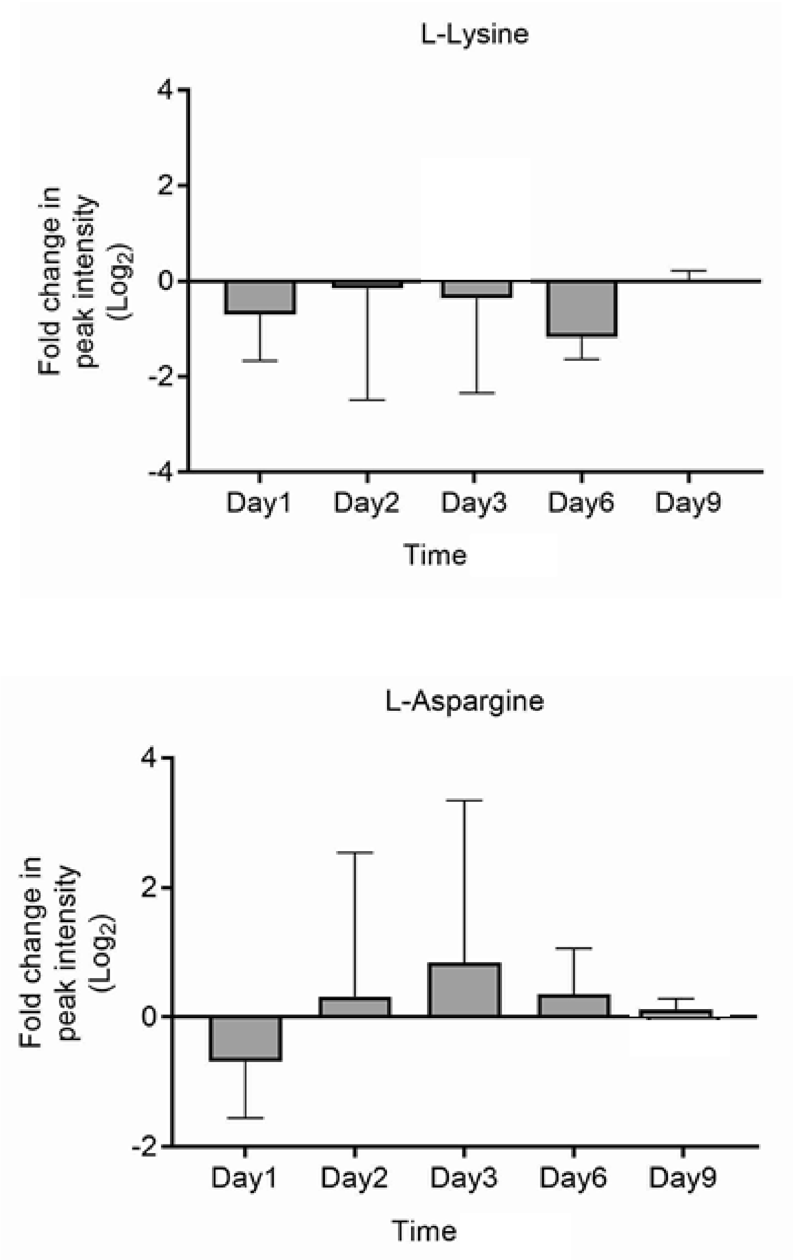

Figure 6.8 Changes of relative peak intensities of positively charged amino acids calculated from the exo-metabolome data.

Supernatant collected from 4 x 10^7 cells on Day 0, 1, 2, 3, 6, and 9 from the start of culture initiation n=3, Error bars = mean ± SD., Histograms expressed as log2 fold change from the baseline (medium only samples from fresh medium incubated to similar times) over the course of growth from Day 0 to Day 9 of *L. mexicana* promastigotes in Defined medium.

Amongst the positively charged side groups, L-Lysine was taken up moderately from the medium, whilst L-Asparagine was found secreted as shown in Figure 6.8.

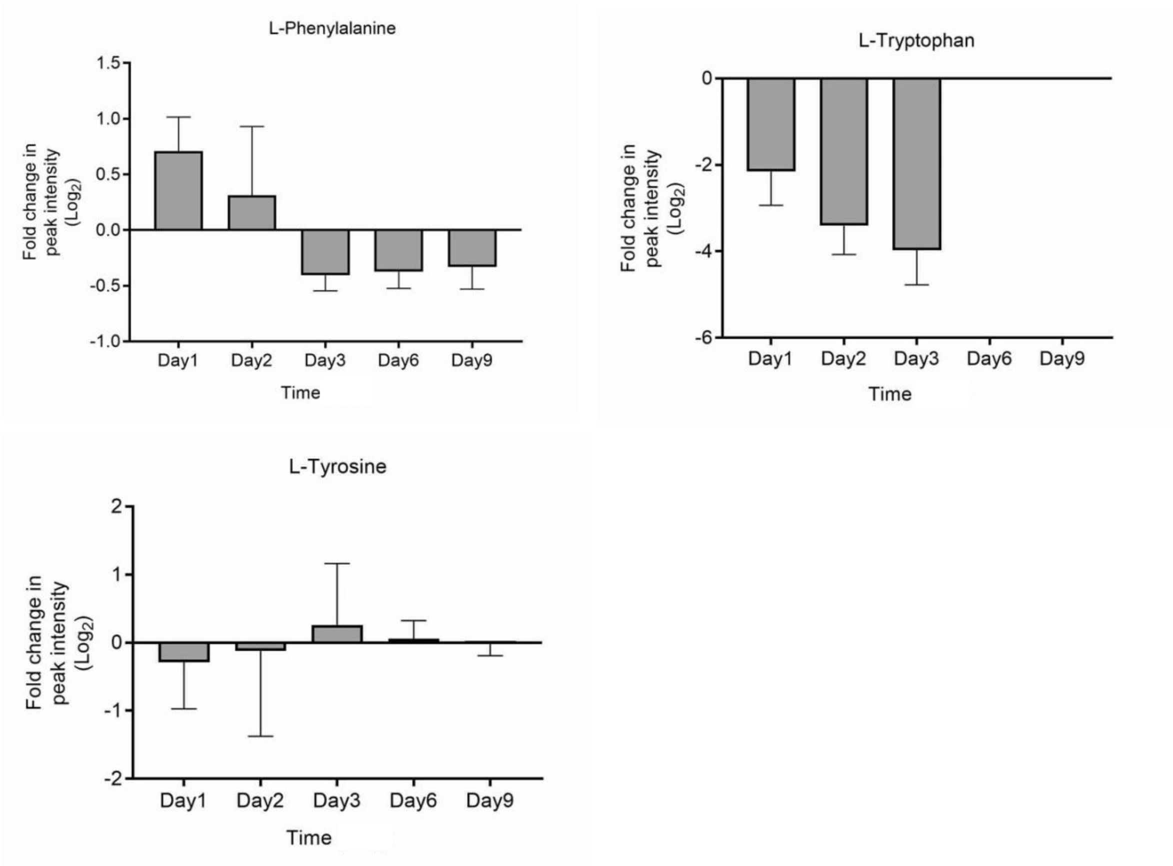

Figure 6.9 Uptake of aromatic amino acids represented from the changes of relative peak intensities from the metabolomics data.

Supernatant collected from 4 x 10^7 cells on Day 0, 1, 2, 3, 6, and 9 from the start of culture initiation n=3, Error bars = mean ± SD. Histograms expressed as log2 fold change from the baseline (medium only samples from fresh medium incubated to similar times) over the course of growth from Day 0 to Day 9 of *L. mexicana* promastigotes in Defined medium. L-Histidine not detected.

Phenylalanine is transiently released in the system as shown in Figure 6.9 but taken up during at later stages of growth cycle especially from day 3 to Day 9. Tyrosine is moderately utilised without much changes in the level of extra-cellular L-Tyrosine. L-Tryptophan was taken up more than 2 fold changes in the extracellular level from Day 0 to Day 3 and consumed completely with not intensity detection on Day 6/9 compared to other amino acids from the medium. Histidine was not detected in this study, raw files were manually checked for retention time and mass which did not match the known values.

Other medium components

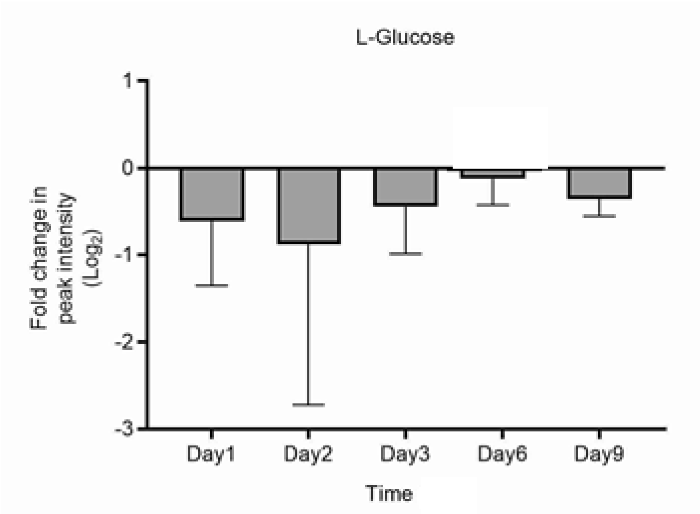

Figure 6.10 Uptake of six carbon sugar such as L-Glucose represented from the changes of relative peak intensities from the metabolomics data.

Six carbon sugar L-Glucose has been depicted in Figure 6.10; however, it is to be noted that these are putative identifications at that stage. The method of LC-MS adopted in this study would not allow to completely differentiate between six carbon sugars such as L-Glucose, L-Fructose or L-Galactose.

Supernatant collected from 4 x 10^7 cells on Day 0, 1, 2, 3, 6, and 9 from the start of culture initiation with n=3, Error bars = mean ± SD. Histograms expressed as log2 fold change from the baseline (which is the fresh medium only samples incubated to similar times) over the course of growth from Day 0 to Day 9 of *L. mexicana* promastigotes in Defined medium.

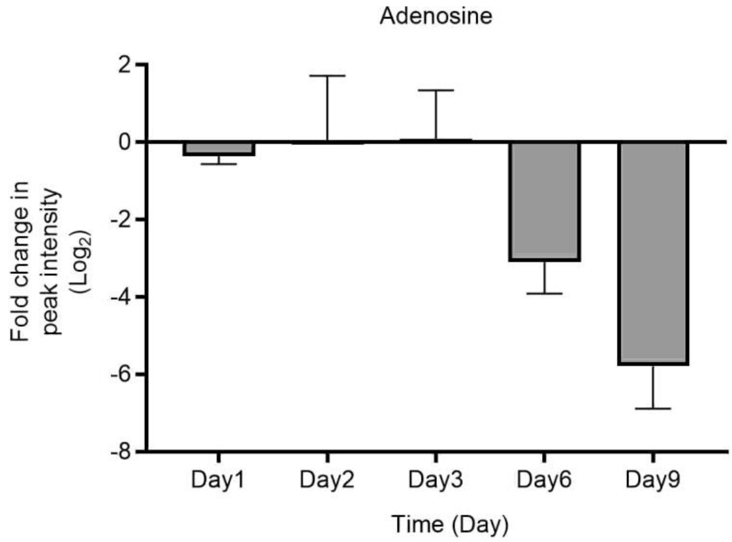

Figure 6.11 Uptake of adenosine represented from the changes of relative peak intensities from the metabolomics data.

Supernatant collected from 4 x 10^7 cells on Day 0, 1, 2, 3, 6, and 9 from the start of culture initiation n=3, Error bars = mean ± SD. Histograms expressed as log2 fold change from the baseline (fresh medium only samples incubated to similar times) over the course of growth from Day 0 to Day 9 of *L. mexicana* promastigotes in Defined medium.

From these results, Glucose and adenosine was recorded to be consumed throughout the growth cycle since the extra-cellular level was completely depleted by day 9 as shown in Figure 6.10 and Figure 6.11.

6.2.7 Classification of amino acids based on depletion rate from the culture medium.

Individual metabolites shown to be divided into 3 main categories, based on degree of change from base level in naïve medium (either metabolites >50% depleted, metabolites <50% depleted and metabolites enriched) from the defined medium at different phases of growth in culture. The amino acids were divided into three major groups depending upon their dynamic utilisation over time compared with naive medium.

Depending upon the relative rate of depletion from the medium, the amino acids are classified into three groups as follows:

- **Continuously utilised amino acids**
- **Partially utilised amino acids**
- **Continuously secreted amino acids**

6.2.7.1 Continuously utilised amino acids

Amino acids categorised under continuous utilisation are L-Tryptophan, Aspartate, Glutamate, L-Arginine, Methionine and Serine as more than half the initial abundance were consumed from the medium in 9 days growth period as shown in Figure 6.12.

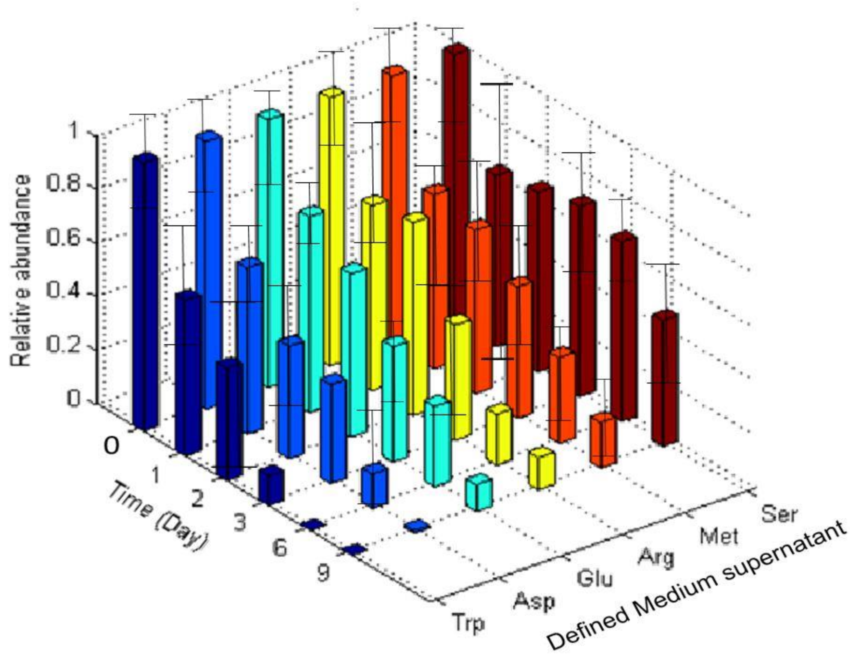

Figure 6.12 Relative abundance of continuously utilised amino acids with more than 50% depleted compared to naïve medium.

(Supernatant collected from 4 x 10^7 cells on Day 0, 1, 2, 3, 6, and 9 from the start of culture initiation n=3, Error bars = mean ± SD. Samples were collected in triplicates from different culture flasks. 3D plot generated using Matlab (code specified in appendix) with changes of metabolites intensities expressed as relative abundance in the form of six column matrix (Y axis) versus time (X axis). Amino acids annotated using three letter abbreviations. Relative abundance of metabolites in samples (Z axis) versus control with peak intensity ratio calculated from mean centred data.

6.2.7.2 Partially utilised amino acids

Amino acids such as L-Leucine, L-Threonine, L-Valine, L-Phenylalanine, L-Tyrosine and L-Lysine as shown in Figure 6.13 were salvaged partially during the entire growth of promastigotes.

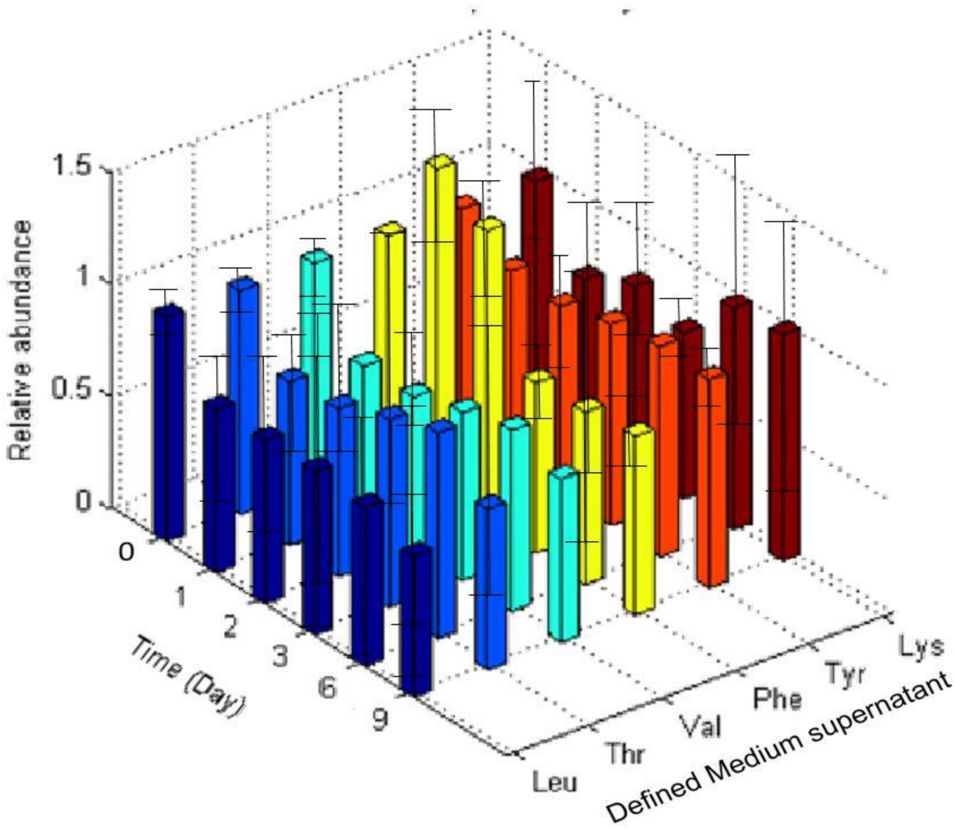

Figure 6.13 Relative abundance of partially utilised amino acids with less than 50% depleted compared to naïve medium.

(Supernatant collected from 4 x 10^7 cells on Day 0, 1, 2, 3, 6, and 9 from the start of culture initiation n=3, Error bars = mean ± SD. Samples were collected in triplicates from different culture flasks. 3D plot generated using Matlab (code specified in appendix) with changes of metabolites intensities expressed as relative abundance in the form of six column matrix (Y axis) versus time (X axis). Amino acids annotated using three letter abbreviations. Relative abundance of metabolites in samples (Z axis) versus control with peak intensity ratio calculated from mean centred data.

6.2.7.3 Continuously secreted amino acids

Glycine, L-Glutamine, L-Asparagine, L-Proline and L-Alanine are secreted in the medium over time with only minor transitory period of utilisation during Day 0 and Day 3 with less than 10% depleted from the medium as shown in **Figure 6.14**.

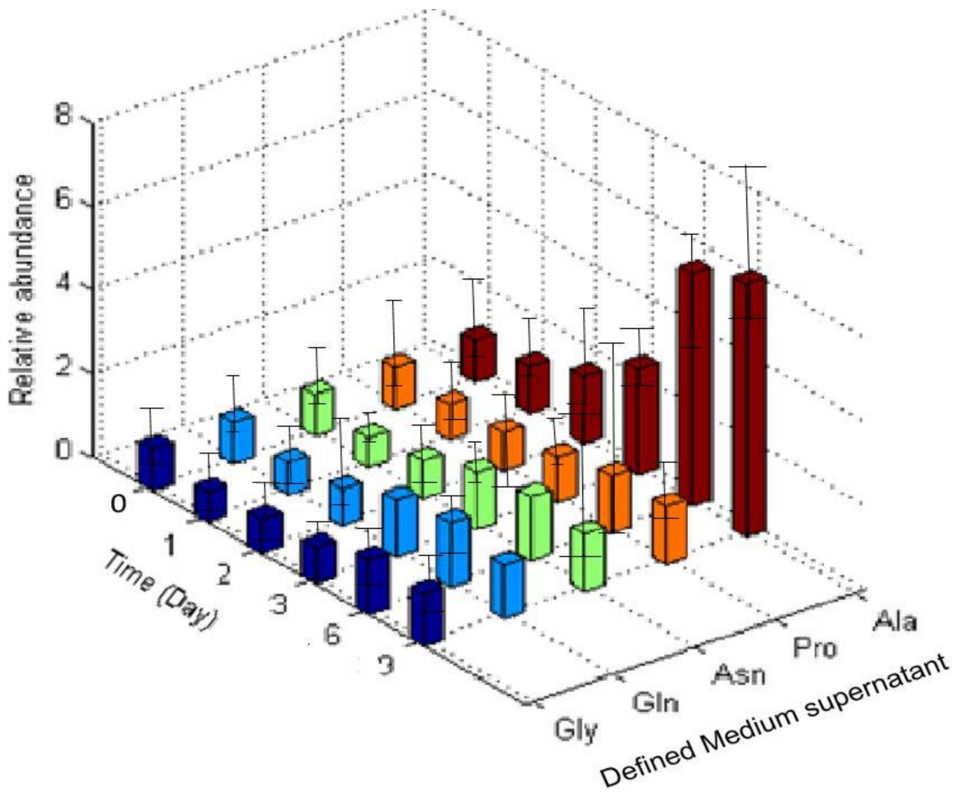

Figure 6.14 Relative abundance of continuously secreted amino acids with more than 50% enriched compared to naïve medium.

(Supernatant collected from 4 x 10^7 cells on Day 0, 1, 2, 3, 6, and 9 from the start of culture initiation n=3, Error bars = mean ± SD. Samples were collected in triplicates from different culture flasks. 3D plot generated using Matlab (code specified in appendix) with changes of metabolites intensities expressed as relative abundance in the form of six column matrix (Y axis) versus time (X axis). Amino acids annotated using three letter abbreviations. Relative abundance of metabolites in samples versus control with peak intensity ratio calculated from mean centred data.

6.2.7.4 Utilisation of other components in the Defined medium

Glucose is consumed by more than 50%, as measured by the relative abundance of the medium alone without cells. Adenosine is completely depleted, suggesting it is growth limiting nutrient of the defined medium composition. Among the vitamins, there were no significant changes in the levels of metabolites from the baseline of naïve medium (cell free medium) as shown in Figure 6.15.

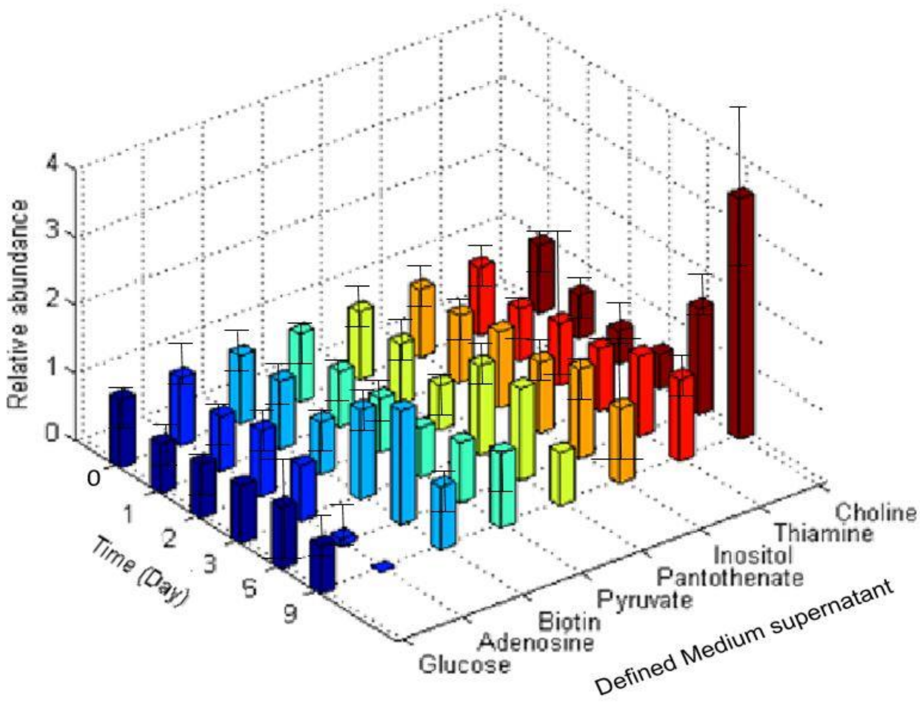

Figure 6.15 Depletion of other components in the defined medium.

(Supernatant collected from 4 x 10^7 cells on Day 0, 1, 2, 3, 6, and 9 from the start of culture initiation n=3, Error bars = mean ± SD. Samples were collected in triplicates from different culture flasks. 3D plot generated using Matlab (code specified in appendix) with changes of metabolites intensities expressed as relative abundance in the form of six column matrix (Y axis) versus time (X axis). Amino acids annotated using three letter abbreviations. Relative abundance of metabolites in samples (Z axis) versus control with peak intensity ratio calculated from mean centred data.

6.2.7.5 Continuously secreted amino acid intermediates

Increasing amounts of indole lactate, 4 hydroxy-phenyl-pyruvate, phenyl-pyruvate, pipecolate, citrulline/argininic acid, potentially derived from L-Tryptophan, L-Tyrosine, L-Phenylalanine, L-Lysine and L-Arginine respectively were observed in the spent medium. The relative abundance of amino acid intermediates in the form of keto acids from L-Tryptophan and L-Arginine were higher compared to amino acid intermediates from L-Phenylalanine and L-Tyrosine, hence these metabolites are represented separately in Figure 6.16 and Figure 6.17.

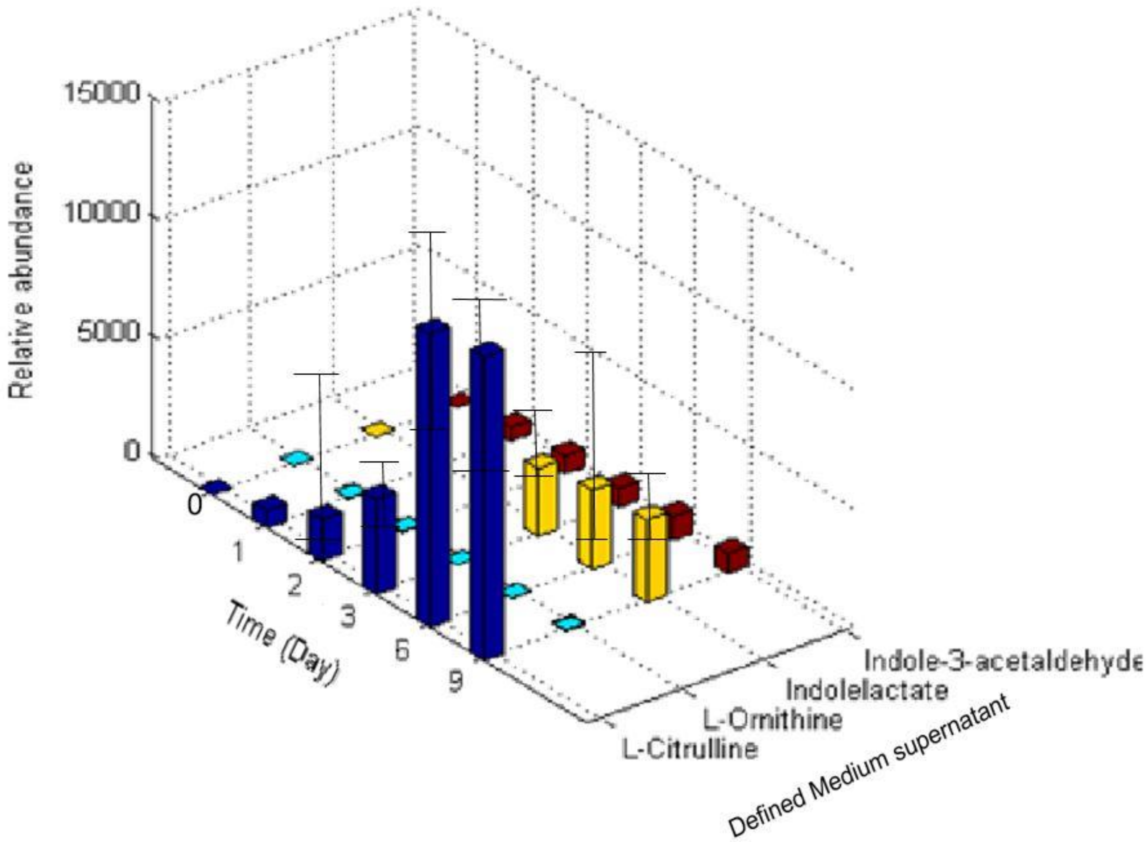

Figure 6.16 Continuously secreted keto acids enriched in the spent medium.

Samples collected at various time as specified 0, 1st, 2nd, 3rd, 6th and 9th day of culture supernatant (Z axis) from the start of culture initiation. Samples were collected in triplicates from different culture flasks. 3D plot generated using Matlab (code specified in appendix) with changes of metabolites intensities expressed as relative abundance in the form of six column matrix (Y axis) versus time (X axis). Peak intensity ratio between the sample and the control calculated from mean centred data.

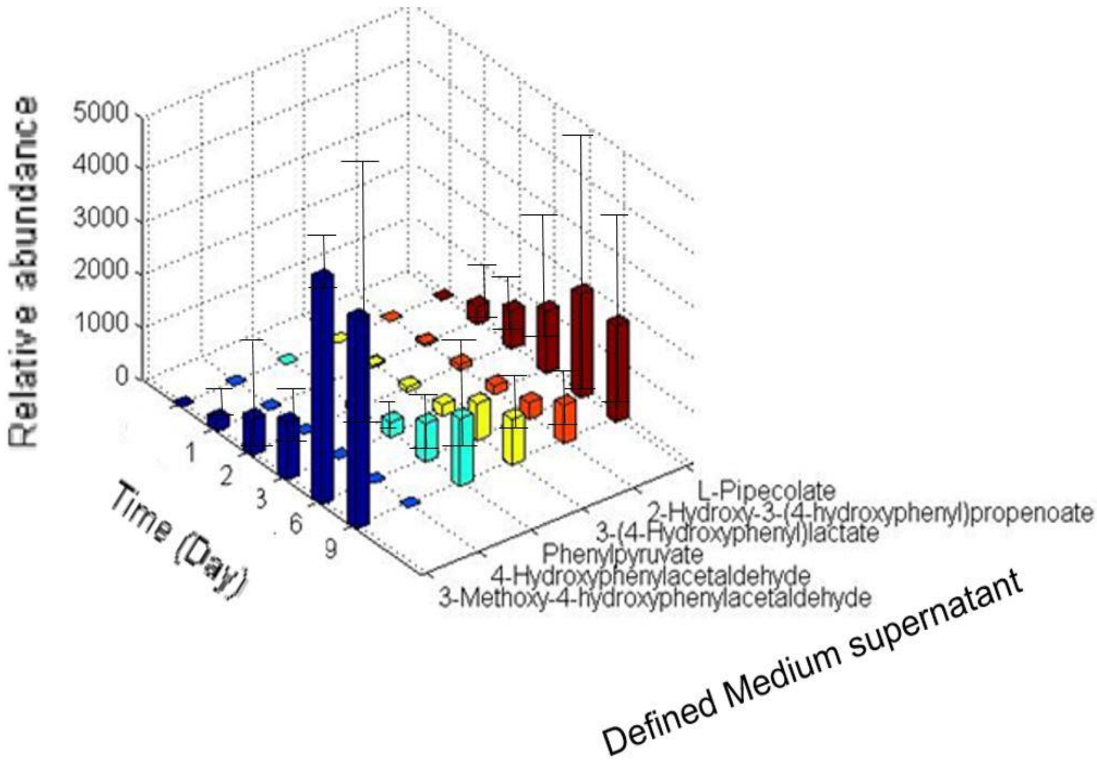

Figure 6.17 Continuously secreted keto acids enriched in the spent medium.

Samples were collected in triplicates from different culture flasks. 3D plot generated using Matlab (code specified in appendix) with changes of metabolites intensities expressed as relative abundance in the form of six column matrix (Y axis) versus time (X axis). Peak intensity ratio between the sample and the control calculated from mean centred log transformed data. Samples collected at various time as specified 0, 1st, 2nd, 3rd, 6th and 9th day of culture supernatant (Z axis) from the start of culture initiation.

The alpha keto acids showed in Figure 6.16 and Figure 6.17 were noted to be derived from continuously utilised amino acids; and showed significant enrichment in the supernatant medium as growth response. Although the trend of enrichment in the supernatant was the same, peak intensities differed between the first set from L-Arginine and L-Tryptophan, whilst the second set from L-Phenylalanine, L-Tyrosine and L-Lysine.

6.2.7.6 Partially secreted amino acid intermediates

Trace amounts of keto acids from partially utilised amino acids such as L-Methionine, L-Threonine, L-Leucine and L-Valine to citraconate, 2-oxo butanoate, 5-guanidino 2 oxopentanoate and 4-guanadino-butanoate respectively were found enriched in the spent medium as shown in Figure 6.18.

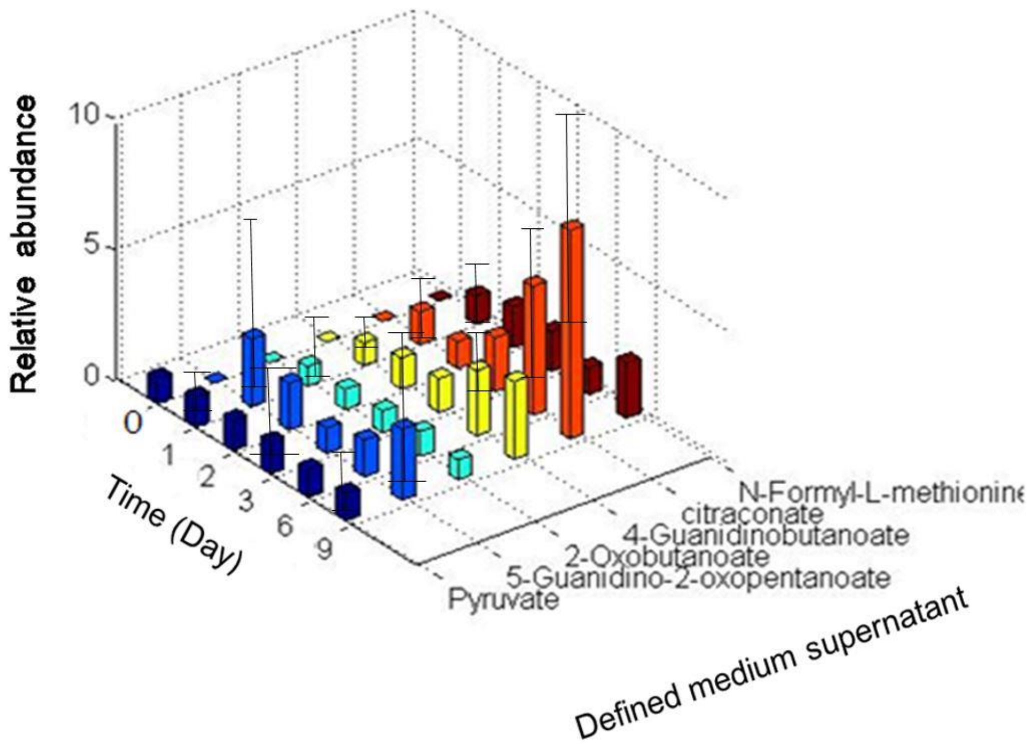

Figure 6.18 Partially secreted keto acids enriched in the spent medium.

Samples were collected in triplicates from three different culture flasks. 3D plot generated using Matlab (code specified in appendix) with changes of metabolites intensities expressed as relative abundance in the form of six column matrix (Y axis) versus time (X axis). Peak intensity ratio between the sample and the control calculated from mean centred data. Samples collected at various time as specified 0, 1st, 2nd, 3rd, 6th and 9th day of culture supernatant (Z axis) from the start of culture initiation.

6.2.7.7 Secretion of intermediates from carbohydrate metabolism and nucleo-lactones

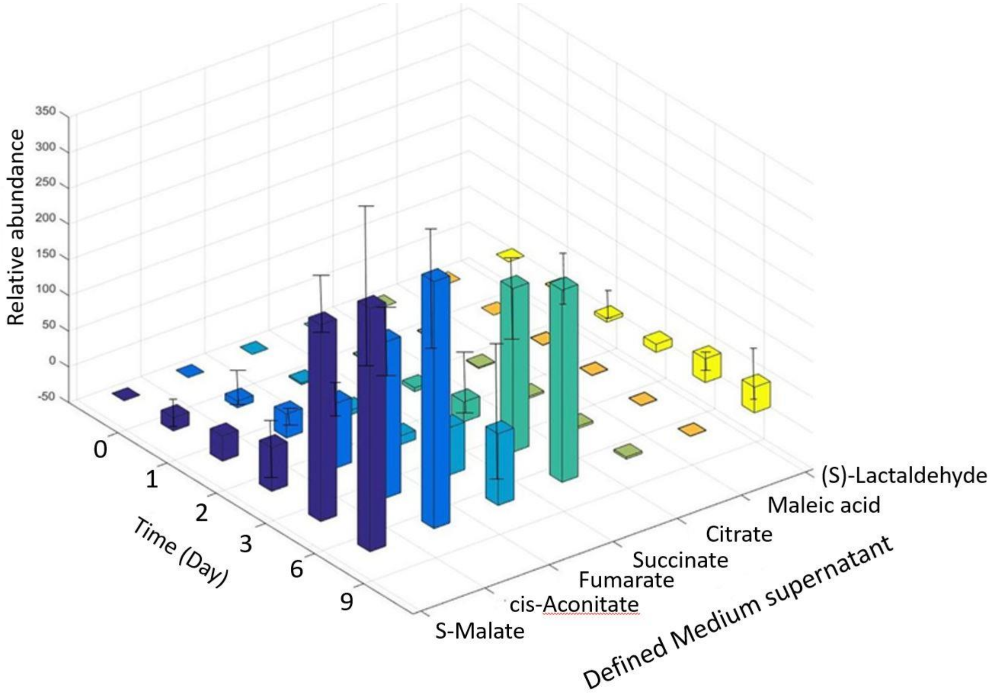

Figure 6.19 Keto acids from carbohydrates metabolism enriched in spent medium

(Supernatant collected from 4 x 10^7 cells on Day 0, 1, 2, 3, 6, and 9 from the start of culture initiation n=3, Error bars = mean ± SD. Samples were collected in triplicates from different culture flasks. 3D plot generated using Matlab (code specified in appendix) with changes of metabolites intensities expressed as relative abundance in the form of six column matrix (Y axis) versus time (X axis). Relative abundance of metabolites (Z axis) in samples versus control with peak intensity ratio calculated from mean centred data).

Significant enrichment of metabolites derived from carbohydrate metabolism such as (S)-Malate, cis-Aconitate, Fumarate, Succinate, Citrate, Maleic acid and L-Lactaldehyde were observed as shown in Figure 6.19. Also, keto acids such as Ascorbate, D-Xylonolactone, Cystathionine, 1,4-Lactone, L-Rhamnono-1,4-lactone were also found enriched in the medium during the course of growth period from Day 0 to Day 9 as shown in Figure 6.20. Nucleolactones such as Orotate, Xanthine, Cytosine, Malonate and D-Ribose were found to be significantly enriched after day 6 from the start of culture initiation as shown in Figure 6.21.

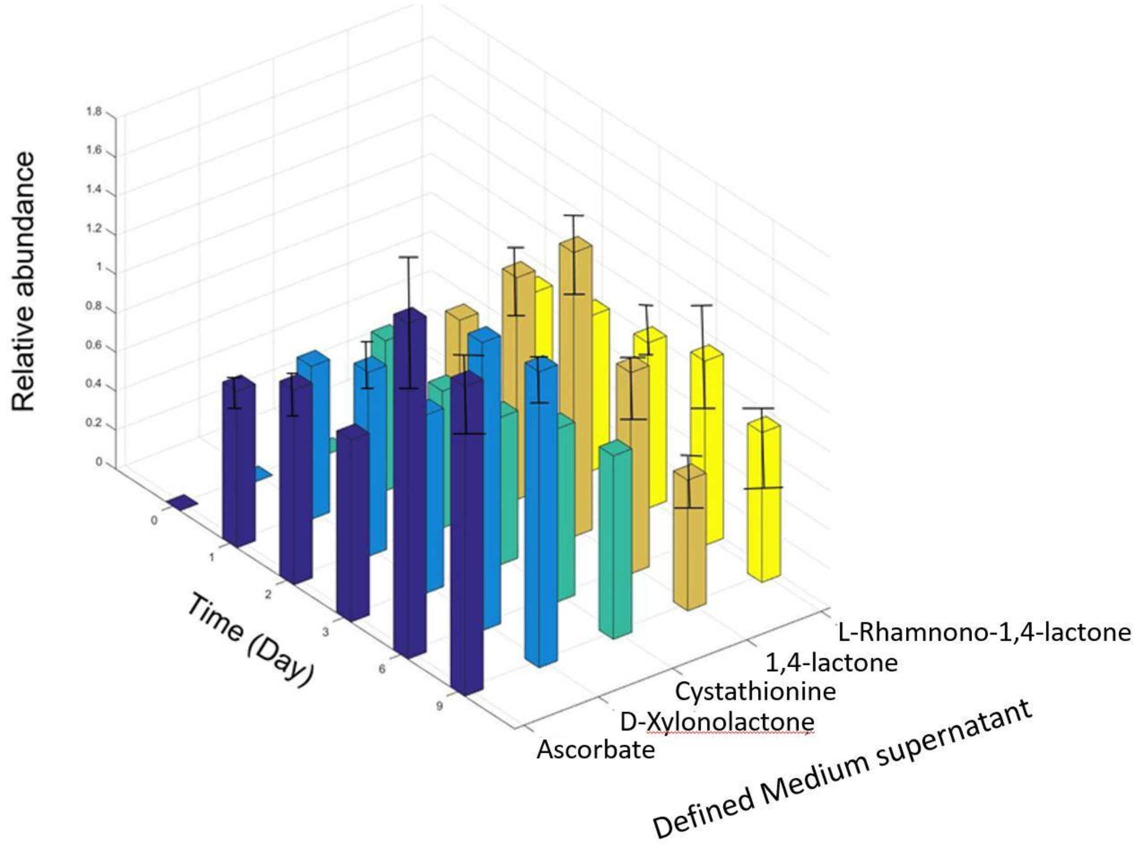

Figure 6.20 Keto acids from carbohydrates metabolism enriched in spent medium

(Supernatant collected from 4 x 10^7 cells on Day 0, 1, 2, 3, 6, and 9 from the start of culture initiation n=3, Error bars = mean ± SD. Samples were collected in triplicates from different culture flasks. 3D plot generated using Matlab (code specified in appendix) with changes of metabolites intensities expressed as relative abundance in the form of six column matrix (Y axis) versus time (X axis). Relative abundance of metabolites (Z axis) in samples versus control with peak intensity ratio calculated from mean centred data).

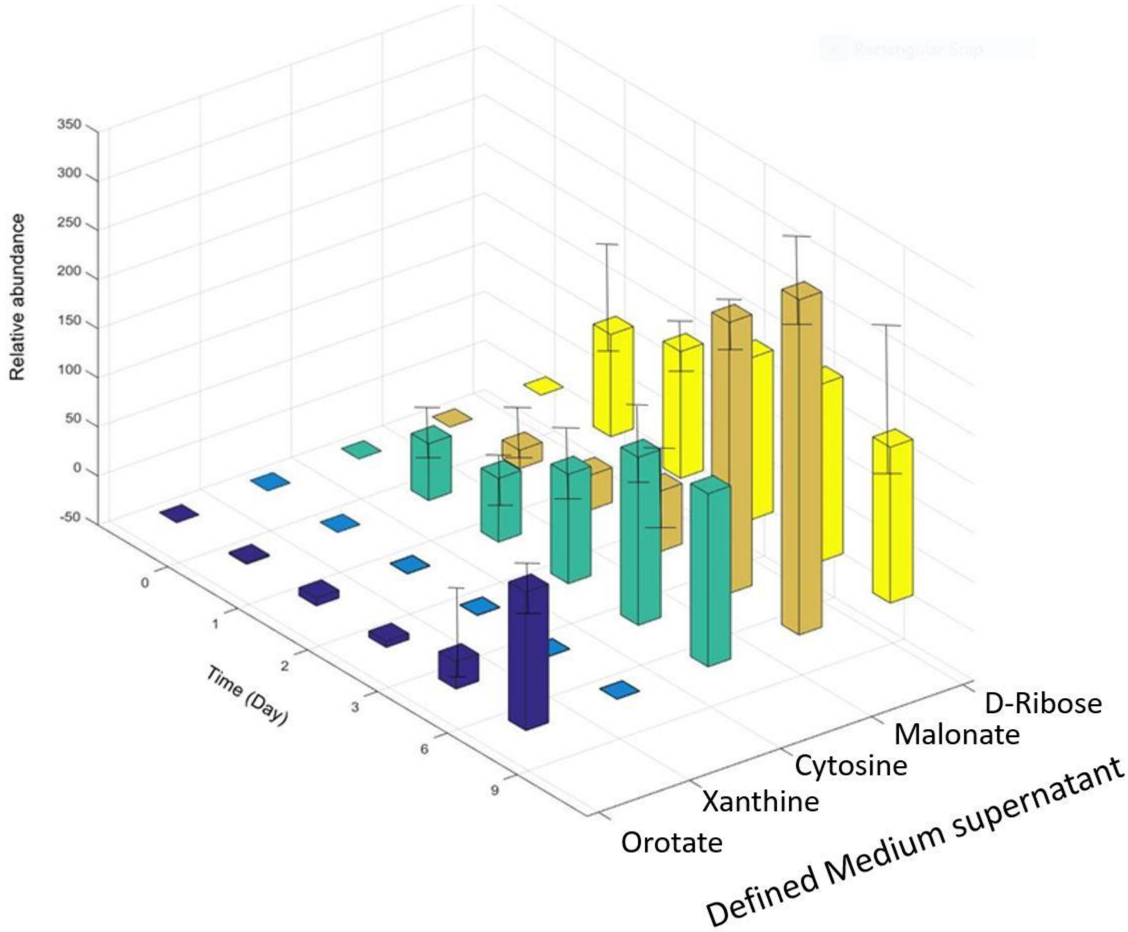

Figure 6.21 Nucleo-lactones enriched in the spent medium

Supernatant collected from 4 x 10^7 cells on Day 0, 1, 2, 3, 6, and 9 from the start of culture initiation n=3, Error bars = mean ± SD. Samples were collected in triplicates from different culture flasks. 3D plot generated using Matlab (code specified in appendix) with changes of metabolites intensities expressed as relative abundance in the form of six column matrix (Y axis) versus time (X axis). Relative abundance of metabolites (Z axis) in samples versus control with peak intensity ratio calculated from mean centred data.

From these results, it showed that amino acids were uniquely metabolised by Leishmania; not only for growth and protein production but metabolic intermediates such as keto acids were secreted into the spent medium (Figure 6.16-Figure 6.20).

Keto acids have a significant ROS scavenging activity and also has been shown to decrease ROS production (Beloborodova et al., 2012, Cotoia et al., 2014) described further in discussion section. Since exometabolome of *L.mexicana* promastigotes show increased accumulation of keto acids towards the metacylic stages; it led to question whether small molecules secreted by the parasite could play a role as antioxidants to support establishment of parasitism with host cells?

To further investigate the holistic nature of these metabolic intermediates secreted by the parasites; certain biochemical assays were carried out as described in 6.2.8 below.

6.2.8 Biochemical assays

These assays was carried out to determine the role of small molecules to test their impact on THP1 differentiated macrophage cells as infection model. Especially, intermediates from the aromatic acids such as L-Tryptophan and L-Phenylalanine were further evaluated since these two amino acids were found to be the most critical exogenous source amongst other amino acids for the viability of the promastigotes (Chapter 4). Samples with aromatic pyruvates found secreted in the extracellular environment throughout the growth period were isolated and tested with pure compounds in various biochemical assays below. Sample preparation and assay methodology has been elaborated in methods section.

6.2.8.1 Evaluation of THP1 viability in the presence of exo-metabolome samples

In order to determine the impact of exometabolome on host cells, the viability of THP1 differentiated macrophages were tested as shown in Figure 6.22

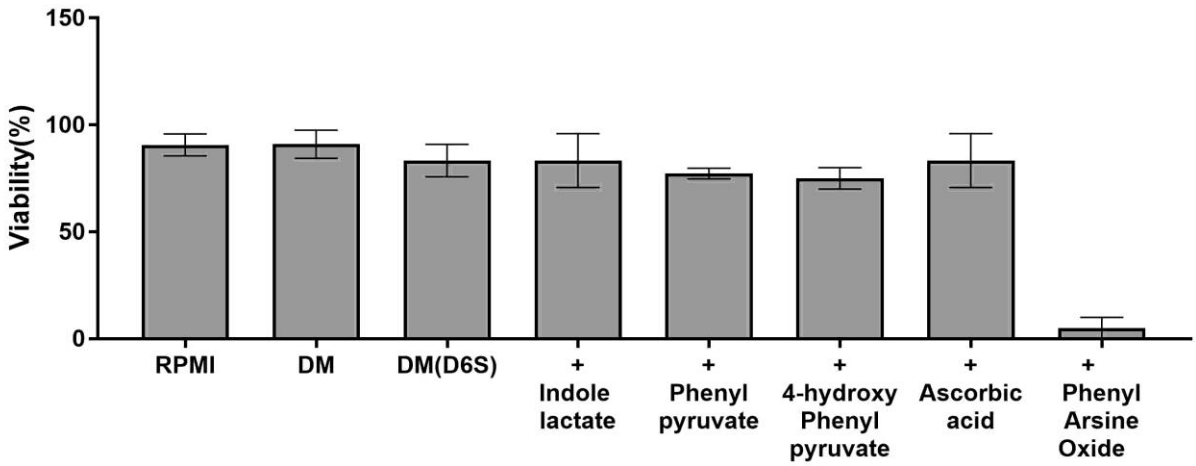

Figure 6.22 Evaluation of viability of THP1 cells

(5 x 10^6 cells/mL cultured in RPMI, DM, DM (D6S) exo-metabolome from Day 6 supernatant and DM with addition of extraneous pure compounds of with various compounds (+ Indole lactate, + phenyl-pyruvate, + 4-hydroxy phenyl pyruvate, +ascorbic acid at 1 mM each and phenyl arsine oxide as negative control at 10 μM) for 24 hours at pH 7.4, 37 ^{o} C, n=6, Error bars = mean ± SD).

It was observed from the results shown in Figure 6.22 that DM with addition of 1mM each of Indole lactate, phenyl-pyruvate, 4-hydroxy phenyl pyruvate, ascorbic acid, or DM (D6S) did not negatively affect viability and growth compared to growth in control samples of THP1 differentiated macrophages in RPMI medium.

6.2.8.2 Evaluation of THP1 viability under oxidative stress in the presence of exo-metabolome samples.

To further investigate the role of exo-metabolome on THP1 viability under oxidative stress by day 6 culture supernatant and pure compounds in biochemical assays for nitrite scavenging activity of *L. mexicana* promastigotes as shown in Figure 6.23 and Figure 6.24.

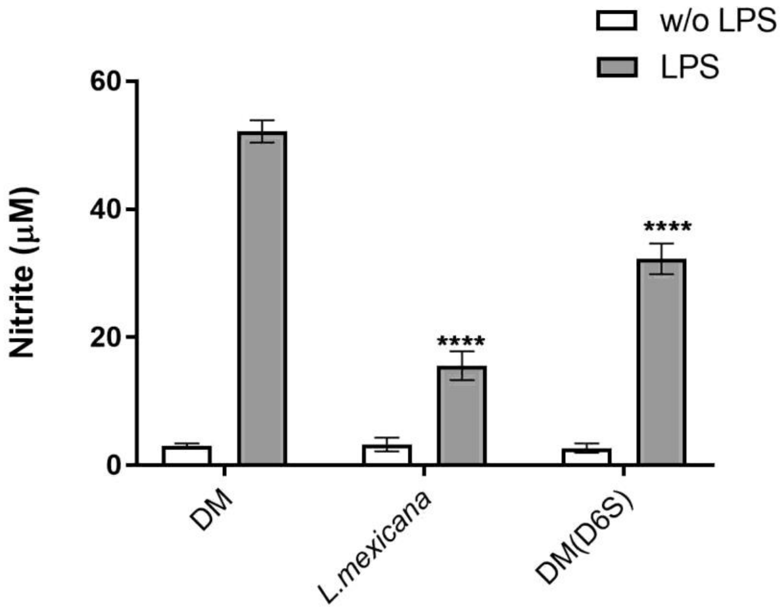

Figure 6.23 LPS stimulated nitric oxide production suppressed by exo-metabolome-treated macrophages.

(5 x10^6 cells/mL of THP1 cells treated with 5 ng/mL PMA for 24 hours undergoes differentiation to macrophages attached to the bottom of the wells in the chamber slides. Differentiated macrophages placed in wells each treated individually with naïve medium (DM), with promastigotes in 1:10 ratio (*L. mexicana*) or incubated with exo-metabolome (DM (D6S) in triplicates in two identical rows. For the wells in the first row, the samples were unstimulated (Control -white bars) and for the second row stimulated with 10ng/mL of LPS for 24 hours (treated - grey solid bars. The nitrite scavenging activity of the exo-metabolome and specific metabolites was analysed as described in methods section using Griess's reagent, at pH 7.4, 37 º C, n=6, Error bars = mean ± SD. Asterisks indicate significant difference in nitrite suppression with ****, $p<0.0001$ compared to DM, one way ANOVA with Dunnett's multiple comparison test).

The amount of nitrite was quantified using standard curve ranging from 0-100 µM and analysed using linear regression analysis of Graph-pad prism software. Stimulation of THP1 cells with LPS triggered nitrite secretion into the extracellular medium and no nitrite was recorded in wells without LPS. The amount of nitrite secreted by THP1 cells in naïve medium DM was recorded to be higher compared incubation with 1:10 *L. mexicana* or exometabolome. It was observed that *L.mexicana* infection inhibits NO production by 70% after 10 ng/mL of LPS stimulation. Exo-metabolome incubation hampers NO production by 30% after 10 ng/mL of LPS stimulation.

Specific compounds of aromatic pyruvates enriched in the exo-metabolome were tested for nitrite scavenging activity as shown in Figure 6.24.

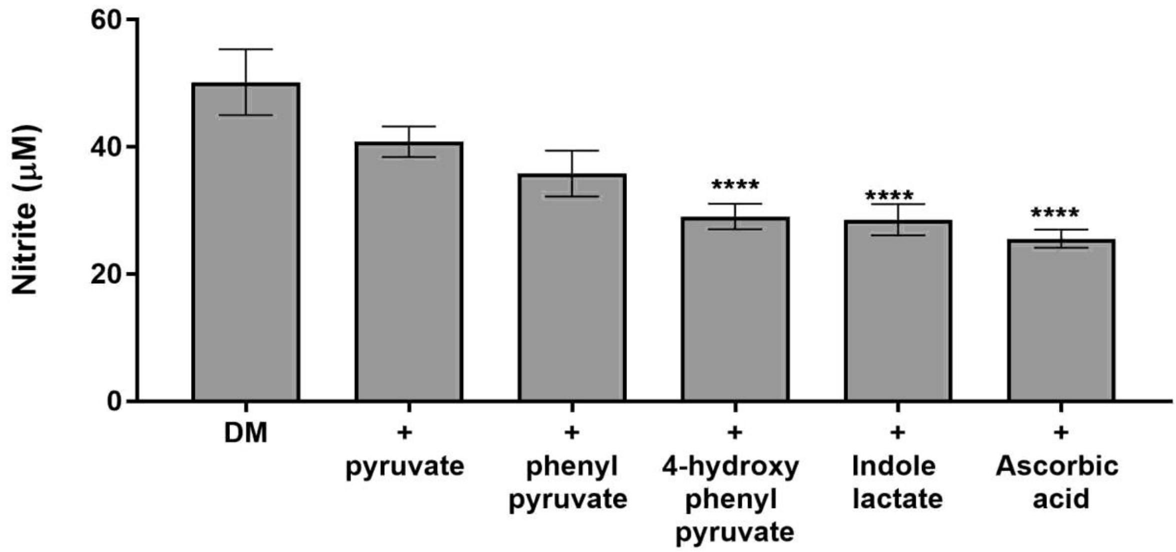

Figure 6.24 LPS stimulated NO production inhibited by aromatic pyruvates and ascorbic acid.

THP1 cells differentiated using 5 ng/mL PMA for 24 hours. Differentiated macrophages were untreated (naïve medium - DM), incubated with DM with various compounds (+pyruvate, + phenyl-pyruvate, + 4-hydroxy phenyl pyruvate, + Indole lactate, +ascorbic acid) for 24 hours at 1 mM each in triplicates. All the wells were stimulated with 10ng/mL of LPS for 24 hours and amount of nitrite recorded using griess assay at pH 7.4, 37 º C, n=6, Error bars = mean ± SD. Asterisks indicate significant values with P value < 0.0001 by one way ANOVA using Dunnett's multiple comparison test of graph-pad prism software.

As shown in Figure 6.24, DM with addition of phenyl pyruvate and 4-hydroxy phenyl pyruvate significantly reduces free nitrite detected by ~20% each. Addition of indole lactate and ascorbic acid reduces amount of free nitrite detected by ~40% after 10 ng/mL of LPS stimulation compared to naïve medium without cells (sample-DM) as shown in Figure 6.24.

6.2.8.3 Determination of antioxidant power by reducing activity measurement.

The antioxidant activity was measured in Figure 6.25 using reducing power of the specific metabolites (aromatic pyruvates) enriched in the spent medium by absorption at 700 nm using range of concentrations from 0-10 mM of ascorbic acid, acetate, phenylpyruvate, hydroxyl-phenylpyruvate and indole lactate.

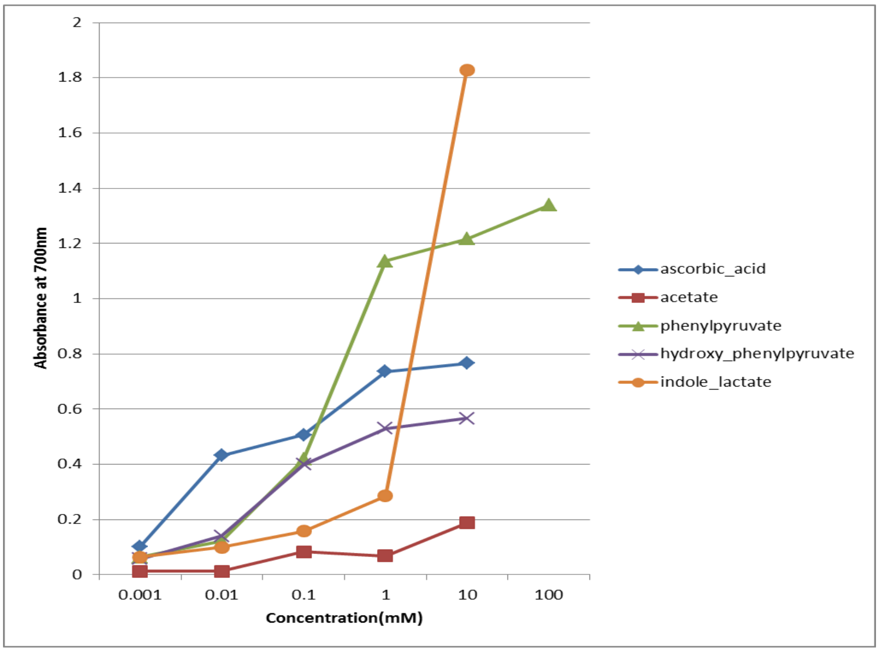

Figure 6.25 Determination of antioxidant power by measurement of reducing activity.

(Ascorbic acid (blue), acetate (red), phenylpyruvate (green), hydroxyl-phenylpyruvate (purple) and indole lactate (orange), n=6, mean centred data)

Specific metabolites enriched in the exo-metabolome such as ascorbic acid, acetate, hydroxy phenyl pyruvate, phenyl pyruvate, indole lactate at a range of different concentrations from 0.001 mM-10 mM was tested were tested for reducing power as a measure of its antioxidant activity. Absorbance read at 700 nm was used to determine the amount of ferric ferrocyanide (Prussian blue) formed. Increase in absorbance indicates linear relationship of the ability of the compounds to reduce ferric complex to ferrous form. Higher absorbance of the reaction mixture indicates higher reducing power of the compounds tested with following order with indole lactate > phenyl pyruvate > ascorbic acid > hydroxy phenyl pyruvate > acetate.

6.2.8.4 Estimation of phenolic content of exo-metabolome samples from different growth stages of promastigotes.

The phenolic content of the exo-metabolome as shown in Figure 6.26 was determined by the number of hydroxyl groups available to react with phosphomolybdic acid in Folin-Ciocalteu reagent in an alkaline medium to produce a blue coloured complex using catechol equivalent standard curve (mg/µL).

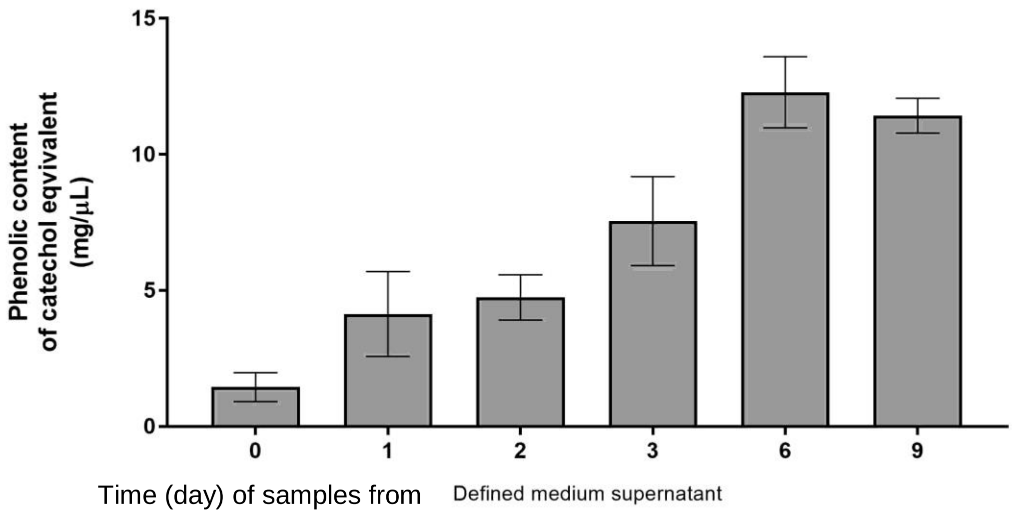

Figure 6.26 Phenolic content of the exometabolome represented as catechol equivalent (mg/µL)

(Supernatant collected from 4 x 10^7 cells on Day 0, 1, 2, 3, 6, and 9 from the start of culture initiation n=6, Error bars = mean ± SD. Samples were collected in triplicates from different culture flasks).

From Figure 6.26, the phenolic content, i.e. the number of free hydroxyl groups have been recorded as increased during the entire growth phase in supernatant samples at various time points from Day 0 to Day 9 as specified from the start of culture initiation (n=6, ANOVA for multiple comparison using graph pad software).

6.2.8.5 Estimation of phenolic content of specific metabolites enriched in the exo-metabolome.

The phenolic content determined by the number of hydroxyl groups available for reaction was measured for specific metabolites enriched in the spent medium as shown Figure 6.27.

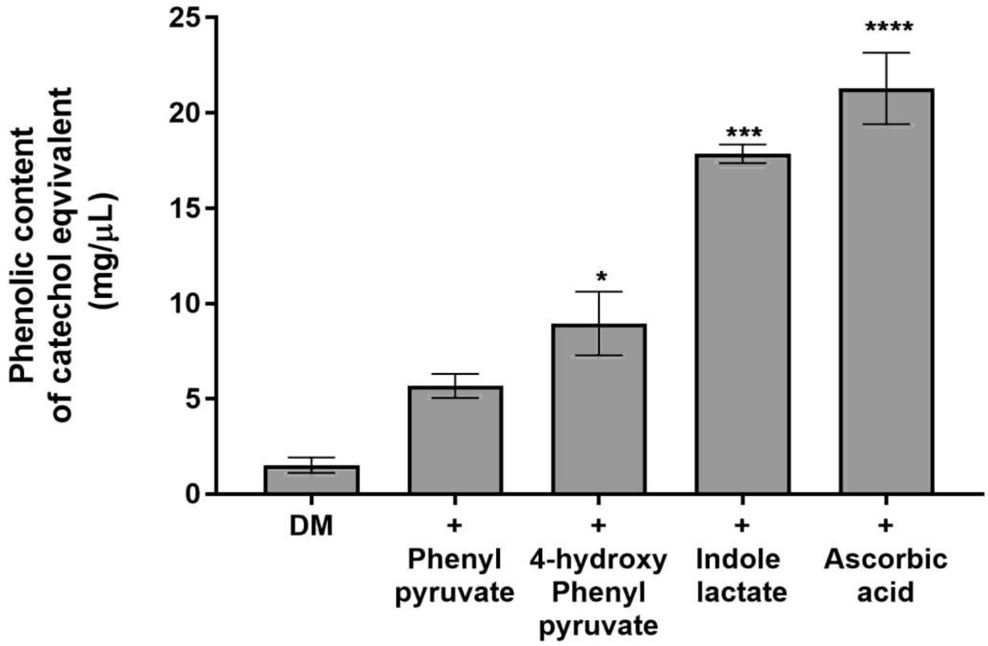

Figure 6.27 Phenolic content of pure compounds represented as catechol equivalent (mg/μL).

(Compounds tested included 1 mM of indole lactate, phenyl- pyruvate, 4-hydroxy-phenyl-pyruvate and ascorbic acid at pH 7.4, 37 º C, n=6, Error bars = mean ± SD. Asterisks indicate significant values with ****p value < 0.0001, ***< 0.0005, *< 0.05 compared to DM alone by one way ANOVA using Dunnett's multiple comparison test of graph-pad prism software.

Phenolic content determines the number of free hydroxyl groups available for complex formation. Increase in absorbance indicates linear relationship of enrichment of free hydroxyl groups available for complex formation with phosphomolybdic acid tested with following order with phenyl pyruvate > hydroxyl phenyl pyruvate > indole lactate > ascorbic acid as shown in Figure 6.27

6.3 Discussion

In this study, an untargeted metabolomics approach was carried out throughout the growth period starting from early log (Day 1 and Day2), mid log (Day 3) and stationary phase (Day 6 and Day 9). Samples from the extracellular supernatant was used to determine uptake and secretion of metabolites during promastigotes growth referred to as time resolved metabolic foot-printing. Using the data, metabolic pathways were differentiated to ascertain specific salvage and biosynthesis pathways of *Leishmania* promastigotes which are parasite specific metabolic pathways as potential drug targets.

Time points chosen for the experimental study was chosen such that the organism growth responses with time is linear during the initial phase and non-linear/exponential during the log phase (Steel, 1967) leading to a mixed model of regression with linear and non-linear curves has been explained elsewhere. For comparative purposes between the six time points, consecutive points were chosen during early stages of growth than during the saturated stationary phase, ensuring proper regression rules were accounted capturing both linear and non-linear responses of growth with time. This allowed for adequate spread among the data taking into consideration the independent variable (time in this experiment) has been measured with 6 time points including control. Day 1, 2 and 3 account for the start point of active uptake of metabolites to mid log phase and then on Day 6 and Day 9 to mark the stationary phase and saturation point respectively. The samples were analysed using LC-MS using both positive and negative ionisation modes with 36 data points of each compound. This approach allowed to identify reproducible metabolic trends with greater confidence statistically with additional spectral filtering algorithm (Scheltema et al., 2011). Data from untargeted metabolomics yields large amount of data which are not selfexplanatory. Inference of meaningful biological information from the data requires careful experimental design, relevant quality control and extensive computational deconvolution of the spectral data to validate the change in metabolite levels (Dunn et al., 2012).

For the pre-processing of data of Defined medium culture supernatant was analysed by LC-MS using orbitrap mass spectrometry in both positive and negative ionisation modes. The mass chromatograms, putative identifications and trends of certain individual metabolites were analysed using IDEOM software (Creek et al., 2012b). Retention time alignment was carried out using XCMS as integrated in the mzMatch software (Scheltema et al., 2011). Manual verification was carried out for metabolites for peak shape verification using PeakML viewer supporting mass and retention time information for metabolite identification.

6.3.1 Multi-variant analysis

Those peaks that were typical contaminants of LC/MS analysis, for example, those with intensity trends that were not subjected to any change or intensities close to the detection limit were removed by manually setting the pre-filter intensity >1000 as rigorous filtering process of peak identification. A list of the detected peaks with intensity trends and stability score values were calculated from the IDEOM software (Creek, 2012). About ~206 putatively identified metabolites were analysed using multi-variant data analysis techniques such as PLS-DA model, principal component analysis (PCA), and hierarchical clustering analysis (HCA) to understand the underlying patterns within the data. PLS-DA model allows for application of supervised machine learning algorithm on the time resolved untargeted metabolomics dataset in an unbiased manner to highlight the underlying pattern within the data (Behrends et al., 2009, Allen et al., 2003). The variance plot as shown in Figure 6.2, the first two components explaining the maximum variability within the data which accounted for 26% and 37% of the variation respectively present in the LC-MS dataset. Visualisation of the data showed the spread of the 18 samples in an unbiased manner across the orthogonal distance on the score plot as shown in observation diagnostics. The score plot (PCA) indicates position of individual samples amongst the 18 samples analysed. The placement of individual metabolites were subdivided into four sections (+/+,

+/-, -/+, -/-) based on the levels of their peak intensities as shown in the Loadings plot as shown in Figure 6.2.

Using PCA analysis, the maximum variance within the data is projected in two or more dimensions or orthogonal components without the loss of vital information to distinguish dominant features of the data set (Dien et al., 2003). Statistically, the mean and variance of the data are used to build the co-variance matrix of the orthogonal components. Computationally, PCA separates the classes based on the orthogonal components across the samples that reduces the dimensions in the data set and highlight underlying metabolites pattern within the data (Fiehn, 2002).

The PCA result as shown in Figure 6.2 showed different clusters with individual growth stages exhibit distinct metabolic signature that uniquely differentiates log phase promastigotes from infective metacyclics. About ~206 metabolites including the base-peaks from the dataset were used to visualise the PCA plot using R software package “ropls” (Thevenot et al., 2015) with appended files and code listed in the appendix. These results also highlight that distinct changes in metabolic profile of the extracellular environment might facilitate the growth and proliferation of promastigotes, thereby supporting the morphological and physiological transformation from procyclics to metacyclics within the 9 day growth period as tested. The HCA analysis as shown in Figure 6.3 confirmed that biological replicates at each time point form a cluster together and the metabolic profile of (naïve culture medium) Cluster 1 were completely separated from Cluster 2 (samples of Day 6 and Day 9) and Cluster 3 (Day 1, Day 2, and Day 3).

Overall about ~205 metabolites that were putatively identified in the extracellular metabolome using IDEOM software. Amongst those ~25 % metabolites depleted from the medium, ~15% not changed significantly and ~40% significantly enriched in the medium over the growth period of 9 days as shown in Figure 6.4. The metabolite variations in the extracellular metabolome reflects the intracellular phenotype, especially about the pathway activities. The nature and pattern of individual metabolites that have been identified with authentic standards as expressed in base 2 logarithmic fold changes of their relative intensities as shown in Figure 6.5 to Figure 6.11.

Amongst the amino acids with polar uncharged side groups, L-Threonine and L-serine were depleted compared to L-Proline and L-Glutamine as shown in Figure 6.5.Those amino acids with non-polar aliphatic side groups, L-Leucine, L-Valine and L-Methionine were depleted compared to L-glycine and L-Alanine as shown in Figure 6.6. With negatively charged side groups, both L-Glutamate and L-Aspartate were consumed as shown in Figure 6.7. Amongst the positively charged side groups, L-Lysine was taken up moderately from the medium, whilst L-Asparagine was found secreted as shown in Figure 6.8. Those with aromatic side groups, L-Tryptophan was depleted compared to L-Phenylalanine and L-Tyrosine as shown in Figure 6.9. Amongst other identified metabolites, L-glucose and L-adenosine were completely depleted as shown in Figure 6.10 and Figure 6.11.

6.3.2 Classification of amino acids based on depletion rate from the media

The overall pattern of utilisation has been further classified under different categories as shown in Figure 6.12 to Figure 6.15. Aspartate, Glutamate, L-Tryptophan, L-Arginine, Methionine and Serine were recorded as continuously utilised amino acids since more than half the initial abundance were consumed from the medium in 9 days growth period as shown in Figure 6.12. During promastigotes growth in defined media, amino acids are consumed at various rates. Aspartate and L-Glutamate are completely consumed as shown in Figure 6.7, indicating their consumption as carbon source, since the corresponding keto acids enter the TCA cycle [22]. It is particularly interesting to correlate that L-Tryptophan and L-Arginine found critical for the growth of promastigotes (Chapter 4) were amongst those amino acids that were continuously up taken from the medium and completely scavenged (Figure 6.9 and Figure 6.5).

It is known that *Leishmania* encode for broad spectrum amino transferase acting on several amino acids such as L-Aspartate, L-Tyrosine, L-Tryptophan, L-Glutamate thus leads to competitive binding amongst these substrates in transamination reactions. The amino group serves as nitrogen donor for other biological reactions (Leblancq and Lanham, 1984). Interestingly, the resulting keto acids were found secreted outside the cells, hence no contribution to the TCA cycle, unlike the situation in mammalian cells (Figure 6.16). Aspartate has been shown to be catabolised by L-Aspartate transaminase, which results in oxaloacetate entering the TCA cycle for energy contribution, as shown in targeted metabolomics using labelled isotope studies (Saunders et al., 2011). Although L-Aspartate in our defined minimal medium at 0.2 mM is less than other amino acids, L-Aspartate uptake is uninhibited by other amino acids at much higher concentration, suggesting the presence of an L-Aspartate-specific transporter. On the other hand, a L-Glutamate transporter with high substrate specificity has been well characterised in *Leishmania amazonensis* (Paes et al., 2008). Glutamate is responsible for 80% of energy generation with maximum flux as alpha keto glutarate enter the TCA cycle (Saunders et al., 2011).

Apart from their importance for growth and viability, metabolic intermediates of these amino acids and their corresponding keto acids were enriched in the spent medium (Figure 6.16 to Figure 6.20). Enrichment of keto acids at the metacylic stages could modulate the host environment, since their chemical structure allows for conversion from keto to enol form. This characteristic of the enone moiety is responsible for scavenging free radicals and reactive oxygen species which may be encountered when the metacylic stages infect the host cells; thereby, favouring a reducing environment and potentially supporting viability of the promastigotes during early attachment and parasitism.

Unlike mammals which elaborate a catabolic pathway for L-Tryptophan contributing to the tricarboxylic acid cycle, radiolabelling experiments in *L. donovani* have reported much simpler pathway (Leelayoova et al., 1992) with the first step in L-Tryptophan catabolism is mediated by L-Tryptophan aminotransferase, a broad spectrum transaminase catalysing the conversion of L-Tryptophan to indole pyruvate and subsequently by hydroxyl-acid dehydrogenase to indole lactate as shown in Figure 6.16. Previous literature also suggest the potential reason for complete consumption of L-Tryptophan from the environment and simplistic pathway could be because of preferred nitrogen donor(Berger, 1996), to deprive host cells from essential amino acids to evade host immune system (Wanasen, 2008).

Interestingly, our time course data indicates that indole lactate is progressively enriched in the spent medium over time (Figure 6.16). It is intriguing the parasite is continuously scavenging L-Tryptophan possibly for NADH regeneration as shown in chapter 4 required for the conversion of L-Tryptophan to indole pyruvate and subsequently indole lactate, which is effluxed out of the cell (Figure 6.16). A recent report suggests that L-Tyrosine transaminase is expressed in *L. infantum* promastigotes (Moreno et al., 2014b). Increased over-expression of the transaminase protein was also observed in nitric oxide resistant species. L-Tryptophan, due to its hydrophobic nature, must rely on a transport process to enter the cell. Transport of L-Tryptophan is uninhibited by other amino acids present at much higher concentration in the Defined medium highlights the probability of transporter protein that have highest affinity and also substrate specificity towards L-Tryptophan alone. However, in the light recent literature and experimental results as described in chapter 5, the hypothesis that aromatic pyruvates could play major role in evading host immune system especially during initial host infection and establishment of parasitism has been tested in this chapter.

L-Arginine has been extensively taken up from the medium, with less than 50% remaining in the medium on day 3 of growth of promastigotes in defined medium. L-Arginine transporter LdAAP3 is well studied in *Leishmania* (Shaked-Mishan et al., 2006), indicating L-Arginine metabolic pathway is unique in kinetoplastids for the synthesis of unique antioxidants such as trypanothione (Colotti and Ilari, 2011). This polyamine pathway mediated by arginase play a pivotal role in *Leishmania* with enzymes localised both in glycosomes and acidocalcisomes, which might serve as intracellular sinks of L-Arginine (Darlyuk et al., 2009). Interestingly, equivalent amount of de-aminated product of L-Arginine enriched in the spent medium during the 9 day growth period is as shown in Figure 6.12. Recent studies confirm that the de-aminated product is arginic acid confirmed through MS-MS fragmentation spectral analysis (Westrop et al., 2015). Results from that particular study (Westrop et al., 2015) were carried out in dialysed serum containing medium which showed only significant L-Arginine and L-Tryptophan consumed from the medium, whilst most other amino acid levels were reported constant due to surplus in the extracellular medium. Here, we show that use of our defined medium allowed to classify six amino acids that are continuously scavenged compared to other amino acids in the next category with moderate utilisation.

As observed from Figure 6.12, more than 50% of serine (0.2mM) was consumed from the extra-cellular system but the amount of serine uptake saturated by day 1 of growth period tested. This could possibly be because of de novo serine biosynthesis that limits the level of uptake of serine as elaborated in discussion section. Uptake of serine (0.2mM) in defined minimal medium not inhibited by other amino acids, suggesting that uptake of serine is mediated by a transporter protein with substrate specificity. Serine is converted into pyruvate entering the TCA cycle (Opperdoes and Coombs, 2007), but there is significant pyruvate enrichment in the spent medium Figure 6.19.

Flux from the TCA cycle via glucose metabolism also results in pyruvate overflow as noted in NMR studies of *Leishmania panamensis* using PBS buffer (Rainey and Mackenzie, 1991). In our data, the pyruvate is enriched in the spent medium with increase in relative abundance over time, although the background signal from the control sample showed high peak intensity with the sterile media composition has 1mM sodium pyruvate.

The exo-metabolome has been shown to decipher gene functions and also highlight disease related biomarkers as shown in yeast systems. Also, time resolved metabolic foot-printing in defined medium has been used to capture drug induced states to unravel the mode of action in yeast systems. This is the first report of its kind to report data about exo-metabolome of *L. mexicana* promastigotes in defined media and colorimetric assays for biochemical studies.
Also, those metabolites enriched in the medium represents metabolic secretion depending upon the internal programming of growth adaptation with the progression of life cycle. Metabolites enriched over time have been shown in Figure 6.16 to Figure 6.20. The major advantage in this study with the use of defined medium, enabled collection and purification of extracellular metabolome samples from different time points. The extracellular metabolites at individual growth stages by time resolved metabolic foot-printing allowed to identify the trend of utilisation of individual metabolites, especially those absent in the medium but enriched over time.

In most organisms, amino acids that are surplus to requirement for protein synthesis enter the TCA cycle as energy intermediates (Sherman, 1977). However, our results from metabolic foot-printing of *L. mexicana* promastigotes in defined medium highlights an intriguing observation that *Leishmania* promastigotes rapidly scavenge amino acids, metabolise into corresponding keto acids and equivalent amounts secreted out of the cell (Figure 6.16, Figure 6.17, Figure 6.18). Berger et al in (Berger et al., 1996) incorporated radiolabelled L-Tryptophan in *L. donovani* promastigotes and reported indole lactate secreted by the cells. In this study, using untargeted metabolomics, we show the presence of various keto acids enriched in the spent medium over time. The question why these parasites increase their transaminase activity in infective forms and secrete equivalent keto acids in their extracellular medium has not been investigated before.

Increasing amounts of arginic-acid, indole lactate, 4 hydroxy-phenyl-pyruvate, phenyl-pyruvate, pipecolate derived from L-Arginine, L-Tryptophan, L-Tyrosine, L-Phenylalanine and L-Lysine are observed in the spent medium (Figure 6.16, Figure 6.17). Also, trace amounts of keto acids from L-Methionine, L-Threonine, L-Leucine, L-Valine to citraconate, 2-oxo butanoate, 5-guanidino 2 oxopentanoate, 4 guanadino butanoate respectively (Figure 6.18) were also enriched in the spent medium. This phenomenon of increased secretion of keto acids has been reported in *Trypanosoma brucei* extracellular medium (Creek et al., 2013, Berger et al., 1996). Alpha keto aciduria has been reported in patients affected with chronic African trypanosomiasis (Hall et al., 1985).

Amino acids such as L-Phenylalanine, L-Tyrosine, L-Leucine, L-Threonine, L-Valine, and L-Lysine as shown in Figure 6.13 were taken up moderately during the entire growth of promastigotes. Berger et al have shown that L-Phenylalanine used as preferential nitrogen donor in *L. mexicana* promastigotes. Studies by Blum et al indicated that (Blum, 1996) the kinetic release of L-Phenylalanine as an adaptive behaviour employed by *Leishmania* promastigotes for osomo-regulation. Initially on Day 1 of the culture, the promastigotes in defined medium released L-Phenylalanine transiently, probably indicating adaptive osomo-regulation.

Moderate consumption of amino acids could also be because of competitive inhibition with other amino acids, for example, L-Methionine and L-Phenylalanine for Locus D (Hasne and Barrett, 2000). Methionine has been classified under category 1 under continuous utilisation which might competitively inhibit L-Phenylalanine uptake, hence the data indicates saturated uptake of this amino acid.

Metabolism of L-Phenylalanine occurs in a series of reactions mainly involving enzymes such as aromatic acid aminotransferase, indolepyruvate oxidoreductase, 3 oxoadipyl CoA thiolase, phenylacetyl CoA isomerase, enoyl CoA hydratase and 3 hydroxybutanoyl CoA dehydrogenase. Although few studies indicates the role of L-Phenylalanine has preferential nitrogen donor, the major metabolic pathway of L-Phenylalanine degradation had not been completely elucidated before. Genome annotation indicates the absence of enzymes for complete L-Phenylalanine degradation to TCA cycle intermediate in *Leishmania* (Opperdoes and Coombs, 2007), however, metabolic intermediates of L-Phenylalanine decarboxylase have been detected in the spent medium (Figure 6.16) with significant amount of phenyl pyruvate, end product of amino transferase activity. Enrichment of these phenyl-pyruvate has been speculated to have potential role in decreasing reactive oxygen species during haemorrhagic shock (Cotoia et al., 2014). Role of this particular metabolite as antioxidant potentially supporting parasitism has been investigated in last section of this chapter.

Leucine, Threonine and Valine show similar depletion profile with active uptake from Day 1 of growth in defined medium and then saturates after until Day 9. Leucine is important amino acid for protein synthesis and also serves as metabolic fuel (Ginger et al., 2001). Leucine is ketogenic in nature and converted to acetoacetyl CoA and acetyl CoA via corresponding keto acid, alpha ketoisocaproate. Subsequent set of oxidative decarboxylation reactions converts alpha ketoisocaproate to isovaleryl CoA, dehydrogenated to betamethylcrotonyl CoA with FAD as hydrogen acceptor. ATP is utilised for the carboxylation of beta-methyl-crotonyl CoA in the presence of biotin as a cofactor for betamethylglutaconyl CoA formation. Hydration reaction of betamethylglutaconyl CoA leads to betahydroxy beta methylglutarylCoA on cleavage results in acetoacetate and acetyl CoA. However, it has been shown in *Leishmania* species that radiolabelled L-Leucine can be directly incorporated into sterol synthase, in contrast to other trypanosomatids or mammalian systems (Ginger et al., 2001).

This is in agreement with our data as there was no detection of this keto acid in the spent medium. Leucine is also shown as important regulator of gene expression by mTOR signalling controlling the rate of protein synthesis (Ginger et al., 1999). Protein production in the absence of L-Leucine has been further explored in Chapter 4 to determine its impact on protein synthesis.

Threonine is moderately utilised (Figure 6.13) during the entire 9 day growth period of *Leishmania* promastigotes. Threonine is very important for protein synthesis; however, it was much less consumed; possibly indicating residual biosynthetic capacity of the parasites. It has been shown that L-Threonine, L-Alanine and L-Proline constitute the major components of free amino acid pool in *Leishmania donovani* promastigotes (Simon et al., 1983) which may be the reason for moderate uptake of L-Threonine from the medium. The enzyme serine/L-Threonine dehydratase, responsible for removing the alpha amino group and the hydroxyl group of serine/L-Threonine to yield alpha keto glutarate and NH4+, is the major route followed by many eukaryotic organisms including mammals. The resulting alpha keto butyrate into succinyl CoA feeds into TCA cycle for energy contribution. In trypanosomatids, an alternative pathway involving serine hydroxyl methyl transferase (SHMT) has been discussed for the formation of glycine and serine, with tetrahydrofolate as an important coenzyme (Williams et al., 2009).

Slow degradation of L-Threonine within the intracellular pool might be another reason for moderate uptake of L-Threonine from the medium. The L-Threonine degradation pathway in *Leishmania* has been of considerable debate (Opperdoes and Coombs, 2007). Enzyme mining for putative L-Threonine pathway components was conducted as described in experimental procedures with a total of 74 different proteins annotated in the KEGG database for L-Threonine degradation pathways across different organisms. Bioinformatics analysis of individual enzymes between pairs of metabolites detected in the L-Threonine degradation leading to isoleucine biosynthesis has been detailed in the next chapter.

Valine is moderately consumed by *L. mexicana* promastigotes as shown in Figure 6.13. Valine is an important regulator for protein synthesis and gene transcription (Sriphochanart et al., 2011). Metabolic end products of L-Valine to its corresponding keto acid from conversion into 3 methyl 3 oxobutanoate to isobutanoyl CoA. The branched chain alpha keto acid dehydrogenase complex is the main linking enzyme for L-Valine utilisation as carbon source. The intermediate, beta hydroxyl acid, is oxidised to methylmalonate semialdehyde and propanoyl CoA (Opperdoes, 2008).

Glycine is enriched in the extracellular medium as the procyclic reach the metacylic infective forms compared to Day 0 to Day 6 spent medium as shown in Figure 6.14. It has been shown that glycine plays important cyto-protective and antioxidant properties (Zhong et al., 2003, Wang et al., 2013) in many organisms. It has been shown that glycine release in the extracellular system hampers reactive oxygen species in human neutrophils (Giambelluca and Gende, 2009). From our dataset, the nature of most small molecules secreted by promastigotes such as keto acids, ascorbate and even glycine have antioxidant properties that modify the extracellular environment. The chemical structure of the small molecules enriched in the extracellular medium has been further discussed as indicated from results of the biochemical assays.

Alanine is commonly produced as a result of proton exchange reactions with alpha keto glutarate, which is a substrate for transamination reactions as shown in Figure 6.14. It has been shown that L-Alanine transaminase in *Leishmania* exhibits narrow specificity compared to L-Alanine transaminases in *Tcruzi*, mammals, yeast and plant counterparts clustered within the same cladogram in the phylogenetic tree (Marciano et al., 2009). Alanine is enriched during stationary phases of growth compared to other amino acids. L-Alanine/L-Proline anti-transporter (Inbar et al., 2013) has been shown to play important role in cell swelling required for osomo-regulation in *Leishmania*. Glutamine and L-Asparagine were transiently utilised on Day 1, however, there is increased secretion into the extracellular medium at later stages of growth as shown in Figure 6.14. The amino acids utilisation from the medium are summarised as shown in Table 6-1.

Table 6-1 Classification of amino acids based on pattern of utilisation during growth of *L. mexicana* promastigotes

Continuously utilised	Partially utilised	Continuously secreted

L-Tryptophan	L-Leucine	L-Glycine
L-Aspartate	L-Threonine	L-Glutamine
L-Glutamate	L-Valine	L-Asparginine
L-Arginine	L-Phenylalanine	L-Proline
L-Methionine	L-Tyrosine	L-Alanine
L-Serine	L-Lysine	

Footnotes- L-Histidine, L-Cysteine and L-Isoleucine were not detected under conditions of exactive orbitrap mass spectrometer used in this study.

Glucose is consumed by more than 50%, as measured by the relative abundance of the medium alone without cells. Adenosine is completely depleted, suggesting it is growth limiting nutrient of the defined medium composition. Among the vitamins, not all of them were matched by authentic standards for mass and retention time. For example, biotin although present in standard list, was not seen in the mass spectrum data on cross verification. This could be because of multiple reasons such as small concentration below detection limit of the instrument, mass drift due to fragmentation, unstable complex and adducts not matching with retention time as explained elsewhere (Dunn et al., 2012). Remaining components such as salts, vitamins, co-factors and metals those below limits of detection, and without comparable standards.

6.3.3 Chemical structural analysis of secreted metabolites

Critical examination of the amino acid derived keto acids enriched in the spent medium showed that there is common “enone” moiety within their chemical structures (Figure 6.28). Chemically the double bond structure of the keto acids has the potential to undergo rapid conversion to enol structure in a reaction with high energy molecules such as reactive oxygen species or free radicals by accepting a proton (Cotoia et al., 2014). This led to the hypothesis that apart from amino acids contribution to protein synthesis and energy metabolism, parasites might have a particular use for amino acid-derived keto acids during infection.

This was further examined by various biochemical assays using THP1 host cells as infection model.

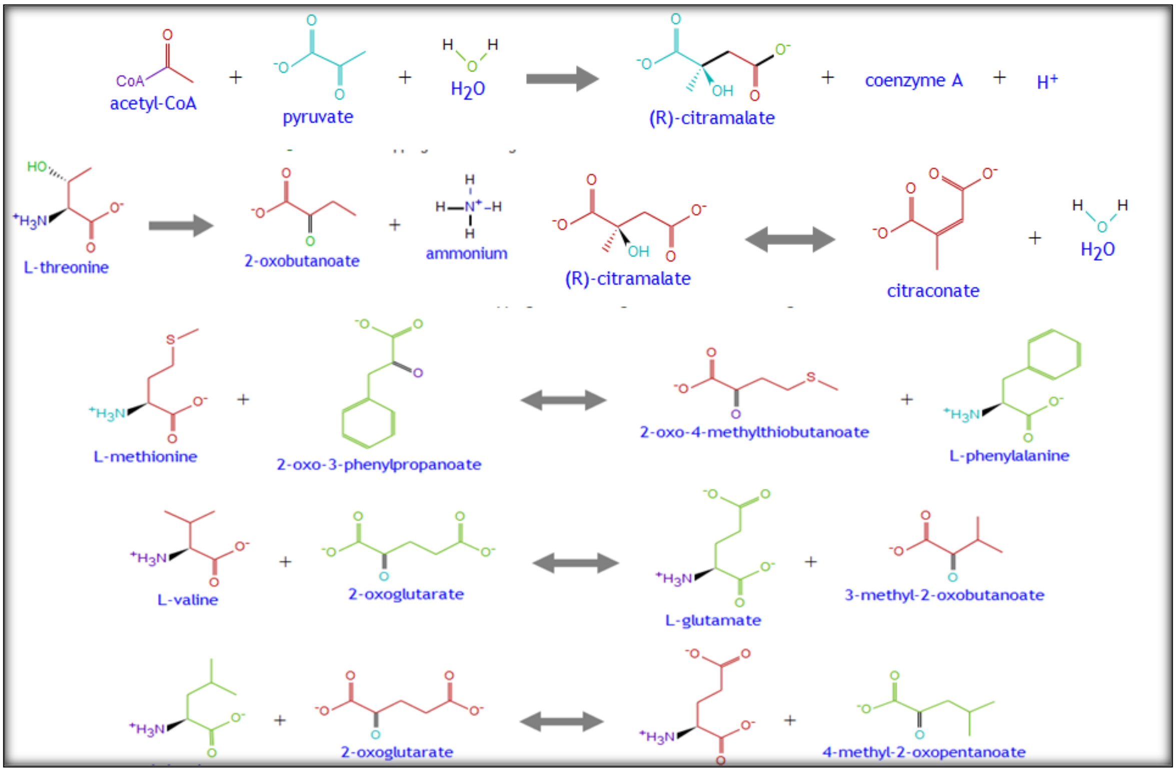

Figure 6.28 Structural representation of amino acid to keto acids production.

(All of the above mentioned show a common side chain with the keto moiety interchangeable with Enol form upon accepting a proton.)

It has been recently shown that keto acids have ROS scavenging action (Beloborodova et al., 2012). Especially, phenolic acids such as phenyl-lactate and p-hydroxy-phenyl-lactate decrease ROS production within mitochondria and neutrophils ofpatients affected with sepsis (Beloborodova et al., 2012). Keto acids such as p-hydroxy-phenyl-pyruvate have been shown as potential therapeutic agents; improving stress condition in haemorrhagic rats as a result of antioxidant activity towards mitochondria generated reactive oxygen species (Cotoia et al., 2014).

Interestingly, the data from this study highlights that the amount of keto acids secreted by *Leishmania* increases with time; especially leading to an accumulation at the infective metacylic stages. This led to further investigate about the role of the exo-metabolome in facilitation of parasitism with host cells. The chemical nature of small molecules were explored using biochemical assays as shown in section 6.2.8. Results indicate that exometabolome fraction of *L. mexicana* have nitrite scavenging activity. Previously, it was shown that secreted proteins alone accounted for 50% of nitrite scavenged versus 70% in infected macrophages (Hassani et al., 2011). The nature of small molecules secreted by *Leishmania* has not been thoroughly investigated before in this context. Hence, it was of interest to test pure compounds detected in the mass spectral data for nitrite scavenging activity to uncover pathophysiological role of these keto acids.

Presence of ascorbate enriched in the spent medium, strengthens the hypothesis that *L. mexicana* promastigotes secrete small molecules possibly for combating oxidative stress. Ascorbic acid was also putatively identified as enriched in the spent medium over time as shown in Figure 6.20. Ascorbic acid has been classified as enol lactone and known for its antioxidant property (Izumi et al., 1989). Ascorbate peroxidase is involved in the reaction of ascorbate quenching hydrogen peroxide (Pal et al., 2010). Literature points to the fact that ascorbate peroxidase characterised in *Leishmania major* is essential for maintenance of infectivity through regulation of oxidative stress (Dolai et al., 2008). It has been explained that ascorbic acid forms a complex with free nitrite to form complex nitroso-ascorbic acid and therefore reduces the free nitrite concentration in aqueous solution (Izumi et al., 1989).

Metabolites significantly enriched in spent medium; such as indole lactate and phenyl pyruvate have been tested for scavenging nitrite levels produced by the host system. The antioxidant activity of the aromatic pyruvates were determined by an assay of reducing power measurement. Briefly, this assay measures the property of the compounds to act as electron donor by potassium ferricyanide reduction. Here the $Fe^{3+/}$ferricyanide complex is reduced to ferrous form. Colour change from yellow to the blue and green range as shown in Figure 6.26 and Figure 6.27. Ascorbic acid is known for its antioxidant properties; thus used as positive control for the assay. Also, ascorbate has been putatively identified in the mass spectrometry data as a metabolite enriched in the spent medium, as shown in Figure 6.20. Ascorbic acid, acetate and aromatic pyruvates such as Indole lactate, phenyl pyruvate, 4 hydroxy phenyl pyruvate significantly enriched in the spent medium were tested in multiple orders of magnitude ranging from 1 µM-100 mM. It was observed that with increasing concentration of ascorbic acid and 4 hydroxy phenyl pyruvate; there was a corresponding increase in absorbance indicating greater reducing power of these metabolites compared to others tested at the same time

Among the compounds tested, indole lactate at more than 1mM concentration, there was sharp rise in the absorbance observed due to increased ferrous complex formation. Phenyl pyruvate showed sharp increase in absorbance between 0.1-1mM and then saturated at increasing concentration. These results indicate small molecules secreted by *L. mexicana* promastigotes could act as natural antioxidants similar to ascorbate action, possibly conferring protection during initial host infection stages. This is in agreement with studies showing that incubation of sandfly *Lutzomiya* sp. saliva alone has a significant effect on supporting infection of *Leishmania* to host cells (Menezes et al., 2008).

Parasites secreted several low molecular weight metabolites bearing an enone moiety, as observed from metabolomics spent medium analysis. In order to analyse their chemical nature over time, the phenolic content of spent medium was assessed. Aromatic compounds with hydroxyl groups react with phosphomolybdic acid in Folin-Ciocalteu reagent in an alkaline medium to produce a blue coloured complex (Lee et al., 2014). It has been reported elsewhere that increase in phenolic content is positively correlated with increase in the number of hydroxyl groups. Results from mass spectrometry data (Figure 6.16-Figure 6.20) highlight that the supernatant medium is enriched by low molecular weight compounds such as indole lactate, phenyl pyruvate, 4-hydroxy-phenyl-pyruvate. Enrichment of these compounds allow for increased hydroxyl groups available for scavenging free radicals by stimulated macrophages within the host system. Phenolic content increase in supernatant samples at various time points as specified from culture initiation, especially during the metacyclics stages with molecules that act as natural antioxidants.

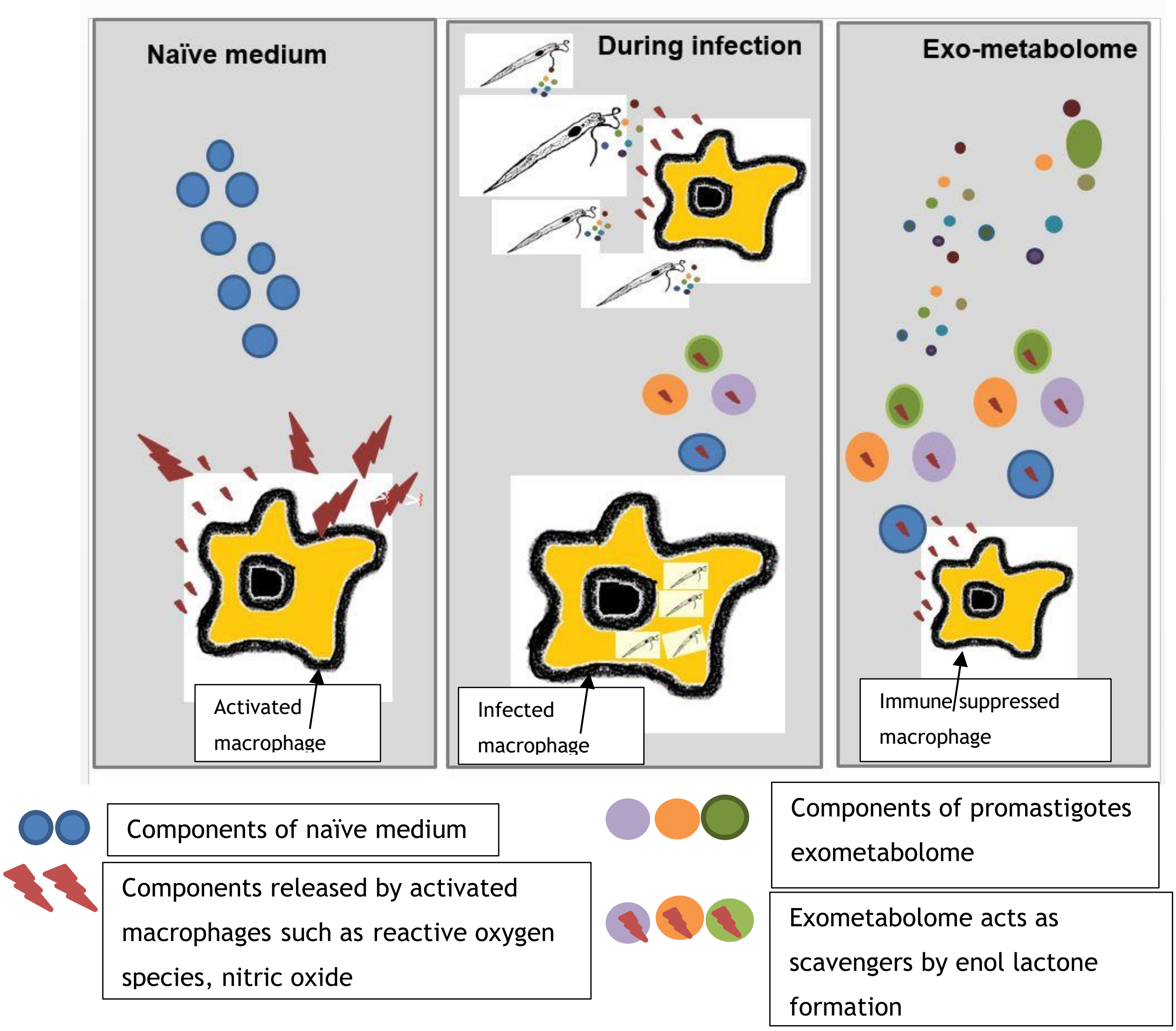

Figure 6.29 Pictorial summary to demonstrate unique role of exo-metabolome in scavenging reactions to defend against macrophage immune responses to support establishment of infection.

(Diagrammatic representation of exo-metabolome from *Leishmania* promastigotes able to scavenge reactive oxygen species, free radicals and supress nitric oxide production from activated macrophages potentially supporting establishment of infection with the host cells).

In summary, adaptable consumption of broad range of amino acids and simultaneous substrate (glucose and purines) utilisation in *L. mexicana* promastigotes is as shown in

Figure 6.29. Although amino acids contribute to the TCA cycle, our results show novel pathway of secretion of multiple keto acids enriched in the extracellular

medium. Keto acids with interchangeable to enone forms upon accepting protons have been tested for ability to scavenge nitrite, reactive oxygen species and free radicals as shown in Figure 6.22 to Figure 6.27. This might suggest pre-adaptive metabolic changes to modify immediate extracellular environment to support parasitism with host cells during macrophage infection.

Thus, during promastigote growth in defined media, amino acids are consumed at various rates. Aspartate and L-Glutamate are completely consumed as shown in Figure 6.12, indicating their consumption as carbon source with their corresponding keto acids enter the TCA cycle. Threonine is very important for protein synthesis; however, it was much less consumed; possibly indicating residual biosynthetic capacity of the parasites as shown in Figure 6.13. It is particularly interesting to note that L-Tryptophan and L-Arginine are amongst those amino acids that are completely scavenged (Figure 6.12) compared to other amino acids such as L-Phenylalanine, L-Leucine, L-Valine and L-Lysine (Figure 6.13) are much less consumed, albeit essential for the viability of the parasites as explained in earlier report. Despite their importance for growth and viability, concentrations of the corresponding keto acids are enriched in the spent medium (Figure 6.16, Figure 6.17, Figure 6.18, Figure 6.19, Figure 6.20). Enrichment of keto acids at the metacylic stages could modulate the host environment, since their chemical structure allows for conversion from keto to enol form. This characteristic of the enone moiety is responsible for scavenging free radicals and reactive oxygen species which may be encountered when the metacylic stages infect the host cells; thereby, favouring a reducing environment and potentially supporting viability of the promastigotes during early attachment and parasitism. These results are in agreement with recent studies by Moreno et al demonstrated that protein expression of L-Tyrosine transaminases were found to be increased in infective and nitric oxide resistant species compared to wild type forms. It has also been proved that L-Tyrosine transaminases have structural differences with no homology to human L-Tyrosine transaminases (Moreno et al; 2014b).

Thus, *Leishmania* aromatic acid transaminases have been proposed as potential as drug targets. Especially, inhibition of parasite specific L-Tryptophan and L-Phenylalanine metabolism using aromatic analogues as insecticides as novel strategy leading to disruption of *Leishmania* promastigotes development within sand-fly insects and combat the spread on this lethal disease. Targeting L-Tryptophan and L-Phenylalanine metabolism as preferential drug targets amongst the other amino acids utilised by *Leishmania* would also inhibit the enrichment of keto acids in the exometabolome, thereby preventing establishment of infection and strengthening the pro-inflammatory activities of the mammalian host system against parasite proliferation.

Chapter 7 Discussion

Leishmania promastigotes develop in the midgut of the sand-fly vector. Sand flies are known to feed on plant phloem, and derivatives of this such as aphid honeydew, rich in sugars and amino acids (Killickkendrick et al; 1990, Pimenta et al., 1992). During blood meal consumption by the sandfly, the transmission of parasites into the mammalian host causes a wide spectrum of clinical diseases associated with leishmaniasis. Increased incidence of leishmaniasis due to global warming, lack of vector control and emergence of resistance to current drugs have necessitated the discovery of novel drug targets (Tiuman et al., 2011, Murray et al., 2005). Perturbations in the nutrient transporters have been discussed as effective drug targets (Dean et al., 2014, Landfear, 2011).

Identification of transport repertoires and characterisation of individual proteins has been greatly facilitated by the availability of whole genome sequences (Ivens et al., 2005). Transporters involved in purines (LdNT1/LdNT2/ LdNT3/ LdNT4, LmaNT1/LmaNT2/LmaNT3/LmaNT4)(Carter et al., 2001, Ortiz et al., 2010), hexoses (LmxGT1, LmxGT2, LmxGT3), iron (LIT1), polyamines (LmaPOT1) and amino acids transportation (LdAAP3/*LdAAP7*/LdAAP24) (Shaked-Mishan et al., 2006, Inbar et al., 2012, Inbar et al., 2013) have been validated as drug targets based on essentiality for the viability of the parasite, functional expression under different environmental conditions and subcellular localisation studies (Landfear, 2011).

However, the nutritional environment encountered by the parasites would vary depending on the feeding frequencies and the diet of the host system. It has been reported that only small percentage of transporter proteins are well characterised compared to the broad range of substrates encountered by the parasites during its developmental cycle within the diverse systems (Dean et al., 2014). This indicates that the parasites must have an adaptive metabolism with activation of the compensatory metabolic pathways under adverse nutrient conditions, often less emphasised.

In this study, efforts have been made to decipher the utilisation of multiple nutrients by *Leishmania* promastigotes using growth and high throughput metabolomics in defined medium. The known medium composition, developed with a minimalistic approach, enabled mapping of multiple nutrient requirements in an unbiased manner.

Furthermore, special emphasis has been drawn to elucidate the importance of amino acids for viability, utilisation and metabolism unique to *L. mexicana* promastigotes. Better understanding about the nutrient requirements and metabolic differences of amino acid pathways within *L. mexicana* promastigotes from their mammalian hosts could accelerate the discovery of novel drug targets.

7.1Conclusions

The first aim addressed in my PhD research was to develop serum and protein free defined medium for *in vitro* culture of *L. mexicana* promastigotes, the insect stage of the parasites. This aim was achieved firstly by systematic literature search of previous *in vitro* medium compositions with individual concentrations collated and compared as shown in Chapter 3. From a minimalistic approach, the Steiger medium (Steiger and Black, 1980) developed for *L. donovani* was chosen as starting point for optimising the growth conditions for *L. mexicana* promastigotes with and without individual components of the medium as shown in Chapter 3. Extensive experiments were carried out to optimise concentrations, especially for zinc and iron which at increasing concentrations were found to have toxic effects on the viability of the parasites. Cofactors and metals tested at optimised concentrations ideal to support growth of *L. mexicana* promastigotes were included in the culture composition. Addition of cofactors such as folic acid, riboflavin, biopterin, lipoic Acid, biotin together metal salts of magnesium, calcium, zinc, iron, manganese and cobalt decreased the lag phase with improved doubling time and growth of *L. mexicana* promastigotes in Nayak medium as shown in Chapter 3 supporting growth in this defined media for continuous passages.

The second aim of my PhD research project was to elucidate the requirements of amino acids in their order of importance for viability, growth and development of parasites using various biochemical assays. It is known that amino acids are classified as essential and non-essential amino acids primarily based on the requirements of mammalian species (Reeds, 2000). Earliest study of amino acids essentiality in parasitic protozoa was reported on studies in lizard parasite *L. tertentole* (Krassner and Flory, 1971) adapted in other protozoa. In this study human infecting *L. mexicana* promastigotes were cultured in single amino acid knock out media and found that exogenous source of L-Tryptophan, L-Phenylalanine, L-Lysine, L-Arginine, L-Leucine and L-Valine as most critical for the viability of parasites as shown in Chapter 4 under identical conditions of starting inoculum, temperature and pH.

The amino acids were also evaluated as relative contribution to growth doubling time, protein synthesis and energy quantification determined by acetate overflow. Owing to *Leishmania* unique acetate succinate CoA transferase (ACST) enzyme, amino acids contributution to acetate production was also evaluated. Acetate overflow is an indirect measure of energy generation in the form of ATP, as a bypass of the extensive oxidative phosphorylation for majority of energy generation not found in mammalian systems. Based on these results for *L. mexicana* promastigotes as shown in Chapter 4, exogenous supply of L-Aspartate, L-Glutamate, L-Glutamine and L-serine significantly promoted growth and exogenous supply of L-Threonine, L-Histidine, L-Methionine and L-Isoleucine were found to increase total intracellular protein content; compared to its absence.

The third aim of my PhD study was to identify *Leishmania* specific amino acid pathways which could serve as potential drug targets. In this study, efforts have been made to highlight amino acids utilisation by unbiased metabolic mapping of amino acid metabolites by network mapping at structural, empirical and functional levels. Unlike mammals which follow an elaborate amino acid degradation pathway, results as shown in Chapter 5 indicate that amino acid utilisation in promastigotes follows a simpler degradation pathway involving a transamination and decarboxylation step. Examination of these individual reactions show that these pathways involved in high energy intermediates such as NADH production. It has been shown in fungal systems that a simpler amino acid degradation as an efficient pathway for NADH regeneration compared to glucose metabolism (Hazelwood et al., 2008). This indicates that amino acids salvaged from the environment has a different metabolic route in parasite to mammals with non-homologous enzymes that could potentially serve as better drug targets. Untargeted metabolomics data was also employed to build novel biosynthetic amino acid pathways which requires further validation. However, one of the main highlights of this study is to show compensatory metabolic processes that might be adapted by the parasite to support its own viability during changing nutritional dynamics of the host system. Understanding these complex biochemical compensatory processes becomes imperative for validation of drug targets.

Furthermore, untargeted metabolomics of the culture supernatant across multiple time points as shown in Chapter 6 allowed for classification of amino acids with L-Tryptophan, L-Aspartate, L-Glutamate, L-Arginine, L-Methionine and L-Serine as continuously utilised amino acids; L-Leucine, L-Threonine, L-Valine, L-Phenylalanine, L-Tyrosine and L-Lysine as partially utilised amino acids and L-Glycine, L-Glutamine, L-Aspargine, L-Proline and L-Alanine as continuously secreted amino acids as observed based on their depletion profile of the exo-metabolome data throughout the growth cycle of *L. mexicana* promastigotes in defined medium. Also, the exometabolome of *L. mexicana* promastigotes showed enrichment of amino acid derived alpha keto acids secreted into the extracellular system. These results highlight the ability of keto acids, especially the aromatic pyruvates to chemically interchange to enol lactones; which are known to scavenge reactive oxygen species, nitric oxide suppression released by activated macrophages as shown in Chapter 6. Hence, unravelling a novel role of amino acids utilisation in supporting early steps of infection and thereby, establishment of parasitism with host cells.

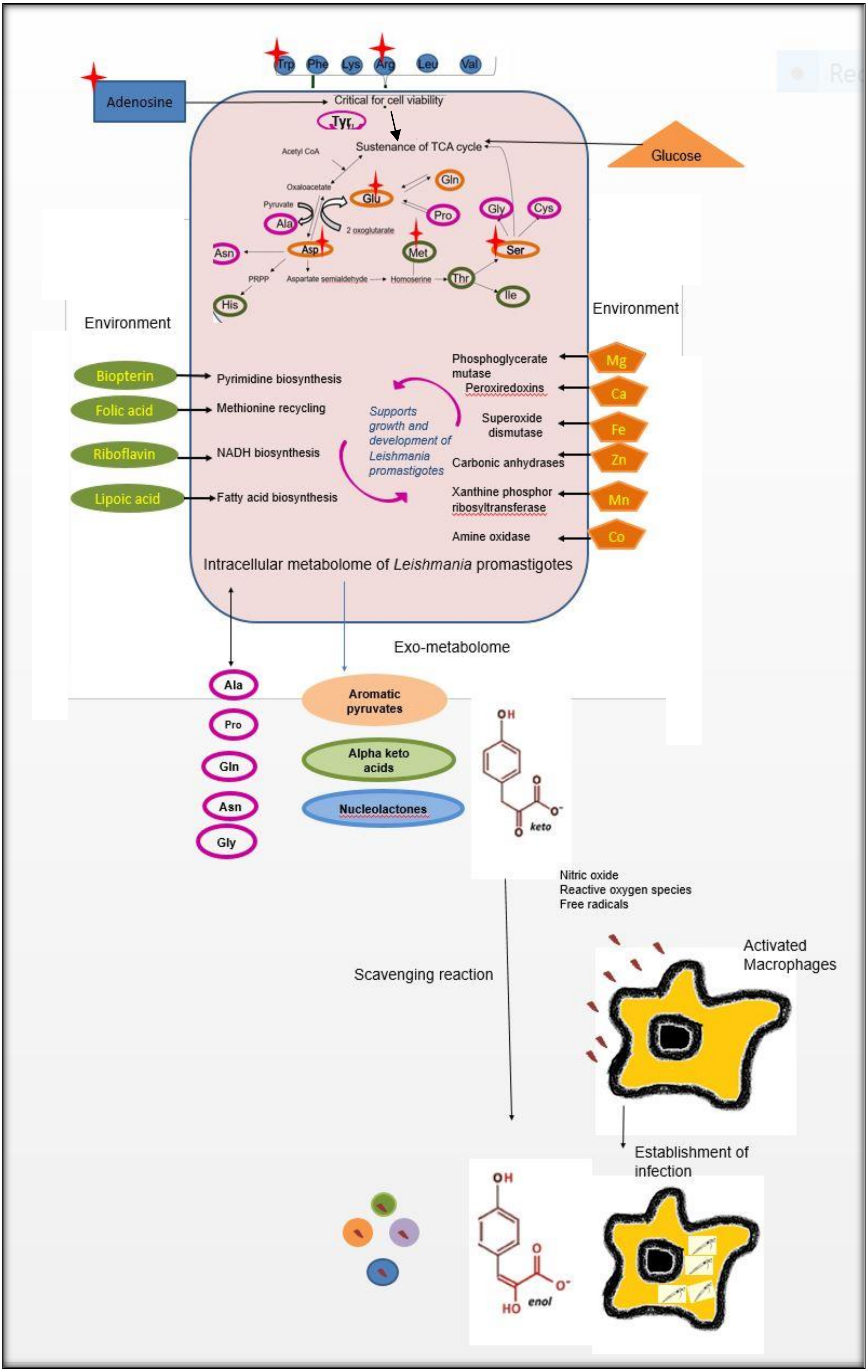

Trp
Phe
Lys
Arg
Leu
Val
Adenosine
Critical for cell viability
Tyr
Sustenance of TCA cycle
Glucose
Acetyl CoA
Oxaloacetate
Pyruvate
Ala
Glu
Gln
Pro
2 oxoglutarate
Gly
Cys
Asn
Asp
Met
Ser
PRPP
Aspartate semialdehyde
Homoserine
Thr
Ile
His
Environment
Environment
Biopterin
Pyrimidine biosynthesis
Folic acid
Methionine recycling
Riboflavin
NADH biosynthesis
Lipoic acid
Fatty acid biosynthesis
Supports growth and development of Leishmania promastigotes
Phosphoglycerate mutase
Mg
Peroxiredoxins
Ca
Superoxide dismutase
Fe
Carbonic anhydrases
Zn
Xanthine phosphor ribosyltransferase
Mn
Amine oxidase
Co
Intracellular metabolome of Leishmania promastigotes
Exo-metabolome
Ala
Pro
Gln
Asn
Gly
Aromatic pyruvates
Alpha keto acids
Nucleolactones
OH
keto
Nitric oxide
Reactive oxygen species
Free radicals
Scavenging reaction
Activated Macrophages
Establishment of infection
OH
HO
enol

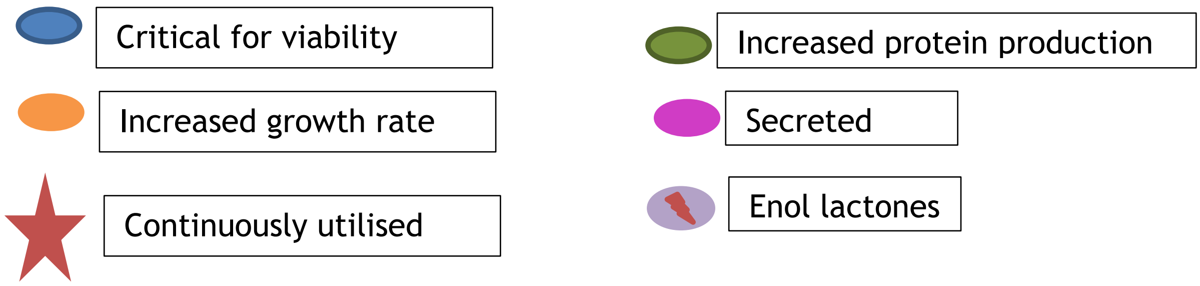

Figure 7.1 Pictorial summary to demonstrate amino acid utilisation in the order of importance for viability, growth and development of *Leishmania* promastigotes supporting establishment of infection with macrophage host cells.

(All amino acids specified using their three letter abbreviation with exogenous supply of amino acids critical for viability are shown in blue circles, (Trp, Phe, Lys, Arg, Leu and Val) Orange circles denotes those required for increased growth rate (Asp, Glu, Gln, Ser) Green circles denotes those required for increased protein production (Thr, Met, His, Ile) Pink circles denotes those secreted (Ala, Pro, Gly, Asn) and Red stars denotes those continuously utilised throughout the growth period from procyclics to metacyclics).

The main findings from this study summarised as follows:

- In chapter 3, progressive steps followed for the development and establishment of defined medium of *L. mexicana* promastigotes has been elaborated. Chemically defined medium for *in vitro* culture allows extensive scientific investigations in controlled environment, especially for antigen isolation for vaccine development, metabolomics, drug therapies and design of novel experimental protocols.
- Elucidation of the nutritional requirements of the parasite by growth analysis in media with and without each individual component in chapter 3 highlights the essentiality of specific co factors and metal ions with data on concentration dependent effect on proliferation. Inhibitors of specific co factors (Biopterin) and metal transport (magnesium and calcium) have been shown as detrimental for the viability of the parasite. Hence, these data could serve useful for vector control strategies especially for sandfly breeding infected areas.
- In Chapter 4, comparative utilisation amongst the 20 proteogenic amino acids on the viability and growth of *L. mexicana* promastigotes has been

reported. For the first time, individual amino acids have been analysed to determine their order of importance by growth analysis. These results of the growth analysis from the single amino acid knockout media were validated by protein and energy quantification; in turn paved way for new type of classification of amino acids based on utilisation.

- Metabolic network mapping using intracellular metabolomics data showed a unique amino acid metabolism pattern in *L. mexicana* promastigotes with a two-step process undergoing transamination and unusual decarboxylation step leading to generation of high energy intermediates such as NADH shown schematically in Chapter 5. Using bioinformatics analysis, the enzyme commission number (EC number) compared between mammalian and parasite species indicated that the enzymes responsible for decarboxylation step are unique parasite specific enzymes that could potentially serve as drug targets.
- In Chapter 6, time resolved metabolic foot-printing of defined medium throughout the growth cycle of *L. mexicana* promastigotes provided novel information about nutrients utilised from the extracellular medium without interference from serum molecules. From this data, it was possible to categorically name amino acids as continuously utilised, partially utilised or continuously secreted based on their nature of depletion during growth of the parasites in the medium.
- Further investigation of the exo-metabolome in Chapter 6 showed that most small molecules secreted by the promastigotes derived from amino acids were metabolic end products with common chemical structure that belonged to the class of enol lactones. Using pure compounds as control samples, experiments were carried out to investigate whether the exo-metabolome played a role during infection with host cells. Results confirm that small molecules of the exo metabolome, especially the aromatic pyruvates have ROS scavenging and reducing activity, leading to anti-inflammatory environment. Thus, indicating a novel role of amino acid utilisation by *Leishmania* in establishment of infection with host cells and to support parasitism.

7.2 Future directions

This study highlights that aromatic amino acids L-Tryptophan and L-Phenylalanine have been found as most important amongst other amino acids for the viability, growth and establishment of parasitism in *L. mexicana* promastigotes by evading host immune responses and supporting infection within host cells. Future work is required with targeted molecular biology approaches to characterise the transport of these aromatic amino acids. Inhibitors for enzymes involved in unique decarboxylation step during indole pyruvate and phenylpyruvate formation in *Leishmania* is proposed as suitable for drugs as it is different from mammals. For example, selected amino acids analogues, especially of L-Tryptophan and L-Phenylalanine tagged with nanoparticles could be useful for targeted studies within insect vectors to investigate their effectiveness against parasite growth (Mitchison and Wilcox 1973, Tiuman et al., 2011).

Also, quantitative data on infection biomarkers and validation of the exploratory biomarker profile gained from the implementation of complementary metabolomics platforms could have tremendous implications for disease diagnosis (Saiki et al, 2013). In particular, amino acids profiling in defined medium could serve as gold standard platform for species comparison, strain identifications, mutant isolation studies, diagnostic tests and others. The knowledge gained from the metabolomics data in this study could also cater for improved predictions from stoichiometric models and genome scale reconstruction (Putri et al., 2013). It would be interesting to understand whether dose dependent inhibition of *Leishmania* exometabolome impacts host gene expression and regulation of niche environment required for the acceleration of infection within the host system as shown in bacterial systems by Beloborodova et al, 2012.

In summary, the results from this study demonstrate the advantages of defined media to gain new insights on nutrients utilisation in *L. mexicana* promastigotes. Growth analysis of individual nutrients under different conditions; with and without individual components was used for the development and establishment of defined minimal medium for *in vitro* culture of *L. mexicana* promastigotes. Cofactors and metal ions were found to exhibit positive growth effect only under optimal concentrations. From single omission of amino acid media, it was demonstrated that six critical amino acids as the most important exogenous sources amongst other amino acids required for the viability of the parasites. It was fascinating that the intracellular data showed putative metabolites that have been shown to build novel biosynthetic pathways which requires further validation as proof for compensatory activation during parasitic adaptation to diverse host nutrient systems.

Thus, these results not only demonstrated the potential of intracellular metabolomics in the study of *L. mexicana* promastigotes but also the changes in time resolved metabolic foot-printing of defined medium, elucidating the constituents of the exometabolome useful for various purposes discussed above. New insights have been gained about the unique amino acid utilisation for the production of exometabolome; enriched in enol lactones that could cater for the establishment of parasitism within host cells. Finally, although the promastigotes life stage of the parasites precedes the clinically significant stage of infection in mammalian cells, the knowledge from this study facilitates designing better chemotherapy and novel drug targets within parasite specific amino acid metabolic pathways which is often less emphasised.

List of References

Akpunarlieva, S., Weidt, S., Lamasudin, D., Naula, C., Henderson, D., Barrett, M., Burgess, K. & Burchmore, R. 2017. Integration of proteomics and metabolomics to elucidate metabolic adaptation in Leishmania. *Journal of Proteomics,* 155, 85-98.

Akhoundi, M., Kuhls, K., Cannet, A., Votypka, J., Marty, P., Delaunay, P. & Sereno, D. 2016. A Historical Overview of the Classification, Evolution, and Dispersion of Leishmania Parasites and Sandflies. *Plos Neglected Tropical Diseases,* 10.

Alexander, J. & Vickerman, K. 1975. Fusion of host-cell secondary lysosomes with parasitophorous vacuoles of *Leishmania mexicana* infected macrophages. *Journal of Protozoology,* 22, 502-508.

Ali, S. A., Iqbal, J., Ahmad, B. & Masoom, M. 1998. A semisynthetic fetal calf serum-free liquid medium for in vitro cultivation of Leishmania promastigotes. *American Journal of Tropical Medicine and Hygiene,* 59, 163-165.

Allen, J., Davey, H. M., Broadhurst, D., Heald, J. K., Rowland, J. J., Oliver, S. G. & Kell, D. B. 2003. High-throughput classification of yeast mutants for functional genomics using metabolic foot-printing. *Nature Biotechnology,* 21, 692-696.

Ameen, M. 2010. Cutaneous leishmaniasis: advances in disease pathogenesis, diagnostics and therapeutics. *Clinical and Experimental Dermatology,* 35, 699-705.

Andreini, C., Bertini, I., Cavallaro, G., Holliday, G. L. & Thornton, J. M. 2008. Metal ions in biological catalysis: from enzyme databases to general principles. *Journal of Biological Inorganic Chemistry,* 13, 1205-1218.

Armstrong, T. C. & Patterson, J. L. 1994. Cultivation of *Leishmania-braziliensis* in an economical serum-free medium containing human urine. *Journal of Parasitology,* 80, 1030-1032.

Attar, Z. J., Chance, M. L., El-Safi, S., Carney, J., Azazy, A., El-Hadi, M., Dourado, C. & Hommel, M. 2001. Latex agglutination test for the detection of urinary antigens in visceral leishmaniasis. *Acta Tropica,* 78, 11-16.

Aurich, M. K., Paglia, G., Rolfsson, O., Hrafnsdottir, S., Magnusdottir, M., Stefaniak, M. M., Palsson, B. O., Fleming, R. M. T. & Thiele, I. 2015. Prediction of intracellular metabolic states from extracellular metabolomic data. *Metabolomics,* 11, 603-619.

Baltz, T., Baltz, D., Giroud, C. & Crockett, J. 1985. Cultivation in a semi-defined medium of animal infective forms of *Trypanosoma-brucei, Trypanosoma-equiperdum, Trypanosoma-evansi, Trypanosoma-rhodesiense and T-gambiense. Embo Journal,* 4, 1273-1277.

Barrett, M. P. 1997. The pentose phosphate pathway and parasitic protozoa. *Parasitology Today,* 13.

Basselin, M., Denise, H., Coombs, G. H. & Barrett, M. P. 2002. Resistance to pentamidine in Leishmania mexicana involves exclusion of the drug from the mitochondrion. *Antimicrobial Agents and Chemotherapy,* 46, 3731-3738.

Basu, S. S. & Blair, I. A. 2012. SILEC: a protocol for generating and using isotopically labeled coenzyme A mass spectrometry standards. *Nature Protocols,* 7, 1-11.

Bates, P. A. 1994. Complete developmental cycle of *Leishmania-mexicana* in axenic culture. *Parasitology,* 108, 1-9.

Bates, P. A. & Tetley, L. 1993. *Leishmania-mexicana* - induction of metacyclogenesis by cultivation of promastigotes at acidic ph. *Experimental Parasitology,* 76, 412-423.

Beach, D. H., Holz, G. G. & Anekwe, G. E. 1979. LIPIDS OF LEISHMANIA PROMASTIGOTES. *Journal of Parasitology,* 65, 203-216.

Beck, J. T. & Ullman, B. 1990. Nutritional-requirements of wild-type and folate transport-deficient *Leishmania-donovani* for pterins and folates. *Molecular and Biochemical Parasitology,* 43, 221-230.

Behrends, V., Ebbels, T. M. D., Williams, H. D. & Bundy, J. G. 2009. Time-Resolved Metabolic Foot-printing for Nonlinear Modeling of Bacterial Substrate Utilization. *Applied and Environmental Microbiology,* 75, 2453-2463.

Beloborodova, N., Bairamov, I., Olenin, A., Shubina, V., Teplova, V. & Fedotcheva, N. 2012. Effect of phenolic acids of microbial origin on production of reactive oxygen species in mitochondria and neutrophils. *Journal of Biomedical Science,* 19.

Berens, R. L., Brun, R. & Krassner, S. M. 1976. Simple Monophasic Medium for Axenic Culture of Hemoflagellates. *Journal of Parasitology,* 62, 360-365.

Berg, K., Zhai, L., Chen, M., Kharazmi, A. & Owen, T. C. 1994. The use of a water-soluble formazan complex to quantitate the cell number and mitochondrial-function of *Leishmania-major* promastigotes. *Parasitology Research,* 80, 235-239.

Berger, B. J., Dai, W. W., Wang, H., Stark, R. E. & Cerami, A. 1996. Aromatic amino acid transamination and L-Methionine recycling in trypanosomatids. *Proceedings of the National Academy of Sciences of the United States of America,* 93, 4126-4130.

Berger, B. J., Dai, W. W. & Wilson, J. 1998. Methionine formation from alpha-ketomethiobuyrate in the trypanosomatid Crithidia fasciculata. *Fems Microbiology Letters,* 165, 305-312.

Berriman, M., Ghedin, E., Hertz-Fowler, C., Blandin, G., Renauld, H., Bartholomeu, D. C., Lennard, N. J., Caler, E., Hamlin, N. E., Haas, B., Bohme, W., Hannick, L., Aslett, M. A., Shallom, J., Marcello, L., Hou, L. H., Wickstead, B., Alsmark, U. C. M., Arrowsmith, C., Atkin, R. J., Barron, A. J., Bringaud, F., Brooks, K., Carrington, M., Cherevach, I., Chillingworth, T. J., Churcher, C., Clark, L. N., Corton, C. H., Cronin, A., Davies, R. M., Doggett, J., Djikeng, A., Feldblyum, T., Field, M. C., Fraser, A., Goodhead, I., Hance, Z., Harper, D., Harris, B. R., Hauser, H., Hostetter, J., Ivens, A., Jagels, K., Johnson, D., Johnson, J., Jones, K., Kerhornou, A. X., Koo, H., Larke, N., Landfear, S., Larkin, C., Leech, V., Line, A., Lord, A., Macleod, A., Mooney, P. J., Moule, S., Martin, D. M. A., Morgan, G. W., Mungall, K., Norbertczak, H., Ormond, D., Pai, G., Peacock, C. S., Peterson, J., Quail, M. A., Rabbinowitsch, E., Rajandream, M. A., Reitter, C., Salzberg, S. L., Sanders, M., Schobel, S., Sharp, S., Simmonds, M., Simpson, A. J., Talton, L., Turner, C. M. R., Tait, A., Tivey, A. R., Van Aken, S., Walker, D., Wanless, D., Wang, S. L., White, B., White, O., Whitehead, S., Woodward, J., Wortman, J., Adams, M. D., Embley, T. M., Gull, K., Ullu, E., Barry, J. D., Fairlamb, A. H., Opperdoes, F., Barret, B. G., Donelson, J. E., Hall, N., Fraser, C. M., et al. 2005. The genome of the African trypanosome Trypanosoma brucei. *Science,* 309, 416-422.

Beverley, S. M., Ellenberger, T. E. & Cordingley, J. S. 1986. PRIMARY STRUCTURE OF THE GENE ENCODING THE BIFUNCTIONAL DIHYDROFOLATE REDUCTASE-THYMIDYLATE SYNTHASE OF LEISHMANIA-MAJOR. *Proceedings of the National Academy of Sciences of the United States of America,* 83, 2584-2588.

Biegel, D., Topper, G. & Rabinovitch, M. 1983. LEISHMANIA-MEXICANA - TEMPERATURE SENSITIVITY OF ISOLATED AMASTIGOTES AND OF AMASTIGOTES INFECTING MACROPHAGES IN CULTURE. *Experimental Parasitology,* 56, 289-297.

Blum, J. J. 1996. Effects of osmotic stress on metabolism, shape, and amino acid content of Leishmania. *Biology of the Cell,* 87, 9-16.

Boitz, J. M., Yates, P. A., Kline, C., Gaur, U., Wilson, M. E., Ullman, B. & Roberts, S. C. 2009. Leishmania donovani Ornithine Decarboxylase Is Indispensable for Parasite Survival in the Mammalian Host. *Infection and Immunity,* 77, 756-763.

Boutry, C., Bos, C. & Tome, D. 2008. Amino acid requirements. *Nutrition Clinique Et Metabolisme,* 22, 151-160.

Bringaud, F., Barrett, M. P. & Zilberstein, D. 2012. Multiple roles of L-Proline transport and metabolism in trypanosomatids. *Frontiers in Bioscience-Landmark,* 17, 349-374.

Burchmore, R. J. S. & Barrett, M. P. 2001. Life in vacuoles - nutrient acquisition by Leishmania amastigotes. *International Journal for Parasitology,* 31, 1311-1320.

Burchmore, R. J. S. & Hart, D. T. 1995. Glucose transport in amastigotes and promastigotes of Leishmania mexicana mexicana. *Molecular and Biochemical Parasitology,* 74, 77-86.

Burchmore, R. J. S., Rodriguez-Contreras, D., Mcbride, K., Barrett, M. P., Modi, G., Sacks, D. & Landfear, S. M. 2003. Genetic characterization of glucose transporter function in Leishmania mexicana. *Proceedings of the National Academy of Sciences of the United States of America,* 100, 3901-3906.

Cairns, B. R., Collard, M. W. & Landfear, S. M. 1989. DEVELOPMENTALLY REGULATED GENE FROM LEISHMANIA ENCODES A PUTATIVE MEMBRANE-TRANSPORT PROTEIN - (PARASITIC PROTOZOAN GENE-EXPRESSION GLUCOSE TRANSPORTER). *Proceedings of the National Academy of Sciences of the United States of America,* 86, 7682-7686.

Capacci, M. L. L., Bernardini, A. P., Silva, A. T., Raia, S. & Faintuch, J. 1984. CIRRHOTIC-LIKE PROFILE OF PLASMA AMINOGRAM IN SYMPTOM-FREE CASES OF LIVER SCHISTOSOMIASIS. *Journal of Parenteral and Enteral Nutrition,* 8, 99-99.

Carter, N. S., Landfear, S. M. & Ullman, B. 2001. Nucleoside transporters of parasitic protozoa. *Trends in Parasitology,* 17, 142-145.

Castro, H. & Tomas, A. M. 2008. Peroxidases of trypanosomatids. *Antioxidants & Redox Signaling,* 10, 1593-1606.

Chang, K. P. & Hendricks, L. D. 1985. *Laboratory cultivation and maintenance of Leishmania.*

Chang, P. C. H. 1956. THE ULTRASTRUCTURE OF LEISHMANIA-DONOV ANI. *Journal of Parasitology,* 42, 126-136.

Chavali, A. K., Whittemore, J. D., Eddy, J. A., Williams, K. T. & Papin, J. A. 2008. Systems analysis of metabolism in the pathogenic trypanosomatid Leishmania major. *Molecular Systems Biology,* 4.

Chokkathukalam, A., Jankevics, A., Creek, D. J., Achcar, F., Barrett, M. P. & Breitling, R. 2013. mzMatch-ISO: an R tool for the annotation and relative quantification of isotope-labelled mass spectrometry data. *Bioinformatics,* 29, 281-283.

Colotti, G. & Ilari, A. 2011. Polyamine metabolism in Leishmania: from L-Arginine to trypanothione. *Amino Acids,* 40, 269-285.

Coombs, G. H., Craft, J. A. & Hart, D. T. 1982. A COMPARATIVE-STUDY OF LEISHMANIA-MEXICANA AMASTIGOTES AND PROMASTIGOTES - ENZYME-ACTIVITIES AND SUB-CELLULAR LOCATIONS. *Molecular and Biochemical Parasitology,* 5, 199-211.

Cotoia, A., Scrima, R., Gefter, J. V., Piccoli, C., Cinnella, G., Dambrosio, M., Fink, M. P. & Capitanio, N. 2014. p-Hydroxyphenylpyruvate, an Intermediate of the Phe/Tyr Catabolism, Improves Mitochondrial Oxidative Metabolism under Stressing Conditions and Prolongs Survival in Rats Subjected to Profound Hemorrhagic Shock. *Plos One,* 9.

Crabtree, M. J., Tatham, A. L., Hale, A. B., Alp, N. J. & Channon, K. M. 2009. Critical Role for Tetrahydrobiopterin Recycling by Dihydrofolate Reductase in Regulation of Endothelial Nitric-oxide Synthase Coupling RELATIVE IMPORTANCE OF THE DENOVO BIOPTERIN SYNTHESIS VERSUS SALVAGE PATHWAYS. *Journal of Biological Chemistry,* 284, 28128-28136.

Creek, D. J., Anderson, J., Mcconville, M. J. & Barrett, M. P. 2012a. Metabolomic analysis of trypanosomatid protozoa. *Molecular and Biochemical Parasitology,* 181.

Creek, D. J. & Barrett, M. P. 2014. Determination of antiprotozoal drug mechanisms by metabolomics approaches. *Parasitology,* 141, 83-92.

Creek, D. J., Jankevics, A., Burgess, K. E. V., Breitling, R. & Barrett, M. P. 2012b. IDEOM: an Excel interface for analysis of LC-MS-based metabolomics data. *Bioinformatics,* 28.

Creek, D. J., Nijagal, B., Kim, D. H., Rojas, F., Matthews, K. R. & Barrett, M. P. 2013. Metabolomics Guides Rational Development of a Simplified Cell Culture Medium for Drug Screening against Trypanosoma brucei. *Antimicrobial Agents and Chemotherapy,* 57, 2768-2779.

Croft, S. L. & Coombs, G. H. 2003. Leishmaniasis - current chemotherapy and recent advances in the search for novel drugs. *Trends in Parasitology,* 19, 502-508.

Cronin, C. N., Nolan, D. P. & Voorheis, H. P. 1989. THE ENZYMES OF THE CLASSICAL PENTOSE-PHOSPHATE PATHWAY DISPLAY DIFFERENTIAL ACTIVITIES IN PROCYCLIC AND BLOOD-STREAM FORMS OF TRYPANOSOMA-BRUCEI. *Febs Letters,* 244, 26-30.

Cross, G. A. M., Klein, R. A. & Baker, J. R. 1975. TRYPANOSOMA-CRUZI - GROWTH, AMINO-ACID UTILIZATION AND DRUG ACTION IN A DEFINED MEDIUM. *Annals of Tropical Medicine and Parasitology,* 69, 513-514.

Cross, G. A. M. & Manning, J. C. 1973. CULTIVATION OF TRYPANOSOMA-BRUCEI SSP IN SEMI-DEFINED AND DEFINED MEDIA. *Parasitology,* 67, 315-331.

Cuperlovic-Culf, M., Barnett, D. A., Culf, A. S. & Chute, I. 2010. Cell culture metabolomics: applications and future directions. *Drug Discovery Today,* 15, 610-621.

Cui, J. J., Liu, Y. T., Hu, Y. H., Tong, J. Y., Li, A. P., Qu, T. L., Qin, X. M. & Du, G. H. 2017. NMR-based metabonomics and correlation analysis reveal potential biomarkers associated with chronic atrophic gastritis. *Journal of Pharmaceutical and Biomedical Analysis,* 132, 77-86.

Darlyuk, I., Goldman, A., Roberts, S. C., Ullman, B., Rentsch, D. & Zilberstein, D. 2009. L-Arginine Homeostasis and Transport in the Human Pathogen Leishmania donovani. *Journal of Biological Chemistry,* 284, 19800-19807.

De Souza, D. P., Saunders, E. C., Mcconville, M. J. & Likic, V. A. 2006. Progressive peak clustering in GC-MS Metabolomic experiments applied to Leishmania parasites. *Bioinformatics,* 22, 1391-6.

Dean, P., Major, P., Nakjang, S., Hirt, R. P. & Embley, T. M. 2014. Transport proteins of parasitic protists and their role in nutrient salvage. *Frontiers in Plant Science,* 5.

Delauney, A. J., Hu, C. A. A., Kishor, P. B. K. & Verma, D. P. S. 1993. Cloning of ornithine delta-aminotransferase cdna from vigna-aconitifolia by transcomplementation in *Escherichia-coli* and regulation of L-Proline biosynthesis. *Journal of Biological Chemistry,* 268, 18673-18678.

Dien, J., Spencer, K. M. & Donchin, E. 2003. Localization of the event-related potential novelty response as defined by principal components analysis. *Brain research. Cognitive brain research,* 17, 637-50.

Dogra, N., Warburton, C. & Mcmaster, W. R. 2007. Leishmania major abrogates gamma interferon-induced gene expression in human macrophages from a global perspective. *Infection and Immunity,* 75, 3506-3515.

Dolai, S., Yadav, R. K., Pal, S. & Adak, S. 2008. Leishmania major ascorbate peroxidase overexpression protects cells against reactive oxygen species-mediated cardiolipin oxidation. *Free Radical Biology and Medicine,* 45, 1520-1529.

Dostalova, A. & Volf, P. 2012. Leishmania development in sand flies: parasite-vector interactions overview. *Parasites & Vectors,* 5.

Drazic, A. & Winter, J. 2014. The physiological role of reversible L-Methionine oxidation. *Biochimica Et Biophysica Acta-Proteins and Proteomics,* 1844, 1367-1382.

Druker, B. J., Talpaz, M., Resta, D. J., Peng, B., Buchdunger, E., Ford, J. M., Lydon, N. B., Kantarjian, H., Capdeville, R., Ohno-Jones, S. & Sawyers, C. L. 2001. Efficacy and safety of a specific inhibitor of the BCR-ABL L-Tyrosine kinase in chronic myeloid leukemia. *New England Journal of Medicine,* 344, 1031-1037.

Dujardin, J. C., Campino, L., Canavate, C., Dedet, J. P., Gradoni, L., Soteriadou, K., Mazeris, A., Ozbel, Y. & Boelaert, M. 2008. Spread of vector-borne diseases and neglect of leishmaniasis, Europe. *Emerging Infectious Diseases,* 14, 1013-1018.

Dunn, W. B., Wilson, I. D., Nicholls, A. W. & Broadhurst, D. 2012. The importance of experimental design and QC samples in large-scale and MS-driven untargeted metabolomic studies of humans. *Bioanalysis,* 4, 2249-2264.

Dutta, S., Ray, D., Kolli, B. K. & Chang, K. P. 2005. Photodynamic sensitization of Leishmania amazonensis in both extracellular and intracellular stages with aluminum phthalocyanine chloride for photolysis in vitro. *Antimicrobial Agents and Chemotherapy,* 49, 4474-4484.

Fiehn, O. 2002. Metabolomics - the link between genotypes and phenotypes. *Plant Molecular Biology,* 48, 155-171.

Flavin, M. & Slaughte.C 1967. ENZYMATIC SYNTHESIS OF HOMOCYSTEINE OR METHIONINE DIRECTLY FROM O-SUCCINYL-HOMOSERINE. *Biochimica Et Biophysica Acta,* 132, 400-&.

Franco, A. M. R. & Grimaldi, G. 1999. Characterization of Endotrypanum (Kinetoplastida : Trypanosomatidae), a unique parasite infecting the neotropical tree sloths (Edentata). *Memorias Do Instituto Oswaldo Cruz,* 94, 261-268.

Fuad, F. A. A., Fothergill-Gilmore, L. A., Nowicki, M. W., Eades, L. J., Morgan, H. P., Mcnae, I. W., Michels, P. A. M. & Walkinshaw, M. D. 2011. Phosphoglycerate mutase from *Trypanosoma brucei* is hyperactivated by cobalt in vitro, but not in vivo. *Metallomics,* 3, 1310-1317.

Funayama, S., Ito, I. Y. & Veiga, L. A. 1977. TRYPANOSOMA-CRUZI - KINETIC-PROPERTIES OF GLUCOSE-6-PHOSPHATE-DEHYDROGENASE. *Experimental Parasitology,* 43, 376-381.

Geraldo, M. V., Silber, A. M., Pereira, C. A. & Uliana, S. R. B. 2005. Characterisation of a developmentally regulated amino acid transporter gene from Leishmania amazonensis. *Fems Microbiology Letters,* 242, 275-280.

Giambelluca, M. S. & Gende, O. A. 2009. Effect of glycine on the release of reactive oxygen species in human neutrophils. *International Immunopharmacology,* 9, 32-37.

Gillespie, P. M., Beaumier, C. M., Strych, U., Hayward, T., Hotez, P. J. & Bottazzi, M. E. 2016. Status of vaccine research and development of vaccines for leishmaniasis. *Vaccine,* 34, 2992-2995.

Ginger, M. L., Chance, M. L. & Goad, L. J. 1999. Elucidation of carbon sources used for the biosynthesis of fatty acids and sterols in the trypanosomatid *Leishmania mexicana. Biochemical Journal,* 342, 397-405.

Ginger, M. L., Chance, M. L., Sadler, I. H. & Goad, L. J. 2001. The biosynthetic incorporation of the intact L-Leucine skeleton into sterol by the trypanosomatid *Leishmania mexicana. Journal of Biological Chemistry,* 276, 11674-11682.

Glaser, T. A. & Mukkada, A. J. 1992. PROLINE TRANSPORT IN LEISHMANIA-DONOVANI AMASTIGOTES - DEPENDENCE ON PH GRADIENTS AND MEMBRANE-POTENTIAL. *Molecular and Biochemical Parasitology,* 51, 1-8.

Goldman-Pinkovich, A., Darlyuk, I., Rentsch, D. & Zilberstein, D. 2011. L-Arginine transport in the human pathogen Leishmania and its possible role in parasite-host interactions. *Amino Acids,* 41, S21-S21.

Gossage, S. A., Rogers, M. E. & Bates, P. A. 2003. Two separate growth phases during the development of Leishmania in sand flies: implications for understanding the life cycle. *International Journal for Parasitology,* 33, 1027-1034.

Hall, J. E., Seed, J. R. & Sechelski, J. B. 1985. MULTIPLE ALPHA-KETO ACIDURIA IN MICROTUS-MONTANUS CHRONICALLY INFECTED WITH TRYPANOSOMA-BRUCEI-GAMBIENSE. *Comparative Biochemistry and Physiology B-Biochemistry & Molecular Biology,* 82, 73-78.

Hanada, K. 2004. Serine palmitoyltransferase, a key enzyme of sphingolipid metabolism (vol 1632, pg 16, 2003). *Biochimica Et Biophysica Acta-Molecular and Cell Biology of Lipids,* 1682, 128-128.

Handman, E. 2001. Leishmaniasis: Current status of vaccine development. *Clinical Microbiology Reviews,* 14, 229-+.

Hart, D. T. & Coombs, G. H. 1982. *Leishmania-mexicana* - energy-metabolism of amastigotes and promastigotes. *Experimental Parasitology,* 54, 397-409.

Hasne, M. P. & Barrett, M. P. 2000. Transport of L-Methionine in Trypanosoma brucei brucei. *Molecular and Biochemical Parasitology,* 111, 299-307.

Hassani, K., Antoniak, E., Jardim, A. & Olivier, M. 2011. Temperature-Induced Protein Secretion by Leishmania mexicana Modulates Macrophage Signalling and Function. *Plos One,* 6.

Hazelwood, L. A., Daran, J. M., Van Maris, A. J. A., Pronk, J. T. & Dickinson, J. R. 2008. The ehrlich pathway for fusel alcohol production: a century of research on Saccharomyces cerevisiae metabolism. *Applied and Environmental Microbiology,* 74, 2259-2266.

Hellemond, J. J. V., Bakker, B. M. & Tielens, A. G. M. 2005. Energy metabolism and its compartmentation in Trypanosoma brucei. *Advances in microbial physiology,* 50.

Henriques, C., Moreira, T. L. B., Maia-Brigagao, C., Henriques-Pons, A., Carvalho, T. M. U. & De Souza, W. 2011. Tetrazolium salt based methods for high-throughput evaluation of anti-parasite chemotherapy. *Analytical Methods,* 3, 2148-2155.

Hisamatsu, T., Okamoto, S., Hashimoto, M., Muramatsu, T., Andou, A., Uo, M., Kitazume, M. T., Matsuoka, K., Yajima, T., Inoue, N., Kanai, T., Ogata, H., Iwao, Y., Yamakado, M., Sakai, R., Ono, N., Ando, T., Suzuki, M. & Hibi, T. 2012. Novel, Objective, Multivariate Biomarkers Composed of Plasma Amino Acid Profiles for the Diagnosis and Assessment of Inflammatory Bowel Disease. *Plos One,* 7.

Hu, C. A. A., Delauney, A. J. & Verma, D. P. S. 1992. A BIFUNCTIONAL ENZYME (DELTA-1-PYRROLINE-5-CARBOXYLATE SYNTHETASE) CATALYZES THE 1ST 2 STEPS IN PROLINE BIOSYNTHESIS IN PLANTS. *Proceedings of the National Academy of Sciences of the United States of America,* 89, 9354-9358.

Hulse, J. D., Ellis, S. R. & Henderson, L. M. 1978. CARNITINE BIOSYNTHESIS - BETA-HYDROXYLATION OF TRIMETHYLLYSINE BY AN ALPHA-KETOGLUTARATE DEPENDENT MITOCHONDRIAL DIOXYGENASE. *Journal of Biological Chemistry,* 253, 1654-1659.

Inbar, E., Canepa, G. E., Carrillo, C., Glaser, F., Grotemeyer, M. S., Rentsch, D., Zilberstein, D. & Pereira, C. A. 2012. Lysine transporters in human trypanosomatid pathogens. *Amino Acids,* 42, 347-360.

Inbar, E., Schlisselberg, D., Grotemeyer, M. S., Rentsch, D. & Zilberstein, D. 2013. A versatile L-Proline/L-Alanine transporter in the unicellular pathogen Leishmania donovani regulates amino acid homoeostasis and osmotic stress responses. *Biochemical Journal,* 449, 555-566.

Ivens, A. C., Peacock, C. S., Worthey, E. A., Murphy, L., Aggarwal, G., Berriman, M., Sisk, E., Rajandream, M. A., Adlem, E., Aert, R., Anupama, A., Apostolou, Z., Attipoe, P., Bason, N., Bauser, C., Beck, A., Beverley, S. M., Bianchettin, G., Borzym, K., Bothe, G., Bruschi, C. V., Collins, M., Cadag, E., Ciarloni, L., Clayton, C., Coulson, R. M. R., Cronin, A., Cruz, A. K., Davies, R. M., De Gaudenzi, J., Dobson, D. E., Duesterhoeft, A., Fazelina, G., Fosker, N., Frasch, A. C., Fraser, A., Fuchs, M., Gabel, C., Goble, A., Goffeau, A., Harris, D., Hertz-Fowler, C., Hilbert, H., Horn, D., Huang, Y. T., Klages, S., Knights, A., Kube, M., Larke, N., Litvin, L., Lord, A., Louie, T., Marra, M., Masuy, D., Matthews, K., Michaeli, S., Mottram, J. C., Muller-Auer, S., Munden, H., Nelson, S., Norbertczak, H., Oliver, K., O'neil, S., Pentony, M., Pohl, T. M., Price, C., Purnelle, B., Quail, M. A., Rabbinowitsch, E., Reinhardt, R., Rieger, M., Rinta, J., Robben, J., Robertson, L., Ruiz, J. C., Rutter, S., Saunders, D., Schafer, M., Schein, J., Schwartz, D. C., Seeger, K., Seyler, A., Sharp, S., Shin, H., Sivam, D., Squares, R., Squares, S., Tosato, V., Vogt, C., Volckaert, G., Wambutt, R., Warren, T., Wedler, H., Woodward, J., Zhou, S. G., Zimmermann, W., Smith, D. F., Blackwell, J. M., Stuart, K. D., Barrell, B., et al. 2005. The genome of the kinetoplastid parasite, Leishmania major. *Science,* 309, 436-442.

Izumi, K., Cassens, R. G. & Greaser, M. L. 1989. Reaction of nitrite with ascorbic-acid and its significant role in nitrite-cured food. *Meat Science,* 26, 141-153.

Johnson, H. E., Broadhurst, D., Goodacre, R. & Smith, A. R. 2003. Metabolic finger-printing of salt-stressed tomatoes. *Phytochemistry,* 62**,** 919-928.

Kamhawi, S. 2006. Phlebotomine sand flies and Leishmania parasites: friends or foes? *Trends in Parasitology,* 22**,** 439-445.

Kamleh, A., Barrett, M. P., Wildridge, D., Burchmore, R. J. S., Scheltema, R. A. & Watson, D. G. 2008. Metabolomic profiling using Orbitrap Fourier transform mass spectrometry with hydrophilic interaction chromatography: a method with wide applicability to analysis of biomolecules. *Rapid Communications in Mass Spectrometry,* 22.

Kandpal, M., Tekwani, B. L., Chauhan, P. M. S. & Bhaduri, A. P. 1996. Correlation between inhibition of growth and L-Arginine transport of Leishmania donovani promastigotes in vitro by diamidines. *Life Sciences,* 59**,** 75-80.

Kar, K. 1997. Folic acid the essential supplement to brain heart infusion broth for cultivation and cloning of Leishmania donovani promastigotes. *Parasitology,* 115**,** 231-235.

Karimpour, M., Surowiec, I., Wu, J., Gouveia-Figueira, S., Pinto, R., Trygg, J., Zivkovic, A. M. & Nording, M. L. 2016. Postprandial metabolomics: A pilot mass spectrometry and NMR study of the human plasma metabolome in response to a challenge meal. *Analytica Chimica Acta,* 908**,** 121-131.

Kaur, K., Coons, T., Emmett, K. & Ullman, B. 1988. Methotrexate-resistant *Leishmania-donovani* genetically deficient in the folate-methotrexate transporter. *Journal of Biological Chemistry,* 263**,** 7020-7028.

Kaye, P. & Scott, P. 2011. Leishmaniasis: complexity at the host-pathogen interface. *Nature Reviews Microbiology,* 9**,** 604-615.

Kell, D. B., Brown, M., Davey, H. M., Dunn, W. B., Spasic, I. & Oliver, S. G. 2005. Metabolic foot-printing and systems biology: The medium is the message. *Nature Reviews Microbiology,* 3**,** 557-565.

Killickkendrick, R. 1990. Phlebotomine vectors of the leishmaniases - a review. *Medical and Veterinary Entomology,* 4**,** 1-24.

Klein, C. C., Alves, J. M. P., Serrano, M. G., Buck, G. A., Vasconcelos, A. T. R., Sagot, M. F., Teixeira, M. M. G., Camargo, E. P. & Motta, M. C. M. 2013. Biosynthesis of Vitamins and Cofactors in Bacterium-Harbouring Trypanosomatids Depends on the Symbiotic Association as Revealed by Genomic Analyses. *Plos One,* 8.

Koutmos, M., Datta, S., Pattridge, K. A., Smith, J. L. & Matthews, R. G. 2009. Insights into the reactivation of cobalamin-dependent L-Methionine synthase. *Proceedings of the National Academy of Sciences of the United States of America,* 106**,** 18527-18532.

Krassner, S. M. & Flory, B. 1971. Essential amino acids in culture of *Leishmania-tarentolae. Journal of Parasitology,* 57**,** 917-&.

Kumar, P., Kumar, A., Verma, S. S., Dwivedi, N., Singh, N., Siddiqi, M. I., Tripathi, R. P. & Dube, A. 2008. Leishmania donovani pteridine reductase 1: Biochemical properties and structure-mode ling studies. *Experimental Parasitology,* 120, 73-79.

Lafon, S. W., Nelson, D. J., Berens, R. L. & Marr, J. J. 1982. PURINE AND PYRIMIDINE SALVAGE PATHWAYS IN LEISHMANIA-DONOVANI. *Biochemical Pharmacology,* 31, 231-238.

Lainson, R., Shaw, J. J. & Silveira, F. T. 1987. DERMAL AND VISCERAL LEISHMANIASIS AND THEIR CAUSATIVE AGENTS. *Transactions of the Royal Society of Tropical Medicine and Hygiene,* 81, 702-703.

Landfear, S. M. 2011. Nutrient Transport and Pathogenesis in Selected Parasitic Protozoa. *Eukaryotic Cell,* 10, 483-493.

Leader, D. P., Burgess, K., Creek, D. & Barrett, M. P. 2011. Pathos: A web facility that uses metabolic maps to display experimental changes in metabolites identified by mass spectrometry. *Rapid Communications in Mass Spectrometry,* 25, 3422-3426.

Leblancq, S. M. & Lanham, S. M. 1984. Aspartate-aminotransferase in leishmania is a broad-spectrum transaminase. *Transactions of the Royal Society of Tropical Medicine and Hygiene,* 78, 373-375.

Lee, D. R., Lee, S. K., Choi, B. K., Cheng, J. H., Lee, Y. S., Yang, S. H. & Suh, J. W. 2014. Antioxidant activity and free radical scavenging activities of Streptomyces sp strain MJM 10778. *Asian Pacific Journal of Tropical Medicine,* 7, 962-967.

Leelayoova, S., Marbury, D., Rainey, P. M., Mackenzie, N. E. & Hall, J. E. 1992. INVITRO L-TRYPTOPHAN CATABOLISM BY LEISHMANIA-DONOVANI-DONOVANI PROMASTIGOTES. *Journal of Protozoology,* 39, 350-358.

Leslie, G., Barrett, M. & Burchmore, R. 2002. Leishmania mexicana: promastigotes migrate through osmotic gradients. *Experimental Parasitology,* 102, 117-120.

Levinthal, M., Williams, L. S., Levintha.M & Umbarger, H. E. 1973. ROLE OF THREONINE DEAMINASE IN REGULATION OF ISOLEUCINE AND VALINE BIOSYNTHESIS. *Nature-New Biology,* 246, 65-68.

Lima, C. V. D., Batista, M., Kugeratski, F. G., Vincent, I. M., Soares, M. J., Probst, C. M., Krieger, M. A. & Marchini, F. K. 2014. LM14 defined medium enables continuous growth of Trypanosoma cruzi. *Bmc Microbiology,* 14.

Limoncu, M. E., Balcioglu, I. C., Yereli, K., Ozbel, Y. & Ozbilgin, A. 1997. A new experimental in vitro culture medium for cultivation of Leishmania species. *Journal of Clinical Microbiology,* 35, 2430-2431.

Lye, L. F., Kang, S. O., Nosanchuk, J. D., Casadevall, A. & Beverley, S. M. 2011. Phenylalanine hydroxylase (PAH) from the lower eukaryote Leishmania major. *Molecular and Biochemical Parasitology,* 175, 58-67.

Marciano, D., Maugeri, D. A., Cazzulo, J. J. & Nowicki, C. 2009. Functional characterization of stage-specific aminotransferases from trypanosomatids. *Molecular and Biochemical Parasitology,* 166, 172-182.

Marini, J. C., Didelija, I. C., Castillo, L. & Lee, B. 2010. Glutamine: precursor or nitrogen donor for citrulline synthesis? *American Journal of Physiology-Endocrinology and Metabolism,* 299, E69-E79.

Marr, J. J., Berens, R. L. & Nelson, D. J. 1978. PURINE METABOLISM IN LEISHMANIA-DONOVANI AND LEISHMANIA-BRAZILIENSIS. *Biochimica Et Biophysica Acta,* 544, 360-371.

Mashego, M. R., Rumbold, K., De Mey, M., Vandamme, E., Soetaert, W. & Heijnen, J. J. 2007. Microbial metabolomics: past, present and future methodologies. *Biotechnology Letters,* 29, 1-16.

Maugeri, D. A., Cazzulo, J. J., Burchmore, R. J. S., Barrett, M. P. & Ogbunude, P. O. J. 2003. Pentose phosphate metabolism in Leishmania mexicana. *Molecular and Biochemical Parasitology,* 130, 117-125.

Mackenzie, N. E., Hall, J. E., Flynn, I. W. & Scott, A. I. 1983. C-13 nuclear magnetic-resonance studies of anaerobic glycolysis in *Trypanosoma-brucei* spp. *Bioscience Reports,* 3, 141-151.

Mcconville, M. J. & Naderer, T. 2011. Metabolic Pathways Required for the Intracellular Survival of Leishmania. *Annual Review of Microbiology, Vol 65,* 65, 543-561.

Mccoy, R. H., Meyer, C. E. & Rose, W. C. 1935. Feeding experiments with mixtures of highly purified amino acids - VIII. Isolation and identification of a new essential amino acid. *Journal of Biological Chemistry,* 112, 283-302.

Meade, J. C., Glaser, T. A., Bonventre, P. F. & Mukkada, A. J. 1984. ENZYMES OF CARBOHYDRATE-METABOLISM IN LEISHMANIA-DONOVANI AMASTIGOTES. *Journal of Protozoology,* 31, 156-161.

Melo, N. M., Deazevedo, H. P., Roitman, I. & Mayrink, W. 1985. A new defined medium for cultivating *Leishmania* promastigotes. *Acta Tropica,* 42, 137-141.

Menezes, M. J., Costa, D. J., Clarencio, J., Miranda, J. C., Barral, A., Barral, M., Brodskyn, C. & De Oliveira, C. I. 2008. Immunomodulation of human monocytes following exposure to Lutzomyia intermedia saliva. *Bmc Immunology,* 9.

Merlen, T., Sereno, D., Brajon, N., Rostand, F. & Lemesre, J. L. 1999. Leishmania spp.: Completely defined medium without serum and macromolecules (CDM/LP) for the continuous in vitro cultivation of infective promastigote forms. *American Journal of Tropical Medicine and Hygiene,* 60, 41-50.

Michels, P. A. M., Hannaert, V. & Bringaud, F. 2000. Metabolic aspects of glycosomes in trypanosomatidae - New data and views. *Parasitology Today,* 16, 482-489.

Millward, D. J. & Rivers, J. P. W. 1988. THE NUTRITIONAL ROLE OF INDISPENSABLE AMINO-ACIDS AND THE METABOLIC BASIS FOR THEIR REQUIREMENTS. *European Journal of Clinical Nutrition,* 42, 367-393.

Monge-Maillo, B. & Lopez-Velez, R. 2013. Therapeutic Options for Old World Cutaneous Leishmaniasis and New World Cutaneous and Mucocutaneous Leishmaniasis. *Drugs,* 73, 1889-1920.

Montemartini, M., Santome, J. A., Cazzulo, J. J. & Nowicki, C. 1994. Production of aromatic alpha-hydroxyacids by epimastigotes of *Trypanosoma-cruzi,* and its possible role in nadh reoxidation. *Fems Microbiology Letters,* 118, 89-92.

Momen, H. & Cupolillo, E. 2000. Speculations on the origin and evolution of the genus Leishmania. *Memorias Do Instituto Oswaldo Cruz,* 95, 583-588.

Moore, G. E., Gerner, R. E. & Franklin, H. A. 1967. Culture of normal human leukocytes. *Journal of the American Medical Association,* 199, 519-&.

Moreno, M. A., Abramov, A., Abendroth, J., Alonso, A., Zhang, S., Alcolea, P. J., Edwards, T., Lorimer, D., Myler, P. J. & Larraga, V. 2014a. Structure of L-Tyrosine aminotransferase from Leishmania infantum. *Acta Crystallographica Section F-Structural Biology Communications,* 70, 583-587.

Moreno, M. A., Alonso, A., Alcolea, P. J., Abramov, A., De Lacoba, M. G., Abendroth, J., Zhang, S., Edwards, T., Lorimer, D., Myler, P. J. & Larraga, V. 2014b. Tyrosine aminotransferase from Leishmania infantum: A new drug target candidate. *International Journal for Parasitology-Drugs and Drug Resistance,* 4, 347-354.

Mukkada, A. J. 1985. Macromolecular-synthesis in leishmania-donovani amastigotes. *Journal of Parasitology,* 71, 365-366.

Murray, H. W., Berman, J. D., Davies, C. R. & Saravia, N. G. 2005. Advances in leishmaniasis. *Lancet,* 366, 1561-1577.

Naderer, T., Ellis, M. A., Sernee, M. F., De Souza, D. P., Curtis, J., Handman, E. & Mcconville, M. J. 2006. Virulence of Leishmania major in macrophages and mice requires the gluconeogenic enzyme fructose-1,6-bisphosphatase. *Proceedings of the National Academy of Sciences of the United States of America,* 103, 5502-5507.

Naula, C. M., Logan, F. M., Wong, P. E., Barrett, M. P. & Burchmore, R. J. 2010. A Glucose Transporter Can Mediate Ribose Uptake DEFINITION OF RESIDUES THAT CONFER SUBSTRATE SPECIFICITY IN A SUGAR TRANSPORTER. *Journal of Biological Chemistry,* 285, 29721-29728.

Nicolle, C. 1908. Culture of the parasite of cutaneous leishmaniasis. *Comptes Rendus Hebdomadaires Des Seances De L Academie Des Sciences,* 146, 842-843.

Noguchi, Y., Zhang, Q. W., Sugimoto, T., Furuhata, Y., Sakai, Y., Mori, M., Takahashi, M. & Kimura, T. 2006. Network analysis of plasma and tissue amino acids and the generation of an amino index for potential diagnostic use. *American Journal of Clinical Nutrition,* 83, 513S-519S.

Novy, F. G. & Mac Neal, W. J. 1904. On the cultivation of Trypanosoma brucei. *Journal of Infectious Diseases,* 1, 1-30.

Oliver, S. G., Winson, M. K., Kell, D. B. & Baganz, F. 1998. Systematic functional analysis of the yeast genome. *Trends in Biotechnology,* 16, 373-378.

Ong, H. B., Lee, W. S., Patterson, S., Wyllie, S. & Fairlamb, A. H. 2015. Homoserine and quorum-sensing acyl homoserine lactones as alternative sources of L-Threonine: a potential role for homoserine kinase in insect-stage Trypanosoma brucei. *Molecular Microbiology,* 95, 143-156.

Opperdoes, F. R. & Coombs, G. H. 2007. Metabolism of Leishmania: proven and predicted. *Trends in Parasitology,* 23, 149-158.

Ortiz, D., Valdes, R., Sanchez, M. A., Hayenga, J., Elya, C., Detke, S. & Landfear, S. M. 2010. Purine restriction induces pronounced translational upregulation of the NT1 adenosine/pyrimidine nucleoside transporter in Leishmania major. *Molecular Microbiology,* 78, 108-118.

Ouellette, M., Drummelsmith, J., El Fadili, A., Kundig, C., Richard, D. & Roy, G. 2002. Pterin transport and metabolism in Leishmania and related trypanosomatid parasites. *International Journal for Parasitology,* 32, 385-398.

Paes, L. S., Rojas, R. L. G., Daliry, A., Floeter-Winter, L. M., Ramirez, M. I. & Silber, A. M. 2008. Active Transport of Glutamate in Leishmania (Leishmania) amazonensis. *Journal of Eukaryotic Microbiology,* 55, 382-387.

Pal, S., Dolai, S., Yadav, R. K. & Adak, S. 2010. Ascorbate Peroxidase from Leishmania major Controls the Virulence of Infective Stage of Promastigotes by Regulating Oxidative Stress. *Plos One,* 5.

Palmer, K. L., Aye, L. A. & Whiteley, M. 2007. Nutritional cues control Pseudomonas aeruginosa multicellular Behavior in cystic fibrosis sputum. *Journal of Bacteriology,* 189, 8079-8087.

Papadopoulou, B., Roy, G., Breton, M., Kundig, C., Dumas, C., Fillion, I., Singh, A. K., Olivier, M. & Ouellette, M. 2002. Reduced infectivity of a Leishmania donovani biopterin transporter genetic mutant and its use as an attenuated strain for vaccination. *Infection and Immunity,* 70, 62-68.

Paselk, R. A. 1983. PRINCIPLES OF BIOCHEMISTRY - LEHNINGER,AL. *Journal of Chemical Education,* 60, A201-A202.

Payne, S. H. & Loomis, W. F. 2006. Retention and loss of amino acid biosynthetic pathways based on analysis of whole-genome sequences. *Eukaryotic Cell,* 5, 272-276.

Pfaller, M. A. & Marr, J. J. 1974. ANTILEISHMANIAL EFFECT OF ALLOPURINOL. *Antimicrobial Agents and Chemotherapy,* 5, 469-472.

Pimenta, P. F. P., Turco, S. J., Mcconville, M. J., Lawyer, P. G., Perkins, P. V. & Sacks, D. L. 1992. STAGE-SPECIFIC ADHESION OF LEISHMANIA PROMASTIGOTES TO THE SANDFLY MIDGUT. *Science,* 256, 1812-1815.

Piper, R., Lebras, J., Wentworth, L., Hunt-Cooke, A., Houze, S., Chiodini, P. & Makler, M. 1999. Immunocapture diagnostic assays for malaria using Plasmodium lactate dehydrogenase (pLDH). *American Journal of Tropical Medicine and Hygiene,* 60, 109-118.

Podinovskaia, M., Lee, W., Caldwell, S. & Russell, D. G. 2013. Infection of macrophages with Mycobacterium tuberculosis induces global modifications to phagosomal function. *Cellular Microbiology,* 15, 843-859.

Prasuna, M. L., Mujahid, M., Sasikala, C. & Ramana, C. V. 2012. L-Phenylalanine catabolism and L-phenyllactic acid production by a phototrophic bacterium, Rubrivivax benzoatilyticus JA2. *Microbiological Research,* 167, 526-531.

Putri, S. P., Nakayama, Y., Matsuda, F., Uchikata, T., Kobayashi, S., Matsubara, A. & Fukusaki, E. 2013. Current metabolomics: Practical applications. *Journal of Bioscience and Bioengineering,* 115, 579-589.

Rainey, P. M. & Mackenzie, N. E. 1991. A C-13 NUCLEAR-MAGNETIC-RESONANCE ANALYSIS OF THE PRODUCTS OF GLUCOSE-METABOLISM IN LEISHMANIA-PIFANOI AMASTIGOTES AND PROMASTIGOTES. *Molecular and Biochemical Parasitology,* 45, 307-316.

Rakotomanga, M., Blanc, S., Gaudin, K., Chaminade, P. & Loiseau, P. A. 2007. Miltefosine afects lipid metabolism in Leishmania donovani promastigotes. *Antimicrobial Agents and Chemotherapy,* 51, 1425-1430.

Ralton, J. E., Naderer, T., Piraino, H. L., Bashtannyk, T. A., Callaghan, J. M. & Mcconville, M. J. 2003. Evidence that intracellular beta 1-2 mannan is a virulence factor in Leishmania parasites. *Journal of Biological Chemistry,* 278, 40757-40763.

Raz, B., Iten, M., Gretherbuhler, Y., Kaminsky, R. & Brun, R. 1997. The Alamar Blue(R) assay to determine drug sensitivity of African trypanosomes (T-b-rhodesiense and T-b-gambiense) in vitro. *Acta Tropica,* 68, 139-147.

Reeds, P. J. 2000. Dispensable and indispensable amino acids for humans. *Journal of Nutrition,* 130, 1835S-1840S.

Rees, J. D., Ingle, R. A. & Smith, J. A. C. 2009. Relative contributions of nine genes in the pathway of L-Histidine biosynthesis to the control of free L-Histidine concentrations in Arabidopsis thaliana. *Plant Biotechnology Journal,* 7, 499-511.

Richmond, M. H. 1962. EFFECT OF AMINO ACID ANALOGUES ON GROWTH AND PROTEIN SYNTHESIS IN MICROORGANISMS. *Bacteriological Reviews,* 26, 398-&.

Romao, P. R. T., Fonseca, S. G., Hothersall, J. S., Noronha-Dutra, A. A., Ferreira, S. H. & Cunha, F. Q. 1999. Glutathione protects macrophages and Leishmania major against nitric oxide-mediated cytotoxicity. *Parasitology,* 118, 559-566.

Ross, R. 1903. Further notes on Leishmans bodies. *British Medical Journal,* 1903, 1401-1401.

Rowe, P. B. & Lewis, G. P. 1973. MAMMALIAN FOLATE METABOLISM - REGULATION OF FOLATE INTERCONVERSION ENZYMES. *Biochemistry,* 12, 1962-1969.

Ramirez JR, Adugelo S, Muskus C (2000) Diagnosis of cutaneous leishmaniasis in Colombia: the sampling site within lesions influences the sensititivity of parasitological diagnosis. J Clin Microbiol 38: 3768-3773.

Blum J, Desjeux P, Schwartz E, Beck B, Hazt C (2004) Treatament of cutaneous leishmaniasis among travellers. J Antimicrob Chemother 53: 158-166.

Attar ZJ, Chance ML, el-Safi S, Carney J, Azazy A, El-Hadi M, Dourado C, Hommel M (2001) Latex agglutination test for the detection of urinary antigens in visceral leishmaniasis. Acta Trop 78: 11-16.

Malaei S, Mohebali M, Akhoundi B, Zarei Z (2006) Evaluation of latex agglutination test (Katex) for the detection of urinary antigens in human visceral leishmaniasis. J Tehran Un Med Sci 4: 101-108.

Diro E, Techane Y, Tefera T (2007) Field evaluation of FD-DAT rK39 dipstick and KATEX (urine latex agglutination)

Vilaplana C, Blanco S, Domínguez J, Giménez M, Ausina V, Tural C, Muñoz C (2004) Noninvasive method for diagnosis of visceral leishmaniasis by a latex agglutination test for detection of antigens in urine samples. J Clin Microbiol 42: 1853-1854.

Boelaert M, Rijal S, Regmi S, Singh R, Karki B, Jacquet D, Chappuis F, Campino L, Desjeux P, Le Ray D, Koirala S, Van der Stuyft P (2004) A comparative study of the effectiveness of diagnostic tests for visceral leishmaniasis. Am J Trop Med Hyg 70: 72-77. 42.

Iqbal J, Hira PR, Saroj G, Philip R, Al-Ali F, Madda PJ, Sher A (2002) Imported visceral leishmaniasis: diagnostic dilemmas and comparative analysis of three assays. J Clin Microbiol 40: 475-479. 43.

Badaró R, Reed SG, Carvalho EM (1983) Immunofluorescent antibody test in American visceral leishmaniasis: sensitivity and specificity of different morphological forms of two Leishmania species. Am J Trop Med Hyg 32: 480-484

John C. Lindon. Elaine Holmes. Jeremy K. Nicholson. Imperial College, London (U.K.). September 1, 2003 / Analytical Chemistry 385 So What's the Deal with Metabonomics?

Raamsdonk, L.M. Raamsdonk LM1, Teusink B, Broadhurst D, Zhang N, Hayes A, Walsh MC, Berden JA, Brindle KM, Kell DB, Rowland JJ, Westerhoff HV, van Dam K, Oliver SG. A functional genomics strategy that uses metabolome data to reveal the phenotype of silent mutations. Nat. Biotechnol. 19, 45–50 (2001).

J.K. Nicholson, I.D. Wilson High resolution proton magnetic resonance spectroscopy of biological fluids. Prog Nucl Magnetic Reson Spectrosc, 21 (4) (1989/01/01), pp. 449-501

Reithinger R, Dujardin JC, Louzir H, Pirmez C, Alexander B, et al. (2007) Cutaneous leishmaniasis. The Lancet infectious diseases 7: 581–596. pmid:17714672

Lepesheva GI, Waterman MR (2011) Sterol 14alpha-demethylase (CYP51) as a therapeutic target for human trypanosomiasis and leishmaniasis. Current topics in medicinal chemistry 11: 2060–2071. pmid:21619513

Moreira, W., Leblanc, E. & Ouellette, M. 2009. The role of reduced pterins in resistance to reactive oxygen and nitrogen intermediates in the protozoan parasite Leishmania. Free Radical Biology and Medicine, 46, 367-375.

Smith, C. A., Want, E. J., O'maille, G., Abagyan, R. & Siuzdak, G. 2006. XCMS: Processing mass spectrometry data for metabolite profiling using Nonlinear peak alignment, matching, and identification. Analytical Chemistry, 78, 779-787.

Saiki, E., Nagao, K., Aonuma, H., Fukumoto, S., Xuan, X. N., Bannai, M. & Kanuka, H. 2013. Multivariable analysis of host amino acids in plasma and liver during infection of malaria parasite Plasmodium yoelii. *Malaria Journal,* 12.

Salotra, P., Sreenivas, G., Pogue, G. P., Lee, N., Nakhasi, H. L., Ramesh, V. & Negi, N. S. 2001. Development of a species-specific PCR assay for detection of Leishmania donovani in clinical samples from patients with kala-azar and post-kala-azar dermal leishmaniasis. *Journal of Clinical Microbiology,* 39, 849-854.

Sanderson, S. J., Pollock, K. G. J., Hilley, J. D., Meldal, M., St Hilaire, P., Juliano, M. A., Juliano, L., Mottram, J. C. & Coombs, G. H. 2000. Expression and characterization of a recombinant cysteine proteinase of Leishmania mexicana. *Biochemical Journal,* 347, 383-388.

Sarkari, B., Chance, M. & Hommel, M. 2002. Antigenuria in visceral leishmaniasis: detection and partial characterisation of a carbohydrate antigen. *Acta Tropica,* 82, 339-348.

Saunders, E. C., De Souza, D. P., Naderer, T., Sernee, M. F., Ralton, J. E., Doyle, M. A., Macrae, J. I., Chambers, J. L., Heng, J., Nahid, A., Likic, V. A. & Mcconville, M. J. 2010. Central carbon metabolism of Leishmania parasites. *Parasitology,* 137, 1303-1313.

Saunders, E. C., Ng, W. W., Chambers, J. M., Ng, M., Naderer, T., Kroemer, J. O., Likic, V. A. & Mcconville, M. J. 2011. Isotopomer Profiling of Leishmania mexicana Promastigotes Reveals Important Roles for Succinate Fermentation and Aspartate Uptake in Tricarboxylic Acid Cycle (TCA) Anaplerosis, Glutamate Synthesis, and Growth. *Journal of Biological Chemistry,* 286, 27706-27717.

Saunders, E. C., Ng, W. W., Kloehn, J., Chambers, J. M., Ng, M. & Mcconville, M. J. 2014. Induction of a Stringent Metabolic Response in Intracellular Stages of Leishmania mexicana Leads to Increased Dependence on Mitochondrial Metabolism. *Plos Pathogens,* 10.

Scheltema, R. A., Decuypere, S., T'kindt, R., Dujardin, J.-C., Coombs, G. H. & Breitling, R. 2010. The potential of metabolomics for Leishmania research in the post-genomics era. *Parasitology,* 137.

Scheltema, R. A., Jankevics, A., Jansen, R. C., Swertz, M. A. & Breitling, R. 2011. PeakML/mzMatch: A File Format, Java Library, R Library, and Tool-Chain for Mass Spectrometry Data Analysis. *Analytical Chemistry,* 83.

Scolamiero, E., Cozzolino, C., Albano, L., Ansalone, A., Caterino, M., Corbo, G., Di Girolamo, M. G., Di Stefano, C., Durante, A., Franzese, G., Franzese, I., Gallo, G., Giliberti, P., Ingenito, L., Ippolito, G., Malamisura, B., Mazzeo, P., Norma, A., Ombrone, D., Parenti, G., Pellecchia, S., Pecce, R., Pierucci, I., Romanelli, R., Rossi, A., Siano, M., Stoduto, T., Villani, G. R. D., Andria, G., Salvatore, F., Frisso, G. & Ruoppolo, M. 2015. Targeted metabolomics in the expanded newborn screening for inborn errors of metabolism. *Molecular Biosystems,* 11, 1525-1535.

Scott, D. A., Coombs, G. H. & Sanderson, B. E. 1987. FOLATE UTILIZATION BY LEISHMANIA SPECIES AND THE IDENTIFICATION OF INTRACELLULAR DERIVATIVES AND FOLATE-METABOLIZING ENZYMES. *Molecular and Biochemical Parasitology,* 23, 139-149.

Serafim, T. D., Figueiredo, A. B., Costa, P. A. C., Marques-Da-Silva, E. A., Goncalves, R., De Moura, S. A. L., Gontijo, N. F., Da Silva, S. M., Michalick, M. S. M., Meyer-Fernandes, J. R., De Carvalho, R. P., Uliana, S. R. B., Fietto, J. L. R. & Afonso, L. C. C. 2012. Leishmania Metacyclogenesis Is Promoted in the Absence of Purines. *Plos Neglected Tropical Diseases,* 6, 10.

Sernee, M. F., Ralton, J. E., Dinev, Z., Khairallah, G. N., O'hair, R. A., Williams, S. J. & Mcconville, M. J. 2006. Leishmania beta-1,2-mannan is assembled on a mannose-cyclic phosphate primer. *Proceedings of the National Academy of Sciences of the United States of America,* 103, 9458-9463.

Shaked-Mishan, P., Suter-Grotemeyer, M., Yoel-Almagor, T., Holland, N., Zilberstein, D. & Rentsch, D. 2006. A novel high-affinity L-Arginine transporter from the human parasitic protozoan Leishmania donovani. *Molecular Microbiology,* 60, 30-38.

Shaw, J. J. 1994. TAXONOMY OF THE GENUS LEISHMANIA - PRESENT AND FUTURE-TRENDS AND THEIR IMPLICATIONS. *Memorias Do Instituto Oswaldo Cruz,* 89, 471-478.

Sherman, I. W. 1977. AMINO-ACID METABOLISM AND PROTEIN-SYNTHESIS IN MALARIAL PARASITES. *Bulletin of the World Health Organization,* 55, 265-276.

Silber, A. M., Colli, W., Ulrich, H., Alves, M. J. M. & Pereira, C. A. 2005. Amino acid metabolic routes in Trypanosoma cruzi: Possible therapeutic targets against Chagas' disease. *Current Drug Targets - Infectious Disorders,* 5, 53-64.

Silber, A. M., Tonelli, R. R., Martinelli, M., Colli, W. & Alves, M. J. M. 2002. Active transport of L-Proline in Trypanosoma cruzi. *Journal of Eukaryotic Microbiology,* 49, 441-446.

Silva, A. M., Cordeiro-Da-Silva, A. & Coombs, G. H. 2011. Metabolic Variation during Development in Culture of Leishmania donovani Promastigotes. *Plos Neglected Tropical Diseases,* 5.

Simon, M. W., Jayasimhulu, K. & Mukkada, A. J. 1983. THE FREE AMINO-ACID POOL IN LEISHMANIA-TROPICA PROMASTIGOTES. *Molecular and Biochemical Parasitology,* 9, 47-57.

Solano-Gallego, L., Morell, P., Arboix, M., Alberola, J. & Ferrer, L. 2001. Prevalence of Leishmania infantum infection in dogs living in an area of canine leishmaniasis endemicity using PCR on several tissues and serology. *Journal of Clinical Microbiology,* 39, 560-563.

Sporn, M. B., Dingman, W. & Defalco, A. 1959. A METHOD FOR STUDYING METABOLIC PATHWAYS IN THE BRAIN OF THE INTACT ANIMAL - THE CONVERSION OF PROLINE TO OTHER AMINO ACIDS. *Journal of Neurochemistry,* 4, 141-147.

Sriphochanart, W., Skolpap, W., Scharer, J. M., Moo-Young, M. & Douglas, P. L. 2011. Effect of amino acid requirements on the growth and lactic acid production of Pediococcus acidilactici culture. *African Journal of Microbiology Research,* 5, 3815-3822.

Steel, G. G. 1967. Cell loss as a factor in the growth rate of human tumors. *Eur J Cancer,* 3, 381-387.

Steeleda.F & Krassner, S. M. 1971. ASSIMILATORY SULFATE REDUCTION BY HEMOFLAGELLATE LEISHMANIA-TARENTOLAE. *Journal of Protozoology,* 18, 718-&.

Steiger, R. F. & Black, C. D. V. 1980. SIMPLIFIED DEFINED MEDIA FOR CULTIVATING LEISHMANIA DONOVANI PROMASTIGOTES. *Acta Tropica,* 37, 195-198.

Steiger, R. F. & Steiger, E. 1976. DEFINED MEDIUM FOR CULTIVATING LEISHMANIA-DONOVANI AND LEISHMANIA-BRAZILIENSIS. *Journal of Parasitology,* 62, 1010-1011.

Steiger, R. F. & Steiger, E. 1977. CULTIVATION OF LEISHMANIA-DONOVANI AND LEISHMANIA-BRAZILIENSIS IN DEFINED MEDIA - NUTRITIONAL-REQUIREMENTS. *Journal of Protozoology,* 24, 437-441.

Sundar, S., Agrawal, S., Pai, K., Chance, M. & Hommel, M. 2005. Detection of leishmanial antigen in the urine of patients with visceral leishmaniasis by a latex agglutination test. *American Journal of Tropical Medicine and Hygiene,* 73, 269-271.

Swartzla.Ee 1974. INTRODUCTION TO STATISTICAL PATTERN RECOGNITION - FUKUNAGA,K. *Ieee Transactions on Systems Man and Cybernetics,* MC 4, 238-238.

T'kindt, R., Jankevics, A., Scheltema, R. A., Zheng, L., Watson, D. G., Dujardin, J.-C., Breitling, R., Coombs, G. H. & Decuypere, S. 2011. Towards an unbiased metabolic profiling of protozoan parasites: optimisation of a Leishmania sampling protocol for HILIC-orbitrap analysis (vol 398, pg 2059, 2010). *Analytical and Bioanalytical Chemistry,* 400.

Thevenot, E. A., Roux, A., Xu, Y., Ezan, E. & Junot, C. 2015. Analysis of the Human Adult Urinary Metabolome Variations with Age, Body Mass Index, and Gender by Implementing a Comprehensive Workflow for Univariate and OPLS Statistical Analyses. *Journal of Proteome Research,* 14, 3322-3335.

Tikunov, Y., Lommen, A., De Vos, C. H. R., Verhoeven, H. A., Bino, R. J., Hall, R. D. & Bovy, A. G. 2005. A novel approach for nontargeted data analysis for metabolomics. Large-scale profiling of tomato fruit volatiles. *Plant Physiology,* 139, 1125-1137.

Tiuman, T. S., Santos, A. O., Ueda-Nakamura, T., Dias, B. P. & Nakamura, C. V. 2011. Recent advances in leishmaniasis treatment. *International Journal of Infectious Diseases,* 15, E525-E532.

Vecsei, A. K. W., Kastner, U., Trebo, M., Kornmuller, R., Picher, O., Schratzberger-Vecsei, E. & Gadner, H. 2001. Pediatric visceral leishmaniasis in Austria: Diagnostic difficulties in a non-endemic region. *Wiener Klinische Wochenschrift,* 113, 102-106.

Vendelbo, M. H., Moller, A. B., Christensen, B., Nellemann, B., Clasen, B. F. F., Nair, K. S., Jorgensen, J. O. L., Jessen, N. & Moller, N. 2014. Fasting Increases Human Skeletal Muscle Net Phenylalanine Release and This Is Associated with Decreased mTOR Signaling. *Plos One,* 9.

Vickerman, K. 1994. THE EVOLUTIONARY EXPANSION OF THE TRYPANOSOMATID FLAGELLATES. *International Journal for Parasitology,* 24, 1317-1331.

Vickers, T. J. & Beverley, S. M. 2011. Folate metabolic pathways in Leishmania. *Essays in Biochemistry: Molecular Parasitology,* 51, 63-80.

Vincent, I. M. & Barrett, M. P. 2015. Metabolomic-Based Strategies for Anti-Parasite Drug Discovery. *Journal of Biomolecular Screening,* 20, 44-55.

Vincent, I. M., Creek, D. J., Burgess, K., Woods, D. J., Burchmore, R. J. S. & Barrett, M. P. 2012. Untargeted Metabolomics Reveals a Lack Of Synergy between Nifurtimox and Eflornithine against Trypanosoma brucei. *Plos Neglected Tropical Diseases,* 6.

Vincent, I. M., Weidt, S., Rivas, L., Burgess, K., Smith, T. K. & Ouellette, M. 2014. Untargeted metabolomic analysis of miltefosine action in Leishmania infantum reveals changes to the internal lipid metabolism. *International Journal for Parasitology-Drugs and Drug Resistance,* 4, 20-27.

Vitreschak, A. G., Lyubetskaya, E. V., Shirshin, M. A., Gelfand, M. S. & Lyubetsky, V. A. 2004. Attenuation regulation of amino acid biosynthetic operons in proteobacteria: comparative genomics analysis. *Fems Microbiology Letters,* 234, 357-370.

Voncken, F., Gao, F., Wadforth, C., Harley, M. & Colasante, C. 2013. The Phosphoarginine Energy-Buffering System of Trypanosoma brucei Involves Multiple L-Arginine Kinase Isoforms with Different Subcellular Locations. *Plos One,* 8.

Walker, J., Vasquez, J. J., Gomez, M. A., Drummelsmith, J., Burchmore, R., Girard, I. & Ouellette, M. 2006. Identification of developmentally-regulated proteins in Leishmania panamensis promastigotes and by proteome profiling of axenic amastigotes. *Molecular and Biochemical Parasitology,* 147, 64-73.

Walters, L. L. 1993. LEISHMANIA DIFFERENTIATION IN NATURAL AND UNNATURAL SAND FLY HOSTS. *Journal of Eukaryotic Microbiology,* 40, 196-206.

Wanasen, N. & Soong, L. 2008. L-Arginine metabolism and its impact on host immunity against Leishmania infection. *Immunologic Research,* 41, 15-25.

Wang, W. W., Wu, Z. L., Dai, Z. L., Yang, Y., Wang, J. J. & Wu, G. Y. 2013. Glycine metabolism in animals and humans: implications for nutrition and health. *Amino Acids,* 45, 463-477.

Wellen, K. E. & Thompson, C. B. 2012. A two-way street: reciprocal regulation of metabolism and signalling. *Nature Reviews Molecular Cell Biology,* 13, 270-U1.

Westrop, G. D., Williams, R. A. M., Wang, L. J., Zhang, T., Watson, D. G., Silva, A. M. & Coombs, G. H. 2015. Metabolomic Analyses of Leishmania Reveal Multiple Species Differences and Large Differences in Amino Acid Metabolism. *Plos One,* 10.

Whitfiel.Cd, Steers, E. J. & Weissbac.H 1970. PURIFICATION AND PROPERTIES OF 5-METHYLTETRAHYDROPTEROYLTRI-GLUTAMATE-HOMOCYSTEINE TRANSMETHYLASE. *Journal of Biological Chemistry,* 245, 390-&.

Williams, R. A. M., Westrop, G. D. & Coombs, G. H. 2009. Two pathways for cysteine biosynthesis in Leishmania major. *Biochemical Journal,* 420, 451-462.

Wilson, M. E., Lewis, T. S., Miller, M. A., Mccormick, M. L. & Britigan, B. E. 2002. Leishmania chagasi: uptake of iron bound to lactoferrin or transferrin requires an iron reductase. *Experimental Parasitology,* 100, 196-207.

Wishart, D. S., Tzur, D., Knox, C., Eisner, R., Guo, A. C., Young, N., Cheng, D., Jewell, K., Arndt, D., Sawhney, S., Fung, C., Nikolai, L., Lewis, M., Coutouly, M. A., Forsythe, I., Tang, P., Shrivastava, S., Jeroncic, K., Stothard, P., Amegbey, G., Block, D., Hau, D. D., Wagner, J., Miniaci, J., Clements, M., Gebremedhin, M., Guo, N., Zhang, Y., Duggan, G. E., Macinnis, G. D., Weljie, A. M., Dowlatabadi, R., Bamforth, F., Clive, D., Greiner, R., Li, L., Marrie, T., Sykes, B. D., Vogel, H. J. & Querengesser, L. 2007. HMDB: the human metabolome database. *Nucleic Acids Research,* 35, D521-D526.

Womack, M. & Rose, W. C. 1934. Feeding experiments with mixtures of highly purified amino acids VI. The relation of L-Phenylalanine and L-Tyrosine to growth. *Journal of Biological Chemistry,* 107, 449-458.

Womack, M. & Rose, W. C. 1947. THE ROLE OF PROLINE, HYDROXYPROLINE, AND GLUTAMIC ACID IN GROWTH. *Journal of Biological Chemistry,* 171, 37-50.

Wood, T. 1986. PHYSIOLOGICAL FUNCTIONS OF THE PENTOSE-PHOSPHATE PATHWAY. *Cell Biochemistry and Function,* 4, 241-247.

Woods, D. D. 1962. BIOCHEMICAL MODE OF ACTION OF SULPHONAMIDE DRUGS. *Journal of General Microbiology,* 29, 687-&.

Yin, J., Garen, G., Garen, C. & James, M. N. G. 2011. Expression, purification and preliminary crystallographic analysis of Rv3002c, the regulatory subunit of acetolactate synthase (IlvH) from Mycobacterium tuberculosis. *Acta Crystallographica Section F-Structural Biology and Crystallization Communications,* 67, 933-936.

Zech, H., Hensler, M., Kossmehl, S., Drueppel, K., Woehlbrand, L., Trautwein, K., Colby, T., Schmidt, J., Reinhardt, R., Schmidt-Hohagen, K., Schomburg, D. &

Rabus, R. 2013. Dynamics of amino acid utilisation in Phaeobacter inhibens DSM 17395. *Proteomics,* 13, 2869-2885.

Zelmer, D. A. 1998. An evolutionary definition of parasitism. *International Journal for Parasitology,* 28, 531-533.

Zhong, Z., Wheeler, M. D., Li, X. L., Froh, M., Schemmer, P., Yin, M., Bunzendaul, H., Bradford, B. & Lemasters, J. J. 2003. L-glycine: a novel antiinflammatory, immunomodulatory, and cytoprotective agent. *Current Opinion in Clinical Nutrition and Metabolic Care,* 6, 229-240.

Zilberstein, D. 1993. TRANSPORT OF NUTRIENTS AND IONS ACROSS MEMBRANES OF TRYPANOSOMATID PARASITES. *Advances in Parasitology, Vol 32,* 32, 261-291.

Zilberstein, D. & Gepstein, A. 1993. REGULATION OF L-PROLINE TRANSPORT IN LEISHMANIA-DONOVANI BY EXTRACELLULAR PH. *Molecular and Biochemical Parasitology,* 61, 197-205.

Books

Culture of animal cells, Freshney.

Leishmania, After the genome, Myler and Fasel.

Lehninger Principles of Biochemistry, Cox and Nelson

Appendices

Concentration (mM)	Concentration (M)	Log(M)
10	0.01	-2
5	0.005	-2.301
2.5	0.0025	-2.6021
1.25	0.00125	-2.9031
0.625	0.000625	-3.2041
0.3125	0.0003125	-3.5051
0.15625	0.00015625	-3.8062
0.078125	0.000078125	-4.1072
0.0390625	3.90625E-05	-4.4082
0.01953125	1.95313E-05	-4.7093
0.009765625	9.76563E-06	-5.0103
0.004882813	4.88281E-06	-5.3113
0.002441406	2.44141E-06	-5.6124
0.001220703	1.2207E-06	-5.9134
0.000610352	6.10352E-07	-6.2144
0.000305176	3.05176E-07	-6.5154
0.000152588	1.52588E-07	-6.8165
7.62939E-05	7.62939E-08	-7.1175
3.8147E-05	3.8147E-08	-7.4185
1.90735E-05	1.90735E-08	-7.7196
9.53674E-06	9.53674E-09	-8.0206

Appendix Table 1- Amino acid concentraions used for alamar blue assay as shown in Figure 4.5.

Concentration (mM)	Concentration (M)	Log(M)
100	0.0001	-4
50	0.00005	-4.301
25	0.000025	-4.6021
12.5	0.0000125	-4.9031
6.25	0.00000625	-5.2041
3.125	0.000003125	-5.5051
1.5625	1.5625E-06	-5.8062
0.78125	7.8125E-07	-6.1072
0.390625	3.90625E-07	-6.4082
0.1953125	1.95313E-07	-6.7093
0.09765625	9.76563E-08	-7.0103
0.048828125	4.88281E-08	-7.3113

Appendix table 2- Amino acid analogues tested in 12 different concentrations with serial dilutions starting from 100 µM to 49 nM depicted as log of molar concentration described in Figure 4.13

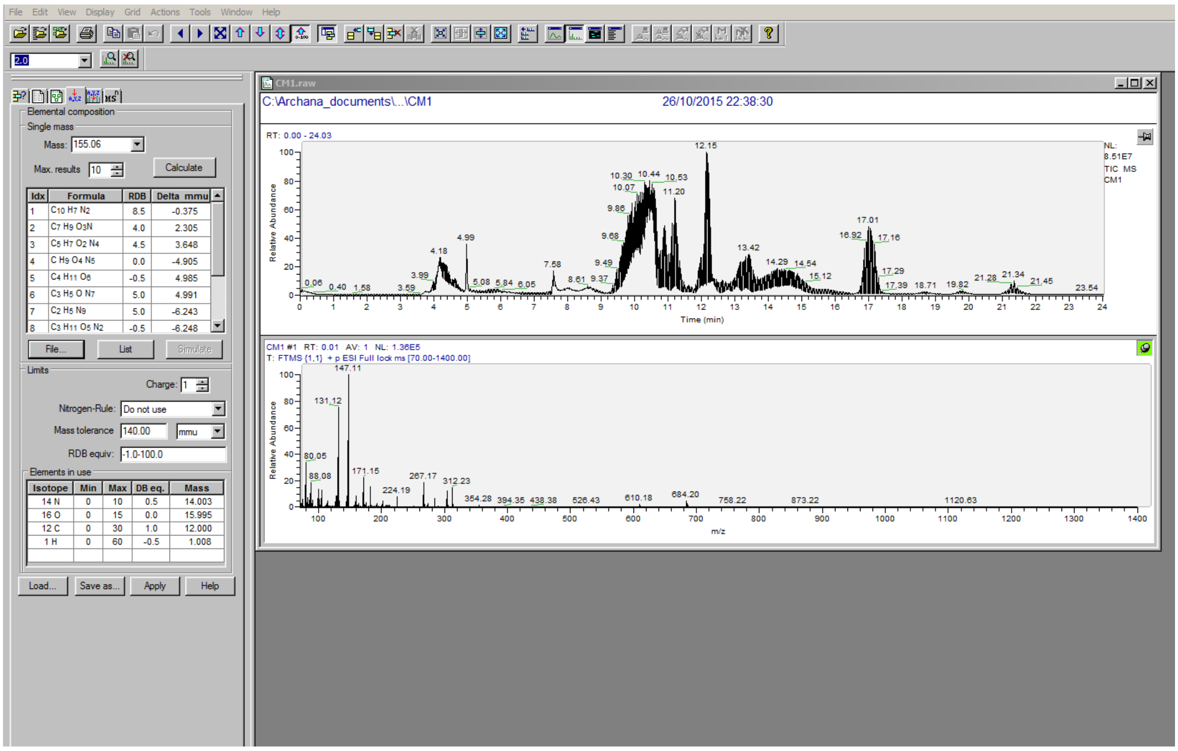

Appendix Figure 1- Raw spectral investigation of L-Histidine not detected in LC-MS in the conditions used in the study.

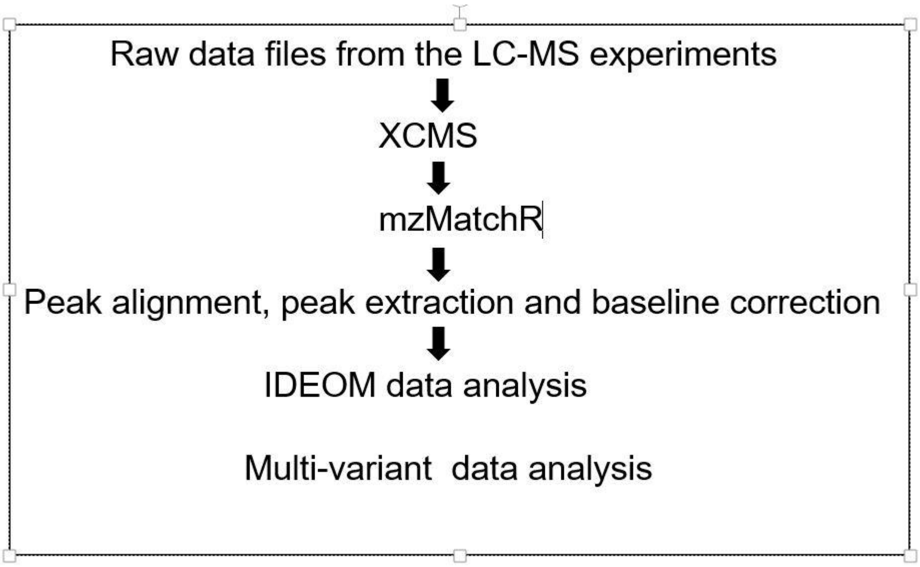

Appendix Figure 2- Schematic representation of the software used for LC-MS data analysis.

P_Id	Mass	RT	**FORMULA**	**Putative metabolite**	p_cells
1	175.0957	13.41808	C6H13N3O3	**L-Citrulline**	4.27
2	159.0685	5.618025	C10H9NO	Indole-3-acetaldehyde	3.67
3	129.079	11.54965	C6H11NO2	L-Pipecolate	3.61
4	156.0535	10.39066	C6H8N2O3	Imidazole lactate	3.38
5	138.0429	10.22049	C6H6N2O2	Urocanate	4.16
6	131.0694	12.93816	C4H9N3O2	Creatine	6.16
7	132.0899	18.04894	C5H12N2O2	**L-Ornithine**	3.89

8	173.0801	12.75051	C6H11N3O3	5-Guanidino-2-oxopentanoate	2.96
9	188.1525	17.78643	C9H20N2O2	N6,N6,N6-Trimethyl-L-Lysine	6.32
10	205.0739	7.337082	C11H11NO3	Indolelactate	2.06
11	246.1327	18.26903	C9H18N4O4	N2-(D-1-Carboxyethyl)-L-Arginine	0.44
12	360.6442	15.63521	C27H47N9O10S2	Trypanothione disulfide	4.85
13	188.1161	11.70094	C8H16N2O3	N6-Acetyl-L-Lysine	2.27
14	103.0997	18.50945	C5H13NO	**Choline**	2.16
15	145.0851	13.23628	C5H11N3O2	4-Guanidinobutanoate	0.60
16	89.04766	12.96275	C3H7NO2	**L-Alanine**	1.93
17	145.074	13.22288	C6H11NO3	[FA oxo,amino(6:0)] 3-oxo-5S-amino-hexanoic acid	0.58
18	130.1106	16.46056	C6H14N2O	N-Acetylputrescine	0.52
19	146.1055	19.2855	C6H14N2O2	D-Lysine	0.48
20	131.0946	10.78067	C6H13NO2	**L-Leucine**	0.53
21	142.0379	11.42419	C5H6N2O3	4-Imidazolone-5-acetate	0.53

22	144.1011	20.72059	C5H12N4O	4-Guanidinobutanamide	0.55
23	115.0633	11.78636	C5H9NO2	**L-Proline**	0.67
24	177.0789	11.89642	C10H11NO2	indole-3-glycol	0.59
25	149.051	10.90539	C5H11NO2S	**L-Methionine**	0.52
26	237.086	10.78591	C9H19NO2S2	8-[(aminomethyl)sulfanyl]-6-sulfanyloctanoic acid	1.25
27	208.0848	10.50189	C10H12N2O3	**L-Kynurenine**	0.60
28	119.0583	12.65871	C4H9NO3	**L-Threonine**	0.55
29	219.1107	8.41133	C9H17NO5	**Pantothenate**	0.58
30	221.0899	11.21216	C8H15NO6	**N-Acetyl-D-glucosamine**	0.61
31	155.0695	12.76548	C6H9N3O2	**L-Histidine**	0.67
32	131.0582	13.0044	C5H9NO3	L-Glutamate 5-semialdehyde	0.51
33	174.1116	20.61022	C6H14N4O2	**L-Arginine**	0.53
34	236.0795	11.04945	C11H12N2O4	L-Formylkynurenine	0.46
35	128.0951	16.49121	C6H12N2O	L-Lysine 1,6-lactam	0.69

36	103.0633	11.98415	C4H9NO2	N,N-Dimethylglycine	1.02
37	161.0688	13.15719	C6H11NO4	O-Acetyl-L-homoserine	0.44
38	117.0789	11.5409	C5H11NO2	**L-Valine**	0.65
39	190.0953	19.27863	C7H14N2O4	LL-2,6-Diaminoheptanedioate	0.47
40	181.0739	11.88295	C9H11NO3	**L-Tyrosine**	0.55
41	165.079	9.979617	C9H11NO2	**L-Phenylalanine**	0.57
42	126.043	10.66894	C5H6N2O2	**Imidazole-4-acetate**	0.97
43	165.046	11.84004	C5H11NO3S	L-Methionine S-oxide	0.52
44	132.0535	13.12173	C4H8N2O3	**L-Asparagine**	0.59
45	160.0848	7.624052	C6H12N2O3	N-gamma-Acetyldiaminobutyrate	2.24
46	240.0237	13.37166	C6H12N2O4S2	**L-L-Cysteine**	0.38
47	146.0691	13.00351	C5H10N2O3	**L-Glutamine**	0.76
48	75.03201	13.49975	C2H5NO2	**Glycine**	0.68
49	204.0899	11.07232	C11H12N2O2	**L-Tryptophan**	0.48
50	105.0426	13.48736	C3H7NO3	**L-Serine**	0.39
51	174.0793	12.27298	C10H10N2O	Indole-3-acetamide	0.97

52	147.0531	12.51229	C5H9NO4	**L-Glutamate**	0.85
53	133.0375	12.7177	C4H7NO4	**L-Aspartate**	0.55
54	173.0478	4.912758	C10H7NO2	indole-3-glyoxal	0.73
55	175.0633	7.36051	C10H9NO2	Indole-3-acetate	0.52
56	113.0477	7.412061	C5H7NO2	(S)-1-Pyrroline-5-carboxylate	0.82
57	129.079	7.30733	C6H11NO2	N4-Acetylaminobutanal	3.12
58	188.1273	19.06158	C7H16N4O2	Homoarginine	3.84
59	145.1579	13.60492	C7H19N3	**Spermidine**	1.01
60	307.0835	12.22601	C10H17N3O6S	**Glutathione**	3.98
61	216.1109	10.57162	C9H16N2O4	gamma-Glutamyl-gamma-aminobutyraldehyde	3.98
62	250.0623	12.13837	C8H14N2O5S	**gamma-L-Glutamyl-L-cysteine**	3.46
63	169.0851	11.5219	C7H11N3O2	**N(pi)-Methyl-L-Histidine**	3.15

Appendix table 3 Table with metabolites in the intracellular samples enriched over time compared to naïve medium without cells. Metabolites in yellow are matched to authentic standards. Chemical formula in red are those with more than one isomeric peak.

Table 1 Enzymes involved in phenylalanine degradation pathway						
			GenBank accession number(s)			
EC Number	Name	Reaction Number	L.major	T.brucei	T.cruzi	H.sapiens
1.11.1.7	Peroxidase	R07443				PRDX6
1.13.11.27	4-hydroxyphenylpy	R02521				HPD
1.14.16.1	Phenylalanine 4-mo	R07211	LmjF.28.1280			PAH
1.2.1.5	Aldehyde dehydrog	R08307				ALDH3A1
1.4.3.2	L-amino-acid oxida	R06124				IL41
1.4.3.21	Primary-amine oxic	R06740				AOC2
1.4.3.4	Monoamine oxidas	R08348				MAOA
2.3.1.13	Glycine N-acyltrans	R05841				GLYAT
2.6.1.1	Aspartate transami	R05052	LmjF.35.0820	Tb927.10.3660		GOT1
2.6.1.5	Tyrosine transamin	R07396	LmjF.36.2360		Tc00.1047(	TAT
4.1.1.28	Aromatic-L-amino-a	R04909				DDC
5.3.2.1	Phenylpyruvate tau	R03342				MIF
1.1.1.157	3-hydroxybutyryl-C	R01976				NA
1.1.1.222	(R)-4-hydroxyphen	R03339				NA
1.1.1.237	Hydroxyphenylpyru	R03373				NA
1.1.1.90	Aryl-alcohol dehydi	R05348				NA
1.13.11.16	3-carboxyethylcate	R06788				NA
1.13.11.16	3-carboxyethylcate	R06788				NA
1.13.12.9	Phenylalanine 2-mo	R00690				NA
1.14.12.19	3-phenylpropanoat	R06783				NA
1.14.12.19	3-phenylpropanoat	R06783				NA
1.14.13.-	With NADH or NAD	R09353				NA
1.14.13.-	With NADH or NAD	R09353				NA
1.14.13.-	With NADH or NAD	R09353				NA
1.14.13.11	Trans-cinnamate 4-	R08815				NA
1.14.13.14	Trans-cinnamate 2-	R02254				NA
1.14.13.4	Melilotate 3-mono	R03369				NA
1.17.5.1	Phenylacetyl-CoA d	R07222				NA
1.2.1.10	Acetaldehyde dehy	R01172				NA
1.2.1.39	Phenylacetaldehyd	R02536				NA
1.2.1.58	Phenylglyoxylate d	R02450				NA
1.3.1.11	2-coumarate reduc	R03709				NA
1.3.1.31	2-enoate reductase	R02252				NA
1.4.1.20	Phenylalanine dehy	R00688				NA
1.4.99.1	D-amino-acid dehy	R07166				NA
1.5.1.18	Ephedrine dehydro	R03614				NA
2.1.1.-	Methyltransferases	R09371	LmjF.36.5360	Tb927.8.31	Tc00.1047(	NA
2.1.1.-	Methyltransferases	R09371	LmjF.36.5360	Tb927.8.31	Tc00.1047(	NA
2.1.1.104	Caffeoyl-CoA O-me	R06578				NA
2.3.1.-	Transferring groups	R09258	LmjF.29.1310	Tb927.5.43	Tc00.1047(	NA
2.3.1.14	Glutamine N-pheny	R04776				NA
2.3.1.36	D-amino-acid N-ac	R03903				NA
2.3.1.53	Phenylalanine N-ac	R00693				NA
2.3.1.71	Glycine N-benzoylt	R02452				NA
2.6.1.-	Transaminases (am	R09373				NA
2.6.1.21	D-amino-acid trans	R05053				NA
2.6.1.57	Aromatic-amino-ac	R07396				NA
2.6.1.58	Phenylalanine(histi	R09254				NA
2.6.1.9	Histidinol-phospha	R03243				NA
3.1.2.-	Thiolester hydrolas	R08273				NA
3.1.2.25	Phenylacetyl-CoA h	R07294				NA
3.5.1.32	Hippurate hydrolas	R01424				NA
3.5.1.4	Amidase	R06134				NA
3.7.1.-	In ketonic substanc	R09238				NA
3.7.1.-	In ketonic substanc	R09238				NA
4.1.1.-	Carboxy-lyases.	R09208	LmjF.28.1580			NA
4.1.1.43	Phenylpyruvate de	R01974				NA
4.1.1.53	Phenylalanine deca	R00699				NA
4.1.2.41	Vanillin synthase	R05773				NA
4.1.3.39	4-hydroxy-2-oxoval	R05298				NA
4.2.1.101	Trans-feruloyl-CoA	R05772				NA
4.2.1.17	Enoyl-CoA hydratas	R08093	LmjF.32.3680	Tb927.3.48	Tc00.1047(	NA
4.2.1.80	2-oxopent-4-enoat	R05864				NA
4.3.1.24	Phenylalanine amm	R06132				NA
4.3.1.25	Phenylalanine/tyro	R06132				NA
5.1.1.11	Phenylalanine race	R00686				NA
6.2.1.12	4-coumarate--CoA	R06583	LmjF.19.1005			NA
6.2.1.30	Phenylacetate--CoA	R02539				NA

Appendix table 3 Enzymes in aromatic amino acids metabolism compared between mammals and kinetoplastid species. Specified in blue are those enzymes with no homologues enzymes in mammals.

```
plot<-read.csv('amino_acid_intermediates(recent analysis).xlsx')
symbols(plot$Mass, plot$RT, circles=plot$p_cells)
radius <- sqrt( plot$p_cells/ pi )
symbols(plot$Mass, plot$RT, circles=radius)symbols(plot$Mass, plot$RT,
circles=radius, inches=0.35, fg="black", bg="yellow", xlab="Mass", ylab="RT")
text(plot$Mass, plot$RT, plot$P_id, cex=1.0)
```

Appendix code 1 R script written for data analysis and visualisation as shown in Figure 5.4 Bubble plot of all metabolites detected in the intracellular dataset

```
data<-read.csv('inensity_time_course.csv')
library(ropls)
sample<-read.csv('sample.csv')
group<-sample[,'Group']
data.plsda <- opls(data[-1], group)
data.pca <- opls(data[-1])
plot(data.pca), typeVc = "x-score",
parAsColFcVn = group, parEllipsesL = TRUE
```

Appendix code 2 R script written for data analysis and visualisation as shown in Figure 6.2 PLS-DA model of exo-metabolome at six different time points during the growth of *L. mexicana* promastigotes cultured in Defined medium.

```
inputdata <- read.csv("StatsTable3.csv", header=TRUE,
row.names=1,stringsAsFactors=FALSE)
inputdata <- read.csv("int", header=TRUE, row.names=1,stringsAsFactors=FALSE)
inputdata <- read.csv("inensity_time_course.csv", header=TRUE,
row.names=1,stringsAsFactors=FALSE)
inputdata [is.na(inputdata)] <- 0
colnames (inputdata) <- abbreviate(colnames(inputdata), minlength = 64)
PeakTable <- inputdata[-c(1)]
prelog_data <- inputdata
prelog_data[prelog_data==0] <- 0.5*(min(PeakTable[PeakTable>0],na.rm=TRUE))
library (metabolomics)
```

```
log_data <- LogTransform(prelog_data, base = 2,saveoutput = FALSE,
outputname = "log.results2")
sampleclasses <- log_data$Group
HeatMap(log_data$output, colramp = redgreen(75), scale = c("row"),dendrogram
= c("none"),distmethod = "euclidean", aggmethod = "complete", margins = c(5, 8),
key = TRUE, keysize = 1.5, cexRow = 2.0, ColSideColors = NULL)
```

Appendix code 3 R script written for data exploration and visualisation Figure 5.4 Bubble plot of all metabolites detected in the intracellular dataset

```
A=importdata('bargraph.txt')
Y = A(1:6,:);
width = 0.25;
figure
bar3(Y,width)
set(gca,'XTickLabel',{'metabolites names;},'FontSize',12)
set(gca,'YTickLabel',{'Ctrl';'D1';'D2';'D3';'D6';'D9'})
title('Other DM components')
```

Appendix code 4 Matlab script for data analysis and visualisation as shown in Figure 6.12 to Figure 6.21

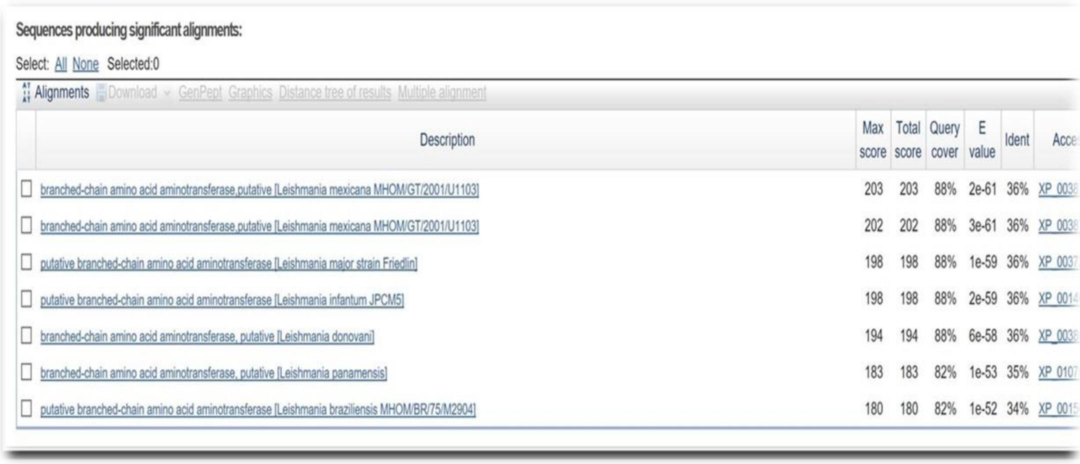
Sequences producing significant alignments:

Select: All None Selected:0

Alignments Download GenPept Graphics Distance tree of results Multiple alignment

Description	Max score	Total score	Query cover	E value	Ident	Acce
branched-chain amino acid aminotransferase,putative [Leishmania mexicana MHOM/GT/2001/U1103]	203	203	88%	2e-61	36%	XP_0038
branched-chain amino acid aminotransferase,putative [Leishmania mexicana MHOM/GT/2001/U1103]	202	202	88%	3e-61	36%	XP_0038
putative branched-chain amino acid aminotransferase [Leishmania major strain Friedlin]	198	198	88%	1e-59	36%	XP_0037
putative branched-chain amino acid aminotransferase [Leishmania infantum JPCM5]	198	198	88%	2e-59	36%	XP_0014
branched-chain amino acid aminotransferase, putative [Leishmania donovani]	194	194	88%	6e-58	36%	XP_0038
branched-chain amino acid aminotransferase, putative [Leishmania panamensis]	183	183	82%	1e-53	35%	XP_0107
putative branched-chain amino acid aminotransferase [Leishmania braziliensis MHOM/BR/75/M2904]	180	180	82%	1e-52	34%	XP_0015

Sequences producing significant alignments:

Select: All None Selected:0

Alignments Download GenPept Graphics Distance tree of results Multiple alignment

	Description	Max score	Total score	Query cover	E value	Ident	Accession
☐	putative pyruvate/indole-pyruvate carboxylase,putative [Leishmania mexicana MHOM/GT/2001/U1103]	110	110	77%	4e-25	26%	XP_003878881.1
☐	putative putative pyruvate/indole-pyruvate carboxylase [Leishmania infantum JPCM5]	110	110	82%	4e-25	25%	XP_001468661.1
☐	putative pyruvate/indole-pyruvate carboxylase, putative [Leishmania donovani]	110	110	82%	8e-25	25%	XP_003864462.1
☐	putative pyruvate/indole-pyruvate carboxylase [Leishmania major strain Friedlin]	108	108	77%	2e-24	26%	XP_001686429.1
☐	putative pyruvate/indole-pyruvate carboxylase, putative [Leishmania panamensis]	99.0	99.0	77%	3e-21	25%	XP_010698497.1
☐	putative putative pyruvate/indole-pyruvate carboxylase [Leishmania braziliensis MHOM/BR/75/M2904]	97.4	97.4	77%	8e-21	25%	XP_001564563.1

Appendix figure 3 Isoleucine biosynthesis enzymes with positive results as verified using blast analysis from NCBI server.

Sort | Trend Sort | Import Peaks | Search | Tools | Graphs | Export

Mass	RT	FORMULA	Isomers	Putative metabolite	confide	Map	Pathway	m…ensity	CM1	D1S	D2S	D3S	D6S	D9S
156.05	10.79	C6H8N2O3	4	4-Imidazolone-5-propanoate	8	Amino Acid Metabolism	Histidine metabolism	1707537	1.00	**1921.78**	**3753.56**	**11181.67**	**35656.35**	**42625.76**
257.1	12.9	C8H20NO6P	1	**sn-glycero-3-Phosphocholine**	8	Lipid Metabolism	Glycerophospholipid metabolism __Ether lipid metabolism	1923617	1.00	862.63	**1032.95**	**572.37**	**50.18**	**71.49**
175.1	13.75	C6H13N3O3	3	**L-Citrulline**	10	Amino Acid Metabolism	L-Arginine and L-Proline metabolism	6208916	1.00	**734.99**	1759.32	**3989.82**	**12313.99**	**12744.22**
519.33	4.611	C26H50NO7P	3	[PC (18:2)] 1-(9Z,12Z-octadecadienoyl)-sn-glycero-3-phosphocholine	7	Lipids: Glycerophospholipids	Glycerophosphocholines	2059070	**0.00**	**690.16**	**1611.81**	**175.94**	**0.00**	**0.00**
183.07	12.	C5H14NO4P	1	**Choline phosphate**	10	Lipid Metabolism	Glycerophospholipid metabolism	1389125	1.	687.93	1394	584.21	131.48	106.10

	92						__Glycine, serine and L-Threonine metabolism		00		.29			
159.07	6.0477	C10H9NO	4	Indole-3-acetaldehyde	8	Amino Acid Metabolism	L-Tryptophan metabolism	392015	1.00	573.02	756.73	**785.29**	**1008.04**	**831.63**
205.07	7.578	C11H11NO3	5	Indolelactate	8	Amino Acid Metabolism	L-Tryptophan metabolism	3719187	**0.00**	**532.54**	**1404.26**	**2836.50**	**3316.32**	**3465.79**
129.08	11.9	C6H11NO2	9	L-Pipecolate	8	Amino Acid Metabolism	Lysine degradation__Alkaloid biosynthesis II	2666796	1.00	**345.73**	727.27	**1181.19**	**1964.20**	**1831.33**
166.06	4.95	C9H10O3	17	3-Methoxy-4-hydroxyphenylacetaldehyde	8	Amino Acid Metabolism	Tyrosine metabolism	333543	1.00	**223.28**	701.36	1088.96	**4273.73**	3981.13
150.05	11.26	C5H10O5	37	**D-Ribose**	10	Carbohydrate Metabolism	Pentose phosphate pathway	148782	1.00	**105.05**	129.96	**165.80**	**181.21**	**159.66**
112.03	8.918	C4H4N2O2	2	Uracil	6	Nucleotide Metabolism	Pyrimidine metabolism__beta-Alanine metabolism__Pantothenate and CoA biosynthesis	92483	1.00	95.96	177.37	**190.30**	**368.35**	**505.22**
98.048	9.492	C4H6N2O	1	Imidazole-4-methanol	7	0	0	270967	1.00	**58.12**	123.82	**193.82**	**397.85**	**446.89**
156.02	9.982	C5H4N2O4	2	**Orotate**	10	Nucleotide Metabolism	Pyrimidine metabolism	125153	**0.00**	**57.77**	**64.80**	**111.31**	**170.97**	**176.22**
180.04	7.576	C9H8O4	11	2-Hydroxy-3-(4-hydroxyphenyl)propenoate	6	Amino Acid Metabolism	Tyrosine metabolism	199864	**0.00**	**43.75**	**107.22**	**171.50**	**313.77**	**725.13**
164.05	4.8	C9H8O3	13	Caffeic aldehyde	7	Biosynthesis of	Phenylpropanoid	44650	1.	**40.93**	119.90	**289.57**	**725.41**	**1289.87**

	56					Secondary Metabolites	biosynthesis		00					
152.03	11.098	C5H4N4O2	3	**Xanthine**	8	Nucleotide Metabolism	Purine metabolism__Caffeine metabolism	75823	0.00	34.52	71.28	43.00	112.24	133.11
182.06	8.863	C9H10O4	13	3-(4-Hydroxyphenyl)lactate	8	Amino Acid Metabolism	Tyrosine metabolism	245243	0.00	34.09	89.64	214.97	703.32	869.44
204.07	13.03	C7H12N2O5	4	Glu-Gly	5	Peptide(di-)	Acidic peptide	75903	0.00	30.42	46.79	47.04	93.97	126.24
146.02	13.08	C5H6O5	7	5-hydroxy-2,4-dioxopentanoate	8	0	0	294884	1.00	24.57	42.55	41.56	87.78	75.63
276.02	11.08	C6H14O8P2	1	3,4-epoxy-3-methyl-1-butyl diphosphate	7	0	0	70420	0.00	22.84	53.15	54.56	132.63	135.78
132.09	18.62	C5H12N2O2	6	**L-Ornithine**	8	Amino Acid Metabolism	L-Arginine and L-Proline metabolism__D-L-Arginine and D-ornithine metabolism__Glutathione metabolism	83635	1.00	20.67	21.92	11.04	22.57	68.56
134.02	13.28	C4H6O5	4	**(S)-Malate**	10	Carbohydrate Metabolism	Citrate cycle (TCA cycle)__Glutamate metabolism__Alanine and L-Aspartate metabolism__Pyruvate metabolism__Glyoxylate and dicarboxylate	3083134	1.00	19.69	36.38	62.42	276.81	342.30

							metabolism__Carbon fixation__Reductive carboxylate cycle (CO2 fixation)							
133.07	12.57	C5H11NO3	4	1-deoxyxylonojirimycin	7	0	0	155426	1.00	**16.59**	35.35	**50.00**	**102.77**	**117.92**
174.02	14.17	C6H6O6	3	**cis-Aconitate**	10	Carbohydrate Metabolism	Citrate cycle (TCA cycle)__Glyoxylate and dicarboxylate metabolism__C5-Branched dibasic acid metabolism__Reductive carboxylate cycle (CO2 fixation)	148120	1.00	10.38	34.64	91.81	**219.81**	**347.33**
130.06	4.79	C6H10O3	18	Ethyl 3-oxobutanoate	7	0	0	80288	1.00	**7.56**	**17.60**	**11.31**	**2.41**	6.11
430.16	4.189	C23H26O8	4	Sesartemin	5	0	0	909926	1.00	5.77	3.46	0.83	0.69	1.99
256.24	3.74	C16H32O2	27	Hexadecanoic acid	8	Lipid Metabolism	Fatty acid biosynthesis__Fatty acid elongation in mitochondria__Fatty acid metabolism__Biosynthesis of unsaturated fatty acids	3208385	1.00	5.22	3.14	1.43	0.76	0.56
394.15	10.7	C14H26N4O7S	4	Ala-Met-Ser-Ser	5	Peptide(tetra-)	Hydrophobic peptide	33891	**0.00**	**5.11**	**11.25**	**29.82**	**147.61**	**215.28**

173.08	13.07	C6H11N3O3	1	5-Guanidino-2-oxopentanoate	8	Amino Acid Metabolism	D-L-Arginine and D-ornithine metabolism	538852	1.00	3.67	**2.84**	**2.01**	**2.46**	**3.81**
196.06	12.49	C6H12O7	11	L-Gulonate	6	Carbohydrate Metabolism	Pentose and glucuronate interconversions__Ascorbate and aldarate metabolism	54277	1.00	**3.43**	12.38	**7.17**	**17.21**	**24.92**
228.21	3.803	C14H28O2	23	Tetradecanoic acid	6	Lipid Metabolism	Fatty acid biosynthesis	1085479	1.00	3.37	4.09	1.11	0.64	0.31
116.01	13.28	C4H4O4	3	**Fumarate**	8	Carbohydrate Metabolism	Citrate cycle (TCA cycle)__Oxidative phosphorylation__L-Arginine and L-Proline metabolism__Glutamate metabolism__Alanine and L-Aspartate metabolism__L-Arginine and L-Proline metabolism__Tyrosine metabolism__Phenylalanine metabolism	126139	1.00	3.34	**7.38**	**13.44**	**67.63**	**101.49**
325.37	7.602	C22H47N	1	di-n-Undecylamine	7	0	0	1209569	1.00	3.07	2.13	1.73	0.92	0.82
206.17	4.155	C14H22O	6	[PR] (+)-15-nor-4-thujopsen-3-one	7	Lipids: Prenols	Isoprenoids	126749	1.00	3.03	1.25	2.88	1.91	0.90

286.1	4.942	C12H18N2O4S	1	4-Hydroxytolbutamide	7	0	0	153270	1.00	2.87	2.99	2.30	0.58	0.31
118.03	12.81	C4H6O4	7	**Succinate**	10	Carbohydrate Metabolism	Citrate cycle (TCA cycle)__Oxidative phosphorylation__Glutamate metabolism__Alanine and L-Aspartate metabolism__Tyrosine metabolism__Phenylalanine metabolism__gamma-Hexachlorocyclohexane degradation__Glyoxylate and dicarboxylate metabolism	6522799	1.00	2.34	6.41	**28.97**	**230.39**	**270.35**
74.037	8.763	C3H6O2	7	(S)-Lactaldehyde	8	Carbohydrate Metabolism	Fructose and mannose metabolism__Pyruvate metabolism	176117	1.00	2.31	5.65	**12.34**	**34.28**	**36.82**
459.26	4.061	C26H37NO6	1	Militarinone A	5	0	0	276821	1.00	2.14	0.14	3.92	3.61	0.24
192.03	14.34	C6H8O7	12	Citrate	8	Carbohydrate Metabolism	Citrate cycle (TCA cycle)__Glutamate metabolism__Alanine and L-Aspartate metabolism__Glyoxylate and dicarboxylate	1913894	1.00	1.90	2.67	3.81	**4.22**	**4.01**

							metabolism__Reductive carboxylate cycle (CO2 fixation)							
111.04	11.258	$C_4H_5N_3O$	1	**Cytosine**	10	Nucleotide Metabolism	Pyrimidine metabolism	6845	**0.00**	**1.89**	**8.08**	**6.35**	**27.91**	**141.14**
176.05	8.585	$C_4H_8N_4O_4$	1	Allantoate	6	Nucleotide Metabolism	Purine metabolism	670058	1.00	1.86	2.04	2.65	**3.40**	2.41
189.04	7.526	$C_{10}H_7NO_3$	6	Kynurenate	6	Amino Acid Metabolism	L-Tryptophan metabolism	14176	1.00	1.76	3.50	**5.55**	**38.33**	**77.26**
136.07	10.45	$C_5H_{12}O_4$	2	D-Apiitol	7	0	0	77858	1.00	1.60	1.90	1.15	0.54	2.65
113.08	5.968	$C_6H_{11}NO$	1	epsilon-Caprolactam	5.5	Xenobiotics Biodegradation and Metabolism	Caprolactam degradation	325476	1.00	1.47	0.89	1.16	1.06	0.52
165.08	10.38	$C_9H_{11}NO_2$	7	**L-Phenylalanine**	10	Amino Acid Metabolism	Phenylalanine metabolism__Phenylalanine, L-Tyrosine and L-Tryptophan biosynthesis__Phenylpropanoid biosynthesis__Alkaloid biosynthesis II	1489027	1.00	1.44	1.30	**0.76**	**0.77**	**0.80**
193.07	7.549	$C_{10}H_{11}NO_3$	10	5,6-Dihydroxy-3-methyl-2-oxo-1,2,5,6-tetrahydroquinoline	5	0	3-methylquinoline degradation	1808267	1.00	1.41	1.38	1.84	2.10	2.67

329.18	5.7333	C16H27NO6	1	Europine	5	0	0	100583	1.00	1.34	1.51	0.30	0.48	3.94
100.05	7.5222	C5H8O2	18	Tiglic acid	5	Lipids: Fatty Acyls	Fatty Acids and Conjugates	156424	1.00	1.26	5.09	22.57	**86.64**	**74.68**
136.05	4.934	C8H8O2	16	4-Hydroxyphenylacetaldehyde	8	Amino Acid Metabolism	Tyrosine metabolism__Alkaloid biosynthesis I	479641	1.00	1.25	1.01	1.13	1.50	**1.64**
250.06	8.457	C8H14N2O5S	2	Glu-Cys	7	Peptide(di-)	Acidic peptide	392820	1.00	1.25	1.39	1.54	1.61	1.05
294.18	3.86	C17H26O4	3	[6]-Gingerol	5	0	0	163936	1.00	1.20	1.41	1.14	0.84	**0.35**
182.08	12.83	C6H14O6	6	D-Sorbitol	6	Carbohydrate Metabolism	Fructose and mannose metabolism__Galactose metabolism	67503	1.00	1.17	2.32	1.10	5.99	**20.72**
289.12	9.726	C29H34N6O5S	1	Met-Trp-Trp-Gly	7	Peptide(tetra-)	Hydrophobic peptide	219750	1.00	1.16	1.92	2.76	**2.66**	**2.68**
193.07	4.987	C10H11NO3	10	Cichorine	7	0	0	413715	1.00	1.14	1.00	1.09	0.94	1.09
89.048	13.29	C3H7NO2	9	**L-Alanine**	10	Amino Acid Metabolism	Alanine and L-Aspartate metabolism__Cysteine metabolism__Taurine and hypotaurine metabolism__Selenoamino acid metabolism__D-Alanine metabolism__Carbon fixation__R	2806218	1.00	1.12	1.61	**2.54**	**5.55**	**6.04**

							eductive carboxylate cycle (CO2 fixation)							
385.19	11.26	C22H27NO5	1	O-methylandrocymbine	7	Biosynthesis of Secondary Metabolites	colchicine biosynthesis	90259	1.00	1.11	0.92	**1.48**	**2.30**	**2.77**
79.966	12.8	[PO3]3-	1	Phosphite	5	0	0	82116	1.00	1.11	**1.71**	1.27	0.43	2.98
81.982	12.8	H3O3P	1	Phosphonate	7	0	0	524381	1.00	1.10	1.54	1.11	0.56	2.75
164.07	17.559	C6H12O5	25	L-Rhamnulose	6	Carbohydrate Metabolism	Fructose and mannose metabolism	302140	1.00	1.08	1.06	0.20	0.47	4.42
116.01	11.16	C4H4O4	3	**Maleic acid**	8	Carbohydrate Metabolism	Butanoate metabolism __Nicotinate and nicotinamide metabolism	170705	1.00	1.04	1.61	1.60	1.59	0.46
104.01	13.19	C3H4O4	3	**Malonate**	8	Nucleotide Metabolism	Pyrimidine metabolism __beta-Alanine metabolism	74828	1.00	1.00	**1.53**	1.48	**3.36**	**5.09**
244.09	9.016	C10H16N2O3S	1	Biotin	8	Metabolism of Cofactors and Vitamins	Biotin metabolism	477019	1.00	1.00	0.76	1.31	1.68	0.92
180.06	16.38	C6H12O6	57	myo-Inositol	8	Carbohydrate Metabolism	Inositol metabolism __Galactose metabolism __Ascorbate and aldarate metabolism __Streptomycin biosynthesi	457081	1.00	0.98	1.12	1.04	1.31	1.10

								s__Inositol phosphate metabolism						
97.967	14.37	H2O4S	1	Sulfate	8	Nucleotide Metabolism	Purine metabolism __Cysteine metabolism __Sulfur metabolism	837950	1.00	0.96	1.23	1.54	**1.78**	1.60
88.052	7.578	C4H8O2	8	Butanoic acid	6	Carbohydrate Metabolism	Butanoate metabolism	354951	1.00	0.90	1.78	**2.93**	**6.56**	**7.54**
219.11	8.904	C9H17NO5	1	**Pantothenate**	10	Amino Acid Metabolism	beta-Alanine metabolism __Pantothenate and CoA biosynthesis	1271112	1.00	0.89	0.65	1.32	1.35	0.78
145.09	13.64	C5H11N3O2	3	4-Guanidinobutanoate	8	Amino Acid Metabolism	L-Arginine and L-Proline metabolism	44422	1.00	0.89	1.23	1.33	**2.57**	**3.06**
130.03	11.04	C5H6O4	7	2,5-Dioxopentanoate	6	Carbohydrate Metabolism	Ascorbate and aldarate metabolism __L-Arginine and L-Proline metabolism	192938	1.00	0.88	1.50	1.69	1.66	0.59
102.07	7.532	C5H10O2	9	Pentanoate	7	Lipids: Fatty Acyls	Fatty Acids and Conjugates	150728	1.00	0.88	**1.91**	4.44	**12.78**	**13.28**
177.05	7.573	C6H11NO3S	3	N-Formyl-L-Methionine	8	Amino Acid Metabolism	Methionine metabolism	382845	1.00	0.88	0.38	0.43	0.95	2.18
381.15	12.27	C17H23N3O7	3	Phe-Thr-Asp	5	Peptide(tri-)	Hydrophobic peptide	100050	1.00	0.87	0.70	0.83	**1.40**	0.87
218.06	12.69	C13H21N6O9P	1	(L-Seryl)adenylate	7	0	0	12092	1.00	0.86	5.02	1.25	15.24	27.76
155.07	13.53	C6H9N3O2	5	3-(Pyrazol-1-yl)-L-Alanine	7	0	beta-pyrazole-1-ylalanine	734849	1.00	0.86	0.99	1.15	**1.62**	1.66

							biosynthesis							
181.07	12.34	C9H11NO3	11	**L-Tyrosine**	10	Amino Acid Metabolism	Tyrosine metabolism__Phenylalanine, L-Tyrosine and L-Tryptophan biosynthesis__Novobiocin biosynthesis__Thiamine metabolism__Phenylpropanoid biosynthesis__Alkaloid biosynthesis I	1662601	1.00	0.86	0.84	0.90	0.94	0.93
287.1	7.744	C12H17NO7	1	Volkenin	5	0	0	176987	1.00	0.85	0.94	1.07	**1.78**	1.54
200.18	3.896	C12H24O2	15	Dodecanoic acid	8	Lipid Metabolism	Fatty acid biosynthesis	380864	1.00	0.85	1.45	1.26	0.89	0.08
115.06	12.09	C5H9NO2	4	**L-Proline**	10	Amino Acid Metabolism	L-Arginine and L-Proline metabolism__Novobiocin biosynthesis	41316036	1.00	0.85	0.92	1.09	**1.37**	**1.39**
300.1	10.45	C17H16O5	48	Farrerol	5	Lipids: Polyketides	Flavonoids	1113104	1.00	0.85	0.83	0.93	1.08	0.96
140.98	15.8	CH4NO5P	1	Carbamoyl phosphate	6	Amino Acid Metabolism	L-Arginine and L-Proline metabolism__Purine metabolism__Pyrimidine metabolism__Glutamate metabolism	103727	1.00	0.84	0.71	0.55	**0.61**	0.69

							__Nitrogen metabolism							
116.08	4.881	C6H12O2	24	4-Hydroxyhexan-3-one	5	0	0	332290	1.00	0.83	1.73	1.62	1.16	0.22
173.14	5.611	C9H19NO2	4	[FA amino(9:0)] 3R-aminononanoic acid	7	Lipids: Fatty Acyls	Amino Fatty Acids	127567	1.00	0.82	2.12	1.43	0.47	1.54
88.016	8.049	C3H4O3	3	**Pyruvate**	10	Carbohydrate Metabolism	Glycolysis / Gluconeogenesis__Citrate cycle (TCA cycle)__Pentose phosphate pathway__Ascorbate and aldarate metabolism__Biosynthesis of steroids__Alanine and L-Aspartate metabolism__Glycine, serine and L-Threonine metabolism	3073406	1.00	0.81	0.79	0.73	0.88	1.10
95.988	14.04	CH4O3S	1	Methanesulfonic acid	7	0	dimethylsulfide degradation II (oxidation)__methanesulfonate degradation	115076	1.00	0.81	0.95	1.01	1.15	0.99
176.03	12.9	C6H8O6	15	**Ascorbate**	10	Carbohydrate Metabolism	Ascorbate and aldarate metabolism__Glutathione metabolism	3344115	1.00	0.80	1.00	0.94	1.72	1.59

267.1	9.483	C10H13N5O4	3	**Adenosine**	10	Nucleotide Metabolism	Purine metabolism	6507491	1.00	0.80	0.97	0.82	**0.11**	**0.00**
165.05	12.227	C5H11NO3S	4	L-Methionine S-oxide	6	Amino Acid Metabolism	Methionine metabolism	999396	1.00	0.80	0.94	0.96	1.17	1.17
558.18	7.529	C23H34N4O8S2	1	Asp-Met-Met-Tyr	5	Peptide(tetra-)	Hydrophobic peptide	7066	1.00	0.79	3.38	**7.08**	**62.72**	**266.66**
129.04	10.09	C5H7NO3	6	**5-Oxoproline**	10	Amino Acid Metabolism	Glutathione metabolism	622228	1.00	0.79	0.71	0.82	**0.78**	**0.64**
214.19	3.865	C13H26O2	23	CAI-1	5	0	0	118105	1.00	0.79	1.32	1.25	0.86	0.03
148.04	12.52	C5H8O5	18	D-Xylonolactone	8	Carbohydrate Metabolism	Pentose and glucuronate interconversions	3140493	1.00	0.79	0.95	0.92	**1.48**	1.52
102.03	13.49	C4H6O3	8	2-Oxobutanoate	6	Amino Acid Metabolism	Glycine, serine and L-Threonine metabolism__Methionine metabolism__Valine, L-Leucine and isoleucine biosynthesis__Propanoate metabolism__C5-Branched dibasic acid metabolism	1494387	1.00	0.78	0.81	0.88	0.98	**0.79**
505.2	9.53	C26H27N5O6	1	Trp-Trp-Asp	5	Peptide(tri-)	Hydrophobic peptide	2250961	1.00	0.78	0.70	0.54	**0.15**	**0.00**
146.07	13.36	C5H10N2O3	6	**L-Glutamine**	8	Amino Acid Metabolism	Glutamate metabolism__Purine metabolism__Pyrimidine metabolism	3970343	1.00	0.78	0.88	1.37	1.55	1.29

							__D-Glutamine and D-L-Glutamate metabolism __Nitrogen metabolism							
88.016	13.04	C3H4O3	3	3-Oxopropanoate	6	Carbohydrate Metabolism	Inositol metabolism __Alanine and L-Aspartate metabolism __beta-Alanine metabolism __Propanoate metabolism __3-Chloroacrylic acid degradation	567445	1.00	0.78	0.98	0.89	**1.66**	1.52
222.07	11.87	C7H14N2O4S	4	Cystathionine	8	Energy Metabolism	Sulfur metabolism	409615	1.00	0.77	0.70	0.76	0.89	0.94
264.1	19.66	C12H16N4OS	1	**Thiamin**	10	Metabolism of Cofactors and Vitamins	Thiamine metabolism	238196	1.00	0.77	0.92	0.92	1.18	1.21
129.15	14.62	C8H19N	2	Octylamine	7	0	0	72650	1.00	0.77	1.33	0.78	**0.59**	2.57
238.1	10.45	C8H18N2O4S	1	**HEPES**	9	Medium Component	0	30417826	1.00	0.77	0.77	0.98	1.08	0.97
123.98	11.09	C2H4O4S	1	Sulfoacetaldehyde	6	Amino Acid Metabolism	Taurine and hypotaurine metabolism	875203	1.00	0.76	0.80	0.71	0.90	0.79
130.11	17.05	C6H14N2O	2	N-Acetylputrescine	8	Amino Acid Metabolism	L-Arginine and L-Proline metabolism	19542322	1.00	0.76	0.84	0.95	**1.16**	**1.20**
114.03	13.	C5H6O3	6	2-Hydroxy-2,4-	6	Amino Acid	Phenylalanine metabolism	1068293	1.	0.75	0.78	0.85	0.97	**0.78**

	57			pentadienoate		Metabolism	__Benzoate degradation via hydroxylation__Biphenyl degradation__Toluene and xylene degradation__1,4-Dichlorobenzene degradation__Fluorene degradation__Carbazole degradation__Ethylbenzene degradation__Styrene degradation		00					
131.09	11.16	C6H13NO2	12	**L-Isoleucine**	10	Amino Acid Metabolism	Valine, L-Leucine and isoleucine degradation__Valine, L-Leucine and isoleucine biosynthesis__Alkaloid biosynthesis II	29328974	1.00	0.73	0.73	**0.73**	**0.71**	**0.63**
86.037	7.682	C4H6O2	7	Diacetyl	8	Carbohydrate Metabolism	Butanoate metabolism	164774	1.00	0.73	1.14	1.46	1.03	0.67
147.05	12.77	C5H9NO4	14	**L-Glutamate**	10	Amino Acid Metabolism	L-Arginine and L-Proline metabolism__Glutamate metabolism__Histidine metabolism__D-Glutamine and D-L-	1774838	1.00	0.73	0.61	**0.43**	**0.30**	**0.10**

119.06	13.06	C4H9NO3	11	**L-Threonine**	10	Amino Acid Metabolism	Glutamate metabolism__Glutathione metabolism_Butanoate metabolism_C5-Branched dibasic acid metabolism_Porphyrin and chlorophyll metabolism_Nitrogen metabolism Glycine, serine and L-Threonine metabolism__Valine, L-Leucine and isoleucine biosynthesis__Porphyrin and chlorophyll metabolism	3478770	1.00	0.73	0.75	0.84	0.92	0.72
162.05	13.01	C6H10O5	24	2-Dehydro-3-deoxy-L-rhamnonate	8	Carbohydrate Metabolism	Fructose and mannose metabolism	1538890	1.00	0.73	0.80	0.85	0.95	0.77
75.032	13.87	C2H5NO2	3	**Glycine**	8	Amino Acid Metabolism	Bile acid biosynthesis__Purine metabolism__Glycine, serine and L-Threonine metabolism__Lysine degradation__Cyanoamino acid metabolism__Glutathione metabolism__Methane metabolism__Thiamine	103574	1.00	0.72	0.82	0.88	1.32	**1.25**

							metabolism__Porphyrin and chlorophyll metabolism__Nitrogen metabolism							
180.06	13.4	C6H12O6	57	**D-Glucose**	10	Carbohydrate Metabolism	Glycolysis / Gluconeogenesis__Pentose phosphate pathway__Galactose metabolism__Starch and sucrose metabolism__Streptomycin biosynthesis__Indole and ipecac alkaloid biosynthesis	6816792	1.00	0.72	0.79	0.85	0.90	0.71
135.05	9.496	C5H5N5	1	**Adenine**	10	Nucleotide Metabolism	Purine metabolism__Zeatin biosynthesis	514516	1.00	0.72	0.77	**0.53**	**0.06**	**0.00**
132.04	13.47	C5H8O4	16	2-Acetolactate	6	Carbohydrate Metabolism	Butanoate metabolism__Pantothenate and CoA biosynthesis	421507	1.00	0.72	0.77	0.82	0.92	**0.74**
130.03	14.07	C5H6O4	7	citraconate	8	Amino Acid Metabolism	Valine, L-Leucine and isoleucine biosynthesis__C5-Branched dibasic acid metabolism	35419	1.00	0.71	1.06	2.14	5.10	**8.24**
150.05	13.39	C5H10O5	37	D-Xylulose	6	Carbohydrate Metabolism	Pentose and glucuronate interconversions	242820	1.00	0.71	0.77	0.82	0.94	0.70
146.11	19.	C6H14N2O2	8	D-Lysine	8	Amino Acid	Lysine degradation	1135781	1.	0.70	0.81	0.74	0.99	1.02

	83					Metabolism			00					
132.05	13.48	$C_4H_8N_2O_3$	6	**L-Asparagine**	8	Amino Acid Metabolism	Alanine and L-Aspartate metabolism__Tetracycline biosynthesis__Cyanoamino acid metabolism__Nitrogen metabolism	578127	1.00	0.69	0.86	1.12	1.37	1.13
174.11	21.3	$C_6H_{14}N_4O_2$	2	**L-Arginine**	10	Amino Acid Metabolism	L-Arginine and L-Proline metabolism__Clavulanic acid biosynthesis__D-L-Arginine and D-ornithine metabolism	4497884	1.00	0.69	0.72	**0.43**	**0.19**	**0.12**
353.16	12.13	$C_{21}H_{23}NO_4$	2	(S)-N-Methylcanadine	5	0	0	122945	1.00	0.68	0.80	0.93	1.23	1.17
117.08	11.89	$C_5H_{11}NO_2$	17	**L-Valine**	10	Amino Acid Metabolism	Valine, L-Leucine and isoleucine degradation__Valine, L-Leucine and isoleucine biosynthesis__Penicillin and cephalosporin biosynthesis__Propanoate metabolism__Pantothenate and CoA biosynthesis	9778422	1.00	0.68	0.68	**0.75**	**0.81**	**0.73**
266.09	12.	$C_{12}H_{14}N_2O_5$	1	p-aminobenzoyl L-	5	0	0	1484037	1.	0.68	0.61	0.82	0.86	**0.69**

	38			Glutamate					00					
505.2	9.578	C18H31N7O8S	2	Asn-Met-Asn-Gln	5	Peptide(tetra-)	Hydrophobic peptide	129970	1.00	0.67	**0.38**	**0.23**	**0.02**	0.00
237.09	11.19	C9H11N5O3	6	6-Pyruvoyltetrahydropterin	6	Metabolism of Cofactors and Vitamins	Folate biosynthesis	198858	1.00	0.67	0.76	0.78	1.14	**1.11**
173.04	11.6	C5H7N3O4	1	L-azaserine	7	0	0	317947	1.00	0.67	0.83	0.89	1.12	1.07
172.07	10.59	C8H12O4	4	[FA dioxo(8:0)] 4,7-dioxo-octanoic acid	7	Lipids: Fatty Acyls	Fatty Acids and Conjugates	165190	1.00	0.67	1.46	1.51	1.02	0.03
186.16	3.965	C11H22O2	25	[FA (11:0)] undecanoic acid	5	Lipids: Fatty Acyls	Fatty Acids and Conjugates	160958	1.00	0.65	1.46	1.43	0.97	0.02
149.05	11.33	C5H11NO2S	5	**L-Methionine**	10	Amino Acid Metabolism	Methionine metabolism	4880753	1.00	0.65	0.61	**0.49**	**0.32**	**0.17**
105.04	13.81	C3H7NO3	4	**L-Serine**	10	Amino Acid Metabolism	Glycine, serine and L-Threonine metabolism __Methionine metabolism __Cysteine metabolism __Cyanoamino acid metabolism __Sphingolipid metabolism __Methane metabolism __Sulfur metabolism	330243	1.00	0.64	0.67	0.71	**0.67**	**0.47**
103.1	18.68	C5H13NO	1	**Choline**	10	Amino Acid Metabolism	Glycine, serine and L-Threonine metabolism	1012113	1.00	0.63	0.48	**0.51**	**1.55**	**3.54**

							__Glycerophospholipid metabolism							
122.04	7.517	C7H6O2	6	4-Hydroxybenzaldehyde	5.5	Xenobiotics Biodegradation and Metabolism	Benzoate degradation via hydroxylation__Bisphenol A degradation__Toluene and xylene degradation	2815339	1.00	0.62	1.21	1.38	1.11	0.10
133.04	12.95	C4H7NO4	4	**L-Aspartate**	10	Amino Acid Metabolism	Alanine and L-Aspartate metabolism__L-Arginine and L-Proline metabolism__Glycine, serine and L-Threonine metabolism__Lysine biosynthesis__L-Arginine and L-Proline metabolism__Histidine metabolism__beta-Alanine metabolism__Cyanoamino acid metabolism__Carbon fixation	1764351	1.00	0.62	0.42	**0.37**	**0.13**	**0.01**
216.04	13.12	C5H13O7P	1	2-C-Methyl-D-erythritol 4-phosphate	6	Lipid Metabolism	Biosynthesis of steroids	909305	1.00	0.61	0.99	0.92	1.24	0.98
158.13	4.113	C9H18O2	25	Nonanoic acid	7	Lipids: Fatty Acyls	Fatty Acids and Conjugates	2087005	1.00	0.60	1.35	1.41	1.03	0.05

144.12	4.268	$C_8H_{16}O_2$	23	ethyl caproate	7	0	0	565099	1.00	0.59	1.36	1.36	1.03	0.11
204.09	11.155	$C_{11}H_{12}N_2O_2$	6	**L-Tryptophan**	10	Amino Acid Metabolism	L-Tryptophan metabolism__Phenylalanine, L-Tyrosine and L-Tryptophan biosynthesis__Indole and ipecac alkaloid biosynthesis	910128	1.00	0.58	0.42	**0.11**	0.00	0.00
172.15	4.013	$C_{10}H_{20}O_2$	23	Decanoic acid	8	Lipid Metabolism	Fatty acid biosynthesis	591091	1.00	0.58	1.40	1.39	1.03	0.04
130.1	4.569	$C_7H_{14}O_2$	21	Ethyl isovalerate	7	0	0	1635749	1.00	0.58	1.38	1.69	1.12	0.03
278.08	7.612	$C_{12}H_{14}N_4O_2S$	1	Thiamin acetic acid	6	Metabolism of Cofactors and Vitamins	Thiamine metabolism	123267	1.00	0.58	0.65	0.77	1.03	0.75
122.05	7.609	$C_6H_6N_2O$	4	Picolinamide	7	0	Glycerophosphoinositols	2900646	1.00	0.57	0.67	0.77	**0.74**	**0.32**
118.06	7.582	$C_5H_{10}O_3$	13	5-Hydroxypentanoate	5	Lipids: Fatty Acyls	Fatty Acids and Conjugates	116956	1.00	0.55	1.02	0.82	0.78	0.29
252.08	9.592	$C_{16}H_{12}O_3$	6	4'-O-Methylisoflavone	7	0	0	463774	1.00	0.54	0.62	0.75	0.87	0.81
369.19	10.776	$C_{22}H_{27}NO_4$	2	Corydaline	7	0	0	1712253	1.00	0.52	0.79	0.60	**0.54**	**0.40**
122.04	5.027	$C_7H_6O_2$	6	Salicylaldehyde	5.5	Xenobiotics Biodegradation and	Naphthalene and anthracene degradation	328827	1.00	0.52	1.34	1.71	1.39	0.34

						Metabolism								
495.22	3.7228	C30H29N3O4	1	GW 1929	7	0	0	162794	1.000	0.43	0.58	0.42	0.33	1.54
145.05	7.591	C9H7NO	7	3-Methyleneoxindole	5	0	0	199390	1.000	0.41	0.46	0.53	0.67	0.57
177.08	7.534	C10H11NO2	3	indole-3-glycol	7	Amino Acid Metabolism	L-Tryptophan degradation V (side chain pathway)	134220	1.000	0.41	0.12	0.06	0.09	0.11
177.08	5.8336	C10H11NO2	3	5-Hydroxytryptophol	7	0	0	448237	1.000	0.39	0.10	0.05	0.09	0.08
266.16	3.955	C12H27O4P	1	Tributyl phosphate	7	0	0	221258	1.000	0.34	0.69	1.10	0.68	0.42
191.09	4.918	C11H13NO2	1	5-Methoxytryptophol	7	0	0	274319	1.000	0.33	0.09	0.05	0.08	0.13
173.05	7.55	C10H7NO2	4	2-Quinolinecarboxylic acid	5	0	0	217573	1.000	0.33	0.44	0.41	0.52	0.35
222.09	4.123	C12H14O4	8	Apiole	7	0	0	165388	1.000	0.28	0.71	0.55	0.37	0.13
174.08	7.559	C10H10N2O	4	3-Indoleacetaldoxime	6	0	glucosinolate biosynthesis from L-Tryptophan __ camalexin biosynthesis __ IAA biosynthesis I	126636	1.000	**0.28**	**0.28**	**0.15**	**0.10**	**0.06**
251.1	8.742	C10H13N5O3	4	5'-Deoxyadenosine	7	Nucleotide Metabolism	0	125061	1.000	0.23	0.15	0.01	0.00	0.02
200.01	12.	C4H9O7P	4	D-Erythrose 4-	6	Carbohydrate	Pentose phosphate pathway__	11773	**0.**	**0.00**	**2.30**	**8.97**	**20.27**	**156.58**

	82	phosphate			Metabolism	Phenylalanine, L-Tyrosine and L-Tryptophan biosynthesis__Carbon fixation__Vitamin B6 metabolism		**00**					
403.2	4.17			-			21802438	1.00	2.14	1.42	1.13	0.90	1.68
179.09	5.359		0	4.5			8536973	1.00	1148.56	1672.62	**2285.40**	**3363.02**	**1980.98**
334.1	4.187		0	3			7750327	1.00	2.77	2.74	2.70	3.07	2.79
308.12	4.374			-			6189894	1.00	0.98	1.72	1.43	1.96	2.39
352.11	8.625			-			3935026	1.00	1.95	1.65	**2.59**	**3.17**	2.30
366.13	3.983			-			3480084	1.00	1.64	2.24	1.96	0.61	0.88
191.15	5.848			-			3097652	1.00	1.31	1.97	0.97	0.87	1.58
450.16	3.751		0	3			2455992	1.00	0.67	1.09	0.48	0.43	1.25
76.016	7.531		0	4			2168501	1.00	1.11	1.15	1.10	1.13	1.38
145.98	14.65			-			2091254	1.00	1.08	1.00	0.86	1.02	0.88
467.18	3.756		0	3			2046583	1.00	0.65	1.01	0.51	0.39	1.51

254.09	11.64				-			1693676	1.00	1.03	1.21	1.34	**1.89**	**1.69**
352.11	7.57				-			1398134	1.00	1.59	2.25	**2.36**	**3.02**	**2.77**
127.95	14.45				-			1230764	1.00	1.01	0.88	0.67	0.76	0.77
189.95	14.41				-			1047265	1.00	1.07	0.95	0.63	0.93	0.77
315.2	4.358		0		4.5			835249	1.00	1.84	0.72	2.38	1.32	0.78
146.11	0.121		0		4			748721	1.00	1.21	1.38	1.28	1.00	0.92
386.19	4.117				-			707323	1.00	0.81	1.45	1.02	0.20	1.14
132.05	13.44	$C_4H_8N_2O_3$	6	**L-Asparagine**	10	Amino Acid Metabolism	Alanine and L-Aspartate metabolism__Tetracycline biosynthesis__Cyanoamino acid metabolism__Nitrogen metabolism	563455	1.00	0.70	0.91	1.36	1.53	1.37
284.13	5.49				-			543784	1.00	0.75	0.99	0.12	0.59	**5.83**
527.17	4.681				-			541667	1.00	2.00	1.75	1.94	2.41	2.57
243.06	13.05				-			404653	1.00	0.50	0.47	0.55	0.50	1.13
117.97	15.				-			373821	1.	0.98	0.84	0.64	0.70	0.71

	91				00					
283.16	10.67		-	363264	1.00	0.73	0.58	0.75	0.60	0.89
170.92	0.097		-	353892	1.00	1.18	1.09	1.25	1.57	0.78
266.04	7.572		-	322795	1.00	0.37	0.32	0.35	0.12	0.03
299.19	3.986		-	313356	1.00	1.22	0.53	1.60	0.99	0.68
383.77	4.021		-	305819	1.00	1.83	0.22	1.79	2.67	0.24
209.04	12.81		-	266998	1.00	2.44	2.23	2.29	0.69	0.24
74.037	12.92		-	235259	1.00	1.17	2.79	12.15	**101.30**	**123.27**
200.05	10.72		-	232292	1.00	0.52	1.26	0.70	0.31	1.75
164.08	4.764	0	4.5	219920	1.00	1.55	2.03	2.08	1.90	**0.00**
694.29	4.4		-	206764	1.00	3.58	1.31	2.95	3.72	**6.71**
188.05	12.26		-	187963	**1.00**	190.10	249.27	421.96	**679.35**	**858.26**
379.89	14.57		-	182975	1.00	0.98	0.75	0.54	**0.60**	0.66
292.16	12.64		-	182839	1.00	0.60	0.54	0.74	0.84	0.92

202.05	13.32				-			163459	1.00	0.93	0.82	0.88	1.02	0.95
290.11	7.94				-			152095	1.00	1.14	1.30	1.26	1.34	1.09
183.94	15.42				-			151722	1.00	1.05	0.75	0.60	0.60	0.64
163.91	14.41				-			133717	1.00	0.89	1.08	1.05	**1.48**	1.36
255.12	4.971		0		3			128665	1.00	**0.32**	1.46	0.52	**0.20**	1.34
308.1	7.6				-			125208	1.00	0.50	0.72	0.70	1.45	**3.15**
296.05	12.02				-			113549	**1.00**	3.83	4.59	**5.01**	**7.85**	**6.93**
387.19	4.105				-			112543	1.00	0.84	1.24	1.07	0.21	1.47
171.84	12.6				-			106523	1.00	0.63	0.85	0.78	1.36	1.11
306.1	4.26		0		3			105782	1.00	0.83	2.17	1.13	2.20	2.21
89.019	7.66				-			103367	1.00	0.81	0.78	0.69	0.87	1.10
236.1	4.049		0		3			102091	1.00	1.45	0.58	1.98	1.40	0.65
165.05	12.28	C5H11NO3S	4	L-Methionine S-oxide	8	Amino Acid Metabolism	Methionine metabolism	97370	1.00	0.68	0.83	0.85	1.07	1.05

483.18	3.77		-	96792	1.00	1.65	2.10	2.01	2.43	3.34
116.06	12.27		-	90856	1.00	0.82	0.90	1.09	**1.41**	**1.38**
212.08	12.85		-	88456	1.00	0.71	0.82	0.86	1.04	0.94
142.07	7.857	0	4	80185	1.00	1.11	1.26	1.22	**1.47**	0.75
204.06	12.89	0	3	61256	1.00	1.18	1.48	1.75	**6.28**	**14.18**

Appendix table 6 metabolites in the exometabolome samples enriched over time compared to naïve medium without cells. Metabolites in yellow are matched to authentic standards. Chemical formula in red are those with more than one isomeric peak.